Evaluation of the zebrafish embryo as an alternative model for hepatotoxicity testing

Driessen, M.

Evaluation of the zebrafish embryo as an alternative model for hepatotoxicity testing

Marja Driessen

Evaluation of the zebrafish embryo as an alternative model for hepatotoxicity testing

Proefschrift

ter verkrijging van
de graad van Doctor aan de Universiteit Leiden,
op gezag van de Rector Magnificus prof. mr. C.J.J.M. Stolker,
volgens besluit van het College voor Promoties
te verdedigen op woensdag 17 december 2014
klokke 10.00 uur

door

Marja Driessen
geboren te Breda,
23 januari 1985

ISBN
978-94-6259-475-3

Design and lay-out
Promotie In Zicht, Arnhem

Print
Ipskamp Drukkers, Enschede

Illustrations chapter pages: Simona M Ceccarelli Pharmaceuticals Division, F. Hoffmann-La Roche Ltd. , CH- 4070 Basel, Switzerland. simona_m.ceccarelli@roche.com
Cover illustration based on a photograph of Marianne Roodbergen

This research was financially supported by the Netherlands Genomics Initiative/ Netherlands Organization for Scientific Research (NWO) (grant number 050-060-510)

Financial support for the printing costs of this thesis by the National Institute for Public Health and the Environment (RIVM) is gratefully acknowledged.

Promotiecommissie

Promotor:	Prof. dr. B. van de Water	Universiteit Leiden/LACDR
Co-promotores:	Dr. L.T.M. van der Ven	RIVM
	Dr. A.S. Kienhuis	RIVM
Overige leden:	Prof. dr. P.H. van der Graaf	Universiteit Leiden
	Prof. dr. J. Kuiper	Universiteit Leiden/LACDR
	Prof. dr. Ir. J. Legler	Vrije Universiteit Amsterdam/IVM
	Prof. dr. A. H. Piersma	Universiteit Utrecht/RIVM
	Prof. dr. H.P. Spaink	Universiteit Leiden/IBL

Voor Marcel

Table of contents

Chapter 1	General Introduction	9
Chapter 2	Exploring the Zebrafish Embryo as an alternative Model for the Evaluation of Liver Toxicity by Histopathology and Expression Profiling	27
Chapter 3	Gene Expression Markers in the Zebrafish Embryo Reflect a Hepatotoxic Response in Animal Models and Humans	55
Chapter 4	Gene and Protein Expression Markers of Hepatotoxicity in Zebrafish Embryo Model	75
Chapter 5	A Transcriptomics-based Hepatotoxicity Comparison between the Zebrafish Embryo and established Human and Rodent *in vitro* and *in vivo* Model Using Cyclosporine A, Amiodarone and Acetaminophen	103
Chapter 6	General Discussion	121
Chapter 7	English Summary	133
	Nederlandse Samenvatting	141
	References	145
	Curriculum Vitae	153
	List of Publications	155
	Supplementary Tables Chapter 2	157
	Supplementary Tables Chapter 3	210
	Supplementary Tables Chapter 5	232

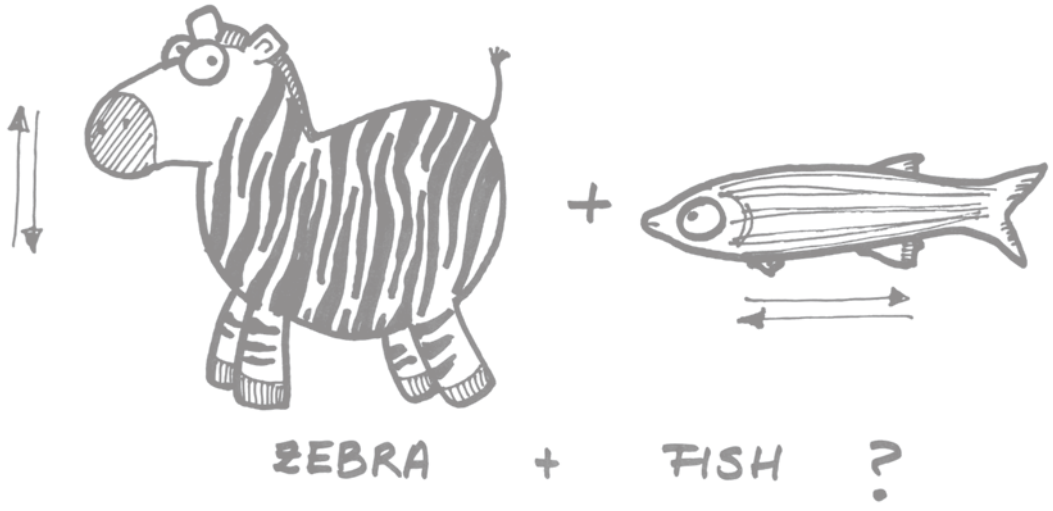

1

General Introduction

In part published as:
Hepatotoxicity screening on *in vitro* models and the role of Omics

Marja Driessen and Leo T.M van der Ven

in: Toxicogenomics-Based Cellular Models: Alternatives to Animal Testing for Safety Assessment
15 Mar 2014 ISBN-10: 0123978629

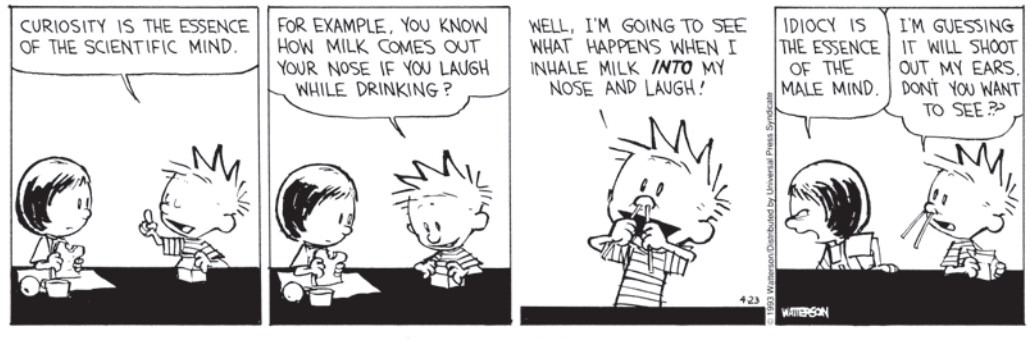

Humans are exposed throughout their entire life to multitude of diverse xenobiotic compounds, such as industrial chemicals and pharmaceuticals. This exposure is either intended, *e.g.* when prescribed as drug, or unintended, *e.g.* as contaminants in food or the environment. Xenobiotic exposure may pose health risks; when a hazardous concentration is reached adverse biological effects may occur. Toxicological research aims to identify these adverse health effects (hazard) and compare hazard threshold levels with real-life exposure levels to estimate the risk associated with actual exposure. The liver is one of the major targets of toxicological effects, because it is the first organ to be encountered after absorption from the gastro-intestinal tract, and it is therefore important to assess hepatotoxic properties of xenobiotics that humans are exposed to[1]. Traditionally hepatotoxicity is studied mainly in animal studies, but observations in animal exposure studies appeared to be not fully predictive for the effects in humans[2]. The predictivity of animal studies is limited mainly by physiological differences between species, leading to differences in toxicokinetic fate, *i.e.* absorption, distribution, metabolism, and excretion of the xenobiotic, and differences in sensitivity of target cells[2]. These differences are the cause of uncertainties associated with extrapolation from animal to man and from short-term to long-term exposure. Thus, effects that occur in humans may remain undetected in animals. Therefore, there is an imperative need to improve toxicological testing, and develop strategies that do not rely on traditional testing in rodents. Development of new screening methods should build on new *in silico* and *in vitro* methods, which can also help to implement the 3R strategy to Replace, Reduce and Refine the use of animals. An approach is to analyze the molecular mechanisms that underlay toxicological effects facilitating comparison across models and species, through the use of 'omics-technologies'. A promising alternative testing model is the zebrafish embryo, which we evaluate here for its application in hepatotoxicity testing through the use of several toxicogenomics tools.

The liver as critical target organ for toxicity

The liver is an important target for adverse effects of xenobiotics, as it is the first organ to pass after enteric absorption, positioned between the gastro-intestinal tract and systemic circulation. The liver has metabolic activity, which allows deactivation or detoxication of xenobiotics, thereby facilitating their excretion. This process is called biotransformation, which is a multistep process including Phase I and Phase II metabolism. Phase I metabolism can be divided into by three steps including modification, oxidation and reduction preparing the xenobiotics for Phase II metabolism. In Phase II metabolism, the xenobiotics are conjugated resulting in clearance[3]. Due to the position of the liver and its metabolic function, it serves as a 'first pass' organ resulting in relatively high concentrations of xenobiotics that depend on oral uptake. This may lead to toxic activity of the xenobiotic and thereby to the induction of liver injury[1,4–6].

The liver consists of several cell types. Hepatocytes are the most predominant cell type, covering approximately 60% of the liver and carrying out most of the metabolic functions.

Furthermore, they express a wide scale of circulating plasma proteins including albumin[1,3,7]. Less than 40% of the liver is comprised of sinusoid endothelial cells, Kuppfer cells, and stellate cells[1,3,7]. Sinusoidal endothelial cells are the largest group of non-parenchymal cells compromising around 19% of the total liver cell mass. These cells are a physical barrier for blood circulation allowing the interchange of nutrients, toxicants, hormones and other molecules from the plasma to the hepatotocytes. In addition, these cells play an important role in the inflammatory reactions[7,8]. Kuppfer cells compromise 15% of the total liver mass and in healthy situations these cells are present as resting macrophages. However, upon activation, for example due to liver damage, these cells will excrete pro-inflammatory cytokines potentially aggravating the damage in the hepatocytes and promoting the pro-apoptotic responses[7,9,10]. Stellate cells are the smallest non-parenchymal cells in the liver, only compromising 6% of the total liver mass. Their function in the liver is to store vitamin A, however, under toxic stress these cells have various other functions including the secretion of chemokines and activation of natural killer cells[7]. This shows that hepatotoxicity may occur through interaction of a xenobiotic with various cell types within the liver. Depending on the toxic functions and pathways that are activated, xenobiotic interaction may lead to a variety of liver pathologies including cholestasis (intra- or extracellular bile accumulation), steatosis (fatty liver), and necrosis (cell death)[1,4,6,11]. These specific toxic phenotypes are explained below in more detail, together with actions of some reference toxicants.

Cholestasis. Cholestasis is one of the main xenobiotic-induced liver pathologies resulting from either impairment in bile secretion or obstruction in bile flow[12–14]. Bile and bile acids are not only important for the digestion of fat from the diet, but also for the clearance of xenobiotics from the liver[1]. Cholestasis occurs when there is either an impaired bile transport or an inhibition of bile transporters[12]. Several drugs are known to induce cholestasis via different molecular mechanisms.

First, 17α-ethinylestradiol (EE2), a synthetic estrogen derivative, is used in combined oral contraceptive pills, which reduces bile flow by inhibiting bile acid active transporters at the hepatic canalicular membrane. EE2 also increases the permeability of cells in the bile ductules elevating the reabsorption of bile components[1,15].

Second, cyclosporine A (CsA) is widely used as an immunosuppressant in organ transplantation to avoid rejection. In humans, it induces cholestasis by interacting with and inhibiting the bile transporter, also known as the bile salt export pump (BSEP)[12].

Third, chlorpromazine (CPZ) is used to treat acute and chronic psychoses[16]. CPZ induces cholestasis by directly acting at the intracellular membrane thereby decreasing bile acid-dependent bile flow resulting in a loss of bile acids via defective bile canaliculi. In addition, the Na^+/K^+ pump and hydroxylation of cholesterol to bile acids are inhibited by CPZ[16].

Furthermore, all of these compounds are frequently used in *in vivo* and *in vitro* studies to induce cholestasis[1,12,15–17].

Several studies have shown that these model compounds are able to induce cholestasis in a wide variety of models including *in vivo* mouse and rats, and also *in vitro* mouse liver slices, primary hepatocytes and many more.

Steatosis. Fat metabolism is another important function of the liver, specifically through fatty acid synthesis and promoting lipid circulation by lipoprotein synthesis[1,3]. Changes in fat metabolism may result from an increase in uptake of lipids, elevation of the *de novo* synthesis of fatty acids, an impairment of lipoprotein synthesis/secretion, and/or a reduction in fatty acid oxidation[19]. The accumulation of cytoplasmic fatty acids in the form of lipid droplets is known as steatosis[11,19]. Disrupted fat metabolism is manifested as

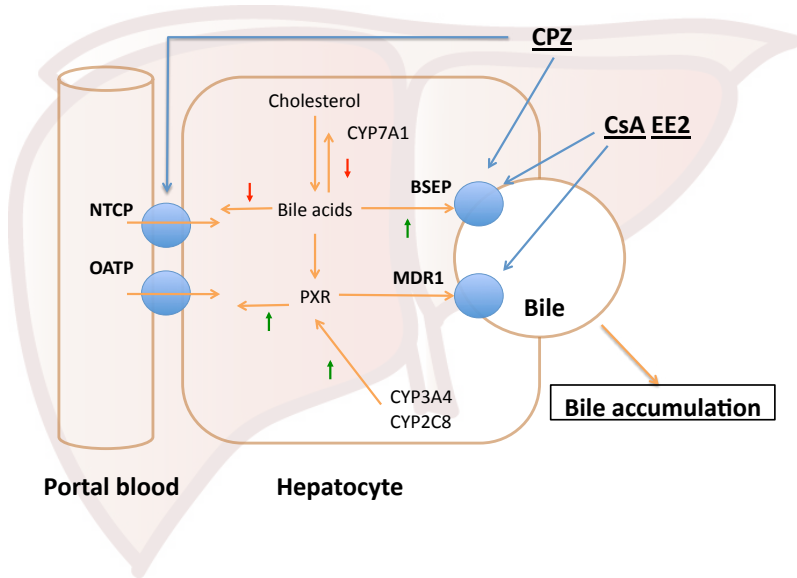

Figure 1 Toxicity pathway of cholestasis.
Cyclosporine A (CsA) and 17α-ethinylestradiol (EE2) block the transporters regulating bile flow from hepatocyte to bile duct (bile salt pump (BSEP) and multidrug resistance protein 1 (MDR1)), resulting in accumulation of bile in the hepatocyte. Chlorpromazine (CPZ) and EE2 act on the uptake transporters Na^+-dependent taurocholic cotransporting polypeptide (NTCP) and organic anion-transporting polypeptide (OATP), but also inhibit the excretion transporters BSEP and MDR1. This inhibition of bile acid excretion leads to accumulation of intracellular bile acids. Cholesterol is known to be converted to bile acids by cytochrome P450 CYP7A1 into bile acids, which in turn activate pregnane X receptor (PXR) leading to an increase in expression of MDR1 and OATP (Adapted from Jansen *et al.,* and Zimmerman[1,18])

either microvesicular (multiple small vacuoles in the hepatocytes) or macrovesicular steatosis (larger vacuoles that dislocate the nucleus from the center of the cell). Several drugs and chemicals are known to induce steatosis in humans including amiodarone (AM), tetracycline (TET), and valproic acid (VPA).

Amiodarone (2-butyl-3-benzofuranyl 4-[2-(diethylamino)etoxcy]-3,5-diiodophenyl ketone; AM) is a frequently prescribed antiarrythmic agent, to prevent atrial fibrillation. AM induces steatosis in humans, and also in rodent models, probably through inhibiting mitochondrial β-oxidation of long-, medium-, and short-chain fatty acids. Furthermore, this compound inhibits carnitine palmitoyltransferase-I (CPTI)-dependent transport of long-chain fatty acids across the mitochondrial membrane [20] resulting in fatty acid accumulation in hepatocytes.

Tetracycline is a frequently used antibiotic, to fight infections with both gram-positive and gram-negative bacteria. Tetracycline induces microvesicular steatosis in the liver by down-

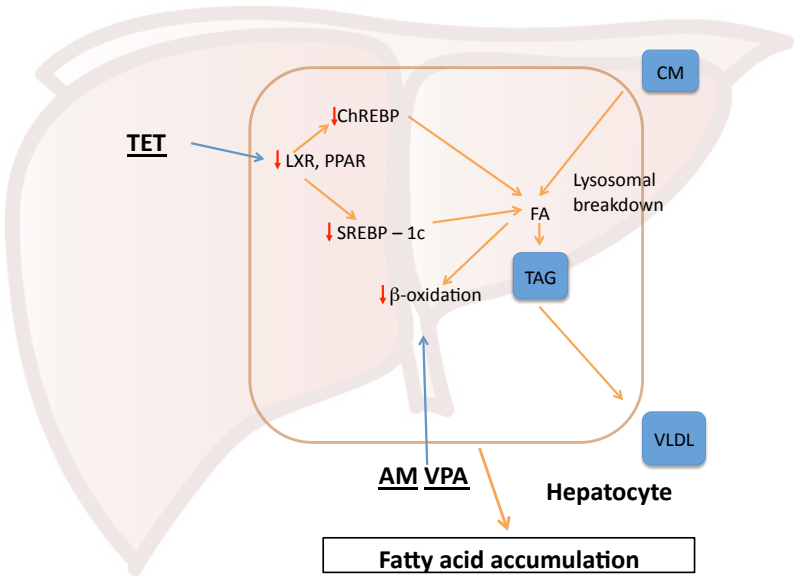

Figure 2 Toxicity pathway of steatosis.
Sources of fatty acids (FA) are triacylglycerol (TAG) and chylomicrons (CM). TAG is exported out of the hepatocytes in the form of very low density lipoproteins (VLDL). Tetracycline (TET) induces steatosis by downregulation of nuclear receptors including liver X receptor (LXR) and peroxisome proliferator receptors (PPARs) and their target genes sterol regulatory element-binding protein 1c (SREBP-1c) and carbohydrate response element-binding protein (chREBP); this in turn leads to an increase in fatty acids (FA) level. Valproic acid (VPA) and amiodarone (AM) inhibit the β-oxidation cycle resulting in decreased metabolism of fatty acids, which then accumulate in the hepatocyte (Adapted from Matsuzaka and Shimano (2011)[26])

regulating the peroxisome proliferator activated receptors (PPARs), which are involved in the development of steatosis through their important role in lipid deposition[21,22].

Valproic acid (VPA) is an antiepileptic agent, used to treat specific types of seizures. VPA hepatotoxicity is believed to be mediated by either an inhibitory effect on the mitochondrial β-oxidation pathway, which gives rise to microvesicular steatosis, or by metabolic effects which promote weight gain and insulin resistance giving rise to macrovesicular steatosis and steatohepatitis[23].

Studies have shown that VPA and TET induce steatosis in mice through an increase in cholesterol and triglyceride biosynthesis and a decrease in fatty acid oxidation[22,24,25]. Furthermore, AMD has been found to promote steatosis in mice through altering lipid homeostasis in the liver[20].

Necrosis. Necrosis, or cell death, is caused by severe metabolic perturbations resulting in ATP depletion. Diminished levels of ATP breakdown and cytoskeleton integrity, which results in the characteristic morphology of cell swelling accompanied by membrane blebbing[11]. Furthermore, mitochondrial permeability transition (MPT) plays an important role in necrosis. MPT is known to lead to either necrosis or apoptosis after mitochondrial oxidative stress[7,27]. Known drugs or compounds that induce necrosis are acetaminophen (APAP), paraquat (PQ) and thioacetamide (TAA).

Acetaminophen (paracetamol; APAP) is an analgesic and antipyretic, which is considered safe at therapeutic doses. In this setting, APAP is inactivated by sulfation and glucuronidation. However, when therapeutic doses are exceeded, APAP causes hepatic damage and may eventually lead to liver failure. APAP toxicity is due to its active metabolic conversion by CYP2E1 to the highly toxic metabolite N-acetyl-p-benzoquinone imine (NAPQI). In normal situations, NAPQI is conjugated to reduced glutathione and is excreted the bile. However, when therapeutic doses are exceeded, NAPQI concentrations increase due to saturation of the sulfation and glucuronidation pathways. Hepatotoxicity occurs when NAPQI binds to macromolecules, for example in the mitochondria, which leads to mitochondrial dysfunction and DNA damage[11,28,29].

Paraquat (PQ), a contact herbicide, is a dehydrate and defoliant used for harvesting cotton, potatoes, and soy beans. PQ is a bipyridyl derivative, which can be taken up by the redox cycle leading to the release of active oxygen radicals, which in turn can induce damage to the hepatocyte[30].

Thioacetamide (TAA) was formerly used as a fungicide. The underlying mechanism of hepatotoxicity of this compound appears to be its metabolism via CYP2E1. TAA is metabolized to di-S-oxide (CH3-C(SO2)NH2), which is a reactive intermediate that covalently binds to hepatic macromolecules resulting in necrosis[31]

Hepatotoxicity testing

Traditionally, rodent studies are used to predict the hepatotoxic effects of xenobiotics. As introduced above, an important scientific argument against the use of rodent studies is that the obtained effects are not always fully predictive for the effects in humans[2]. In general, animal studies are helpful to identify human toxicants, but particularly in the case of hepatotoxicity, the identification remains low due to a poor correlation between human and animals[2,7,11]. Missed hepatotoxic effects in traditional screening assays is a major cause of the high attrition rate in drug development and therewith associated with high cost[1,4,6]. From the perspective of animal welfare it is unfavorable that animals need to be exposed to high doses of compounds for extended periods of time. Therefore, there is an imperative need to develop alternative models to assay the hepatotoxic potential of xenobiotics. Currently, multiple alternatives are available for hepatotoxicity testing, including single liver cell systems, liver slices and whole organisms[7,11].

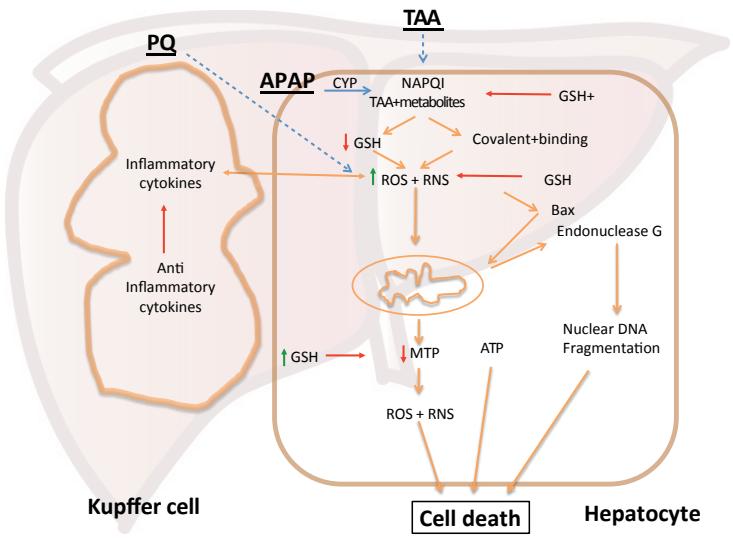

Figure 3 Toxicity pathway of hepatic necrosis.
Necrosis is the consequence of induction of reactive oxygen species (ROS) and reactive nitrogen species (RNS), which eventually leads to a decrease of glutathione (GSH). GSH depletion eventually leads excess of ROS/RNS, oxidative damage and hence to cell death. Acetaminophen (APAP) induces ROS/RNS through its toxic metabolite N-acetyl-p-benzoquinone imine (NAPQI) to which it is converted by cytochrome P450 (CYP) enzymes. Thioacetamide (TAA) is also metabolised by CYP enzymes to a reactive metabolite which increases the ROS production. Mechanism of paraquat (PQ) is not completely understood, but it probably also induces an increase in ROS production. One important damaging action of ROS/RNS is the decrease of mitochondrial permeability transition (MPT) leading to loss of ATP, which contributes to cell death. Kupffer cells secrete cytokines which may aggravate ROS/RNS production leading to cell death (Adapted from Hinson *et al.* (2010) and Jaeschke et al. (2012) [32,33])

The *in vitro* cell system of primary hepatocytes is one of the most prominent models for studying hepatotoxicity and allows for easy interspecies comparison[7,11,37]. Generally, these cells maintain expression of Phase I and Phase II metabolic enzyme activities for longer periods of time, however, they are not fully representative of the *in vivo* liver due to a loss of original cell shape and a deviating gene expression response to xenobiotics[7,11,37].
Alternatively, several permanent, immortalized cell models are available for toxicity screening. Of these, the frequently used human hepatocarcinoma derived HepG2 cell line has a long history in xenobiotics testing. The advantage of this cell line is that it provides an infinite reservoir of identical cells[7,11,37]. HepG2 cells show activity of several Phase I and Phase II metabolic enzymes, however, not all metabolizing enzymes are present and otherwise the expression level is generally much lower than in the *in vivo* situation or primary human hepatocyes, leading to a different response after compound exposure[7,11,37]. However, recent advances allowed to improve the expression of Phase I enzymes in the HepG2 cells constructing Adv-HepG2 cell line[38].

Table 1 Reference compounds and phenotypes.

Phenotype	Compound	Proposed mechanism of action	References
Cholestasis	17α-ethinylestradiol	Inhibition of bile acid transporters	Wagner *et al.,*[12,34]
	Cyclosporine A	Inhibition of BSEP	Antherieu *et al.,*[12]
	Chlorpromazine	Decreases bile acid dependent bile flow	Yamamoto *et al,.*[16]
Steatosis	Amiodarone	Inhibition of mitochondrial β-oxidation and CPTI dependent transport	Anderson and Borlak[19]
	Tetracycline	Down-regulation of PPARs which play a role in lipid desposition	Yin *et al.,*[21,22]
	Valproic acid	Inhibition of mitochondrial β-oxidation	Silva *et al.,*[23]
Necrosis	Acetaminophen	CYP2E1 metabolism releasing NAPQI (toxic metabolite) inducing mitochondrial dysfunction	McGill *et al.*[35]
	Paraquat	Taken up by redox cycle inducing release of active oxygen radicals	Burk *et al.,* and Bus and Gordon[30,36]
	Thioacetamide	Metabolism via CYP2E1 resulting in reactive intermediate	Hunter *et al.,*[31]

An overview of the phenotypes of interest in this thesis and the associated reference compounds

Other hepatocyte cell lines are also used, and HepaRG is an example of a recently isolated and cultured hepatoma cell line. Several studies have shown the presence of xenobiotic metabolizing enzymes, much similar to the primary hepatocytes, enabling them to be suitable in assessing the xenobiotic compounds hepatotoxicity potential[39–41]. Another recent advancement is use of 3D cell culture systems. HepG2 cells cultured in 3D stopped proliferating, self-organize and differentiate to form multiple polarized spheroids acquiring hepatotocyte functions including glycogen storage, transportation of bile salts and the formation of structures resembling bile canaliculi[42].

The isolated perfused liver and liver slices are considered to be the system closest related to the *in vivo* condition, because these systems maintain 3D-architecture including bile flow and cell-cell interactions. Furthermore, these systems contain the non-parenchymal cells which have an important role in mediating the toxicity[7,43]. A downside of these systems is the relative short period of viability, limiting these models to test only compounds which are expected to have an effect within a few hours[7,43].

Toxicological science is in need of a model that combines these advantages and overcomes the drawbacks of these systems. In this respect, the zebrafish embryo could be considered as a complementary alternative model to screen for potential hepatotoxic compounds and to investigate the mechanisms by which chemicals induce liver injury[44–49].

The zebrafish embryo

The zebrafish (*Danio rerio*) is a diploid minnow of the teleost family Cyprinidae and was introduced several decades ago to study development and neurobiology. Thereof, the zebrafish emerged as a powerful model to study human disease and the effects of chemical exposure[45,50–53]. Several features make the zebrafish embryo attractive as an experimental model, among which are the potential for use in a high-throughput screening setting and the small size of both the adult zebrafish and zebrafish embryo. Furthermore, maintenance in large stocks is easy due to their high fecundity. In the embryo, direct observation and experimental manipulation of tissue and organs is relatively simple due to the transparency and the rapid development. As a result of the rapid development, most organs become fully functional between three and five days post fertilization[50]. In addition, during the earliest developmental stages (until independent, free-feeding) the zebrafish embryo is not a protected animal under present European legislation (Directive 2010/63/EU) and can therefore be considered as an alternative to animal experimentation[54]. A fully functional liver is present in the zebrafish embryo by three days post fertilization, at which time it is perfused with blood. In terms of xenobiotic biotransformation capacity, zebrafish embryos express 94 cyps, which occur in the same 18 gene families as in humans, and most of them are human cyp orthologs. The cyp1-4 families are mainly involved in metabolizing xenobiotics, similar to humans. Most important is the presence of the human CYP3A4 ortholog, *cyp3a65*, because this cyp catalyzes the majority of known drug-metabolizing reactions[46,55,56].

The zebrafish embryo and hepatotoxicity testing. While most of the important cytochromes are present in the zebrafish embryo, this model might be suitable to detect hepatotoxicity. Some studies showed that zebrafish embryos are suitable to detect hepatotoxicants. In a study by Jones *et al*., the whole zebrafish embryo model was evaluated through morphological endpoints after exposure to a set of compounds, including falsely classified DILI drugs by HepG2 cells. In this study, the whole zebrafish embryo model successfully detected hepatotoxicants with higher specificity than the HepG2 cells[49]. In another study, Amali *et al*., carried out histopathological, molecular and biochemical analysis in zebrafish embryos exposed to a single dose of thioacetamide and showed that the whole zebrafish embryo model is suitable to detect steatohepatitis[57]. These studies indicate the potential of the zebrafish embryo as a model for hepatotoxicity testing at the level of the phenotype, but they provide limited insights into the underlying mechanisms of toxicity[58]. Toxicogenomics is hypothesized to contribute understanding of the underlying mechanisms of hepatotoxicity and discrimination between various hepatotoxic phenotypes, such as cholestasis, steatosis and necrosis.

Toxicogenomics

For drug development, understanding the mechanism of toxicity is imperative, not only to compare between reference toxicants and test compounds, but also to differentiate between toxic and targeted effects, and to develop relevant markers of toxicity. The method to analyze and describe mechanisms of toxicity comprises a set of tools, which generally involves toxicogenomics[61].

Traditionally, hepatotoxic properties of chemicals and compounds are determined using rodent studies which rely on different toxicity endpoints including body and organ weight, death rate, serum toxicity biomarkers and histopathological changes[11]. Although these phenotypical endpoints give an indication of toxicity, they do, however, not provide insight into the underlying molecular mechanisms of hepatotoxicity. By applying molecular techniques, such as transcriptomics, proteomics and next generation sequencing, in the toxicology setting will provide an insight into the underlying molecular mechanisms[61–63]. The assumption is that changes in for example toxicity markers and histopathology are preceded by changes on gene and/or protein level after exposure to compounds. The changes in genes and/or proteins will provide us with a more detailed view on the onset of the toxic events.

Transcriptomics analysis can be implemented in different ways including the use of micro arrays and the more recent technique next generation sequencing. Next generation sequencing provides multiple advantages over the traditionally used mRNA microarrays. In contrast to microarrays, NGS does not rely on the probe design and probe selection, thus enabling detection of non-predefined transcripts, including diverse splicing variants of a single gene.

Another advantage of the implementation of molecular techniques in toxicology research is that it allows the researcher to extrapolate the findings to other organisms. In the area of

Table 2 Testing models for hepatotoxicity.

Model	Strength	Weakness
Liver slices	Fairly high throughput Retain liver structure; contain all cell types Functional bile canaliculi Good *in vitro/in vivo* correlation of xenobiotic metabolism Maintain zone-specific CYP activity; maintain toxicity mechanisms Stability of phase II enzymes, albumin production, gluconeogenesisis for 20-96 hours	Cellular necrosis after 48-72 hours CYP levels quickly decrease (6-72 hours) Poor concordance with liver for intrinsic clearance rates and *Km* values Diffusion-limited gradient of the exposure to a compound across the slice
Immortalized hepatic cell lines	Throughput depends on application Unlimited amount of cells available Some cell lines retain expression of many liver-specific functions	Lacking most phenotypic and functional characteristics of the liver tissue
Primary hepatocyte suspensions	Fairly high throughput Better estimate of internal clearance than monolayer cultures Retain high level of enzyme functionality (close to *in vivo*)	Loss of cell-cell interactions Loss of cell-matrix interactions Limited viability allows short-term use only (<4 hours) Loss of cellular polarity No bile canaliculi
Primary hepatocyte cultures	Throughput depends on the application Cells can re-establish cell-cell interactions and polarity Cells retain some morphology and liver specific functionality in short-term cultures (2-4 days) Induction/inhibition of the metabolizing enzymes can be studied	Inability to maintain *in vivo* liver-specific functionality for long-term culture Quick reduction in functionality and phenotype (24-48 hours) May not develop functional bile canaliculi
Primary hepatocyte cultures Sandwich	Throughput depends on the application Restores *in vivo* polygonal morphology Better maintains liver-specific functionality Prevents loss of viability Functional bile canaliculi	Loss of liver-specific functionality, morphology and phenotype in long-term cultures Decline in metabolic enzyme activity in long-term culture
HepaRG cell line	Functional activities remain stable for long time period Enzyme activity can be modulated allowing to more closely mimic inter-individual variations in xenobiotics metabolizing enzymes	Loss of cell-cell interactions Loss of cell-matrix interactions No bile canaliculi
Zebrafish embryo	*Ex vivo* development and optical clarity of the embryo Embryogenesis is completed at 72 hpf, liver is fully functional Biological complexity of *in vivo* models Easy to handle and cheap Genome of the zebrafish is sequenced. Molecular biology tools are available for genetic manipulation High-throughput screening	Developmental stage of the hepatocytes Extrapolation to human First pass effect Teleost fish possess two copies of many mammalian genes due to gene duplication events

Adapted from Delvecchio *et al.* (2011), Guillouzo (1998) and Soldatow *et al.* (2013)[37,59,60]

hepatotoxicity, several studies have shown that toxicogenomics can be applied to investigate the underlying molecular mechanisms leading to toxicity[61,64]. Mostly, these toxicogenomics techniques are applied in traditionally used models for hepatotoxicity including mice, rats and *in vitro* models[64,65]. With regards to the ZFE, several recent studies show that toxicogenomics can be applied to investigate the underlying mechanisms of toxicity. For example, the study of Yang *et al.*, showed that the ZFE allows for the robust identification of genes to distinguish between toxicants[53]. More specifically, several transcriptomics studies identified the underlying mechanisms of teratogenicity[66–70] of compounds showing the suitability of applying toxicogenomics in the ZFE. Few studies have been performed with toxicogenomics in ZFE with regard to hepatotoxicity[46,49,57]. Nevertheless, these transcriptomics studies show that the zebrafish embryo model is suitable for detecting differences between chemical classes illustrating the possibilities of this model. Several proteomics studies have been performed in other models, such as *in vitro* and *in vivo* systems, to gain further insight into the differences in proteomes after exposure to hepatotoxicants[17,71,72]. These studies show the potential of this technique to assess the molecular mechanisms of hepatotoxicity.

With regard to the ZFE, proteomics studies have been performed, but are mainly targeted at the differences between proteomes during different life-stages. Less is known about

the changes occurring after exposure to hepatotoxicants. The most practical way to study hepatic gene expression in ZFE is to use whole ZFE RNA extract for analysis, instead of liver extracts, but this may result in masking of signals or lowering the signal/noise ratio of the regulated genes. Although available, sophisticated methods such as micro-dissection to study hepatic gene expression in small organism hinder the throughput of the system[73].

Toxicogenomics data analysis. The amount of data generated by applying these molecular techniques in such a toxicology experiment is enormous, and it is therefore imperative that the proper methods are applied which might translate to biological conclusions. For all the "omics-techniques" analysis, the data needs to be corrected for the background and normalized after the samples are either hybridized to the array (transcriptome) or measured by mass spectrometry (proteome). Background corrections are applied to improve the signal of the measurements, and thus adjust for artifacts, including non-specific hybridizations of the samples on the arrays or peak distributions in proteins[74]. After background correction, the data is routinely log-transformed. This improves the characteristics of the data distribution and enables the use of classical parametric statistics[75,76]. In the next step, the gene expression data is normalized, which corrects for the systematic difference between the arrays. After the preprocessing phase, the analysis of the data is continued by identifying the genes/proteins which differ from the control situation. This is mostly achieved by a selection based on significance level using *p-values*, or false discovery rate (FDR) combined with a fold change (FC). Genes/proteins fitting the selection criteria can be visualized using different methods including biplots, PCA and hierarchical clustering methods. By using these available tools, it is possible to identify the mode-of-action of compounds. In this case, certain groups of compounds are used to establish a 'fingerprint' for certain classes of toxicity. A new compound can thus be identified as toxic based on the basis of overlap based on the fingerprint of the toxicity classes, thereby contributing to the predictive toxicology.
To compare the results from the experiments with the literature, several databases are available, for example Gene Ontology[77], UniProt[78,79], National Center for Biotechnology Information (NCBI)[80], comparative toxicology database[81], and specific for the zebrafish is the Zebrafish Model Organism Database from the Zebrafish Information Network (ZFIN)[82]. Identification of genes which differ from the control situation is not enough to improve the understanding of the molecular mechanism behind the toxic event. Therefore, the genes are tested for overrepresentation in certain biological processes (Gene Ontology[77]) or pathways (KEGG, Wikipathways, MetaCore, Tox-Profiler, DAVID)[83–89]. Also for proteomic expression several databases exist to compare the results to literature. The analysis for proteomics expression can be done using Trans Proteomic Pipeline (TPP) which is a completely open-source analysis method for MS/MS-based proteomics[90]. For example, STITCH, UNIPROT, and again DAVID. STITCH is a resource to explore known and predicted interactions of chemicals and proteins which is based on literature and experiments[91–94].

UniProt (Universal Protein database) provides a freely accessible resource of protein sequence and functional information[78,79].
The implementation of toxicogenomics in the area of hepatotoxicity testing has advanced the understanding of the underlying molecular mechanisms of the different hepatotoxic classes[65]. In addition, this technique allows to extrapolate the findings to the human situation.

Aim and outline of this thesis

Aim of this thesis. The hepatotoxic potential of compounds and chemicals are traditionally assessed using *in vivo* rodent studies. Since these *in vivo* rodents studies are associated with scientific issues (limited predictivity for effects in humans), economical (high costs due to high doses and long experimental periods), and ethical (large numbers of animals to be exposed), there is a need to develop and validate alternative approaches. As such, the zebrafish embryo is presented as an alternative test model that may replace or support the traditional *in vivo* rodent studies. This zebrafish embryo model combines the benefits of an *in vivo* model, namely biological complexity including interactions between tissues and cells[49,54,95], with the advantages of *in vitro* models, that is, the ability for medium to high throughput testing. Therefore, the objective of this thesis is to evaluate the whole zebrafish embryo as an alternative model system to screen for the hepatotoxic potential of compounds using different "-omics" technologies including next-generation sequencing, transcriptomics, and proteomics, thereby improving the prediction for effects in humans. To achieve this objective, a dedicated set of approaches was applied in the studies schematically represented in Fig. 4 and outlined below.

Outline of this thesis. First, we evaluated whether the whole zebrafish embryo can be used for the determination of hepatotoxicity. In **Chapter 2**, we determined whether hepatotoxicity-associated gene expression was detectable in whole zebrafish embryos using next-generation sequencing.
To unravel the underlying molecular mechanisms, we investigated in **Chapter 3** whether gene expression analysis after hepatotoxicant exposure could produce a limited set of informative biomarkers for human hepatotoxicity. To characterize the model even further, we applied proteomics in **Chapter 4**, to strengthen the applicability of the model.
To assess the additonal value of the zebrafish embryo as a model for hepatotoxicity, we performed a meta-analysis based on gene-expression changes including different species in **Chapter 5**.
A general discussion and possible future perspectives are discussed in **Chapter 6** including discussion on the implementation of a better toxicokinetics characterization of the model, while a summary is provided in **Chapter 7**.

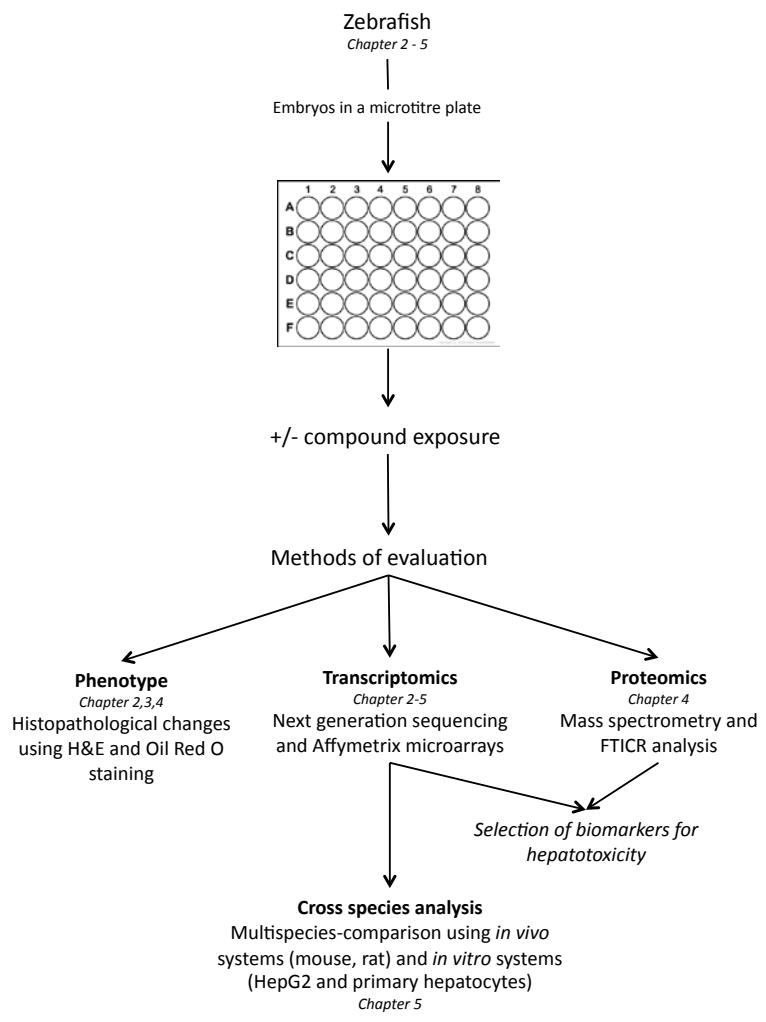

Figure 4 Schematic representation of experiments in this thesis.

2

Exploring the Zebrafish Embryo as an alternative Model for the Evaluation of Liver Toxicity by Histopathology and Expression Profiling

Marja Driessen, Anne S. Kienhuis, Jeroen L.A. Pennings, Tessa E. Pronk, Evert-Jan van den Brandhof, Marianne Roodbergen, Herman P. Spaink, Bob van de Water, Leo T.M. van der Ven

Archives of Toxicology (2013) May;87(5):807-23

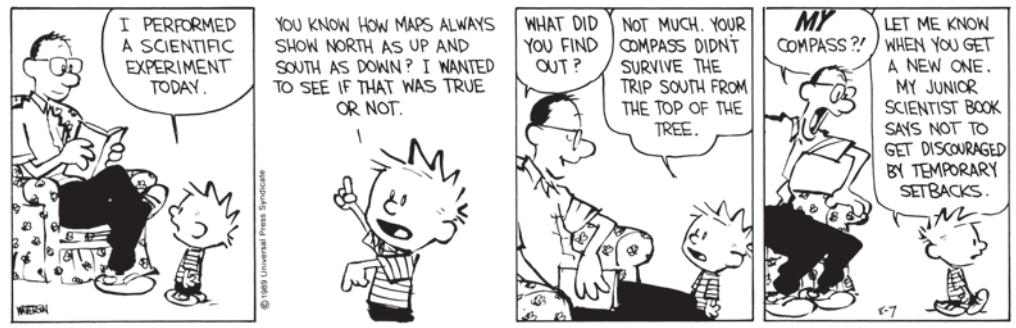

Abstract

The whole zebrafish embryo model (ZFE) has proven its applicability in developmental toxicity testing. Since functional hepatocytes are already present from 36-hours post fertilization (hpf) onwards, whole zebrafish embryo have been proposed as an attractive alternative to mammalian *in vivo* models in hepatotoxicity testing. The goal of the present study is to further underpin the applicability of whole zebrafish embryo for hepatotoxicity testing by combining histopathology and next generation sequencing-based gene expression profiling. To this aim, whole zebrafish embryo and adult zebrafish were exposed to a set of hepatotoxic reference compounds. Histopathology revealed compound and life-stage specific effects indicative of toxic injury in livers of whole zebrafish embryo and adult zebrafish. Next generation sequencing (NGS) was used to compare transcript profiles in pooled individual RNA samples of whole zebrafish embryo and livers of adult zebrafish. This revealed that hepatotoxicity-associated expression can be detected beyond the overall transcription noise in the whole embryo. *In situ* hybridization verified liver specificity of selected highly expressed markers in whole zebrafish embryo. Finally, cyclosporine A (CsA) was used as an illustrative case to support applicability of zebrafish embryo in hepatotoxicity testing by comparing CsA-induced gene expression between zebrafish embryo, *in vivo* mouse liver, and HepaRG cells on the levels of single genes, pathways and transcription factors. While there was no clear overlap on single gene level between the whole zebrafish embryo and *in vivo* mouse liver, strong similarities were observed between whole zebrafish embryo and *in vivo* mouse liver in regulated pathways related to hepatotoxicity, as well as in relevant overrepresented transcription factors. In conclusion, both the use of NGS of pooled RNA extracts analysis combined with histopathology, as well as traditional microarray in single case showed the potential to detect liver-related genes and processes within the transcriptome of a whole zebrafish embryo. This supports the applicability of the whole zebrafish embryo model for compound-induced hepatotoxicity screening.

Introduction

The liver is a critical target for xenobiotic-induced toxicity, and drug-induced liver injury is a major contributor in attrition of drugs in pre-clinical development. A first factor in hepatic susceptibility is that active hepatic processing leads to high intracellular concentrations of xenobiotics. Secondly, hepatocellular biotransformation of xenobiotics, which normally protects against the direct-acting toxicity through inactivation and facilitation of excretion, may also lead to reactive metabolites that are more toxic than the parent compound, resulting in liver cell injury[4]. Xenobiotic-induced hepatotoxicity occurs through different mechanisms associated with distinct histopathological and clinical phenotypes, including cholestasis, steatosis and necrosis, which will be further referred to as nominal phenotypes. These pathological conditions represent the consequences of respectively impaired hepatocellular bile excretion, triglyceride accumulation resulting from disruption of fatty-acid oxidation, and hepatocellular cell death[4]. Traditionally, histopathology and clinical chemistry are used to detect hepatotoxic properties of chemicals in *in vivo* rodent studies. Such studies require high numbers of animals, interfere with animal welfare, and are associated with high costs and are not always predictive for the human situation. Therefore, alternative test systems are needed to improve predictivity, and to contribute to reduction, refinement and replacement of *in vivo* rodent studies.

Following this necessity, several alternative methods to monitor liver injury have been proposed, including liver slices[96], cultured primary hepatocytes[97,98], and continuous cell lines, particularly the human hepatoma derived HepG2 line[99,100] and the more recently derived human hepatocyte HepaRG line[40]. However, these *in vitro* systems each have their limitations related to their reductionistic nature and to loss of functionality compared to the liver *in vivo*[101].

The zebrafish (*Danio rerio*) is a widely used model organism to study human biology and pathology, because physiological and molecular functions at the organ and cell level are highly comparable between the zebrafish and humans[44]. Consequently its value in the area of toxicology testing as well as drug discovery has also been recognized, making it a potentially important alternative for *in vivo* testing in rodents[102]. The zebrafish has several experimental advantages such as its short life cycle, accessibility and availability, and the power to generate high numbers of embryos easily, which makes the model suitable for high throughput testing. Moreover, the zebrafish genome is completely sequenced and a wide variety of genetic, molecular and cellular manipulation tools are available[103].

As a particular refinement, the use of the whole zebrafish embryo (ZFE) is advantageous since the early embryo is considered not to perceive pain or otherwise discomfort. According to legislation[104], whole ZFE can be considered as an alternative model system and it is already applied for studying chemical toxicity using developmental and lethality endpoints[47,66]. In contrast to *in vitro* cell cultures, *in vivo* cell type and organ interactions are maintained in the whole zebrafish embryo. These aspects may contribute to a better representation of hepatotoxic responses that occur *in vivo*.

From a hepatotoxicity testing perspective, the liver in the zebrafish embryo is fully functioning with active drug metabolism at 72-hpf[105]. A few promising studies showed that zebrafish embryos are suitable to detect human hepatotoxicants. In a study by Jones *et al.*, the whole zebrafish embryo model was evaluated through morphological endpoints after exposure to a set of compounds including drugs which were falsely identified by the HepG2 cells. In this design, whole zebrafish embryo successfully detected more hepatotoxicants with higher specificity than the HepG2 cells[49]. In another study, Amali *et al.* carried out histopathological, molecular and biochemical analysis in zebrafish embryo exposed to a single dose of thioacetamide and showed that the whole zebrafish embryo model is suitable to detect steatohepatitis[57]. These descriptive studies certainly indicate the potential of the whole zebrafish embryo model for hepatotoxicity testing, but further validation of the model is needed. A potential addition in this perspective is toxicogenomics, as it enables detailed analysis of the underlying mechanisms of cellular responses upon xenobiotics exposure. The most practical way to study hepatic gene expression in zebrafish embryo is to use whole zebrafish embryo RNA extract for analysis, instead of liver extracts, but this may result in masking of signals or lowering the signal/noise ratio of the regulated genes. Although available, sophisticated methods such as micro-dissection to study hepatic gene expression in small organism hinder the throughput of the system[73].
The main objective of this study was to further substantiate the applicability of whole zebrafish embryo as a model for testing hepatotoxicity by combining histopathology with toxicogenomics, by means of next generation sequencing (NGS)-based gene expression profiling. To this end, histopathology in the zebrafish embryo and adult zebrafish liver was studied after exposure to a set of hepatotoxic reference compounds to confirm hepatocellular pathology and to extrapolate between developmental stages. Subsequently, induction of hepatoxicity relevant genes was analyzed in a single RNA pool composed from a set of whole zebrafish embryo and adult zebrafish liver, individually exposed to one out of a range of reference hepatotoxicants, using NGS. The use of such a single combined pool of RNA is a cost-effective way to obtain robustly expressed transcripts after treatment with compounds of a similar toxicity class[106]. The advantage of NGS is that, in contrast to expression arrays, it does not build on sequence- specific probe hybridization and does not suffer from background and cross-hybridization problems. Furthermore, it provides an absolute measure of all transcripts, not just the relative abundance in an array selection, enabling to assess the whole transcriptome[107]. The zebrafish embryo and adult zebrafish liver transcriptomes were then compared to reveal whether hepatotoxicity associated signals, as present in the overlap between zebrafish embryo and adult liver, can be detected in the noise of other tissues that contribute to the whole zebrafish embryo RNA. Highly expressed markers in zebrafish embryo were confirmed for liver specificity through *in situ* hybridization. Further analysis of the transcriptome was on regulation of pathways related to liver toxicity. General conclusions on hepatotoxic responses in the zebrafish embryo were verified in a dedicated case, i.e. cyclosporine A (CsA), where zebrafish embryo data was compared with available data from *in vivo* mouse liver and from the HepaRG cell line, at the levels of single genes, pathways, and transcription factors. Pathway and transcription factor-based analyses attractively leveled out differences between models due to species variation, model sensitivity and power.
Altogether, using pooled RNA extracts in NGS analysis combined with histopathology, followed by case-directed traditional microarray, we supportively demonstrate the applicability of the whole zebrafish embryo model for toxicogenomics-based compound-induced hepatotoxicity screening.

Materials and Methods

Materials. Exposure studies were performed with reference compounds known to induce nominal hepatotoxic phenotypes in humans (cholestasis, steatosis and necrosis; Table 1). All test chemicals were purchased from Sigma Aldrich (Zwijndrecht, the Netherlands), and included acetaminophen or paracetamol (N-actyl-para-aminophenol; APAP, CAS no.103-90- 2), paraquat (1,1'-Dimethyl-4,4'-bipyridinium dichloride, PQ, CAS no.1910-42-5), thioacetamide((CH3-C(S)NH2); TA, CAS no.62-55-5), amiodarone hydrochloride (2-butyl- 3-benzofuranyl-4-[2-(diethylamino)ethoxy]-3,5-diiodophenyl ketone hydrochloride; AM, CAS no.19774-82-4), valproic acid (2-propylpentanoic acid sodium; VPA, CAS no.1069-66- 5), tetracycline (TET, CAS no.64-75-5), cyclosporine A (CsA, CAS no.59865-13-3),17α- ethinyl-estradiol (17α-Ethinyl-1,3,5(10)-estratriene-3,17β-diol; EE2, CAS no.57-63-6) and chlorpromazine (2-Chloro-10-(3-dimethylaminopropyl)phenothiazine hydrochloride; CPZ, CAS no.69-09-0), tricaine methansulfonate (MS-222; CAS no. 886-86-2). Dimethylsulfoxide (DMSO, CAS no. 67-68-5) was ordered from Fisher-Scientific. The RNeasy MinElute Cleanup kit (Cat. No. 74204) and the QIAzol Lysis reagent (Cat. No. 79306) were obtained from Qiagen Benelux B.V. (Venlo, the Netherlands). Phase-lock Gel Heavy (Cat. No. 2302870) and the metal micro pestle (P985.1) were purchased from VWR International B.V. (Amsterdam, the Netherlands).

Zebrafish. Wild-type zebrafish (*Danio rerio*) were originally obtained as commercially bred Singapore import (Ruinemans Aquarium BV, Montfoort, The Netherlands), which were maintained and bred in our facilities for more than 5 generations. Adult zebrafish (aZF) used in this study were approximately 14 months of age. For generation of zebrafish embryos, two male and two female adulte zebrafish were set together one day before spawning, after a period of four day separation to improve egg production. The breeding tank was constructed to prevent egg predation and after spawning, a glass siphon was used to collect the eggs. All eggs were checked for fertility and thereafter pooled in a single petri dish containing Dutch Standard Water (DSW; demineralized water supplemented with $NaHCO_3$ (100 mg/l), $KHCO_3$ (20 mg/l), $CaCl_2 \cdot 2H_2O$ (200 mg/l), and $MgSO_4 \cdot 7H_2O$ (180 mg/l) aerated for 24h at 27°C) until the start of the exposure.

Table 1 Reference compounds.

Compound	Nominal phenotype	Test concentrations (µM)[1]	Vehicle control
Chlorpromazin (CPZ)	Cholestasis	3 - 1 - 0.3[2]	DMSO[3]
Cyclosporin A (CsA)	Cholestasis	6 - 2 - 0.7	DMSO
17α-ethynylestradiol (EE2)	Cholestasis	3.5 - 1.2 - 0.4	DMSO
Amiodarone (AM)	Steatosis	10 - 3.3 - 1.1	DMSO
Valproic acid (VPA)	Steatosis	600 - 200 - 67	DSW[4]
Tetracycline (TET)	Steatosis	200 - 66.7 - 22.2	DMSO
Acetaminophen (APAP)	Necrosis	660 - 220 - 73.3	DMSO
Paraquat (PQ)	Necrosis	3,000 - 1,000 - 330	DSW
Thioacetamide (TA)	Necrosis	10,000 - 3,333 - 1,111	DSW

[1] Test concentrations of the reference compounds for transcriptomics and histopathology
[2] aZF were exposed to a different range of CPZ, i.e. 1 - 0.3 µM - 0.1 µM.
[3] Compounds initially dissolved in DMSO and diluted further in DSW with a final DMSO concentration of 0.2% v/v. DSW and DMSO 0.2% v/v were included as vehicle controls.
[4] Dutch Standard Water, demineralized water supplemented with $NaHCO_3$ (100 mg/l), $KHCO_3$ (20 mg/l), $CaCl_2 \cdot 2H_2O$ (200 mg/l), and $MgSO_4 \cdot 7H_2O$ (180 mg/l) aerated for 24h at 27 °C.

Exposure conditions. All zebrafish embryo exposures started at 3 days post fertilization (3dpf) with embryos which were randomly derived from at least 2 spawning units. Exposures were performed in 48-well plates (BD Biosciences) containing 1 ml of test medium per well. Exposures were performed in an incubator at 26.5 ± 1°C in a static way, and lasted for 48 hrs. Concentrations for the expression study were defined in a range finding study conducted with zebrafish embryo, where respectively 6 and 7 exposures were tested for DMSO and water diluted compounds, with 12 zebrafish embryos per condition, each embryo in a single well. The exposures in the expression study were conducted with three concentrations (Table1), where the highest concentration was defined as the no effect concentration in zebrafish embryo (no mortality or teratogenicity) in the range finding study. Each concentration was performed in five replicate units, where each unit had 15 embryos (three wells each with five embryos). Each plate was set up to have 6 vehicle control wells. After exposure, the 15 embryos of each replicate unit were sampled in a single tube and snap frozen in liquid nitrogen.
aZF were transferred to the static test system 3 days prior to testing for acclimatization, and this consisted of full-glass aquaria containing three liters of DSW covered by a glass plate. The water was continuously aerated and ambient conditions were daily monitored. The temperature was kept at 27 ± 2 °C, pH between 7.4 to 9.0, and oxygen > 7.10 mg/l at all times. The light/dark cycle was 14 hours light and 10 hours dark. Each experimental group consisted of four male zebrafish. Test concentrations and exposure duration were as for zebrafish embryo (except CPZ; Table 1). After the exposure, the zebrafish were euthanized with a solution of 100 mg/l MS-222 buffered with sodium bicarbonate. Following decapitation, the fish were slit ventrally from heart to anus and livers were dissected and snap frozen in liquid nitrogen zebrafish embryo and aZFL samples were stored at -80°C until RNA extraction.
Experiments with adult zebrafish were approved by the RIVM Animal Experimentation Ethical Committee and carried out in accordance with relevant Dutch national legislation, including the 1997 Dutch Act on Animal Experimentation.

Histopathology. For histopathology, zebrafish embryo were sampled from three highest concentrations without mortality or teratogenicity of the concentration range finding study and adult zebrafish livers were dissected from adult fish exposed in the expression study. Whole zebrafish embryo and aZFL were fixed in 4% paraformaldehyde for 24 hrs, then transferred and stored in 70% ethanol until use. Samples were first embedded in a specially designed 1% agarose mold for adequate positioning of the embryos[108,109], and then transferred to paraffin, whereafter 4 µm sections were routinely stained with hematoxylin and eosin (H& E) and covered with a glass coverslip. Additional cryosections from AM, VPA and TET were stained with Oil Red O to determine fatty droplet accumulation in zebrafish embryo and aZFL. Furthermore, in aZFL, additional sections from CPZ, EE2 and CsA were stained with Fouchet staining to detect bile accumulation. For the aZFL only one replicate per compound was included. As for the zebrafish embryo, approximately 12 replicates were included per compound.

RNA isolation and processing. Total RNA was isolated using the MinElute Clean up kit according to the protocol of de Jong *et al.,*[110]. RNA concentration was measured spectrophotometrically (ND1000; NanoDrop technologies, Wilmington, DE) and RNA integrity was assessed using Bioanalyzer 2100 (Agilent Technologies, Amstelveen, the Netherlands). All samples contained intact total RNA with RNA Integrity Number (RIN) > 8. To reduce cost of NGS, RNA extracts of all zebrafish embryo of the highest exposure concentration of each compound were combined to a single pool. This is justified because our primary interest was in responsiveness potency of the zebrafish embryo, not in effects of single compounds, and pooling of samples has analytical advantages (see Discussion). We added control samples to be able to pick up any transcripts that are highly expressed in control conditions and down regulated in samples treated with liver toxicants, although, these transcripts may be harder to detect because they now have their highest expression level only in a minority of the pooled samples (2 control samples versus 9 hepatotoxicants). A pool contained 500 ng/µl RNA, with equal quantities derived from approximately 45 embryos per compound (Fig.1). A similar RNA pool was prepared from three adult zebrafish livers per compound at the same concentration.

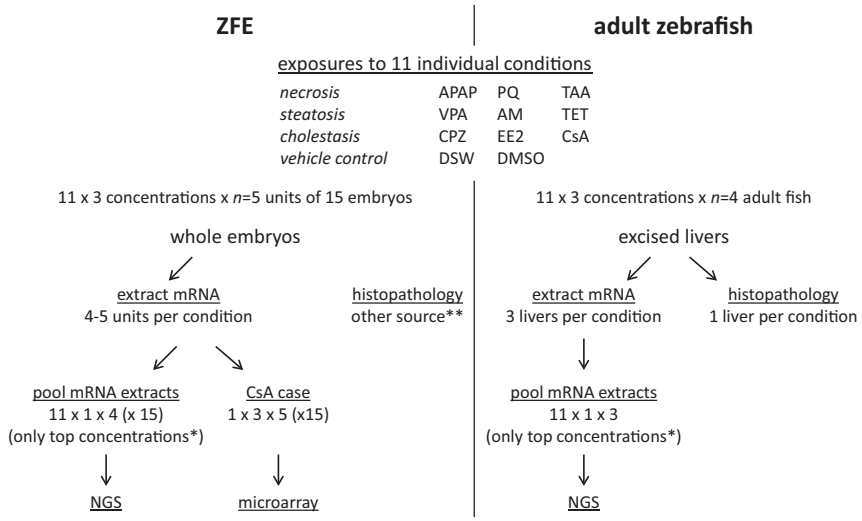

* The 2 lower concentrations were for contingency in case of toxicity in the top concentration, and could be included in the CsA case study.
** Embryos for histopathology were sampled from the concentration range finding study.

Figure 1 Study design for next generation sequencing analysis.
Each pool contained 500ng/µl total RNA, consisting of equal absolute quantities of total RNA from each exposure to the highest concentration of each compound

RNA NGS sequencing. NGS sequencing was performed by BaseClear B.V. (Leiden, the Netherlands) using the Illumina GAII instrument. RNA seq libraries were made from 10 µg total RNA for each pool using the Illumina mRNA-Seq Sample Preparation Kit according to manufacturer's instructions (Illumina, Inc., San Diego). In brief, this included purification of the RNA, fragmentation through divalent cations under elevated temperatures, followed by cDNA synthesis. Next, adaptors were ligated and the product was again purified and then amplified. A quantity of 4 pmol of each library was transferred to a flow cell, there again amplified to produce clusters of fragment copies, which were then paired end sequenced with a read length of 51 nucleotides. Fragments in a cluster were sequenced twice (forward and reverse), ensuring highly accurate alignment of the reads. Paired end sequences can be considered as technical duplicates, to control for reliability of the procedure. The Illumuna system is based on fluorometric image analysis, in which base calling and tag counting were performed using the Illumina pipeline. The sequence reads were mapped to the reference genome (Ensemble, Zv8, Release 59, August 2010) using the CLC Genomics Workbench (version 4.0.3., October 28, 2010).

GeneChip hybridization. For control and CsA , RNA samples were used as produced for the RNA NGS sequencing (Fig. 1). Sample labeling and hybridization to Affymetrix GeneChip zebrafish ST Genome Arrays were performed by ServiceXS B.V. (Leiden, the Netherlands). The Ambion WT Expression kit (#4411974) was used to synthesize labeled sense stranded cDNA starting from 100 ng total RNA. The minimal yield of the cRNA product is 10 µg. The Affymetrix Terminal Labeling Kit (901524) was used to perform the fragmentation and terminal labeling step using 5.5 µg of the ss cDNA. The concentration and the quality of the cRNA and fragmented ss cDNA samples were assessed using the Nanodrop and the BioAnalyzer. A total amount of 2.9 µg (25 ng/µl) fragmented ss cDNA was finally utilized for the hybridization on the Affymetrix Zebrafish ST Array. The Ambion WT Wash and Stain Kit for GeneTitan Hybridization (#901622) was used for the hybridization, washing, staining and scanning of the chips. The entire experimental procedure was carried out according to ServiceXS Standard Operating Procedures (SOPs) which have been validated for use with the Affymetrix kits and GeneChips and Array Plates and are completely compatible with the Affymetrix protocols.
The software program Affymetrix GeneChip Command Console (v3.2) was used for fully automated operation of the Affymetrix fluidics stations, which process the washing and staining of the cartridges. After scanning, the array images (DAT files) as well as the correct alignment of the grid were inspected using the program Affymetrix Command Console Viewer software.

Data analysis. In the NGS output file, transcripts were quantified to reads per kilobase of exon model per million mapped reads (RPKM) values, which are expression values corrected for library size and transcript length. These RPKM values were calculated with the CLC Genomics Workbench software[111]. Previous RNA NGS studies of zebrafish embryos indicated that this technique is extremely sensitive and can even detect gene expression at levels that are hard to detect with other high density technologies such as microarrays[112–114]. On the other hand, at extremely low expression levels, exact quantification and reproducibility are often impaired. We therefore used a filter level to exclude unreliable values. Based on previous experience (unpublished results), this filter level was set at an RPKM of 0.12 and only genes with a higher RPKM value were included in the analyses. Statistical analyses were carried out using the R statistical software environment (http://www.r-project.org). To investigate the expression of genes associated with hepatotoxicity, gene lists were made using a text-mining tool (Anni2.1, April, 2010)[115]. This tool provides an interface to Medline and retrieves associations for several classes of biomedical concepts. For determining the relevance to the applied search term, every concept is given a concept weight. The used search terms were 'hepatotoxicity' and 'heart-, eye-, brain development', and were based on human data. As a specificity threshold, the maximum value of the multiple search terms combined should exceed 0.01. Functional overrepresentation analysis was performed using the software program PathVisio2 (2.0.11, February,

2011)[116]. A pathway was considered 'overrepresented' when the *Z score* was greater than two and the minimally required number of changed genes was set at two. Pathways were retrieved from Curated collection of Pathways[117], Kyoto Encyclopedia of Genes and Genomes (KEGG), and manually curated collection of Pathways (MC). BLAST was employed to search for homologs of the hypothetical transcripts against the NCBI Non-Redundant database. This procedure was used to assign hypothetical transcripts with a functional annotation, based on protein sequence similarity.

All Affymetrix Cell Intensity Files (*.cel) generated for each Genechip using the Affymetrix GeneChip Command Console (v3.0) software were normalized using the Robust Multichip Average (RMA) algorithm. For all systems, the data was annotated with a MBNI custom CDF specifically designed for the chips (http://brainarray.mbni.med.umich.edu/Brainarray/Database/CustomCDF/CDF/)[118]. Mouse liver expression data were obtained from an exposure study of Kienhuis *et al.*[119], where the mice were exposed to a dose of 26.6 mg/kg b.w. of CsA for 11 days. Expression data of HepaRG cells exposed for 12 hrs to 300 µM was obtained from Jennen *et al.*[120], EBI ArrayExpress (http://www.ebi.ac.uk/microarray-as/ae/) with accession number E-MEXP-2458. All gene expression signals were Log_2 transformed before calculations were performed.

In the CsA case study, comparisons were performed on the level of single significantly expressed genes, pathways and enriched motifs for transcription factors. Significantly expressed genes were selected in whole zebrafish embryo, *in vivo* mouse liver, and the *in vitro* cell line using ANOVA performed over different exposure conditions (concentrations, doses, time- points) with an FDR cut-off of 0.05, 0.1, and 0.01, respectively. Comparison of regulated pathways between the whole zebrafish embryo, mouse *in vivo* and the cell line was done using the T-Profiler software, which enables a threshold and parameter free analysis of genome-wide expression patterns[83]. The input for T-Profiler consisted of individual samples of the three models. After pathway calculation the enrichment score, that is the *t-value*, was averaged per condition per model. Heatmaps are produced using the GeneMaths XT Software (Version, Applied Maths NV). Transcription factor enrichment analysis was performed using the significant genes in whole zebrafish embryo, *in vivo* mouse liver and the *in vitro* cell line.

Transcription factor binding motifs associated with the significant genes were determined using the C3 dataset, which contains transcription factor binding motifs found 2kB up- or downstream of target genes[121]. For optimal retrieval, the zebrafish and mouse gene IDs were converted to their human homologues by using the homologene dataset of the NCBI. To determine which transcription factors binding motifs were present significantly more than random in the gene sets, a random permutation test was applied using a cut-off value of $p < 0.01$. As an additional criterium the transcription factor binding motifs should be found by at least four genes in the set. To calculate the probability of overlap of the transcription factor binding motifs between models, the phyper package in R was used.

RNA probes. Anti-sense RNA probes were designed using Primer-BLAST from the NCBI website[122] based on the complete RefSeq sequence of the gene of interest. Primers were ordered by Invitrogen (Life Technologies, Breda, the Netherlands) and are summarized in Table 2. Primers were used for an RT-PCR with the Titan One Tube RT- PCR System (Roche Applied Science). This PCR product was purified with the QIAquick PCR purification kit (Qiagen, Venlo, the Netherlands) and a nested PCR was then conducted to amplify the PCR product. A synthesis step using T3 and T7 polymerase promoters was then performed to generate DIG-labeled RNA probes.

Table 2 Primer sequences for *in situ* hybridization.

Primer	Strand	PCR	Sequence
fabp10	Forward	1st PCR	AGCGGGACGTGGCAGGTTTAC
fabp10	Reverse	1st PCR	CCTCCGACTGTCAGCGTCTCCAC
fabp10	Forward	Nested PCR	CTCAGAGCCATCTCTCTGCCAGA
fabp10	Reverse	Nested PCR	CCTGGATGTGGGAGAATCGGTCA
pparγ	Forward	1st PCR	GACGTTTGGCTGGCCCGTGG
pparγ	Reverse	1st PCR	CAGGAACAGCGCCATGTCGCA
*pparγ**	Forward	Nested PCR	GAAGATCCGTCTTCATCCTCAC
*pparγ**	Reverse	Nested PCR	GATCTGTCCGTAGGAGATCAGG
zgc:193613	Forward	1st PCR	TGGGCACAGGAATGGCCCGT
zgc:193613	Reverse	1st PCR	TGGACACACAGCTGTCAGATTGGT
zgc:193613	Forward	Nested PCR	TCAAGAGGCTTGTCAATGCTTGGG
zgc:193613	Reverse	Nested PCR	TTCCCTGGGGCAGTACGGTGT
wu:fj16a03	Forward	1st PCR	TTCCAACTTGCTGAACATCCGTGAA
wu:fj16a03	Reverse	1st PCR	ATGTTGCTGCATTGCTGTCGGAT
wu:fj16a03	Forward	Nested PCR	TGTTCCTGCTGCTGCCTGTCTG
wu:fj16a03	Reverse	Nested PCR	AGCATTTCCAGCCTTTCTTCTCGC

* Primer set from literature[123]

***In situ* hybridization.** Whole mount *in situ* hybridization was performed following a protocol adapted from Thisse *et al.*[124]. ZFEs were collected at 5-dpf and fixed overnight in 4% paraformaldehyde. After fixation zebrafish embryos were washed 2 times in 1x PBS, bleached in 3% H_2O_2/0.5% KOH solution to remove pigment and washed in 1x PBS. Following bleaching, the zebrafish embryos were dehydrated in a graded methanol/PBS series and stored in 100% methanol at -20°C. Before *in situ* hybridization zebrafish embryos were rehydrated with 50/50 PBS/MeOH for 5 min, washed 4 times for 5 min with PTW

(1x PBS, 0.1 % Tween20) followed by 40 min incubation in 5µg/ml proteinase K in PTW at 37°C. Embryos were fixated again in 4% paraformaldehyde, followed by 5 times 5 min wash in PTW. Until here, all the washing steps were performed in 24-well plates using small baskets made from 15 ml tubes with a nylon mesh melted to its opened bottom end. After this, the embryos were transferred to transparent 4 ml screw cap vials and prehybridized in hybridization buffer (50% deionized formamide; 5x SSC; 500 µg/ml tRNA; 50 µg/ml heparin; 0.1% Tween20; pH 6.0 with 1M citric acid) for 3 hrs at 70°C. The buffer was then replaced by fresh hybridization buffer (pre-heated for 5-10 min at 70°C) containing digoxigenin labelled RNA probe and incubated overnight at 70°C. After hybridization the embryos were washed twice at 70°C for 20 min with respectively 50% hybridization buffer (without tRNA and heparin)/50% 2xSSC; and 2xSSC. Then the zebrafish embryo were washed twice with 0.2xSSC for 60 min, followed by 5 min washes at room temperature with 50% PBT (PTW with 2% sheep serum and 0.2% BSA)/50% 0.2xSSC and finally 100% PBT. The embryos were incubated at room temperature while shaking with PBT for 3 hrs, followed by incubation overnight at 4°C with anti-DIG antibody solution diluted at 1/2000 with PBT under gentle agitation. The embryos were subsequently washed 6 times 15 min each with PBT at room temperature. Embryos were transferred to a 24-wells plate and washed 4 times for 20 min with staining buffer (100 mM Tris pH 9.5, 50 mM MgCl2, 100 mM NaCl, 0.1% Tween 20, 5 mM levamisole). The first of these washing steps was done with staining buffer without MgCl2. Embryos were stained with 20mL/ml NBT/BCIP staining buffer until an optimal signal was obtained. The staining reaction was stopped by three washes in 0.5 ml PTW, followed by overnight fixation in 4% paraformaldehyde at 4°C. Embryos were subsequently washed 3 times in 0.5 ml PTW and transferred to 100% glycerol, placed on a rocker and agitated gently overnight at room temperature in the dark, mounted in 100% glycerol and observed and photographed microscopically.

Results

Hepatotoxicant-specific liver pathology in zebrafish embryo and adult zebrafish liver. Histopathological examination in the whole zebrafish embryo and aZFL was conducted after 48 hrs of exposure to the model compounds. In H&E staining, hepatocytes of the control adult zebrafish showed a similar morphology as mammalian hepatocytes (Fig. 2a-b). Although the liver as a whole did not show the obvious lobular structure which is present in mammals, substructures such as bile canaliculi could be discerned (Fig. 2b, arrow). Hepatocytes in the control embryos showed a more open cytoplasm, although with varying degrees, indicative of varying levels of glycogen contents (Fig. 3a-b). After 48 hrs of exposure, cholestasis was a remarkably frequent observation in aZFL, with a high incidence in nominal cholestatic compounds (CPZ, EE2, CsA), but also with most of the non-cholestatic compounds (Table 3). Cholestasis appeared as intracellular and intra-

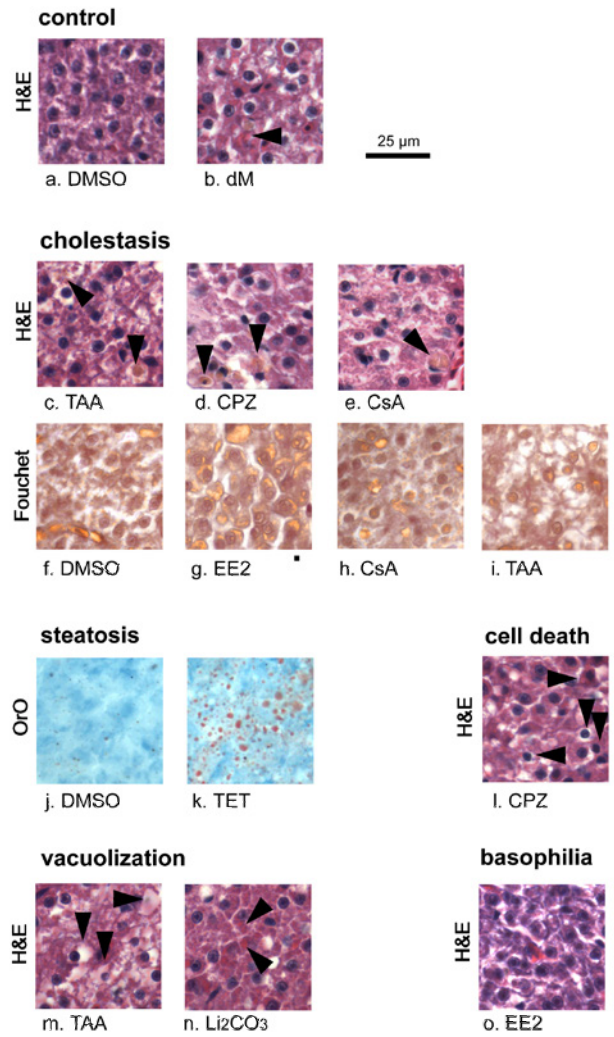

Figure 2 Microphotographs illustrating of various observations.
Reference histology in control (a); arrowhead indicates bile canaliculus. Cholestasis is shown in H&E (b-d) and Fouchet staining (e-h). Arrowheads in b, c intracellular cholestasis, in d, intracanalicular cholestasis. Corresponding intracellular and intracanalicular cholestasis with Fouchet staining are shown in f and g, respectively; additional intranuclear cholestasis in h. Steatosis is shown with Oil red O staining in j, absence of OrO is shown in i. Cell death is indicated by chromatin condensation and eosinophilic cytoplasm (arrowheads in k). Arrowheads in l, chromophobic vacuolization, arrowheads in m, eosinophilic cytoplasm inclusions; n, basophilic cytoplasm. Compound abbreviations are explained in Table 1. Size bar refers to all microphotographs.

Table 3 Histopathological observations in ZFE and aZFL.

	Embryo Liver									Adult Liver									Illustration in Fig.
	Cholestasis			Steatosis			Necrosis			Cholestasis			Steatosis			Necrosis			
	CPZ*	CsA	EE2*	AM	VPA	TET	APAP*	PQ	TAA	CPZ	CsA	EE2	AM	VPA	TET	APAP	PQ	TAA	
n	*7*	*3*	*12*	*6*	*6*	*5*	*10*	*5*	*8*	*3*	*3*	*3*	*3*	*3*	*3*		*3*	*3*	
Cholestasis (H&E)	-	-	-	-	-	-	-	-	-	2	1	3	-	-	-	-	1	3	1c-1e
Cholestasis(Fouchet)											cn	cp						in	1f – 1i
Lipid vacuoles (H&E)	6	-	-	6	6	-	-	-	-	-	-	-	3	3	3	-	-	-	2c-2e
Oil-Red-O (cryosections)				6	6	5							3	3	3				1j-1k
Chromatin condensation	2	-	11	-	-	-	-	2	-	-	-	-	-	-	-	-	-	-	1l
Chromophobic vacuolization	-	1	8	-	-	-	-	-	-	-	3	-	-	-	-	-	-	3	2f-2g 1m-1n
Eosinophilic vacuolization	4	2	-	-	-	-	-	3	5	1	2	3	-	-	-	-	3	-	2h
Cytoplasmic basophilia	4	-	-	-	-	5	7	-	-	-	-	3	-	-	-	-	-	-	1o

Observations are qualitative, *i.e.* without considering severity or intensity of effects, and without considering concentration dependency of effects. Cn, canalicular; cp, cytoplasmatic; in, intranuclear; * CPZ, EE2 and APAP showed remarkable vacuolization in the intestinal epithelium. Empty cells indicate not tested. - sign indicate no observation

canalicular brown pigment accumulation in H&E staining (Fig. 2c-e), and these subtypes were confirmed by Fouchet staining (Fig. 2g-h, compared with control in 2f). In addition, with TAA, Fouchet staining was confined to the nuclei (Fig. 2i). Cholestasis was not observed in zebrafish embryo. Lipid vacuoles as a mark of steatosis were not observed in aZFL, but well discernible in zebrafish embryo with two of the nominal steatotic compounds and one nominal cholestatic compound (Fig. 3c-e). However, Oil Red O staining also revealed lipid droplets in aZFL, with nominal steatotic compounds (illustrated for TET in Fig. 2k, compare with control in 2j). Necrosis did not show in either aZFL or zebrafish embryo, i.e. not in a zonal pattern as can be observed in mammal liver. On the other hand, marks of cell death, particularly chromatin condensation and cytoplasmic eosinophilia, were observed in both aZFL (Fig. 2l) and zebrafish embryo with some compounds, although without much consistency between life stages and clearly more compound than class specific. Additional observations were chromophobic and eosinophilic vacuolization, which occurred in aZFL and zebrafish embryo (Fig. 2m-n, Fig. 3f-h), mainly coinciding with nominal cholestatic and necrotic compounds (Table 3); and cytoplasm basophilia, in aZFL only observed with EE2 (Fig. 2o) and in zebrafish embryo with CPZ (Fig. 3c).

Overall assessment of all exposed animals indicated that simple histopathological effects were mainly observed with nominal steatotic compounds, and that complex histopathology effects were present in most nominal cholestatic and necrotic compounds (Table 3). Furthermore, serial sections of the whole zebrafish embryo revealed additional histopathology in the intestinal epithelium, which showed vacuolization after exposure to CPZ, EE2 and APAP (Table 3). Histopathological observations are summarized in Table 3, without considering the xenobiotic concentration conditions.

Next generation sequencing of the whole zebrafish embryo and adult zebrafish liver transcriptomes. Next-generation RNA sequencing was used to compare the transcriptomes of adult zebrafish liver and whole zebrafish embryo. A number of 21914 transcripts were sequenced from zebrafish embryo (Fig. 4a, blue and yellow area) and 16459 transcripts from the adult zebrafish liver (Fig.4a, blue and green area). There were 15801 overlapping transcripts (Fig. 4a, blue area). These three areas can also be distinguished when comparing relative expression (RPKM values) between zebrafish embryo and adult zebrafish liver (Fig. 4b). Here, the grey diagonal (Fig.4b) separates transcripts that are more highly expressed in the whole zebrafish embryo (above) from those that are more highly expressed in the adult zebrafish liver (below).

PathVisio2 was used to identify overrepresented biological pathways and processes from the uniquely expressed transcripts in zebrafish embryo (6113 transcripts, Fig.4a-b, yellow area) and adult zebrafish liver (658 transcripts, Fig.4a-b, green area). zebrafish embryo thus showed overrepresentation in developmental processes, signaling pathways and in other

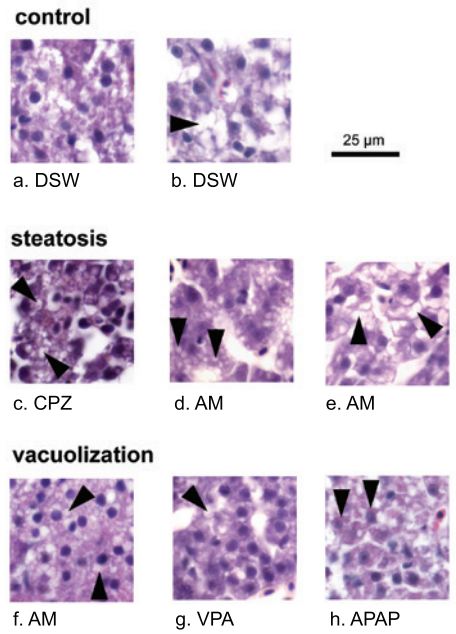

Figure 3 Hepatotoxicant-specific liver pathology in whole zebrafish embryo.
Microphotographs are illustrations of various observations recorded in Table 3. Reference histology in controls (a,b); arrowhead indicates irregular unstained area indicitive of glycogen storage. Lipid vacuoles of varying sizes (arrowheads) as observed in H\&E are illustrated in c-e (small in c-d, larger in e). Arrowheads in f and g indicated chromophobic vacuolization, and eosinophilic inclusions in h.

pathways not obviously related to the liver. In adult zebrafish liver, overrepresented pathways were mainly found in the immune and intracellular processes (Table 4). It should be noted that due to nature of the experimental setup and the pooling of all individual samples that regulation of neither adaptive or toxicity pathways nor of transcription factors can be attributed to any individual of our hepatoxicants.

Hepatotoxicity-associated gene expression in the exposed zebrafish transcriptomes.
Next, to discover whether transcripts related to either human hepatotoxicity or development were expressed in exposed whole zebrafish embryo or adult zebrafish liver, we performed text mining using an automated search strategy (Supplementary Table 1 for hepatotoxicity, supplementary Table 2 for development).
Transcripts specific for hepatotoxicity were evenly distributed in both pooled zebrafish embryo and adult zebrafish liver samples and mainly located in the set of overlapping genes (Fig. 4b, red squares, n=127, and explained in supplementary Table 3). Furthermore,

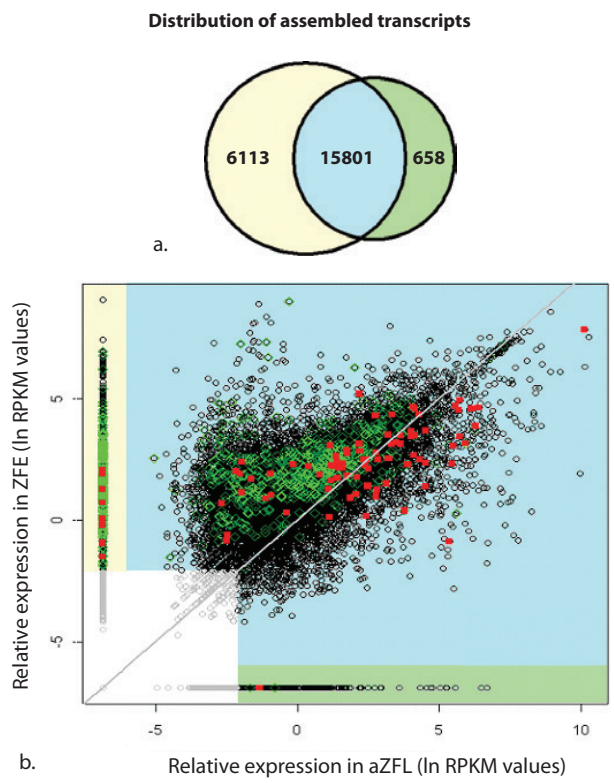

Figure 4 Expression comparison of hepatotoxicity-associated genes and development specific genes for the adult zebrafish liver and zebrafish embryo.
a. Venn diagram showing the number of expressed transcripts per experimental pool and the overlap of these expressed transcripts after exposure to a set of model hepatotoxicants. **b**. Black circles represent genes that were neither related to hepatotoxicity nor involved in development of heart, eye and brain based on the results of the text-mining. Grey circles represent genes that were not included in the analysis due to their RPKM expression below 0.12. Green diamonds indicate genes associated with development, red squares indicate genes associated with hepatotoxicity. Colored areas indicate model specificity of transcripts: green area only expressed in adult zebrafish liver (658), yellow area only expressed in whole zebrafish embryo (6,113), blue area expressed in both model systems (15,801). White shaded area indicate transcripts not involved in analysis (color figure online).

Table 4 Biological pathways and processes in the subset of uniquely expressed transcripts in ZFE and aZFL. Pathways were "overrepresented" when the Z score was > 2 and the minimally required number of changed genes ≥ 2.

Biological System	Pathway	ZFE	aZFL
Development	Neural Crest Development	10.8	-
	Canonical wnt - zebrafish	6.9	-
	Noncanonical wnt Pathway	5.0	-
	Wnt Signaling Pathway	2.6	-
	Endochondral Ossification	2.0	-
	Hedgehog Signaling Pathway	3.9	2.0
	Melanogenesis	4.8	-
	BMP Signaling Pathway	2.8	-
Muscle Systems	Vascular Smooth Muscle Contraction	2.0	-
	Calcium Regulation in the Cardiac Cell	6.4	-
	Striated Muscle Contraction	3.1	-
	Cardiac Muscle Contraction	4.7	-
Metabolism	Glycosphingolipid Biosynthesis - Ganglio Series	2.1	-
	Taurine and Hypotaurine Metabolism	2.3	-
	Biogenic Amine Synthesis	3.8	-
	Nitrogen metabolism	-	5.3
	Alanine, Aspartate and Glutamate Metabolism	-	3.7
Signal transduction, Signaling Molecules and Interaction	Nodal Signaling Pathway	3.7	-
	Peptide GPCRs	3.8	-
	GPCRs, Class C Metabotropic Glutamate, Pheromone	2.4	-
	Monoamine GPCRs	2.3	-
	MAPK Signaling Pathway	3.8	-
	ERK1 - ERK2 MAPK Cascade	2.8	-
	FGF Signaling Pathway	5.0	-
	Myometrial Relaxation and Contraction Pathways	3.3	-
	Calcium Signaling Pathway	8.2	2.1
	Neuroactive Ligand-Receptor Interaction	14.8	2.9
	GnRH Signaling Pathway (signaling)	2.2	-
	Proteasome	-	2.4

Table 4 Continued.

Biological System	Pathway	ZFE	aZFL
Intracellular processes	ECM-Receptor Interaction	3.1	-
	Cell Adhesion Molecules (CAMs)	3.6	-
Immune	Phagosome	-	1.8
	Prostaglandin Signaling	2.7	-
	NOD Pathway	-	2.6
	Cytokine-cytokine Receptor Iinteraction	-	3.0
Other	ACE Inhibitor Pathway	2.3	-
	Phototransduction	5.8	-
	SIDS Susceptibility Pathways	4.5	-
	Oocyte Meiosis	-	2.9
	Ovarian Infertility Genes	-	5.3

Analysis is based on 6113 unique transcripts in zebrafish embryo and 658 unique transcripts in adult zebrafish liver (Fig. 4). - pathway is not overrepresented

transcripts related to development were predominantly present in the whole zebrafish embryo (Fig. 4b, green diamonds, n= 324, and explained in supplementary Table 4). Several hepatotoxicity associated genes (red squares) were uniquely present in zebrafish embryo, namely, *aanat1*, *cyp1b1*, *fabp10a*, *hgfa*, *npy*, *otc*, *pomca*, and, *si:dkey- 22d17.3*. In adult zebrafish liver, the uniquely expressed hepatotoxicity related gene was *faslg* and the uniquely expressed genes for development were *amh* and *bmp10*.

Validation of liver specific gene expression by in situ hybridization. Genes which by text-mining were associated with hepatotoxicity and also were highly expressed in both whole zebrafish embryo and adult zebrafish liver, were selected to verify liver-specificity of the expression using *in situ* hybridization in whole zebrafish embryo. This set included three known genes, *i.e.* fatty acid binding protein 10a (*fabp10a*), peroxisome proliferator activated receptor gamma (*ppar*γ), and apolipoprotein A2 (*apoa2*) and one unannotated hypothetical gene, *wu:fj16a03*. All four genes thus showed expression in the liver region, whereas *ppar*γ and *wu:fj16a03* showed additional staining in the brain and gut (Fig.5). For *fabp10a*, *ppar*γ, and *apoa2* the sense probes were negative, while for *wu:fj16a03* the sense probe stained the same areas as the antisense probe, cautioning for conclusiveness of the *wu:fj16a03* antisense signal. Still, the *in situ* hybridization confirmed the liver specificity as concluded from NGS in at least three of the four analyzed expression markers.

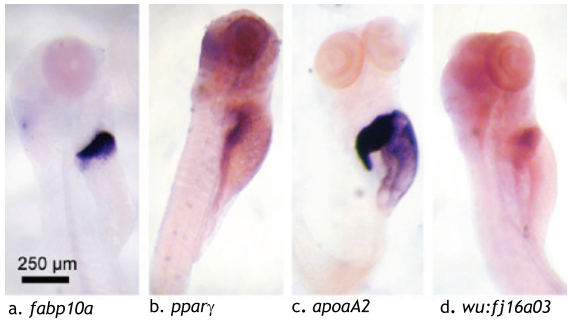

Figure 5 Validation of liver specific gene expression by *in situ* hybridization.
Representative *in situ* hydrization microphotographs for *fabp10a*, *pparγ*, *apoa2*, and *wu:fj16a03* mRNAs in 5-dpf zebrafish embryo. mRNA staining is dark blue. *fabp10a* shows intensely in the liver, and an additional small area in the hindbrain, *pparγ* and *wu:fj16a03* are observed in the liver, gut, and brain, and *apoa2* intensely in liver with additional staining in the yolk sac

Case study cyclosporine A. As a next step, we performed a comparative study using the widely studied hepatotoxicant cyclosporine A (CsA). Here, CsA-regulated gene sets, pathways and transcription factors in zebrafish embryo were compared with existing data from studies of CsA treated *in vivo* mouse livers and HepaRG cells. Statistical analysis of Affymetrix microarray data revealed 72 significantly regulated liver associated genes for the whole zebrafish embryo model. In comparison, 115 significantly regulated genes were observed in the *in vivo* mouse liver; and 262 significantly regulated genes in the HepaRG cell line. On single gene level, there was no overlap observed between the significant CsA induced transcripts of the *in vivo* mouse liver and whole zebrafish embryo, which can be understood from the low number of significant transcripts in each model. For the human HepaRG cell line, 3 transcripts overlapped with the *in vivo* mouse liver. Pathway analysis using all genes is therefore a more informative approach, and when aligning all regulated pathways in the three models in a cluster analysis, this showed good comparability between whole zebrafish embryo and mouse liver *in vivo* (Fig. 6).

These two models had 15 of the 26 regulated pathways regulated in the same direction, whereas the HepaRG cell line showed a deviating regulation of the these 15 pathways, and only 5 pathways regulated in the same direction as compared to mouse. Concordance between mouse liver and the cell line was similar to that between zebrafish embryo and the cell line. While most corresponding pathways between whole zebrafish embryo and mouse *in vivo* included hepatotoxicity related pathways (Fig.6, italics), the pathways that showed overlap between whole the zebrafish embryo and the liver cells included cell cycle-related pathways, which is related to the active proliferation in these two models. Importantly, cholesterol biosynthesis was down regulated in all models.

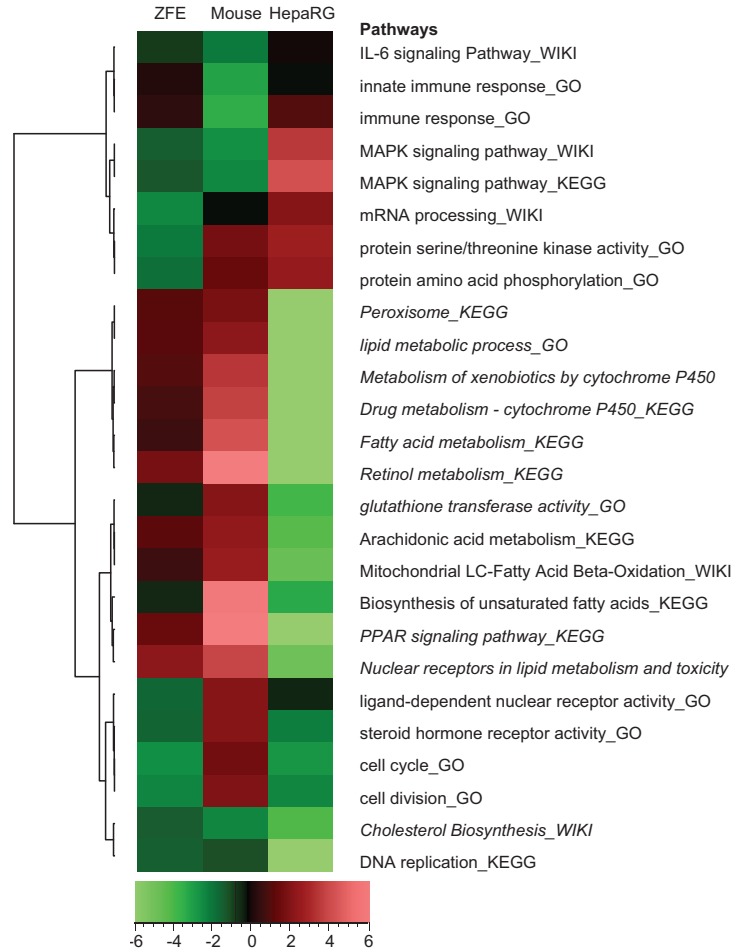

Figure 6 Heatmap of pathway responses upon cyclosporine A exposure.
Pathways regulated in mouse liver *in vivo*, whole zebrafish embryo and the cell line HepaRG. The cluster of pathways that are upregulated in both whole zebrafish embryo and mouse liver *in vivo* is clearly enriched for hepatotoxicity related pathways (indicated in italics). The color scale indicates the T-value, with downregulation in shades of green and upregulation in shades of red

The high concordance in hepatotoxicity pathways between zebrafish embryo and mouse liver is indicative for similar regulation at the level of transcription factors. To verify this we started out with only those genes which were significantly regulated and liver specific in the zebrafish embryo, that is, present in the overlapping genes in the NGS comparison

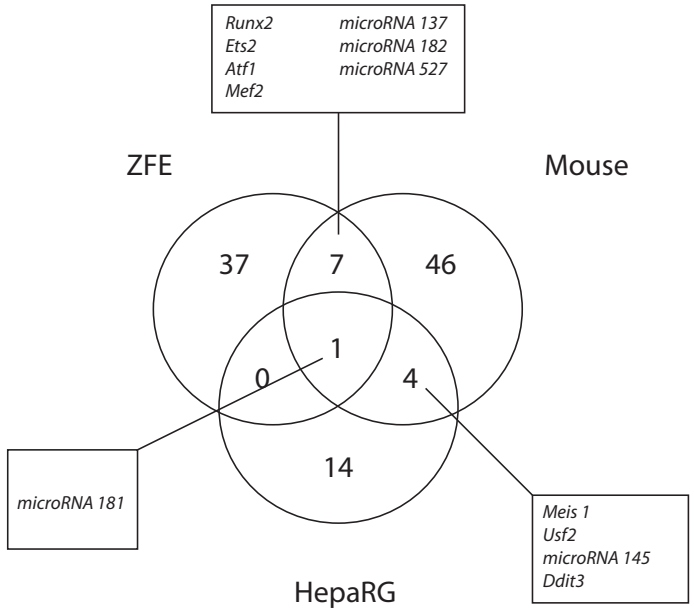

Figure 7 Venn diagram of the enriched transcription factor motifs enriched after CsA exposure.

Venn diagram showing the number of enriched transcription factor motifs in the *in vivo* mouse liver, whole zebrafish embryo model and the two cell lines exposed to CsA. Enrichement of transcription factors is based on the significant genes per system after exposure to CsA using an ANOVA analysis. The overlap of transcription factors between the models is tested for significance with an hypergeometric test

between whole zebrafish embryo and adult zebrafish liver (Fig. 4, blue area). Transcription enrichment analysis thus resulted in 45 enriched transcription factor binding motifs (Fig. 7). In mouse liver, using the whole set of significantly regulated genes, 58 enriched transcription factors were found, and 19 enriched transcription factors in the HepaRG cell line. The overlap between the whole zebrafish embryo and *in vivo* mouse liver was significant (*p-value* < 0.001, hypergeometric test) and showed eight overlapping transcription factor binding motifs, which were *Runx2*, *Ets2*, *Atf1*, *Mef2*, microRNA 137, microRNA 181, microRNA 182, microRNA 527. The overlap between the cell line HepaRG and *in vivo* mouse liver was 5 transcription factor binding motifs, which were *Meis 1*, *Usf2*, microRNA 145, microRNA 181, and *Ddit3*. The overlap between zebrafish embryo, *in vivo* mouse liver and HepaRG cells was one transcription factor binding motif, which was microRNA 181.

Discussion

The zebrafish is a powerful vertebrate model for human biology and disease, and zebrafish liver resembles the mammalian liver on the morphological and functional level[125]. In zebrafish embryo, hepatocytes are present from 36-hpf, and at 72-hpf the liver is fully functioning, including functional activity of the cytochrome P450 system, which is important for metabolizing xenobiotics[105]. Therefore hepatic responses can be expected after exposure to hepatotoxicants in zebrafish embryo. In this paper, we investigated the applicability of the zebrafish embryo as an alternative model system for hepatotoxicity testing. To this aim, we compared hepatotoxic effects induced by a set of reference compounds (Table 1), reflected by histopathology and gene expression profiling, in the whole zebrafish embryo and adult zebrafish liver.

Histopathology indicated that the adult zebrafish liver is particularly sensitive for development of cholestasis, after exposure with both typical and non-typical cholestatic compounds (Table 3). Cholestasis could not be detected in zebrafish embryos. This is probably due to underdevelopment of bile production mechanisms, in line with the observation that genes involved in the formation of bile ducts are first expressed at 48-hpf[126] and that the onset of fully operational bile production in the embryo is only from 5-dpf onwards[44]. On the other hand, comparable para-cholestatic events were present at both life stages reflected by vacuolization observed in both zebrafish embryo and aZF and induced by nominal cholestatic compounds, although vacuolization was a rather generalized observation in zebrafish embryo. Vacuolization might therefore be a non-specific response in zebrafish embryo hepatocytes, e.g. resulting from induction of metabolic activity or as an inhibiting effect on the mitochondrial energy production[127].

The steatotic compounds (AM, VPA and TET) induced an effect that was consistent with the nominal phenotype in both zebrafish life stages, that is lipid accumulation as observed with Oil Red O staining, but lipid accumulation was also present with CPZ in zebrafish embryo. All three necrotic compounds (TAA, PQ and APAP) induced hepatocellular vacuoles at both life stages, with the exception of APAP in adult zebrafish liver, but no apparent apoptosis or necrosis.

There was also additional, mixed effects. Taken together, the nominal phenotypes of the tested compound classes were not simply reproduced in adult zebrafish liver and zebrafish embryo. The final morphology of hepatotoxic effects were related to life stage dependent capability of hepatocytes, and hepatotoxic responses could lead to mixed histopathology. Still, all of the tested hepatotoxicants do induce specific histopathological effects in the liver, which could be interpreted as a different expression of similar mechanisms of hepatotoxicity compared to humans. Since the design of our study aimed at qualitative assessment of histopathological effects, the information on relation to exposure concentration is limited.

The overall aim of the NGS analysis was to confirm that transcripts associated with hepatotoxicity are expressed in the whole zebrafish embryo (by comparison with adult zebrafish liver), and that hepatotoxicity specific signals are detectable over the noise of other tissues. To achieve this aim, NGS provides multiple advantages over mRNA microarrays. In contrast to microarrays, NGS does not rely on the probe design and probe selection, thus enabling detection of non-predefined transcripts, including diverse splicing variants of a single gene. The high expenses that come with NGS in a traditional toxicogenomics study set-up could in our case be avoided by the use of pooled samples. This was justified because this would sufficiently reveal the liver specific response capability of the zebrafish embryo. Working with pools even has a specific advantage, because it eliminates the blur of non or low-responding individuals and of non or less-active compounds[106]. On the other hand, good transcript counts depend on a sufficient number of response-evoking compounds, and information on individual compounds is lost. This was however not considered as a weakness, because compound-specific activity was not the focus here. Nevertheless, hepatotoxicity-associated gene expression could have been too low to support general conclusions on the applicability of the zebrafish embryo model with a specific transcriptional response in only a limited number of compounds.

Bioinformatics-based text mining showed that hepatotoxicity-associated transcripts are detectable in zebrafish embryo as well as adult zebrafish liver, and that they were evenly distributed between the two models (Figure 4, red squares). This indicates that similar processes are active in whole zebrafish embryo and adult zebrafish liver, in spite of the immature hepatocyte morphology in zebrafish embryo, and in spite of a different histopathology between the two models. Apparently, initial cellular responses do overlap as reflectec in similar gene expression changes, but the downstream biological outcomes differ, depending on the developmental stage of the organism.

Besides a major overlap in the NGS transcripts, unique transcripts were found for both zebrafish embryo and adult zebrafish liver conditions. These transcripts were analyzed for underlying pathways and processes. Unique transcripts in zebrafish embryo were mostly related to developmental processes, which is an expected result considering the developmental stage of the embryo. The specific transcripts in adult zebrafish liver were predominantly involved in immune response pathways. Such responses are not likely to happen in zebrafish embryo in view of the immaturity of the immune function at that stage[128]. The gene expression showed that some hepatotoxicity-associated genes were only present in whole zebrafish embryo. These genes were arylalkylamine N-acetyltransferase 1 (*aanat1*), cytochrome P450, family 1, subfamily B, polypeptide 1 (*cyp1b1*), fatty acid binding protein 1a (*fabp1a*), neuropeptide Y (*npy*), ornithine carbamoyltransferase (*otc*) and carbamoyl-phosphate synthase 1, mitochondrial (*cps1*, former *si:dkey-225d17.3*) and are highly expressed in other tissues than liver[82]. The absence of these genes in adult zebrafish liver is either because gene expression is below the RPKM cut-off value or transcripts are in zebrafish embryo expressed in other tissues than the liver. The ability to identify these off-target gene expressions can be interpreted as an advantage of the zebrafish embryo model as it may still contribute to the hepatotoxic response. *Cyp1b1*, for example, is an enzyme for biotransformation of compounds and is highly expressed in the gills of zebrafish[129]. Like the gut in mammals, the gill represents the first-pass organ in fish and its cross-talk with the liver is important for biotransformation of compounds[130]. Such interaction between organs is important for assessment of hepatotoxicity and an advantage of whole zebrafish embryo model. Moreover, the zebrafish embryo model allows for identification of toxic responses in organs outside the liver, shown in the affected intestinal epithelium after exposure to CPZ, EE2 and APAP (Table 3). One hepatotoxicity related gene was uniquely expressed in the adult zebrafish liver, faslg, which is known to be present only in the adult stages[82]. The major conclusion from the comparison ZFE-aZF liver is that using whole zebrafish embryo RNA extract allows for detection of important transcripts for hepatotoxicity, either in the liver or in other tissues. Moreover, none of the important hepatotoxicity pathways as expressed in aZF livers were missed in whole zebrafish embryo exposed to reference hepatotoxicants, providing a promising perspective for use of the whole zebrafish embryo model for (toxicogenomics-based) hepatotoxicity testing.

The liver expression of key hepatotoxicity related genes identified in the whole zebrafish embryo was confirmed by *in situ* hybridization. Liver expression of *fapb10a*, *pparγ*, and *apoa2* was also observed by others[44,131]. Neither function nor site-specificity of the highly expressed hypothetical gene *wu:fj16a03* has been described. The closest observation is that BLAST analysis indicates that this gene has a strong sequence similarity to the toxin-1 gene, which is found in rainbow trout (*Oncorhynchus mykiss*). In trout, expression of this particular gene is found in the liver, spleen and brain, which is similar to our observations in whole zebrafish embryos[82]. Some off-liver expression sites were detected for some of the genes, *e.g.* the *wu:fj16a03* transcript is rather prominent in the head region and in the gut. To further validate the applicability of the zebrafish embryo as a suitable alternative for hepatotoxicity testing, pathways regulated by CsA, which is known to induce cholestasis in humans[6], were compared between our zebrafish embryo model, a mouse model [119] and one *in vitro* model, the HepaRG cell lines[120]. Although CsA doses/concentrations and exposure duration differed between models, they were all selected to optimally induce hepatotoxicity, reflected by clinical chemistry (mouse *in vivo*[119]), histopathology (whole zebrafish embryo) and cytotoxicity (*in vitro* cell line[120]) and therefore allowed for comparison. Pathway and transcription factor based analyses attractively level out differences between models due to species variation, and model sensitivity and power, which can hamper model comparison based on single gene level. Transcription factors are key players in the regulation of a wide variety of cellular processes in health and disease. They play an important role in the development of toxic responses, and transcription factor analysis is therefore an attractive way to interpret gene was

observed in affected significantly different genes between the whole zebrafish embryo and *in vivo* mouse liver. Nevertheless, pathway analysis showed that there is an overlap in regulation of the affected pathways. It appeared that the cluster of pathways showing the same direction of regulation of gene expression was highly enriched for pathways relevant for liver toxicity. The one pathway that was down-regulated in all model systems, the cholesterol biosynthesis pathway, corresponds with the inhibiting effect of CsA on cholesterol 7α-hydroxylase, which is the rate-limiting step in cholesterol conversion to bile acids[132]. In addition, a significant overlap in transcription factors was found between whole zebrafish embryo and *in vivo* mouse liver. These transcription factors (*Runx2, Ets2, Atf1* and *Mef2*) regulate immune processes, which can be understood from the immuno-suppressant function of CsA. For the three microRNAs, not enough information is available to link them to the CsA effects. The overlapping transcription factors between hepaRG cells and *in vivo* exposed mouse liver are mainly involved in wide range of processes which can be linked to DNA binding (*Ddit3, Usf2*) and development (*Meis1*). The absence of immune cells in the HepaRG model can explain the absence of immune-function related transcription factors.

Overall, these results indicate that there is more similarity of responses between the zebrafish embryo and *in vivo* mouse liver after CsA exposure than between HepaRG cells and *in vivo* mouse liver, particularly on the level of pathways and transcription factors. This supports the notion that the whole zebrafish embryo is a better proxy for the traditional *in vivo* model than the human cell line *in vitro* model.

In conclusion, we confirmed that the zebrafish embryo is a promising alternative model for hepatotoxicity testing, as indicated by hepatotoxicant-induced liver histopathology and by induction of hepatotoxicity-associated gene expression. NGS appeared a powerful tool allowing sensitive and specific quantitative comparison of transcripts between zebrafish embryo and adult zebrafish liver. While due to high costs we had to apply NGS on pooled samples from multiple experiments, comparison of gene expression from a single hepatotoxicant experiment between zebrafish embryo, *in vivo* mouse liver, and HepaRG cells further supported the potential of zebrafish embryo in hepatotoxicity testing.

Acknowledgements

The authors acknowledge Erik Steenbergen and Sanne Hermsen for technical assistance with animal handling and necropsies and Joke Robinson for histology. This study was supported by grant nr 050-060-510 from the Netherlands Genomics Initiative/Netherlands Organization for Scientific Research (NWO) to the Netherlands Toxicogenomics Centre.

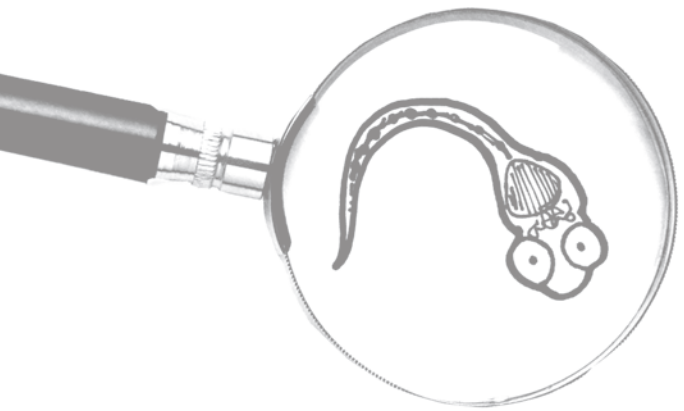

3

Gene Expression Markers in the Zebrafish Embryo Reflect a Hepatotoxic Response in Animal Models and Humans

Marja Driessen, Anne S. Kienhuis, Alexa P. Vitins, Jeroen L.A. Pennings, Tessa E. Pronk, Evert-Jan van den Brandhof, Marianne Roodbergen, Bob van de Water, Leo T.M. van der Ven

Toxicology Letters 2014 July 24;230(1):48-56

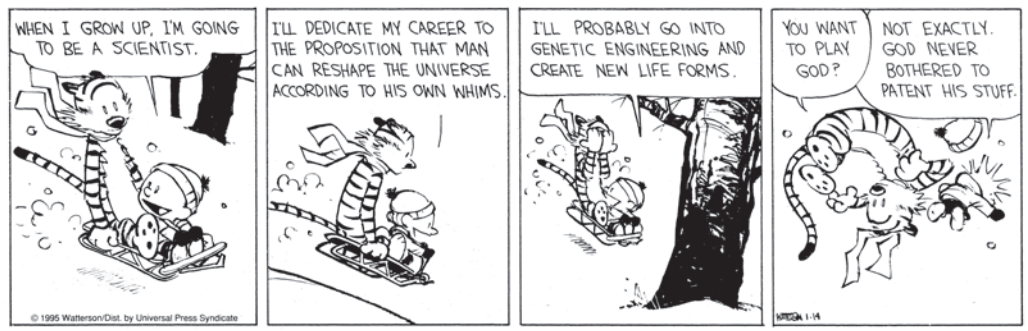

Abstract

The zebrafish embryo (ZFE) is a promising non-rodent model in toxicology, and initial studies suggested its applicability in detecting hepatotoxic responses. Here, we hypothesize that the detailed analysis of underlying mechanisms of hepatotoxicity in ZFE contributes to the improved identification of hepatotoxic properties of new compounds and to the reduction of rodents used for screening. ZFEs were exposed to nine reference hepatotoxicants, targeted at induction of cholestasis, steatosis and necrosis, and two non-hepatotoxic controls. Histopathology revealed various specific morphological changes in the ZFE hepatocytes indicative of cell injury. Gene expression profiles of the individual compounds were generated using microarrays. Regulation of single genes and of pathways could be linked to hepatotoxic responses in general, but phenotype-specific responses could not be distinguished. Hepatotoxicity-associated pathways included xenobiotic metabolism and oxidoreduction related pathways. Overall analysis of gene expression identified a limited set of potential biomarkers specific for a common hepatotoxicity response. This set included several cytochrome P450 genes (*cyp2k19*, *cyp4v7*, *cyp2aa3*), genes related to liver development (*pklr*) and genes important in oxidoreduction processes (*zgc:163022*, *zgc:158614*, *zgc:101858* and *sqrdl*). In conclusion, the ZFE model allows for identification of hepatotoxicants, without discrimination into specific phenotypes.

Introduction

The liver has a central role in the metabolism of xenobiotic substances in an organism, which includes biotransformation targeted at inactivation of toxic parent compounds. However, this biotransformation may also produce toxic reactive metabolites, leading to xenobiotic-induced liver injury[4,6]. Various underlying mechanisms can result in a wide range of xenobiotic-induced liver toxic phenotypes, of which cholestasis, steatosis and necrosis are most frequently observed. Cholestasis is a chronic condition and is phenotypically characterized by bile accumulation as a result of changes in intra- or extracellular bile flow or bile composition[34]. Steatosis may occur chronically as well and is characterized as an increase in cellular lipid content due to an increase in de novo synthesis of fatty acids or reduced lipid secretion or oxidation[19]. Necrosis is an acute condition and is characterized by cell death due to oxidative stress[4,33].

A challenge in toxicology is to predict the hepatotoxic potential of compounds to which humans are exposed. In mammals, and particularly for oral uptake, many compounds provoke first signs of toxicity in the liver (due to the first path effect and activation in liver cells), and therefore hepatotoxicity is an important aspect of adverse drug effects and adverse effects of chemicals. To this end, there is an urging need to develop and validate alternative approaches, since traditional *in vivo* animal studies are associated with ethical (large numbers of animals exposed), economical (high costs and long experimental periods), and scientific issues (not fully predictive for effects in humans). As such, the zebrafish embryo is an alternative screening model with the potential of reducing traditional *in vivo* rodent studies. It combines the benefits of an *in vivo* model, namely complete biological complexity including interaction between tissues and cells[49,54,95], with the advantages of an *in vitro* model, that is, reduced animal discomfort and the ability for medium to high throughput testing. The structure and function of the adult zebrafish liver is similar to the mammalian liver[46,55], and fully functional liver tissue is present in the zebrafish embryo at 72 hours post fertilization (hpf), which is therefore a suitable time point to start hepatotoxicity testing. There is also high genetic conservation between humans and zebrafish, including genes functioning in biotransformation[46,55]. Zebrafish embryos express 94 cytochrome P450 enzymes (CYPs), which occur in the same 18 gene families as in humans. Furthermore, the CYP1-4 families, which are involved in metabolizing xenobiotics, are very similar between the two species, and an ortholog of the human CYP3A4, which catalyzes the majority of known drug-metabolizing reactions, is present in zebrafish as well, namely, *cyp3a65*[46,55].

In a previous study, we showed that the zebrafish embryo can be used to identify human hepatotoxic responses using histopathology and analysis of hepatotoxicity-associated transcripts by next-generation sequencing (NGS)[133]. In that study, we showed that the induced phenotype in zebrafish embryos (summarized in Table 1) differs from histopathology in humans and rodents, partly due to species differences, and partly due

to immaturity of embryonic hepatocytes. The phenotype in humans and rodents is therefore defined as 'nominal', and that in zebrafish embryos as 'observed'. Our NGS results demonstrated that hepatotoxicity-associated gene expression responses remain detectable even in case of a non-tissue specific analysis in whole body homogenates and are distinct from developmental toxicity processes. Furthermore, our initial microarray study with cyclosporin A (CsA) showed that changes in gene expression were reflective of mechanisms underlying the onset of cholestasis[133].

Building on these premises, the hypothesis of the present study was that detailed analysis of mechanisms of hepatotoxicity may contribute to a better description of hepatotoxic responses and to the development of expression markers predictive for hepatotoxicity in humans. The specific objective was to analyze hepatotoxicity related gene expression responses and derive transcriptomics markers. To allow for the comparison of phenotypic responses between zebrafish embryos and humans and for the deduction of transcriptional responses underlying these phenotypes in the zebrafish embryos, we selected nine reference hepatotoxicants based on established major hepatotoxic phenotypes in humans and/or the classical rodent testing models, namely cholestasis (cyclosporine A, chlorpromazine and 17α-ethinylestradiol)[1,15,134,135], steatosis (amiodarone, tetracycline and valproic acid)[23,136,137] and necrosis (acetaminophen, paraquat and thioacetamide)[1,4,138]. Zebrafish embryos were treated with these compounds for 48 hours starting at three days post fertilization. Transcriptional analysis was performed using microarrays followed by both gene and pathway level analysis. The individual gene analysis approach is particularly useful to derive predictive markers for hepatotoxicity, whereas the analysis on the pathway and process level provides more integrative information into the underlying molecular mechanism of hepatotoxicity[61].

Materials and methods

Chemicals. All tested chemicals (purity >95%), were purchased from Sigma Aldrich (Zwijndrecht, the Netherlands), and included acetaminophen (N-actyl-para-aminophenol; paracetamol; APAP, CAS no.103-90-2; 660 µM), paraquat (1,1'-Dimethyl-4,4'-bipyridinium dichloride; PQ, CAS no.1910-42-5; 3000 µM), thioacetamide (CH3-C(S)NH2); TA, CAS no.62-55-5; 10000 µM), amiodarone hydrochloride (2-butyl-3-benzofuranyl-4-[2-(diethylamino)ethoxy]-3,5-diiodophenyl ketone hydrochloride; AM, CAS no.19774-82-4; 10 µM), valproic acid (2-propylpentanoic acid sodium; VPA, CAS no.1069-66-5; 600 µM), tetracycline (TET, CAS no.64-75-5; 200 µM), cyclosporine A (CsA, CAS no.59865-13-3; 6 µM),17α-ethinylestradiol (17α-Ethinyl-1,3,5(10)-estratriene-3,17β-diol; EE2, CAS no.57-63-6; 3.5 µM), chlorpromazine (2-Chloro-10-(3-dimethylaminopropyl)phenothiazine hydrochloride; CPZ, CAS no.69-09-0; 3 µM), D-Mannitol (Mannite; DM, CAS no. 69-65-8; 3000 µM), lithium carbonate (Carbonic acid lithium salt; Li_2CO_3, CAS no. 554-13-2; 1100 µM) and tricaine methanesulfonate (MS-222, CAS no. 886-86-2). Dimethylsulfoxide (DMSO, CAS no. 67-68-5; 0.2%) was ordered from Fisher-Scientific.

Fish treatment. Wild-type zebrafish (*Danio Rerio*) were originally obtained as commercially bred Singapore import (Ruinemans Aquarium BV, Montfoort, The Netherlands), which was maintained and bred in our facilities for more than 5 generations. Egg production was optimized by separation of the male and female fish before spawning, and female zebrafish were fed only thawed Artemia Naupli prior to spawning. Egg predation was prevented by using a breeding tank with a perforated bottom, in which male and female zebrafish were paired in a 2:2 ratio before spawning. Spawning was triggered by morning light and was usually completed within 30 minutes. After spawning, the eggs were collected using a glass siphon and debris was removed to rinse the fertilized batches at least three times in Dutch Standard Water (DSW; demineralized water supplemented with $NaHCO_3$ (100 mg/l), $KHCO_3$ (20 mg/l), $CaCl_2 \cdot 2H_2O$ (200 mg/l), and $MgSO_4 \cdot 7H_2O$ (180 mg/l) aerated for 24h at 27°C). After rinsing, the fertilized eggs from different batches were pooled and placed in a petri dish in an incubator at 26.5 ± 1°C with a photoperiod of 14 hours light/10 hours dark. The used concentration for all compounds including the negative compounds was the highest subtoxic concentration in a range-finding study, *i.e.* the highest concentration that had no observable morphological or teratological effects and no mortality (See Table 1 for histopathological changes). After 72 hours, hatched embryos were randomly distributed over 48-well plates in a density of 5 embryos per well in 1 ml test or control medium. Each test compound had at least four statistical replicates, which consisting of 3 wells (15 embryos) per replicate. In total, 13 conditions were tested including the 9 reference hepatotoxicants, two vehicle controls and two non-hepatotoxicants. At 120 hpf, the embryos were evaluated under a Leica Labovert FS microscope for altered normal development (e.g. delay in development, teratogenic effects) and indications of toxicity (e.g. abnormal swimming behaviour) and snap frozen in liquid nitrogen for microarray analysis. Although we did not analyze compound concentrations during the 48 h exposure period, all compounds were indicated to be relatively stable in the indicated time period according to the NLM Hazardous Substances Database (http://toxnet.nlm.nih.gov/cgi-bin/sis/htmlgen?HSDB).

All procedures were done under licensed conditions for studies with laboratory animals, according to European and Dutch legislation.

Microarray hybridization and quality control. The RNeasy MinElute Cleanup kit (Cat. No. 74204) and the QIAzol Lysis reagent (Cat. No. 79306) were obtained from Qiagen Benelux B.V. (Venlo, the Netherlands). Phase-lock Gel Heavy (Cat. No. 2302870) and the metal micro pestle (P985.1) were purchased from VWR International B.V. (Amsterdam, the Netherlands). For microarray analysis, samples consisting of 15 embryos per concentration per compound were snap frozen in liquid nitrogen. Total RNA was isolated using the

MinElute Cleanup Kit[110]. RNA concentration was measured spectrophotometrically (ND-1000, NanoDrop Technologies Inc., Wilmington, DE) and RNA integrity was assessed by automated gel electrophoresis using the RNA 6000 Nano Chip Kit (Bioanalyzer 2100, Agilent technologies, Amstelveen, The Netherlands). Total RNA samples with an RNA Integrity Number (RIN) > 7 were used for further analysis.
Technical handling of the microarrays (GeneChip hybridization) was outsourced to ServiceXS BV (Leiden, the Netherlands). RNA quality control, hybridisation, microarray quality check and data processing were performed as described previously[133].
For data processing and quality control, affymetrix Cell Intensity Files (*.cel) were normalized using the Robust Multichip Average (RMA) algorithm [76] and the MBNI custom CDF version 15 (http://brainarray.mnbi.medumich.edu/Brainarray/Database/CustomCDF)[118]. RMA normalized data was Log_2 transformed and the quality of micro array images was inspected visually (http://arrayanalysis.org, BiGCaT Maastricht University). Four out of 192 arrays were eliminated from further analysis because they did not meet the quality criteria. Affymetrix internal controls ID were not used in further analyses, leaving a total of 23,758 probe sets corresponding to unique Entrez GeneIDs. R software (Version 2.15.0 R Foundation for Statistical Computing, Vienna, Austria) was used to correct the Log_2-transformed data for the median of the vehicle controls.

Gene expression analysis. Following our hypothesis, the basis for gene expression analysis was histopathological clustering. Clusters were based either on the phenotype as observed in humans after compound exposure (referred to as nominal phenotype) or on actually observed histopathology (observed phenotype, Table 1). The nominal phenotype clusters included three classes, namely cholestasis (CPZ, CsA and EE2), steatosis (AM, TET and VPA) and necrosis (APAP, PQ and TAA). The observed phenotype consisted of four clusters; (1) lipid vacuolization (AM, CPZ and VPA), (2) chromatin condensation (CPZ, EE2 and PQ), (3) chromophobic vacuolization (CsA, EE2, PQ and TAA) and (4) eosinophilic vacuolization (CPZ, CsA, TET and APAP). Processes and pathways regulated after exposure, were determined using T-Profiler. T-Profiler allows genome-wide expression analysis without applying cut-offs on single gene level resulting in the use of all the genes on the array[83]. Compound-specific pathways were identified using the highest concentration of each compound and by averaging the replicates. Pathways were considered significant when the absolute T-value was >3 and the E-value < 0.05 (a Bonferoni corrected two-tailed P-value) in at least one reference hepatotoxicant. Compound specific effects on pathway level were determined using the top-3 up and down regulated pathways per compound. Pathways were included in the top-3 if they had at least an absolute T-value > 4. Next, to assess which pathways were phenotype specific, a two-group comparison was performed using Qlucore Omics Explorer (Qlucore AB, Lund, Sweden). Phenotypic clusters were based on either nominal phenotype, observed phenotype and common hepatotoxicity phenotype. Phenotype-specific pathways were counted as those with a p-value <0.05.

Finally, to detect commonly induced genes between hepatotoxic compounds, the gene expression values for the highest concentration of each compound were analyzed by one-way ANOVA with an FDR<0.05. Genes with an absolute FC > 1.2 were considered to be differentially expressed and were ranked on the number of compounds regulating the gene.

Results

Hepatotoxicity-associated pathways. T-Profiler was used to identify the significantly regulated pathways per compound to confirm a compound's ability to induce hepatotoxicity-associated pathways/processes in the zebrafish embryo. A biological pathway/process with an absolute T-value > 4 and E-value < 0.05 in one of the compounds was considered significant and a heatmap separating up- and down-regulated pathways and processes was generated (Fig. 1). The compounds were clustered using an unsupervised Euclidian distance with Ward linkage clustering method, which revealed that most hepatotoxicants cluster together, with exception of TAA and CPZ, which cluster with the non-hepatotoxicants DM and Li_2CO_3 for the up-regulated pathways. For the down-regulated pathways, a different clustering of the compounds was observed. Here, all hepatotoxicants formed a cluster, whereas the negative compounds, DM and Li_2CO_3, formed a distinct cluster. Distinctive functions can be identified between the up-regulated and down-regulated pathways/processes. Up-regulated pathways/processes were associated with oxidative stress (including oxidoreductase activity, oxidation reduction related pathways/processes) and xenobiotic metabolism (including glutathione metabolism, glutathione transferase activity, metabolism of xenobiotics by cytochrome P450 and drug metabolism-cytochrome P450). Down-regulated pathways/processes were mainly involved in ribosome, protein kinase activity and regulation of transcription. Without considering statistical significance, directions of responses of the regulated pathways/processes were highly concordant between hepatotoxic compounds. Listing of the three most highly up- and down-regulated pathways/processes per compound (Table 2) showed that the most up-regulated pathways over all compounds included oxidoreductase activity, oxidation reduction, heme binding, and iron ion binding. The most down-regulated pathways were involved in ribosome and cytoplasmic ribosomal proteins related processes. CPZ had only 3 significantly regulated pathways/processes, one up-regulated (signal transducer activity) and two down-regulated pathways, which overlapped with other compounds in the set. TAA did not have any significant pathways/processes in either direction.

Phenotype directed clustering of processes and pathways at the transcriptome level. To determine whether the phenotypes, nominal or observed, specifically defined pathways/processes, a phenotype-directed analysis was performed using a two-group comparison, *i.e.* phenotype-related compounds versus all other compounds in the set.

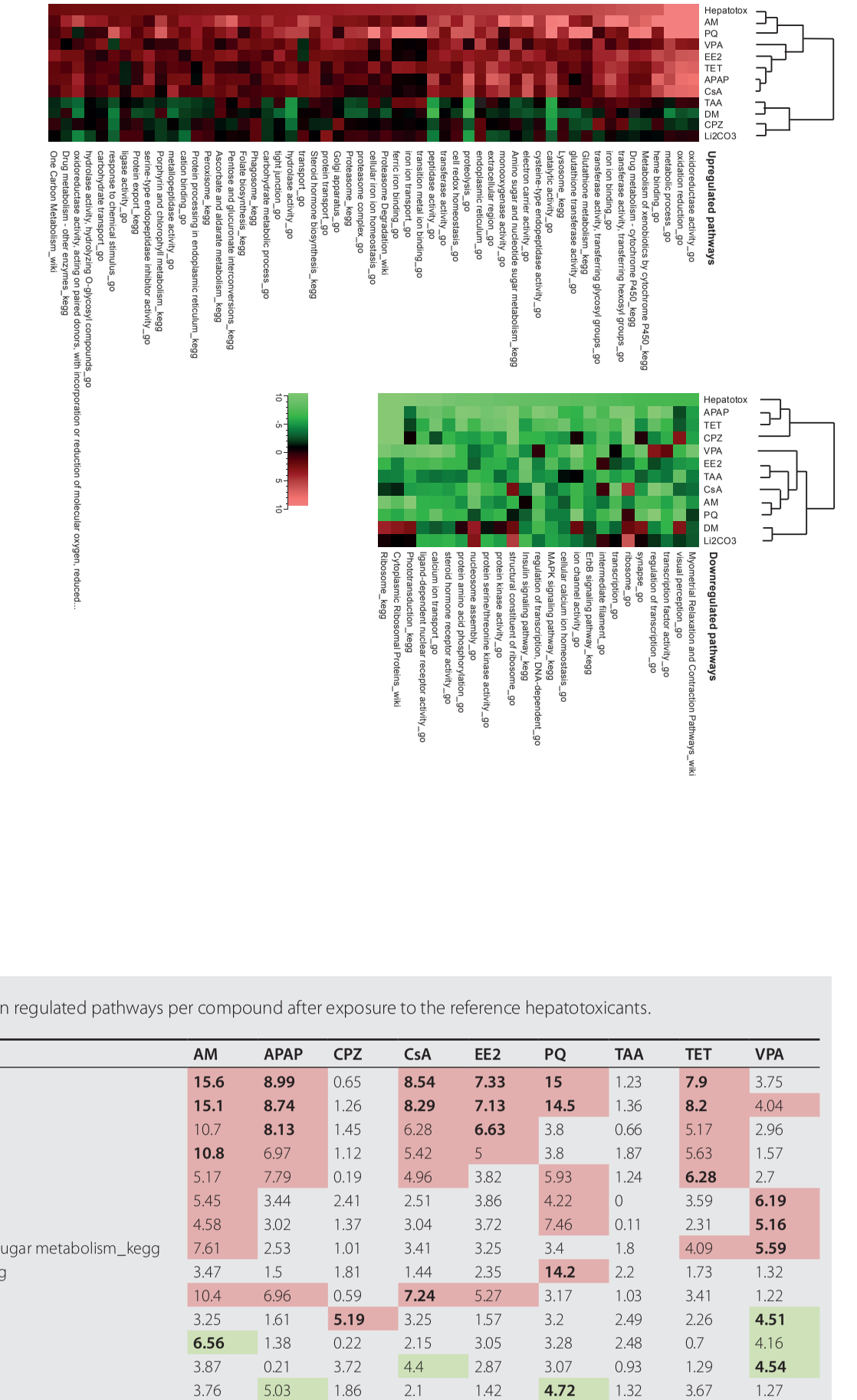

Figure 1 Hepatotoxicant regulated pathways.

Significantly regulated pathways per compound were analyzed using T-Profiler, with significance criteria T-value > 4 and E-value > 0.05, so each pathway has a significant occurrence in at least one compound. _go, _kegg, _wiki indicates pathway origin from The Gene Ontology (GO), Kyoto Encyclopedia of Genes and Genomes (KEGG), and Wikipathways (WIKI). Color shades in the heatmap represent corresponding T-value (see color scale). Left panel: upregulated pathways, right panel downregulated pathways. Pathways and compounds are unsupervisedly clustered using Euclidian distance and Ward linkage

Table 2 Top-3 up and down regulated pathways per compound after exposure to the reference hepatotoxicants.

Pathways	AM	APAP	CPZ	CsA	EE2	PQ	TAA	TET	VPA
oxidoreductase activity_go	**15.6**	**8.99**	0.65	**8.54**	**7.33**	**15**	1.23	**7.9**	3.75
oxidation reduction_go	**15.1**	**8.74**	1.26	**8.29**	**7.13**	**14.5**	1.36	**8.2**	4.04
heme binding_go	10.7	**8.13**	1.45	6.28	**6.63**	3.8	0.66	5.17	2.96
iron ion binding_go	**10.8**	6.97	1.12	5.42	5	3.8	1.87	5.63	1.57
extracellular region_go	5.17	7.79	0.19	4.96	3.82	5.93	1.24	**6.28**	2.7
endoplasmic reticulum_go	5.45	3.44	2.41	2.51	3.86	4.22	0	3.59	**6.19**
cell redox homeostasis_go	4.58	3.02	1.37	3.04	3.72	7.46	0.11	2.31	**5.16**
amino sugar and nucleotide sugar metabolism_kegg	7.61	2.53	1.01	3.41	3.25	3.4	1.8	4.09	**5.59**
glutathione metabolism_kegg	3.47	1.5	1.81	1.44	2.35	**14.2**	2.2	1.73	1.32
electron carrier activity_go	10.4	6.96	0.59	**7.24**	5.27	3.17	1.03	3.41	1.22
signal transducer activity_go	3.25	1.61	**5.19**	3.25	1.57	3.2	2.49	2.26	**4.51**
phototransduction_kegg	**6.56**	1.38	0.22	2.15	3.05	3.28	2.48	0.7	4.16
signal transduction_go	3.87	0.21	3.72	4.4	2.87	3.07	0.93	1.29	**4.54**
homophilic cell adhesion_go	3.76	5.03	1.86	2.1	1.42	**4.72**	1.32	3.67	1.27
visual perception_go	3.65	0.76	1.89	1.13	1.97	**4.34**	3.78	0.95	2.8
DNA replication_go	3.2	0.67	0.09	**4.69**	2.38	2.94	2.06	1.04	0.4
regulation of transcription_go	3.04	**5.04**	1.73	**4.88**	0.75	**5.03**	1.79	3.72	1.93
regulation of transcription, DNA-dependent_go	3.04	4.85	2.67	**4.42**	1.68	3.59	1.86	3.31	0.52
nucleosome assembly_go	3.98	4.74	2.16	4.27	1.06	0.82	2.81	2.89	1.24
cytoplasmic Ribosomal Proteins_wiki	3.53	**6.06**	**5.32**	0.29	1.67	2.4	1.69	**6.02**	4
ribosome_kegg	**4.58**	**7.01**	**6.48**	0.51	2.75	2.79	1.62	**6.79**	**4.61**

Top-3 significantly up- and down-regulated pathways and processes (ranked on either the highest or lowest corresponding T-values) were analyzed using T-Profiler, with significance criteria absolute T-Value > 4 and E-value > 0.05. _go, _kegg, _wiki indicates pathway origin from The Gene Ontology (GO), Kyoto Encyclopedia of Genes and Genomes (KEGG), and Wikipathways (WIKI). Red colored cells and font indicate significant up-regulation of pathways, green colored cells and font indicate significant down-regulation of pathways. Bold font indicates the presence of the pathway in the top-3 either up- or down-regulated pathways per compound

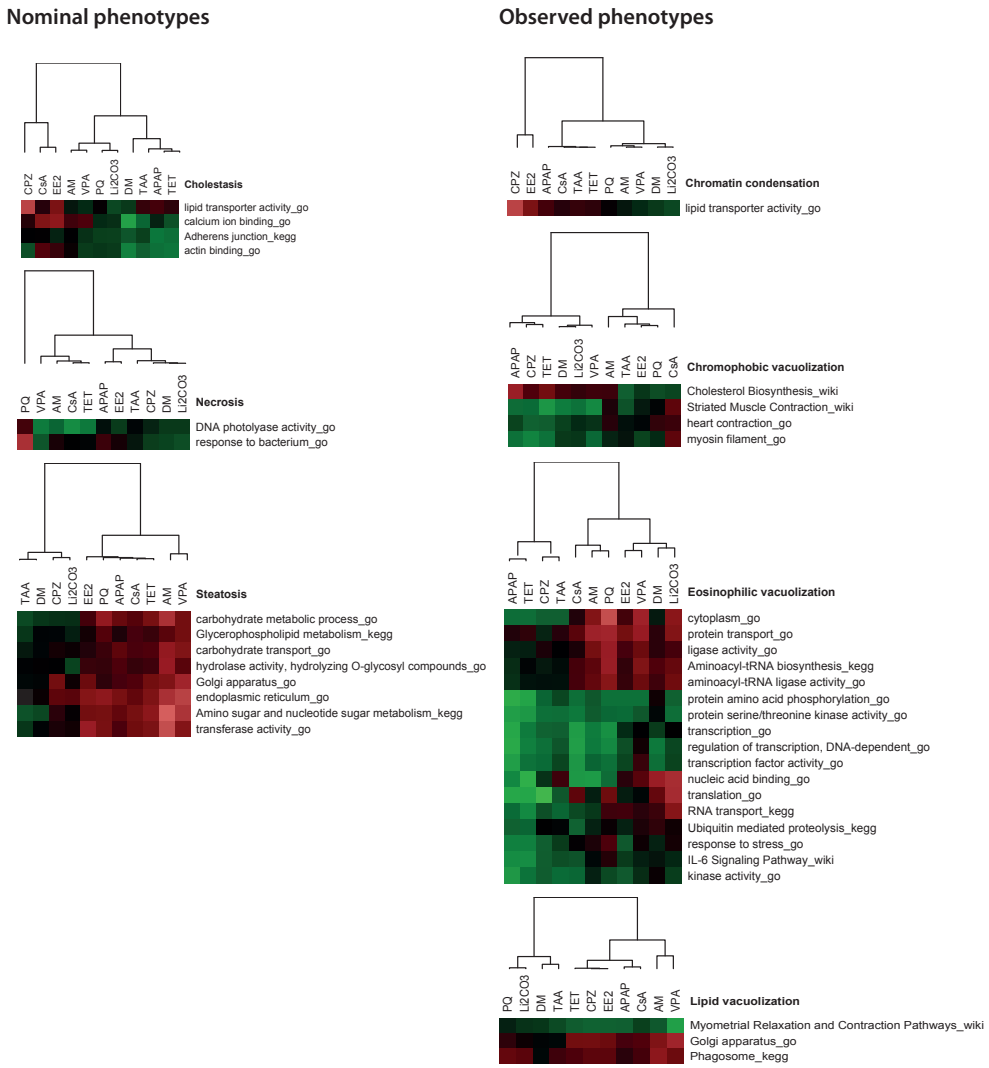

Figure 2 Heatmap of all pathways specific for the nominal, observed and common hepatotoxic phenotype.

Significantly regulated pathways per phenotypic observation based on T-Profiler output and a 2-group comparison in Qlucore. Nominal phenotype indicates the phenotypes as observed in humans, observed phenotype indicates what is seen in ZFE and common hepatotoxicity pathways indicate the response on pathway level without discriminating between phenotypes. _go, _kegg, _wiki indicates pathway origin from The Gene Ontology (GO), Kyoto Encyclopedia of Genes and Genomes (KEGG), and Wikipathways (WIKI). Color shades in the heatmap represent corresponding T-value (see color scale). Pathways and compounds are clustered using euclidian distance with Ward linkage

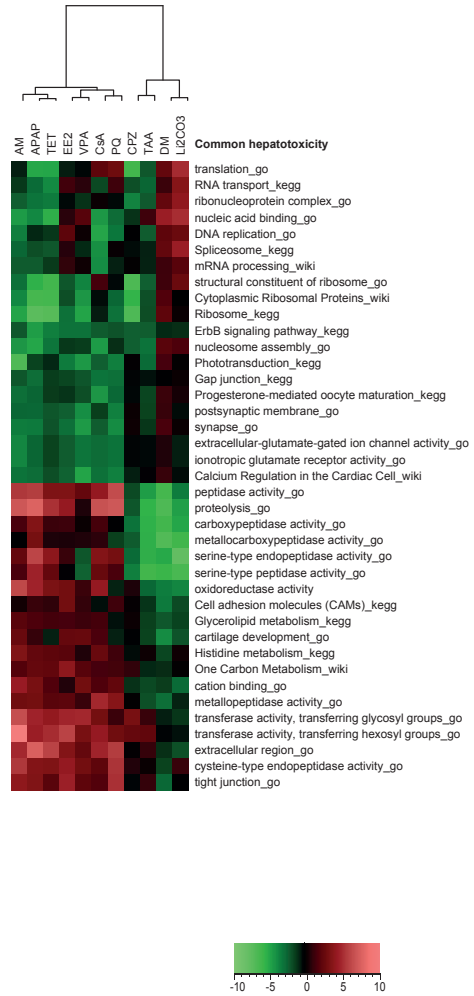

Figure 2 Continued.

The nominal classification followed the selection of reference compounds, i.e. cholestasis (CPZ, EE2, CsA), steatosis (AM, TET, VPA) and necrosis (APAP, PQ, TAA). The observed differed from the nominal phenotypes, probably due to life-stage and species specificity of responses, and the major observed classes were chromatin condensation (CPZ, EE2, PQ), chromophobic condensation (CsA, EE2, PQ, TAA), eosinophilic vacuolization (CPZ, CsA, TET, APAP) and lipid vacuolization (AM, CPZ, VPA); see Driessen *et al.* for further details[133]. This analysis did not reveal unique phenotype-specific patterns for either the nominal (Fig. 2, left) or observed (Fig. 2, middle) phenotypes. Since phenotype-specific pathways/processes could not be identified and the pathway/process listing (Table 2) suggested that there was a more common hepatotoxic response, it was assessed whether common hepatotoxicity pathways/processes could be confirmed using a comparison between all hepatotoxicants and controls (Fig. 2, right). Seven out of the nine compounds showed a uniform response for 39 different pathways/processes, where 19 pathways were up-regulated and 20 down-regulated. Common down-regulated pathways included, for example, translation, DNA replication and mRNA processing. Common up-regulated pathways included, for example, oxidoreductase activity, transferase activity and carboxy-peptidase activity. In line with per compound analysis, CPZ and TAA showed a distinctive and less active pattern of regulated pathways/processes.

Identification of common hepatotoxicity marker genes. As described above, analysis on pathway and process level revealed a uniform response for most of the compounds. To determine marker genes for common hepatotoxicity, a one-way ANOVA with ten groups was performed, i.e. all hepatotoxicants as one group against the controls, which resulted in 732 significantly regulated genes (Fig. 3A; Supplementary Table 1). These significant genes were then ranked by the number of compounds that regulated the specific gene and the following criteria, absolute fold change (FC) > 1.2 and regulation by at least three compounds, were applied to identify the best possible informative marker for a common hepatotoxic response. The 20 best performing up-regulated and down-regulated genes were then selected (Fig. 3B). The top up-regulated genes included several cytochrome P450s (*cyp2k19*, *cyp4v7*, *cyp19a1b*, *cyp24a1* and *cyp2aa3*), genes involved in oxidoreduction processes (*zgc:163022*, *zgc:158614*, *zgc:101858* and *sqrdl*), and a gene in the drug metabolism pathways (*impdh1b*). The top-10 down-regulated genes were related to liver development (*zgc:77778*), glucose transport (*slc2a9l2*), and glycolysis/gluconeo-genesis (*pklr*). Three uncharacterized genes were identified, which were *LOC100003115*, *LOC100538043*, and *LOC100330229*. Furthermore, three genes were involved in neuropeptide signaling (*scg5*), peptidase activity (*zgc:154142*), thrombospondin-1-like (*LOC100535166*), and heart development (*tcap*). It was further assessed whether these marker genes were also present in the significant pathways/processes observed after the phenotype-directed analysis, and this could be confirmed for 10 of the 20 marker genes (Fig. 3B, genes with asterixs). These ten marker genes are listed in Table 3, which also shows that most of the

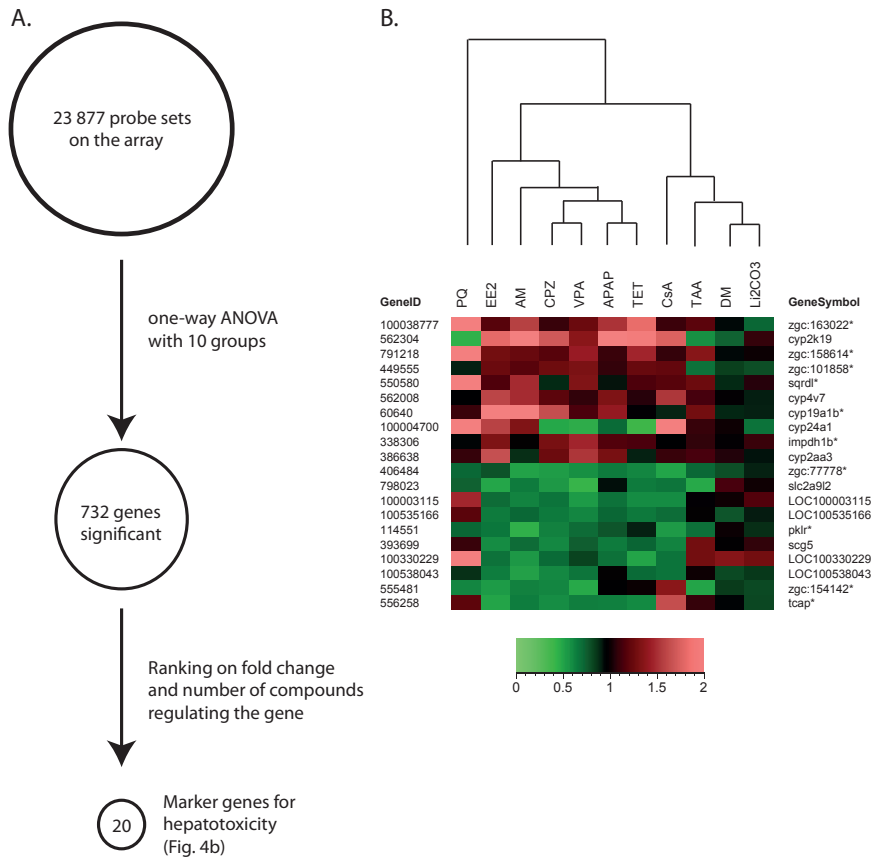

Figure 3 Selection of the proposed marker genes.
3A. Depiction of steps in the analysis leading to marker genes for the prediction of human hepatotoxicity. After one-way ANOVA with 10 groups resulted in 732 significant genes with significance criteria FDR < 0.05 and corrected for the negative compounds. **3B.** Heatmap of the proposed marker genes to predict human hepatotoxicity. Proposed markers for the prediction of human hepatotoxicity using a ranked approach on the number of compounds inducing the gene. Color shades in the heatmap represent corresponding fold change, where green represents down regulation and red presents up regulation (see color scale). Compounds are clustered using Euclidian distance and Ward linkage. Asterixs indicates presence of the gene in phenotype-directed pathways (Table 2)

Table 3 Overview of the ten hepatotoxicity associated markers present in the phenotype directed analysis.

GeneName	GeneID	AM	APAP	CPZ	CsA	EE2	PQ	TAA	TET	VPA	DM	Li2CO3	Phenotype	Pathway
zgc:163022	100038777	1.82	1.76	1.28	1.29	1.38	7.89	1.39	2.1	1.47	0.98	0.76	Fig. 3, common	oxidoreductase activity
zgc:158614	791218	1.28	1.13	1.21	1.12	1.32	3.79	1.39	1.5	1.45	0.98	1.04	Fig. 3, common	oxidoreductase activity
zgc:101858	449555	1.25	1.15	1.34	1.29	1.33	0.97	0.74	1.32	1.39	0.87	0.83	Fig. 3, common	oxidoreductase activity
sqrdl	550580	1.45	0.92	0.89	1.16	1.14	4.37	1.24	1.13	1.31	0.93	1.09	Fig. 3, common	oxidoreductase activity
cyp19a1b	60640	2.11	1.48	1.71	0.96	4.07	1.16	1.35	1.04	1.21	0.93	0.94	Fig. 3, common	oxidoreductase activity
impdh1b	338306	0.98	1.16	1.3	0.97	1.31	0.95	1.08	1.14	1.45	1.02	1.13	Fig. 3, common	oxidoreductase activity
zgc:77778	406484	0.54	0.68	0.56	0.52	0.81	0.74	0.74	0.64	0.6	0.83	0.94	Fig. 3, common	extracellular region_go
zgc:154142	555481	0.62	0.95	0.62	1.33	0.54	0.61	0.51	0.97	0.49	0.88	0.85	Fig. 3, common	peptidase activity_go
tcap	556258	0.65	0.64	0.6	1.6	0.52	1.18	1.07	0.62	0.65	0.99	0.85	Fig. 3, observed	Striated Muscle Contraction_wiki
pklr	114551	0.46	0.78	0.63	0.55	0.67	0.73	0.7	0.9	0.71	1.04	0.92	Fig. 3, nominal and observed	transferase activity_go

The 20 proposed markers were assessed for their presence in the phenotype-directed analysis, where ten of these markers were found. Values indicate the fold change per compound, the column *phenotype* indicates from which phenotype-directed analysis the gene is derived (see Fig. 3) The column *pathway* indicates in which significantly regulated pathway the gene is present (Fig.2 and/or Table 2).

genes were derived from the common hepatotoxic response pathways (Fig. 2, right), and specifically from the oxidoreductase activity pathway therein, whereas only the genes *tcap* and *pklr* were present in the observed and/or nominal phenotypic specific pathways (Fig. 2, left and middle).

Discussion

In this study, we analyzed the transcriptional changes on single gene as well as on pathway level in the zebrafish embryo after exposure to reference hepatotoxicants to verify whether mechanistic information can contribute to the applicability of this model in screening for hepatotoxic potential of compounds. The ultimate objective was to derive predictive markers for hepatotoxicity.

Histopathological analysis showed that the hepatotoxic observed phenotypes differ from those know from mammalian studies. However, specific morphological changes were observed in the zebrafish embryo, which were different from those observed in adult zebrafish liver, the latter more resembling histopathology common in livers of humans and model rodents[133]. This difference indicated that the developmental stage affects the final phenotypical outcome, and the early life stage of the zebrafish embryo, with premature hepatocytes, may lack the modes of action leading to expression of a mature hepatotoxic phenotype. Although, the observed histopathological changes confirmed the responsiveness of the zebrafish embryo to the hepatotoxicants suggesting that initiating mechanisms are already active in the early embryo. We observed that hepatotoxicity-associated gene expression was present in the zebrafish embryo supporting that mechanisms of hepatotoxicity are similar between the embryonic and adult stages. The zebrafish embryo is therefore a potentially suitable model to identify hepatotoxic markers.

In the present study, gene expression analysis was performed at the compound level to investigate whether the molecular changes induced by the reference hepatotoxicants in zebrafish embryos may reflect hepatotoxicity in humans and/or classical rodents to which these reference hepatotoxicants refer.

In the pathway analysis that was based on the compound specific transcriptomes, responses of the significant pathways appeared very similar between compounds in terms of directionality (up- or down-regulated), independent of the phenotype class, but with a few exceptions. The most abundant up-regulated pathways were related to xenobiotic metabolism and oxidoreduction processes. The induction of the cytochrome P450 system confirms the capability of the embryos to carry out this important function

in the detoxification of xenobiotics[4]. The presence of this key function of detoxification is further supported by the high induction of glutathione-related pathways, including glutathione metabolism and glutathione transferase activity[139]. The metabolism-related pathways in our model differ from CYP related processes in zebrafish embryos analyzed for mechanisms of developmental toxicity[67], and are therefore considered to be hepatotoxicity specific. This conclusion is further supported when comparing the regulated pathways between these two models for the same compound: exposure to VPA in the developmental toxicity assay of Hermsen *et al.* [67], using a more development-sensitive exposure time window, shows no overlap of pathways with those identified in our model. CPZ and TAA up-regulated the same pathways as all other hepatotoxicants, albeit to a lesser extent forcing them to cluster with the negative controls. Others showed that TAA[57] and CPZ[105] are active in the zebrafish embryo, excluding low absorption as a cause of this less active regulation of processes. The same references indicate that the effects of TAA and CPZ may be induced acutely, i.e. within a shorter time span than the 48 hours used in our study, and this provides a good explanation for the low activity at our measurement point.

In the down-regulated pathways/processes, a more differentiated response was observed and three clusters were formed. Here, APAP and CPZ clustered together, as did VPA, EE2, TAA, CsA, AM, and PQ, and a third cluster consisted of the negative controls. APAP and CPZ down-regulated the same pathways as all other hepatotoxicants, although to a lesser extent, forcing them to cluster separately. Again, the same reasoning as proposed for the up-regulated pathways could apply to the down-regulated pathways in the case of CPZ exposure. Although APAP was chosen for inducing necrosis, a relative acute condition, regenerative events will also be activated and may even take over[140,141]. The up-regulated pathways have higher *t-values* than the down-regulated pathways suggesting that the up-regulated pathways are more significant when compared to the down-regulated pathways. Furthermore, these up-regulated pathways could more easily be linked to hepatotoxicity than the down-regulated pathways.

The negative controls have no known hepatotoxic activity, but are linked to nephrotoxicity in rodents[142]. Because the gene expression is measured in the whole embryo, a slight, non-significant, induction of similar pathways could follow from this nephrotoxic activity. Downregulation of pathways related to transcription and ribosomal activity by these controls could represent an adaptive response to cell stress. It is known that stalling of the transcription process occurs in response to DNA damage which was observed in cells after exposure to cisplatin[143]. Our observations of gene expression dependent regulation of pathways and processes in zebrafish embryos are in line with those in the rat, as far as available from *in vitro* and *in vivo* studies. AM exposure in rats showed highly enriched pathways related to oxidative stress[144]. For VPA, the pathway amino sugar and nucleotide sugar metabolism[23], and for PQ, an increase in glutathione metabolism was observed which can be correlated to its toxic mechanism. PQ is reduced to a superoxide anion by a

Table 4 Description of the marker genes.

Gene name	Gene symbol	Gene information*
zgc:163022	100038777	oxidoreductase activity
cyp2k19	562304	members of this xenobiotic CYP family no known function no human homolog
zgc:158614	791218	cell redox homeostasis
zgc:101858	449555	oxidoreductase activity
sqrdl	550580	oxidoreductase activity
cyp4v7	562008	members of this xenobiotic CYP family less involvement in xenobiotic metabolism shares synteny with their human counterparts
cyp19a1b	60640	important in synthesis of cholesterol, steroids and other lipids important in estrogen biosynthesis human counterpart
cyp24a1	100004700	important in synthesis of cholesterol, steroids and other lipids important in vitamin D regulation part of the nuclear receptor in toxicity pathway human counterpart
impdh1b	338306	IMP dehydrogenase activity
cyp2aa3	386638	members of this xenobiotic CYP family induced by PXR agonists which are cytochrome P450 inducers to protect the body no human homolog
zgc:77778	406484	liver development
slc2a9l2	798023	glucose transporter
LOC100003115	100003115	unknown function human homolog gene is member of the Fc-receptor like family
LOC100535166	100535166	unknown function
pklr	114551	gluconeogenesis and glycolysis
scg5	393699	neuropeptide signaling
LOC100330229	100330229	unknown function
LOC100538043	100538043	unknown function
zgc:154142	555481	catalytic activity
tcap	556258	T-tubule organization

* Gene information was retrieved from NCBI PubMed Gene[80] and ZFIN[82]
Bold italic gene names indicate association with liver-specific processes

variety of enzymes leading to the production of reactive oxygen species (*in vitro* observation)[145].

Each compound was able to induce pathways relevant for hepatotoxicity. A caveat in our approach is that although producing specific hepatotoxicity, the selected exposure concentration may not be optimally represent the underlying mechanisms. However, the reference compounds were selected for their ability to induce specific phenotypical changes. Therefore, compounds were clustered by nominal (cholestasis, steatosis, necrosis) or by observed histopathological changes, (chromophobic, eosinophilic, and lipid vacuolization, and chromatin condensation). Neither of these two approaches produced overrepresented pathways. Grouping based on all hepatotoxicants versus non-hepatotoxicants revealed discriminative pathways, which overlapped with pathways that resulted from the gene expression analysis per compound. Based on the distinction between hepatotoxicants and non-hepatotoxicants, we aimed to identify a set of key genes for common hepatotoxicity that could be used for the prediction of the hepatotoxic potential of a compound. Ten up-regulated and ten down-regulated genes were identified as sensitive to toxicity based on a gene list ranked on fold change and the number of compounds inducing the gene (Fig. 3B). Functions of these genes and details per gene are summarized in Table 4. Although these genes were associated with hepatotoxicant exposure at concentrations inducing liver histopathology, this does not define their dysregulated expression as adverse per se. Some examples of detected genes that can be linked to adversity are *pklr*, which is a known marker for acute hepatotoxicity[146], and *zgc:77778*, which in case of downregulation (as observed) results in maldevelopment of the liver[147]. Furthermore, many detected genese are associated with oxidoreductase activity, which upon upregulation may cause oxidative stress and thus lead to cell injury. A link to adversity may not be obvious for all individual detected genes, but through these examples of adversity, the set as a whole may be considered as pathognomonic for liver injury.

In conclusion, our exposure study with known hepatotoxicants identified a set of marker genes that could be linked to pathways and processes involved in toxic responses in the liver. These markers and pathways/processes were associated with a general hepatotoxic response, whereas specific hepatotoxic phenotypes or classes could not be distinguished. The identified markers are suitable candidates to predict human hepatotoxicity, because they were anchored in responses induced by known hepatotoxicants in humans and/or traditional rodent models for human hepatotoxicity.

Acknowledgements

This study was supported by grant nr. 050-060-510 from the Netherlands Genomics Initiative/Netherlands Organization for Scientific Research (NOW) to the Netherlands Toxicogenomics Centre.

4

Gene and Protein Expression Markers of Hepatotoxicity in Zebrafish Embryo Model

Marja Driessen, Suzanne Duijvesteijn - van der Plas, Alexa P. Vitins, Anne S. Kienhuis, Jeroen L.A. Pennings, Evert-Jan van den Brandhof, Marianne Roodbergen, Bob van de Water, Herman P. Spaink, Magnus Palmblad, Leo T.M. van der Ven

In preparation

Abstract

The zebrafish embryo (ZFE) is a promising non-rodent model in toxicology, and initial studies suggested its applicability in detecting hepatotoxic responses. Here, we hypothesize that detailed analysis of underlying mechanisms of hepatotoxicity in ZFE contributes to the improved identification of hepatotoxic properties of new compounds and to the reduction of rodents used for hepatotoxicity assessment. ZFEs were exposed to nine reference hepatotoxicants, targeted at induction of cholestasis, steatosis and necrosis and two non-hepatotoxic controls. Protein profiles of the individual compounds were generated using LC-MS/MS. Regulation of single genes and pathways could be linked to hepatotoxic responses in general, but phenotype-specific responses could not be distinguished. While overrepresented processes were mainly associated with cellular adaptive stress-responses, individual proteins could be linked to hepatotoxicity-associated processes. This resulted in a set of possible protein markers, especially *glud1b, hspe1* and *anxa1c,* for the detection of hepatotoxicity in a high-throughput manner.

Introduction

The liver has a central role in the metabolism of xenobiotic substances in an organism, which includes biotransformation targeted at inactivation of toxic parent compounds. However, this biotransformation may also produce toxic reactive metabolites, leading to xenobiotic-induced liver injury[4,6]. Various underlying mechanisms can result in a wide range of xenobiotic-induced liver toxic phenotypes, of which cholestasis, steatosis and necrosis are most frequently observed. Cholestasis is a chronic condition and is phenotypically characterized by bile accumulation as a result of changes in intra- or extracellular bile flow or bile composition[34]. Steatosis may occur chronically as well and is characterized as an increase in cellular lipid content due to an increase in *de novo* synthesis of fatty acids or reduced lipid secretion or oxidation[19]. Necrosis is an acute condition and is characterized by cell death typically due to oxidative stress[4,33].

A challenge in toxicology is to predict hepatotoxic potential of compounds to which humans are exposed. There is an urging need to develop and validate alternative approaches, since the traditional *in vivo* rodent studies are associated with ethical (large numbers of animals need to be exposed), economical (high costs due to high doses and long experimental periods), and scientific issues (the obtained results might not be fully predictive for the effects in humans). As such, the ZFE is an alternative test model that may replace or support the traditional *in vivo* rodent studies. This model combines the benefits of an *in vivo* model, namely complete biological complexity including interactions between tissues and cells[49,54,95], with the advantages of *in vitro* model, that is, the ability for medium to high throughput testing.

The structure and the function of the liver in the adult zebrafish is similar to the mammalian liver[46], and a functional liver is present in the ZFE at three days post fertilization, which is therefore a suitable time point to start hepatotoxicity testing in this model. Furthermore, there is high genetic conservation between humans and zebrafish, including genes important for hepatotoxicity and biotransformation[46,55]. ZFEs express several cytochrome P450 enzymes, CYPs, which are grouped into the same families when compared to humans. In the zebrafish, the CYP families 1-4 are important for metabolizing xenobiotics, and these families are similar between the two species. In humans, the most important CYP responsible for catalyzing the majority of known drug-metabolizing reactions, namely CYP3A4, has an ortholog in the zebrafish, namely, *cyp3a65*[46,55].

In previous studies, we showed that the ZFE not only can be used to identify hepatotoxic responses using histopathology hepatotoxic-associated transcripts by next-generation sequencing (NGS)[133], but is also suitable for the identification of possible biomarkers for general hepatotoxicity by gene expression analysis[133]. Although gene expression analysis resulted in a possible list of biomarkers to predict hepatotoxicity in a high-through put manner, it does not allow to predict the protein concentration or activity from the measurement of mRNA levels[148]. Therefore proteomics analysis has become an additional

tool in understanding the underlying molecular mechanisms of hepatotoxicity while it provides quantitative information of molecular events at a more functional level. Therefore, to obtain full insight into the underlying mechanisms of hepatotoxicity, the proteomic changes are imperative information herein. Proteomics is frequently applied in the ZFE, but is mainly targeted at unraveling the developing proteome. The objective of this study was to identify proteomic signatures which describe hepatotoxic events in the ZFE. Specifically, it is hypothesized that distinct phenotypical classes of interest including cholestasis, steatosis and necrosis can be discerned by a specifically altered proteomics profile. Finally, we assessed whether we can define hepatotoxicity-associated proteomics markers to complement the changes as observed with gene expression after exposure to nine reference hepatotoxicants. These reference hepatotoxicants were confirmed to show hepatotoxic phenotypes in humans and rodent studies, namely cholestasis (cyclosporine A, chlorpromazine and 17α-ethinylestradiol)[1,15,134,135], steatosis (amiodarone, tetracycline and valproic acid)[23,136,137], and necrosis (acetaminophen, paraquat and thioacetamide)[1,4,33]. ZFEs were treated with the nine reference hepatotoxicants for 48 hours starting from three days post fertilization. Gene expression was performed as described previously[149] and the proteomics profiling was done by using liquid chromatography coupled with tandem mass spectometry.

Materials and methods

Chemicals. All tested chemicals (purity >95%), were purchased from Sigma Aldrich (Zwijndrecht, the Netherlands), and included acetaminophen (N-actyl-para-aminophenol; paracetamol; APAP, CAS no.103-90-2; 660 µM), paraquat (1,1'-Dimethyl-4,4'-bipyridinium dichloride; PQ, CAS no.1910-42-5; 3 mM), thioacetamide (CH3-C(S)NH2); TA, CAS no.62-55-5; 10 mM), amiodarone hydrochloride (2-butyl-3-benzofuranyl-4-[2-(diethylamino)ethoxy]-3,5-diiodophenyl ketone hydrochloride; AM, CAS no.19774-82-4; 10 µM), valproic acid (2-propylpentanoic acid sodium; VPA, CAS no.1069-66-5; 600 µM), tetracycline (TET, CAS no.64-75-5; 200 µM), cyclosporine A (CsA, CAS no.59865-13-3; 6 µM),17α- ethinylestradiol (17α-Ethinyl-1,3,5(10)-estratriene-3,17β-diol; EE2, CAS no.57-63-6; 3.5 µM), chlorpromazine (2-Chloro-10-(3-dimethylaminopropyl)phenothiazine hydrochloride; CPZ, CAS no.69-09-0; 3 µM), D-Mannitol (Mannite; DM, CAS no. 69-65-8; 3 mM), Lithium Carbonate (Carbonic acid lithium salt; Li_2CO_3, CAS no. 554-13-2; 1.1 mM) and tricaine methanesulfonate (MS-222, CAS no. 886-86-2). Dimethylsulfoxide (DMSO, CAS no. 67-68-5; 0.2%) was ordered from Fisher-Scientific.

Fish treatment. Wild-type zebrafish (*Danio rerio*) were originally obtained as commercially bred Singapore import (Ruinemans Aquarium BV, Montfoort, The Netherlands), which was maintained and bred in our facilities for more than 5 generations. Egg production was optimized by separation of the male and female fish before spawning, and female zebrafish were fed only thawed *Artemia naupli* prior to spawning. Egg predation was prevented by using a breeding tank with a perforated bottom, in which male and female zebrafish were paired in a 2:2 ratio before spawning. Spawning was triggered by morning light and was usually completed within 30 minutes. After spawning, the eggs were collected using a glass siphon and debris was removed to rinse the fertilized batches of eggs at least three times in Dutch Standard Water (DSW; demineralized water supplemented with $NaHCO_3$ (100 mg/l), $KHCO_3$ (20 mg/l), $CaCl_2{\cdot}2H_2O$ (200 mg/l), and $MgSO_4{\cdot}7H_2O$ (180 mg/l) which was then aerated for 24 h at 27°C). After rinsing, the fertilized eggs from different batches were pooled and placed in a petri dish in an incubator at 26.5 ± 1°C with a photoperiod of 14 hours light/10 hours dark. After 72 hours, hatched embryos were randomly distributed over 48-well plates in a density of 5 embryos per well in 1 ml test or control medium. Three concentrations per test compounds in at least three statistical replicates per concentration consisting of 2 wells (10 embryos) per replicate were used. In total, 12 conditions were tested including 9 human hepatotoxicants, two vehicle controls and one non-hepatotoxicant (Fig.1). The highest concentration that had no observed morphological or teratological effects and no mortality was used. At 120 hpf, the embryos were evaluated under a Leica Labovert FS microscope for deviations from normal development (e.g. delay in development, teratogenic effects) and indications of toxicity (e.g. abnormal swimming behavior) and snap frozen in liquid nitrogen to be used for proteomic analysis. Compound concentration during the 48 hours of exposure period was not analyzed, however, all compounds were indicated to be relatively stable according to NLM Hazardous Substances Database (http://toxnet.nlm.nih.gov/cgi-bin/sis/htmlgen?HSDB).
All procedures were done under licensed conditions for studies with laboratory animals, according to European and Dutch legislation.

Protein extraction and digestion. Protein extraction and digestion was adapted from Van der Plas-Duijvesteijn *et al.*[150] with some modifications. In short, at 120 hpf, 10 embryos from each control and treated groups were homogenized using 0.5 mm zirconium oxide beads and the Bullet Blender (Next Advance, New York, United States) and their proteomes were extracted using a lysis buffer containing 8 M urea, 75 mM NaCL, 50 mM Tris-HCl pH 8.2, 50 U/ml benzonase (E1014-5KU, Sigma-Aldrich), 2mM $MgCl_2$, and protease inhibitors (Complete ULTRA Tablets, mini, EDTA-free, Roche). The lysate was kept at 4°C for 30 minutes, after which it was centrifuged for 30 minutes at maximum speed (16,000×*g*) for another 30 minutes at 4°C. Total protein concentration was estimated by the use of a BCA assay (Product #23235, Bio-Rad) based on a bovine serum albumin as standard. In solution digest of the proteins was performed by adding 60 mM DTT to the protein lysate and incubated for 45 min at 56°C for cystines reduction. For alkylation and protection of the cystitis, 100 mM iodoacetamide was added to the sample and incubated for one hour at room temperature in the dark. Then, the protein mixture was diluted by adding 50 mM

ammonium bicarbonate. Next, the volume of the samples was reduced to 30 µl by centrifuging at room temperature for 30 minutes at 14000×*g* using the Millipore Amicon Centrifugal Filter ultra 0.5 (3,000 Da MWCO). The samples were collected by reversing the column in a new tube and centrifuging at 1000×*g* for 2 minutes. After this, sequencing-grade trypsin which specifically cleaves at the carboxylic side of lysine and arginine residues, was added to each sample to initiate digestion, and after overnight incubation, 10% TFA was added to quench the digestion producing peptides that are readily identified by mass spectometry. Samples were centrifuged at 2,500×*g* for 10 minutes at room temperature; where after, supernatant was transferred to a fresh tube. Peptide digests were stored at -80°C until further analysis.

Liquid chromatography - Tandem Mass Spectrometry. As previously described, two µl of each sample was loaded and desalted on a C18 PepMap 300 µm, 5 mm-i.d., 300 Å precolumn (Thermo Scientific) and separated by reversed-phase liquid chromatography using two identical 150 mm 0.3 mm–i.d. ChromXP C18CL, 120 Å columns (Eksigent, Dublin, CA, USA) coupled parallel and connected to a split less NanoLC-Ultra 2D plus system (Eksigent) with a linear 90-minute gradient from 4% to 35% acetonitrile in 0.05% formic acid and a constant (4 µL/minute) flow rate. The LC system was coupled to an amaZon speed ETD ion trap (Bruker Daltonics, Bremen, Germany) equipped with an Apollo II ESI source. After each MS scan, up to 10 abundant multiply charged species in *m/z* 300-1300 were selected for MS/MS and actively excluded for one minute after having been selected twice. Each individual scan or tandem mass spectrum was saved to the hard drive. The LC system was controlled by HyStar 3.2 and the ion trap by trapControl 7.1.

Data analysis

Data processing. Raw LC-MS/MS data were converted to line spectra mzXML[151] files with the Bruker compassXport tool version 3.05. All further data processing was done with the Trans-Proteomic Pipeline 4.6 rev 3[90,152]. Database search was performed with X!Tandem (2009.10.01.1)[90,153] using the following parameters: precursor mass tolerance window was set between -2.0 and 4.0 Da, while fragment tolerance was set to 0.4 Da, modifications were set for carbamidomethylation of cysteine and oxidation of methionine, k-scoring was enabled, maximum missed cleavages was set to 2 and scoring was done for *b* and *y* ions. The X!Tandem output files were converted to pepXML file format with tandem2xml without applying any cut-offs. X!Tandem pepXML files were merged into PeptideProphet and analyzed with the decoy option enabled[154]. The resulting posterior probabilities for the peptide spectrum matches were further refined by iProphet [155]. Finally, ProteinProphet was used to compute a probability that each protein was present in the sample and to estimate a global false discovery rate (FDR). ProteinProphet output was filtered using the probability threshold that corresponded to an FDR < 1% and proteins with an individual probability of zero were discarded. Filtered protein lists were combined[90,153].

Protein expression analysis. Following our hypothesis, the basis for protein expression analysis was histopathological clustering. Clusters were based either on the phenotype as observed in humans after compound exposure (referred to as nominal phenotype) or on actual observed histopathology (observed phenotype) (detailed information can be found in Driessen *et al*.[133,149]. The nominal phenotype clusters included three classes, namely cholestasis (CPZ, CsA and EE2), steatosis (AM, TET and VPA) and necrosis (APAP, PQ and TAA). The observed phenotypes consisted of four clusters; (1) lipid vacuolization (AM, CPZ and VPA), (2) chromatin condensation (CPZ, EE2, and PQ), (3) chromophobic vacuolization (CsA, EE2, PQ and TAA) and (4) eosinophilic vacuolization (CPZ, CsA, TET and APAP). Overrepresented proteins were determined using a two group-comparison with a $p < 0.05$ in QluCore Omics Explorer (Qlucore AB, Lund, Sweden). Phenotypic clusters were based on either nominal phenotype or observed phenotype and overrepresented pathways per cluster were determined using STITCH with FDR < 0.05[91–94] (Table 1).

Marker protein selection. To detect commonly induced proteins between hepatotoxic compounds, the protein expression values for the highest concentration of each compound were analysed by correcting for negative controls. Proteins with an apparent absolute FC > 1.5 were considered to be differentially expressed and were ranked on the number of compounds regulating the proteins. General hepatotoxicity markers were defined as proteins induced by at least six compounds and FC > 1.5.

Match of transcript and protein expression. Gene expression was obtained from a previous study[149] and matched with the observed proteins in this study. Protein names from UniProt were matched against the microarray transcripts gene IDs[156]. This resulted in a set of 402 proteins/genes. Next, the expression between the gene-protein was matched, whereby the protein should have a FC > 1.5.

Results

Basic proteomics observations. In the present study in total we identified 287,000 Peptide-Spectrum Matches (PSMs) corresponding to 3,461 unique peptides and 1,258 unique proteins with 1% FDR. From these 1,258 proteins identified, 1,012 proteins were present in at least two samples.

Hepatotoxicity-associated pathways. A general view of the enriched pathways based on the 1012 identified proteins revealed enrichment in many biological processes including translation, gene expression and cellular metabolic process (Table 1). The enriched biological processes shared similarities based on single protein levels, whereas for example the protein *rpl4* is present in 18 different biological processes.

Table 1 Description of the marker genes.

Phenotype	GO_id	Term	Number of Genes	p-value	p-value_fdr	p-value_ bonferroni
necrosis	GO:0006412	translation	13	4,34E-14	2,54E-10	2,54E-10
	GO:0044267	cellular protein metabolic process	17	1,09E-07	3,17E-04	6,34E-04
	GO:0010467	gene expression	17	4,96E-07	8,04E-04	2,90E-03
	GO:0044249	cellular biosynthetic process	16	7,03E-07	8,04E-04	4,10E-03
	GO:0034645	cellular macromolecule biosynthetic process	14	9,19E-07	8,04E-04	5,36E-03
	GO:1901576	organic substance biosynthetic process	16	9,34E-07	8,04E-04	5,45E-03
	GO:0009059	macromolecule biosynthetic process	14	9,64E-07	8,04E-04	5,63E-03
	GO:0009058	biosynthetic process	16	1,58E-06	1,16E-03	9,24E-03
	GO:0019538	protein metabolic process	17	3,83E-06	2,48E-03	2,23E-02
	GO:0008152	metabolic process	26	1,33E-05	7,76E-03	7,76E-02
	GO:0044237	cellular metabolic process	22	2,66E-05	1,41E-02	1,55E-01
	GO:0044260	cellular macromolecule metabolic process	18	6,42E-05	3,13E-02	3,75E-01
	GO:0044238	primary metabolic process	22	9,21E-05	4,13E-02	5,37E-01
cholestasis	GO:0006412	translation	10	1,94E-11	1,13E-07	1,13E-07
	GO:0044249	cellular biosynthetic process	13	1,50E-06	2,78E-03	8,77E-03
	GO:0044267	cellular protein metabolic process	13	1,54E-06	2,78E-03	9,00E-03
	GO:1901576	organic substance biosynthetic process	13	1,91E-06	2,78E-03	1,11E-02
	GO:0009058	biosynthetic process	13	2,98E-06	3,48E-03	1,74E-02
	GO:0034645	cellular macromolecule biosynthetic process	11	5,21E-06	4,52E-03	3,04E-02
	GO:0009059	macromolecule biosynthetic process	11	5,42E-06	4,52E-03	3,16E-02
	GO:0019538	protein metabolic process	13	2,49E-05	1,74E-02	1,45E-01
	GO:0006189	'de novo' IMP biosynthetic process	2	2,93E-05	1,74E-02	1,71E-01
	GO:0008152	metabolic process	20	3,01E-05	1,74E-02	1,75E-01
	GO:0010467	gene expression	12	3,27E-05	1,74E-02	1,91E-01
Steatosis	GO:0006412	translation	12	3,86E-13	2,25E-09	2,25E-09
	GO:0034645	cellular macromolecule biosynthetic process	13	1,90E-06	3,87E-03	1,11E-02
	GO:0009059	macromolecule biosynthetic process	13	1,99E-06	3,87E-03	1,16E-02
	GO:0010467	gene expression	15	4,27E-06	6,24E-03	2,49E-02
	GO:0044249	cellular biosynthetic process	14	6,86E-06	8,01E-03	4,01E-02
Lipid	GO:0006412	translation	11	3,42E-12	2,00E-08	2,00E-08
Vacuolization	GO:0010467	gene expression	18	1,54E-09	4,49E-06	8,99E-06
	GO:0044267	cellular protein metabolic process	15	2,38E-07	4,58E-04	1,39E-03
	GO:0044260	cellular macromolecule metabolic process	19	3,34E-07	4,58E-04	1,95E-03
	GO:0034645	cellular macromolecule biosynthetic process	13	5,11E-07	4,58E-04	2,98E-03
	GO:0009059	macromolecule biosynthetic process	13	5,34E-07	4,58E-04	3,12E-03
	GO:0043170	macromolecule metabolic process	20	5,50E-07	4,58E-04	3,21E-03
	GO:0019538	protein metabolic process	16	9,31E-07	6,79E-04	5,43E-03
	GO:0044237	cellular metabolic process	21	1,66E-06	1,08E-03	9,71E-03
	GO:0009058	biosynthetic process	14	3,51E-06	2,05E-03	2,05E-02
	GO:0044238	primary metabolic process	21	6,13E-06	3,26E-03	3,58E-02
	GO:0008152	metabolic process	23	8,16E-06	3,97E-03	4,76E-02
	GO:0071704	organic substance metabolic process	21	9,18E-06	4,12E-03	5,36E-02
	GO:0044249	cellular biosynthetic process	13	1,11E-05	4,62E-03	6,47E-02
	GO:1901576	organic substance biosynthetic process	13	1,39E-05	5,42E-03	8,13E-02

Table 1 Continued.

Phenotype	GO_id	Term	Number of Genes	p-value	p-value_fdr	p-value_ bonferroni
Eosinophilic vacuolization	GO:0030163	protein catabolic process	8	1,26E-09	7,38E-06	7,38E-06
	GO:1901575	organic substance catabolic process	11	5,44E-09	1,52E-05	3,17E-05
	GO:0009056	catabolic process	11	1,18E-08	1,52E-05	6,91E-05
	GO:0051603	proteolysis involved in cellular protein catabolic process	7	1,35E-08	1,52E-05	7,88E-05
	GO:0044257	cellular protein catabolic process	7	1,52E-08	1,52E-05	8,86E-05
	GO:0009057	macromolecule catabolic process	8	1,56E-08	1,52E-05	9,11E-05
	GO:0044265	cellular macromolecule catabolic process	7	9,62E-08	8,03E-05	5,62E-04
	GO:0044248	cellular catabolic process	9	2,78E-07	2,03E-04	1,62E-03
	GO:0044238	primary metabolic process	21	2,56E-06	1,66E-03	1,49E-02
	GO:0009117	nucleotide metabolic process	7	3,17E-06	1,77E-03	1,85E-02
	GO:0006753	nucleoside phosphate metabolic process	7	3,33E-06	1,77E-03	1,94E-02
	GO:0071704	organic substance metabolic process	21	3,86E-06	1,88E-03	2,26E-02
	GO:0044237	cellular metabolic process	20	4,26E-06	1,91E-03	2,49E-02
	GO:0009150	purine ribonucleotide metabolic process	6	4,85E-06	2,02E-03	2,83E-02
	GO:0006163	purine nucleotide metabolic process	6	5,50E-06	2,14E-03	3,21E-02
	GO:0019693	ribose phosphate metabolic process	6	6,81E-06	2,34E-03	3,97E-02
	GO:0009259	ribonucleotide metabolic process	6	6,81E-06	2,34E-03	3,97E-02
	GO:0055086	nucleobase-containing small molecule metabolic process	7	7,34E-06	2,38E-03	4,29E-02
Chromophobic condensation	GO:0006412	translation	10	1,31E-14	7,67E-11	7,67E-11
	GO:0034645	cellular macromolecule biosynthetic process	10	5,33E-08	1,08E-04	3,11E-04
	GO:0009059	macromolecule biosynthetic process	10	5,54E-08	1,08E-04	3,23E-04
	GO:0010467	gene expression	11	1,26E-07	1,84E-04	7,37E-04
	GO:0019538	protein metabolic process	11	5,64E-07	6,07E-04	3,29E-03
	GO:0044249	cellular biosynthetic process	10	7,12E-07	6,07E-04	4,16E-03
	GO:0044267	cellular protein metabolic process	10	7,27E-07	6,07E-04	4,25E-03
	GO:1901576	organic substance biosynthetic process	10	8,67E-07	6,32E-04	5,06E-03
	GO:0009058	biosynthetic process	10	1,25E-06	8,11E-04	7,30E-03
Chromatin condensation	GO:0006412	translation	7	1,49E-07	8,68E-04	8,68E-04

Phenotype clustering. The basis for our current protein expression analysis was the association with histopathological clustering. Clusters were based either on the phenotype as observed in humans after compound exposure (referred to as nominal phenotype) or on actual observed histopathology (observed phenotype). To determine whether the phenotypes, nominal or observed, specifically defined processes, a phenotype-directed analysis was performed. For each specific cluster, a set of discriminating proteins was identified and this set was used for the determination of enriched processes. For the nominal phenotypes, the cluster necrosis resulted in 13 enriched biological processes, steatosis only in 5 biological processes and cholestasis resulted in 11 enriched biological processes. For the observed phenotypes, chromatin condensation resulted in one enriched biological process, whereas lipid vacuolization, eosinophilic vacuolization and chromophobic condensation resulted in 15, 18, and 9 enriched biological process, respectively (see Table 1). It should be noted that much overlap was present in the enriched biological processes, for example the biological process "translation" was enriched in each cluster

# compounds	# of proteins	Regulation
9	13	DOWN
8	41	DOWN
7	77	DOWN
6	94	DOWN
6	102	UP
7	54	UP
8	19	UP
9	2	UP

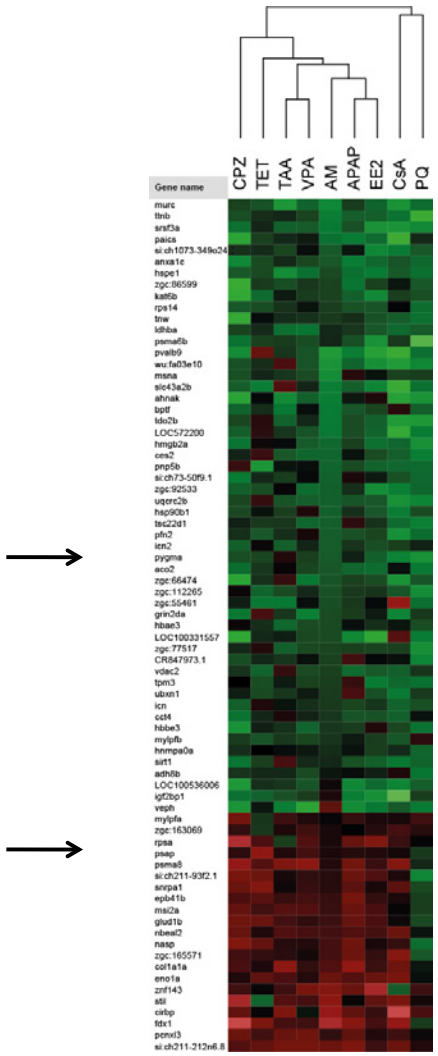

Figure 1 Ranking of the regulated proteins.
Heatmap - regulated proteins per compound were determine using FC > 1.5 and regulation of the protein by at least 6 compounds. Table - indicates the number of proteins regulated by the number of compounds.

except eosinophilic vacuolization (Table 1). The phenotype steatosis completely overlapped with the phenotypes necrosis and cholestasis based on enriched processes, whereas there were three necrosis specific processes and one for steatosis. For the observed phenotypes, eosinophilic vacuolization had 15 specific enriched processes and only shared 3 processes with lipid vacuolization phenotype. The other three observed phenotypes overlap based on the enriched processes (Fig.1) indicating that the ZFE is not able to discriminate between the different hepatotoxic classes using proteomics.

Overlap phenotypes/common hepatotoxicity. Since phenotype-specific processes could not be identified due to large overlap of enriched processes, all hepatotoxicants were grouped together, corrected for the negative controls, and ranked on FC and the number of compounds inducing the protein to identify markers for general hepatotoxicity. This resulted in 427 proteins of the total of 1258 proteins detected having a FC > 1.5 and being modulated by 6 or more compounds. Using these 427 proteins, enriched processes were determined and resulted in 15 up-regulated processes and 10 down-regulated processes. The common up-regulated biological processes included, for example, some relevant processes including translation, gene expression and metabolic processes. Common down-regulated processes included, for example, translation and protein folding (See Table 2) (Supplementary tables 1 and 2 for individual proteins per process).

Identification of common hepatotoxicity marker proteins. Next, we determined marker proteins for common hepatotoxicity. The 427 proteins related to general hepatotoxicity were ranked on FC and the number of compounds inducing the specific protein. A cluster analysis separated proteins into two groups, first CsA and PQ in one group and all the others in the second group (Fig. 2) suggesting that CsA and PQ induce the common proteins to a lesser extent. For the upregulated proteins, two proteins were regulated by all 9 compounds which included *pcnxl3* and *si:ch211-212n6.8*. There were 19 proteins induced by eight compounds and these proteins were *mylpfa, zgc:163069, rpsa, psap, psma8, si:ch211-93f2.1, snrpa1, epb41b, msi2a , glud1b, nbeal2, naps, zgc:165571, col1a1a, eno1a, znf143, still, cirbp* and *fdx1* (Fig.2, table 3).
For the downregulated proteins, 13 proteins were induced by nine compounds and 41 were induced by eight compounds. The 13 proteins induced by nine compounds included *murc, ttnb, srsf3a, paics, si:ch1073-349o24.2, anxa1c, hspe1, zgc:86599, kat6b, rps14, tnw, ldhba* , and *psma6b* (Fig.2, table 3).

Table 2

	GO_id	Term	NumberOfGenes	p-value	p-value_fdr	p-value_ bonferroni
UP	GO:0006412	translation	21	5,18E-19	3,03E-15	3,03E-15
	GO:0010467	gene expression	32	4,41E-10	1,29E-06	2,58E-06
	GO:0044237	cellular metabolic process	46	6,04E-09	1,18E-05	3,53E-05
	GO:0044249	cellular biosynthetic process	28	1,66E-08	2,42E-05	9,69E-05
	GO:1901576	organic substance biosynthetic process	28	2,62E-08	3,06E-05	1,53E-04
	GO:0008152	metabolic process	52	5,24E-08	5,10E-05	3,06E-04
	GO:0009058	biosynthetic process	28	6,12E-08	5,10E-05	3,57E-04
	GO:0044267	cellular protein metabolic process	27	7,54E-08	5,51E-05	4,40E-04
	GO:0034645	cellular macromolecule biosynthetic process	23	1,29E-07	8,09E-05	7,53E-04
	GO:0009059	macromolecule biosynthetic process	23	1,39E-07	8,09E-05	8,09E-04
	GO:0042274	ribosomal small subunit biogenesis	4	1,32E-06	7,02E-04	7,72E-03
	GO:0071704	organic substance metabolic process	44	1,62E-06	7,87E-04	9,44E-03
	GO:0044238	primary metabolic process	43	2,47E-06	1,11E-03	1,44E-02
	GO:0019538	protein metabolic process	28	3,16E-06	1,32E-03	1,85E-02
	GO:0044260	cellular macromolecule metabolic process	33	7,36E-06	2,86E-03	4,30E-02
DOWN	GO:0006412	translation	19	2,20E-12	1,28E-08	1,28E-08
	GO:0006457	protein folding	13	6,13E-11	1,79E-07	3,58E-07
	GO:0044267	cellular protein metabolic process	39	4,06E-09	7,91E-06	2,37E-05
	GO:0019538	protein metabolic process	44	1,40E-08	2,05E-05	8,20E-05
	GO:0044238	primary metabolic process	66	7,96E-08	9,30E-05	4,65E-04
	GO:0044237	cellular metabolic process	62	1,98E-07	1,73E-04	1,15E-03
	GO:0071704	organic substance metabolic process	66	2,07E-07	1,73E-04	1,21E-03
	GO:0008152	metabolic process	74	2,62E-07	1,91E-04	1,53E-03
	GO:0043170	macromolecule metabolic process	52	5,46E-06	3,54E-03	3,19E-02
	GO:0044260	cellular macromolecule metabolic process	47	6,68E-06	3,90E-03	3,90E-02

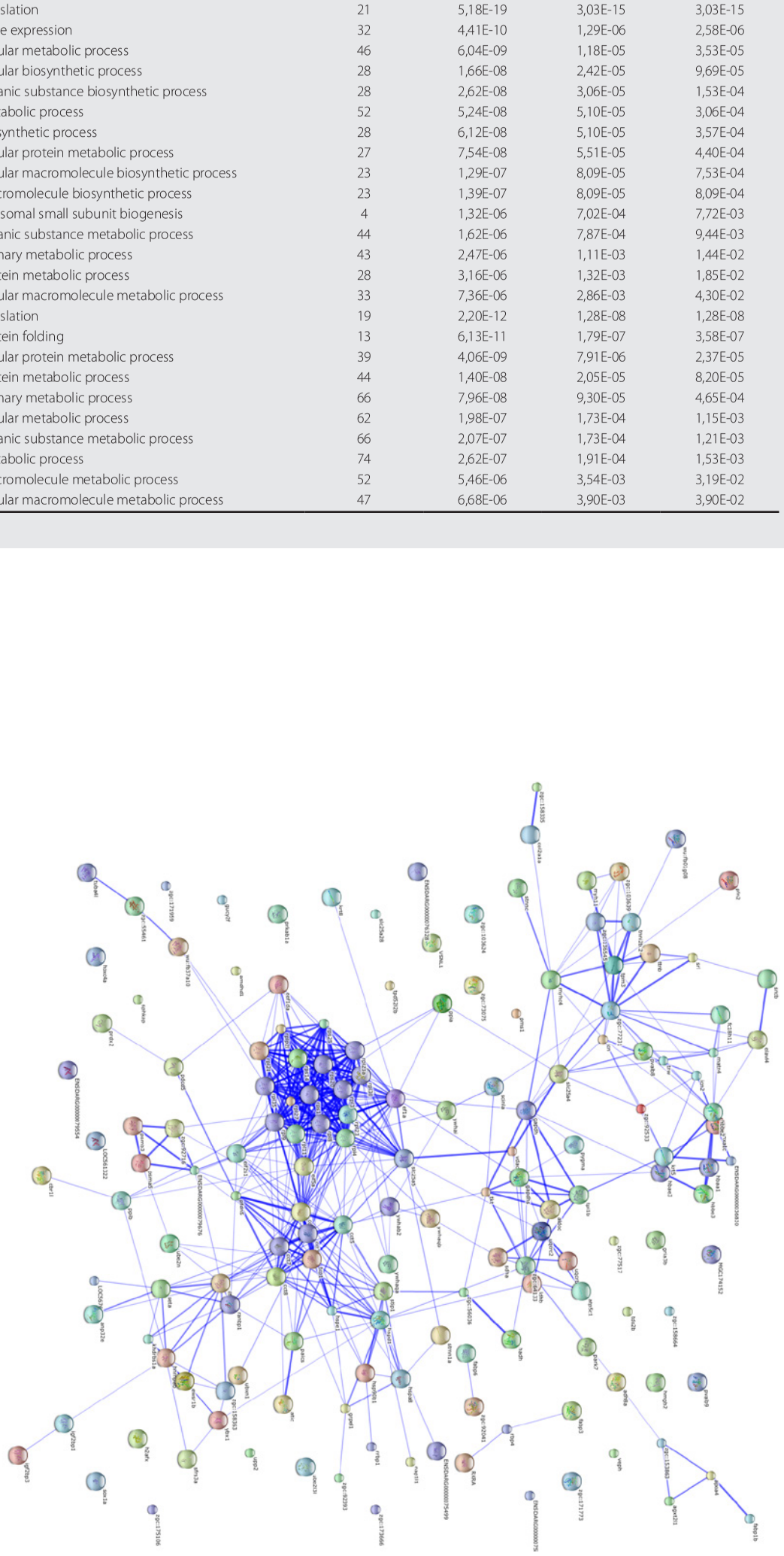

Figure 2 STRING network representation of the down regulated proteins.
STRING network representation of the 402 proteins identified as having a FC > 1.5 and by regulated by more than 6 compounds. Blue lines indicate connects between the proteins.

Table 3

Protein ID	Gene ID	Gene Name	Cluster	Human GeneID	Human Symbol	AM	APAP	CPZ	CsA	EE2	PQ	TAA	TET	VPA	Sum down	Sum Up
A1L260	552940	murc	cell differentiation, muscle organ development, regulation of transcription DNA dependent, transcription DNA dependent		NA	-2,23756	-0,66	-0,77	-2,52	-1,42	-1,58	-2,65	-1,07	-1,40	9	0
B0S6Y0	100333283	ttnb	titin b		NA	-2,00178	-1,29	-0,98	-1,77	-1,30	-3,33	-0,36	-0,43	-0,80	9	0
Q801U3	368925	srsf3a	nucleic acid binding		NA	-1,88251	-1,01	-1,67	-2,55	-2,52	-2,27	-1,34	-0,31	-1,24	9	0
Q7ZUN6	321193	paics	phosphoribosylaminoimidazole carboxylase, phosphoribosylaminoimidazole succinocarboxamide synthetase	10606	PAICS	-1,72851	-1,98	-3,05	-3,41	-1,57	-0,38	-0,36	-0,75	-0,19	9	0
E9QCL0	100333283	si:ch1073-349o24.2		255101	CCDC108	-1,22398	-0,16	-0,51	-1,93	-2,21	-1,17	-0,80	-0,40	-0,08	9	0
Q804H0	494158	anxa1c	annexin A1c		NA	-1,17645	-1,99	-2,24	-1,10	-1,49	-1,48	-0,39	-0,92	-0,86	9	0
Q6IQI7	58041	hspe1	heat shock 10 protein 1 (chaperonin 10)	3336	HSPE1	-0,89881	-1,72	-1,19	-1,20	-1,97	-1,69	-2,38	-0,91	-1,73	9	0
F1RCH5	415253	zgc:86599	zgc:86599	1329	COX5B	-0,78497	-1,80	-3,29	-0,16	-0,76	-1,18	-0,98	-0,64	-0,59	9	0
B7ZD47	568932	kat6b	nucleosome assembly, nucleosome, nucleus, DNA binding, zinc ion binding	23522	KAT6B	-0,77977	-1,35	-3,21	-0,73	-2,27	-1,01	-0,19	-1,57	-0,69	9	0
Q6PBW3	336687	rps14	ribosomal protein S14	6208	RPS14	-0,66654	-1,05	-1,20	-0,01	-1,06	-1,62	-0,49	-0,96	-0,12	9	0
B0S6K6	30234	tnw	ECM-Receptor interaction, Focal adhesion		NA	-0,61845	-0,45	-3,22	-1,26	-1,06	-1,66	-0,41	-0,06	-0,48	9	0
Q9PVK4	30497	ldhba	Cellular carbohydrate metabolic process, glycolysis, cytoplasm, L-lactate dehydrogenase activity		NA	-0,35410	-0,57	-0,79	-1,53	-1,16	-1,24	-1,66	-0,40	-1,81	9	0
Q6DGY8	436862	psma6b	proteasome (prosome, macropain) subunit, alpha type, 6b	5687	PSMA6	-0,33796	-1,02	-1,77	-0,59	-2,49	-4,01	-0,66	-0,75	-0,96	9	0
Q800A1	360209	pvalb9	parvalbumin 9	654231	OCM	-2,71063	-2,01	-2,35	-3,33	-2,92	-1,66	-0,57	1,51	-1,10	8	1
E7F4A4	100004231	wu:fa03e10			NA	-2,53285	-1,41	-1,03	-2,77	-2,40	-2,22	1,01	-0,44	-1,09	8	1
Q66I42	286739	msna	blood vessel lumenization, endoderm development, cytoplasm, cytoskeleton, extrinsic to membrane	4478	MSN	-2,35953	0,45	-1,00	-0,76	-0,12	-0,69	-0,56	-0,33	-0,95	8	1
F1QCB3	494042	slc43a2b	integral to membrane, L-amino acid transmembrane transporter activity	124935	SLC43A2	-2,03292	-1,30	-1,28	-3,29	-2,13	-1,73	1,11	-2,03	-0,33	8	1
F1R1J9	559276	ahnak	oxidoreductase activity	79026	AHNAK	-2,00947	-0,17	-2,99	-2,90	0,30	-2,55	-2,31	-0,03	-1,35	8	1
E7F366	324479	bptf	zinc ion binding	2186	BPTF	-1,93982	-1,13	-1,41	0,44	-0,81	-1,30	-1,88	-0,42	-0,09	8	1
Q7SY53	334082	tdo2b	tryptophan 2,3-dioxygenase b		NA	-1,90317	-0,95	-0,85	-2,71	-1,32	-2,69	-1,37	0,44	-0,37	8	1
F1RA03	572200	LOC572200	similar to vimentin		NA	-1,87826	-0,94	-1,28	-3,23	-1,40	-1,94	-0,56	0,46	-1,08	8	1
B8JL29	641484	hmgb2a		3148	HMGB2	-1,50086	-0,74	-1,78	-1,45	-1,66	-2,43	-0,05	0,15	-1,25	8	1
Q6GMJ1	566132	ces2	hydrolase activity	8824	CES2	-1,44611	-0,12	-0,29	-1,30	-0,95	-2,03	-1,18	0,69	-1,46	8	1
F1QD81	447889	pnp5b	nucleoside metabolic process, purine-nucleoside phosphorylase activity		NA	-1,42661	-0,92	0,66	-1,49	-1,39	-1,55	-0,12	-2,61	-0,08	8	1
F8W4A8	567855	si:ch73-50f9.1	integral to membrane		NA	-1,38696	0,27	-1,97	-1,03	-0,17	-1,50	-0,71	-0,35	-0,04	8	1
Q6DHB6	445051	zgc:92533	zgc:92533	3872	KRT17	-1,35638	-0,45	-1,30	-2,07	-2,35	-1,47	0,06	-0,96	-1,58	8	1
Q6IQ59	322549	uqcrc2b	proteolysis, metal ion binding, metalloendopeptidase activity	7385	UQCRC2	-1,33726	-1,12	-0,84	-2,45	-1,15	-2,17	-1,08	0,63	-1,27	8	1
Q7T3L3	386590	hsp90b1	heat shock protein 90, beta (grp94), member 1	7184	HSP90B1	-1,31686	-0,45	-0,88	-2,02	-1,16	-0,94	-0,72	-0,10	0,30	8	1
F1R1Z6	335842	tsc22d1	zgc:85857	8848	TSC22D1	-1,30107	0,52	-0,26	-1,56	-0,51	-2,07	-0,58	-0,61	-1,47	8	1
Q802D5	394235	pfn2	profilin 2	5217	PFN2	-1,28425	-1,05	-0,45	-2,42	-0,80	-1,63	-0,46	-1,15	0,22	8	1
A3FKT8	100005083	icn2	ictacalcin 2	6275	S100A4	-1,25978	-0,53	-1,30	-0,74	-0,97	-0,28	-1,29	0,12	-0,33	8	1
Q503C7	553655	pygma	carbohydrate metabolic process, glycogen phosphorylase activity, pyridoxal phosphate binding	5837	PYGM	-1,24654	-0,25	-0,99	-2,11	-1,33	-2,48	0,36	-0,83	-0,75	8	1

Table 3 Continued

Protein ID	Gene ID	Gene Name	Cluster	Human GeneID	Human Symbol	AM	APAP	CPZ	CsA	EE2	PQ	TAA	TET	VPA	Sum down	Sum Up
F8W4M7	322670	aco2	aconitase 2, mitochondrial	50	ACO2	-1,16415	-1,46	-1,62	-0,10	-1,58	-1,89	0,06	-0,57	-0,83	8	1
F1QXH7	327500	zgc:66474	zgc:66474		NA	-1,11214	-0,75	-3,03	-2,52	-0,94	-1,12	0,63	-0,48	-1,86	8	1
H9GX84	100003906	zgc:112265		3700	ITIH4	-1,04245	-0,61	0,11	-1,12	-0,53	-2,37	-0,95	-1,44	-0,37	8	1
Q6IQJ2	767806	zgc:55461	zgc:55461; zgc:123194; zgc:153264; zgc:123292; tubulin, beta 2c; zgc:153426		NA	-0,99582	-0,59	-0,22	2,65	-0,04	-1,69	-1,90	-1,89	-0,07	8	1
I3NI77	449864	grin2da	ionotropic glutamate receptor signaling pathway, cell junction, integral to membrane, outer membrane-bounded periplasmic space, plasma membrane, postsynaptic membrane, extracellular-glutamate-gated ion channel activity, ionotropic glutamate receptor activity	2906	GRIN2D	-0,92925	-0,67	-1,86	-2,17	-0,21	-0,60	-0,58	0,92	-2,08	8	1
Q7ZYZ4	30601	hbae3	hemoglobin alpha embryonic-3		NA	-0,91220	-0,07	0,12	-0,14	-0,44	-0,94	-1,50	-0,44	-0,94	8	1
F1QW57	100331557	LOC100331557		0	NA	-0,89687	-2,25	-3,14	1,20	-3,15	-1,95	-0,23	-0,34	-0,87	8	1
A8E5I2	393540	zgc:77517	zgc:77517	3875	KRT18	-0,79947	-0,75	-0,36	-0,75	-0,79	-2,38	-1,33	0,39	-0,89	8	1
E7EYE1	565428	CR847973.1			NA	-0,76208	0,85	-0,96	-0,10	-0,02	-2,16	-0,55	-0,37	-0,09	8	1
Q8AWD0	322126	vdac2	voltage-dependent anion channel 2	7417	VDAC2	-0,75896	-1,56	-0,52	-1,31	-1,17	-0,54	0,60	-1,40	-0,90	8	1
Q803M1	373076	tpm3		7170	TPM3	-0,70343	0,65	-0,00	-1,49	-1,94	-1,73	-0,20	-0,96	-0,78	8	1
Q6NXA9	322073	ubxn1	negative regulation of proteasomal ubiquitin-dependent protein catabolic process, negative regulation of protein ubiquitination, cytoplasm, K6 linked polyubiquitin binding	51035	UBXN1	-0,64131	0,97	-0,22	-1,92	-1,02	-0,62	-0,56	-0,90	-0,19	8	1
Q6XG62	336655	icn	ictacalcin	6275	S100A4	-0,61938	-0,83	-1,29	-1,39	-0,56	-1,00	-0,12	0,33	-0,45	8	1
Q6PH46	393555	cct4	chaperonin containing TCP1, subunit 4 (delta)	10575	CCT4	-0,56944	-1,07	-1,76	-1,35	-1,06	-0,11	0,28	-0,33	-0,29	8	1
Q5BLF6	30596	hbbe3	hemoglobin beta embryonic-3	3046	HBE1	-0,56314	-0,67	-2,49	-0,85	0,35	-1,76	-0,48	-0,25	-1,43	8	1
Q66I73	447930	mylpfb	calcium ion binding	29895	MYLPF	-0,53469	-0,19	-0,66	-1,13	-0,68	0,51	-0,59	-1,07	-0,83	8	1
F1QS28	323529	hnrnpa0a	nucleic acid binding, nucleotide binding	10949	HNRNPA0	-0,41444	-0,11	-0,45	-0,39	-0,71	-1,48	-0,06	0,00	-0,16	8	1
E7F8W3	797132	sirt1	cell migration involved in sprouting angiogenesis, NAD+ binding	23411	SIRT1	-0,34615	-1,03	-1,80	-1,87	-1,29	-1,41	0,94	-0,73	-0,38	8	1
Q7T2J4	402841	adh8b	alcohol dehydrogenase 8a; alcohol dehydrogenase 8b		NA	-0,15260	-0,07	-0,54	0,32	-0,27	-1,82	-0,35	-0,38	-0,90	8	1
H9GYZ0	100536006	LOC100536006			NA	0,15408	-2,22	-2,70	-2,13	-1,57	-1,27	-0,55	-0,46	-1,12	8	1
Q08CK7	558182	igf2bp1	insulin-like growth factor 2 mRNA binding protein 1	10642	IGF2BP1	0,28011	-2,02	-1,73	-4,29	-2,39	-0,71	-1,03	-1,37	-0,68	8	1
A2BID5	405756	veph	brain development, ear morphogenesis, plasma membrane, phospholipid binding	79674	VEPH1	1,39680	-2,32	-2,62	-1,22	-1,88	-1,91	-2,05	-0,15	-3,04	8	1
O93409	30429	mylpfa	calcium ion binding	29895	MYLPF	0,05979	0,58	1,83	0,23	0,27	0,81	0,72	-0,54	0,34	1	8
F1R2V7	100038785	zgc:163069	zgc:163069; wu:fj55c09; zgc:111961		NA	0,22677	0,02	0,60	0,91	0,41	0,46	0,30	-0,59	0,81	1	8
Q803F6	394027	rpsa	ribosomal protein SA	3921	RPSA	0,24968	1,50	3,35	0,68	2,12	0,03	-0,73	1,01	1,10	1	8
F1QMF5	140811	psap	sphingolipid metabolic process, lysosome	5660	PSAP	0,27516	0,41	0,52	0,20	0,37	-0,60	0,35	2,43	0,90	1	8
Q6P0I2	406445	psma8	proteasome (prosome, macropain) subunit, alpha type, 8	143471	PSMA8	0,36309	1,81	2,61	2,14	0,68	-0,36	2,10	1,15	2,40	1	8
F1QLQ9	561967	si:ch211-93f2.1	carboxylesterase activity		NA	0,42594	1,65	1,91	0,29	1,05	-2,18	0,23	1,67	0,56	1	8
F1R300	492511	snrpa1		6627	SNRPA1	0,43642	1,31	1,63	1,31	0,25	-0,87	0,17	2,15	0,63	1	8

Table 3 Continued

Protein ID	Gene ID	Gene Name	Cluster	Human GeneID	Human Symbol	AM	APAP	CPZ	CsA	EE2	PQ	TAA	TET	VPA	Sum down	Sum Up
Q8JG61	326287	epb41b	cortical actin cytoskeleton organization, embryonic hemopoiesis, erythrocyte differentiation, cytoplasm, cytoskeleton, extrinsic to plasma membrane, calmodulin binding		NA	0,63215	1,88	1,01	0,26	0,61	-0,70	0,65	1,24	0,87	1	8
Q7ZW10	100002680	msi2a	musashi homolog 2a (Drosophila)	124540	MSI2	0,65499	1,56	1,48	0,04	0,96	-0,68	1,19	0,82	1,14	1	8
Q6P3L9	373092	glud1b	zgc:192851; glutamate dehydrogenase 1b	2747	GLUD2	0,71978	1,51	1,78	0,14	0,97	-0,87	0,84	1,58	0,53	1	8
E7FAW3	100330830	nbeal2	endoplasmic reticulum	23218	NBEAL2	0,85297	1,10	1,55	1,63	0,91	-0,14	1,11	0,33	0,95	1	8
F1QNE0	799570	nasp	nuclear autoantigenic sperm protein (histone-binding)	4678	NASP	0,86559	1,74	2,13	0,61	0,24	-1,61	0,41	1,44	0,39	1	8
F1Q8B0	335309	zgc:165571			NA	0,89473	1,67	0,83	2,25	0,59	-1,16	0,47	0,62	0,20	1	8
F1QJC9	337158	col1a1a	collagen, type I, alpha 1	1277	COL1A1	1,09770	2,49	0,94	1,72	0,73	-0,16	2,39	0,29	0,58	1	8
Q6PC12	334116	eno1a	glycolysis, phosphopyruvate hydratase complex, magnesium ion binding, phosphopyruvate hydratase activity		NA	1,62171	1,19	0,32	1,94	1,56	-0,08	1,01	1,36	0,40	1	8
Q1LYE3	393954	znf143	zinc finger protein 143	7702	ZNF143	2,13124	1,55	0,80	-1,24	3,16	0,77	0,77	0,09	1,94	1	8
Q8JGS1	192317	stil	body morphogenesis, mitotic spindle organization, multicellular organismal development, neuron homeostasis	6491	STIL	2,40272	0,10	3,16	2,00	1,40	0,18	1,14	-1,44	0,91	1	8
F1R6L4	678563	cirbp	smoothened signaling pathway, spindle assembly, cytoplasm nucleic acid binding, nucleotide binding	1153	CIRBP	2,68568	1,40	1,47	4,09	0,65	0,96	2,06	0,06	-0,13	1	8
E7F7J1	100126232	fdx1	2 iron 2 sulfur cluster binding, electron carrier activity, metal ion binding	2230	FDX1	3,20284	2,24	4,08	2,61	0,88	-0,65	0,91	2,04	0,80	1	8
E7FBX3	100333869	pcnxl3	integral to membrane	NA		0,55653	1,38	1,63	0,74	0,36	0,13	1,54	0,79	1,75	0	9
A6H8Q4	100329887	si:ch211-212n6.8		NA		1,66097	2,06	1,12	1,66	0,76	0,37	1,87	1,43	1,85	0	9

Proteins are linked to hepatotoxicity-associated pathways. We then determined for each of the marker proteins to which processes they belong. The proteins up-regulated by eight or more compounds could be linked to the enriched processes/pathways including zinc ion binding, calcium ion binding, heat shock proteins, but also liver-associated pathways, i.e. carbohydrate metabolism, oxidoreductase activity and alcohol dehydrogenase activation (Fig.3, Table 3).

Proteins downregulated by eight or more compounds were linked to enriched processes/pathways including calcium ion binding, glycolysis and cytoskeleton related processes (Fig. 2, Table 3).

Match transcripts and proteins. In addition, we matched the direction of expression between gene and protein expression, while it is assumed that gene expression levels correlate with protein levels over time. Gene expression data were based on the same time point and published by us before[149]. Analysis was based on the availability of matching protein-gene combinations resulting in a total of 403 direct mRNA-protein comparisons. Matching of direction can be divided into four up-down combinations. This analysis revealed that CsA, EE2, PQ, TAA and VPA were overrepresented in group 'protein – gene down' (Fig 4.). For the other compounds the directionality of expression between protein and gene expression did not match very well. PQ showed the highest correlation (0.82), and the most enriched GO biological processes in the protein – gene down cluster were glutamate receptor signaling pathway, synaptic transmission, translation, cell-cell signaling, nucleosome organization and protein-DNA complex subunit organization (Table 4).

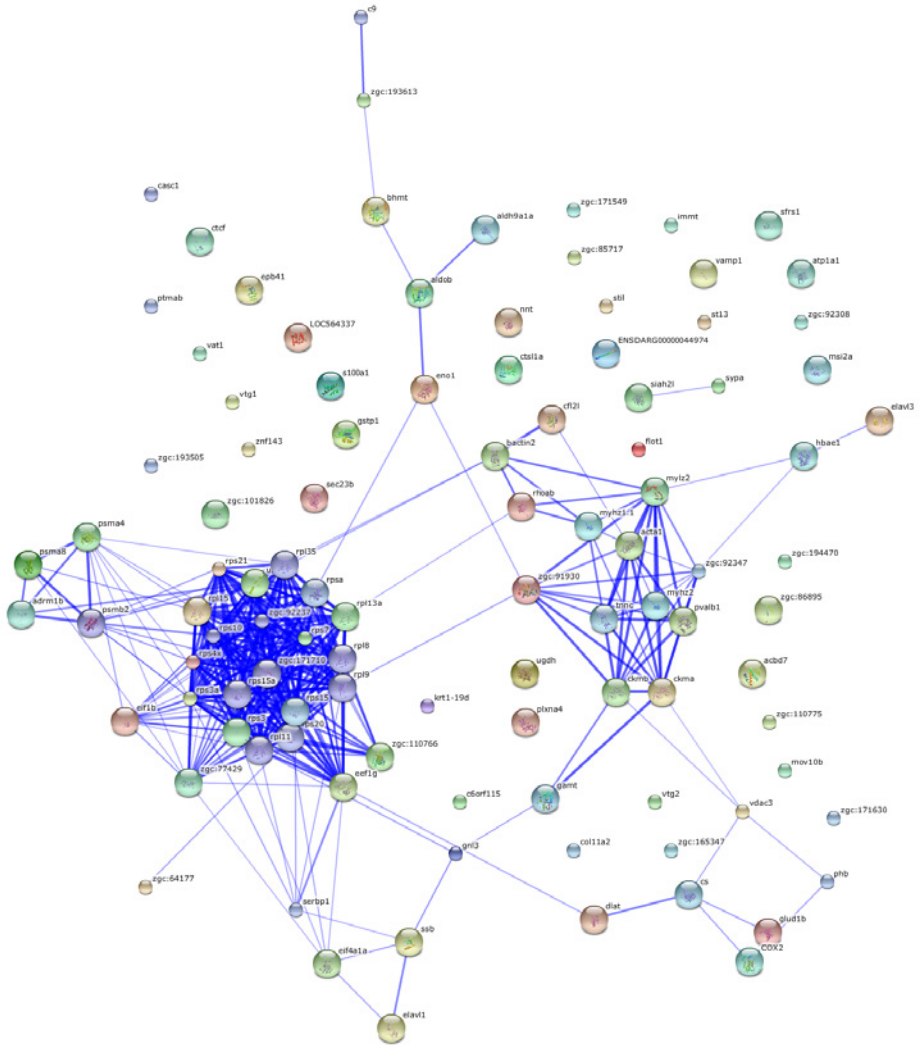

Figure 3 STRING network representation of the up regulated proteins.
STRING network representation of the 402 proteins identified as having a FC > 1.5 and by regulated by more than 6 compounds. Blue lines indicate connects between the proteins.

Table 4 Description of the marker genes.

GO_id	Term	Number OfGenes	p-value	p-value_ fdr	p-value_ bonferroni
GO:0035235	ionotropic glutamate receptor signaling pathway	7	2,58E-11	8,46E-08	1,50E-07
GO:0007215	glutamate receptor signaling pathway	7	4,35E-11	8,46E-08	2,54E-07
GO:0035249	synaptic transmission, glutamatergic	7	4,35E-11	8,46E-08	2,54E-07
GO:0007268	synaptic transmission	8	1,79E-07	2,09E-04	1,04E-03
GO:0006412	translation	12	2,67E-07	2,60E-04	1,56E-03
GO:0007267	cell-cell signaling	8	1,99E-06	1,66E-03	1,16E-02

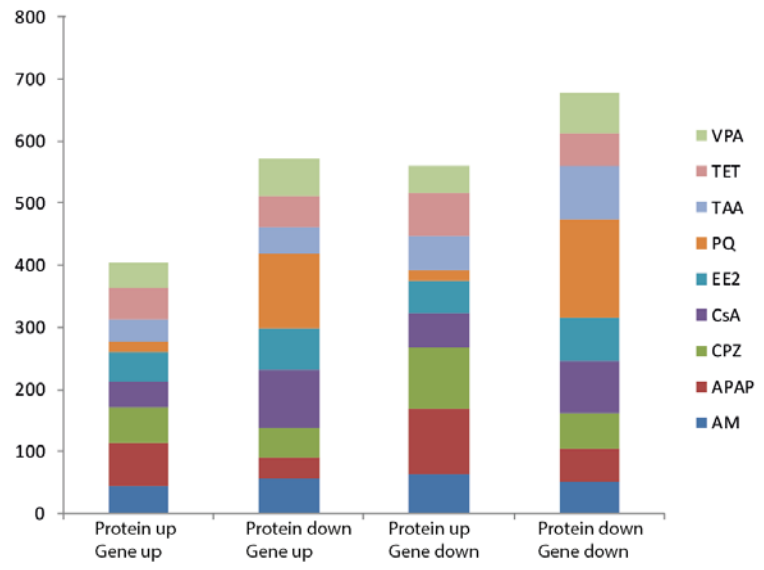

Figure 4 Correlation between gene and protein expression per compound.
Representation of the matched directionality of corresponding gene – protein pair. Directionality of each pair can be placed into four catergories including gene up – protein up, gene up – protein down, gene down – protein down, gene down – protein up. Each color represents a different reference hepatotoxicant.

Discussion

In this study, we analysed the regulation of protein expression in ZFEs after exposure to 9 reference hepatotoxicants, to improve mechanistic understanding of processes underlying hepatotoxicity and derive predictive biomarkers hereof. Furthermore, we compared gene and protein expression to detect interrelations between these levels in the dynamics of liver toxicity.

To investigate whether the significantly expressed proteins underlined the histopathological changes defining phenotypical clusters, overrepresented pathway analysis was performed using STITCH[91–94]. This enrichment analysis showed that the proteomic responses appeared very similar between the phenotypical clusters, resulting in shared pathways and/or processes. One such a shared biological process is "translation", which is known to be disrupted in in global stress responses[157]. "Translation" was highly enriched for both up- and down -regulated proteins, which were mainly characterized by *rps* and *rpl* proteins, respectively. Other detected shared processes, such as the extremely broad "cellular protein metabolic process", "gene expression" and "metabolic process" are also known to be influenced in a general stress response. Altogether, proteome profiling in the ZFE after hepatotoxicant exposure tends to detect a more general stress response which may be linked to oxidative stress, and the large overlap of enriched processes between the phenotypical clusters suggests that this type of broad analysis in the ZFE is not suitable to discriminate between the histopathological phenotypes.

An extended analysis based on common hepatotoxicity produced "translation", "gene expression" and "protein folding" as highly overrepresented processes. The down-regulated process "protein folding" is associated with a stress response involving the endoplasmic reticulum (ER), and a prolonged stress response will eventually lead to apoptosis[158]. The unfolded protein stress response has been found as important for drug induced liver injury (DILI)[159]. The strong upregulation of translation processes indicates that the ZFE is adapting to the stress caused by the xenobiotics[157]. A general stress response thus appears to emerge as an importantly regulated protein expression process after hepatotoxicant exposure.

While there was a large overlap between the phenotypical clusters on pathway and/or process level, we identified a set of predictive key proteins for common hepatotoxicity. For the upregulated proteins, *pcnx l3* and *si:ch211-212n6.8* were regulated by all 9 reference compounds. The first protein, *pcnxl3*, is involved in membrane composition[80]. The other protein is recently annotated as *crygm2d19*, which is a crystallin. Crystallins play an important role in the development of the lens of the eye, but have recently also been observed in other areas of the body, where they might play a role in calcium ion binding[80]. This could be relevant in hepatotoxic processes in view of the role of calcium as an important second messenger in response to stress[80]. In addition, crystallins are found to be regulated after toxic stress in PFOS treated zebrafish larvae[160,161].

Also proteins that were induced by only 8 of the 9 compounds (Table 3) could be linked to hepatotoxic processes. For example, the protein *glud1b* (glutamate dehydrogenase 1b) plays a key role in nitrogen and glutamate metabolism, and also in the energy homeostasis[80]. The human ortholog GLUD1 is a serum marker for hepatotoxicity along with ALT and AST[162]. The *si:ch211-93f2.1* protein is a carboxyl esterase which in humans is known to be involved in the hydrolysis of xenobiotics[80]. The *eno1a* protein is involved in glycolysis and was previously reported to be differentially expressed in ZFE after exposure to CsA[163], supporting a role in hepatotoxicity. The mitochondrial 10 kDa heat shock protein, *hspe1,* was upregulated in our ZFEs after exposure to the hepatotoxicants suggesting the occurrence of oxidative stress. This is in contrast to the observed downregulation in mouse liver slices after CsA exposure, which, however, might be an artifact of exposure duration[164]. Heat-shock proteins are involved in folding/unfolding of proteins and protein translocation. The ER stress after CsA exposure negatively affects the function of heat-shock proteins[164]. Another protein, *anxa1c*, is known to influence hepatocyte differentation[80], and *anxa1c* also appears to play a functional role in the modulation of hepatotoxic inflammation linked to steatosis[165]. In summary, although the regulated processes and/or pathways point towards more general stress and oxidative stress responses, analysis of individual genes/proteins also reveal more hepatotoxicity-associated changes. This supports that protein expression changes can identify hepatotoxicity-specific responses in the ZFE.

An underlying assumption in many biological studies is the concordance of transcripts and protein level[166]. Comparison of protein expression signatures with their corresponding gene expression[149] revealed the best correlation in the cluster were both are down-regulated, with the highest correlation for the compound PQ. The overrepresented GO biological processes for this compound include cell-cell signaling and glutamate receptor signaling, which are suggestive for an oxidative stress response in the cell. This is in line with the known mode-of-action of this compound as observed in multiple species[30,145]. Difficulties in correlating mRNA and protein expression are generally acknowledged, and relate to post-transcriptional processing, different half-lives between mRNAs and proteins, and the noise in both mRNA and protein expression measurements, preventing an easy mechanistic interpretation[166]. Some of this the lack of correlation between mRNA and protein expression in ZFEs was recently shown to derive from three important categories: ribosomal proteins, histones and vitellogenins[156]. The specific noise in our analyses relates to the selective counting of the number of genes and/or proteins being regulated. Furthermore, because mRNA and protein data were derived from the same time point, the different expression kinetics between mRNAs and proteins will also reduce the degree of correlation or even result in negative correlation, particularly for transiently induced genes with slow protein turnover. Despite, or perhaps because of these limitations, mRNA-protein sets with matching expression clusters support the use of these entities as markers for hepatotoxicity, as they suggest non-transiently up- or downregulated gene

expression with a corresponding and rapid change in protein abundance.
In conclusion, our exposure study with a set of reference hepatotoxicants in ZFEs identified proteomics markers for enriched biological processes associated with general hepatotoxicity. The most prominent process was stress response, as indicated by translation, gene expression and metabolic synthetic processes. The identified protein markers, particularly *glud1b, hspe1* and *anxa1c*, are potentially suitable candidates for the prediction of human hepatotoxicants. Such markers could be further developed into high throughput screening using more dedicated methods such as Western blots or ELISA assays.

Acknowledgements

This study was supported by grant nr. 050-060-510 from the Netherlands Genomic Initiative/Netherlands Organization for Scientific Research (NWO) to the Netherlands Toxicogenomics Centre and MP and SDvdP were supported by the NWO Vidi grant 917.11.398.

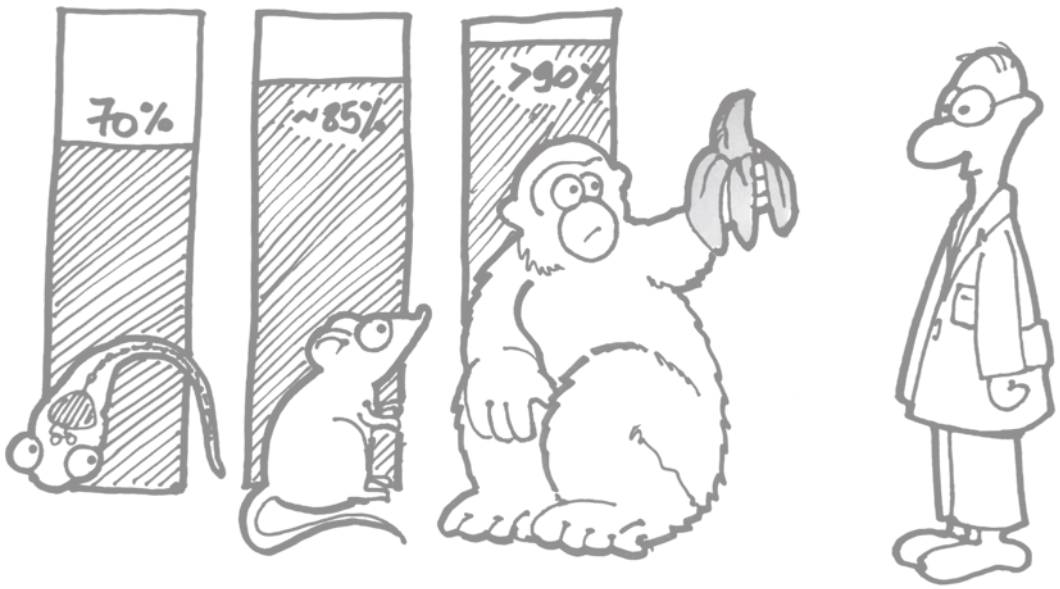

5

A Transcriptomics-based Hepatotoxicity Comparison between the Zebrafish Embryo and established Human and Rodent *in vitro* and *in vivo* models using Cyclosporine A, Amiodarone and Acetaminophen

Marja Driessen[#], Alexa P. Vitins[#], Jeroen L.A. Pennings, Anne S. Kienhuis, Bob van de Water, Leo T.M. van der Ven

[#] Contributed equally

Abstract

The zebrafish embryo (ZFE) is a promising alternative, non-rodent model in toxicology, which has an advantage over the traditionally used models as it contains complete biological complexity, and provides a medium to high-throughput setting. Here, we assess how the ZFE compares to the traditionally used models for liver toxicity testing, i.e. *in vivo* mouse and rat liver, *in vitro* mouse and rat hepatocytes, and primary human hepatocytes. For this comparison we analyzed gene expression changes induced by three model compounds for cholestasis, steatosis, and necrosis. The three compounds, cyclosporine A, amiodarone, and acetaminophen, were chosen because of their relevance to human toxicity and these compounds displayed hepatotoxic-specific changes in the mouse *in vivo* data. Compound induced expression changes in the ZFE model shared similarity with both *in vivo* and *in vitro*. Comparison on single gene level revealed the presence of model specific changes and no clear concordance across models. However, concordance was identified on the pathway level. Specifically the pathway "Regulation of metabolism – bile acids regulation of glucose and lipid metabolism via FXR" was affected across all models and compounds. In conclusion, our study with three hepatotoxic model compounds shows that the ZFE model is at least as comparable to traditional models in identifying hepatotoxic activity, and has the potential for use as a pre-screen to determine hepatotoxic potential of compounds.

Introduction

A challenge in toxicology is to predict the hepatotoxic potential of compounds to which humans are exposed. In mammals and particularly for xenobiotics that rely on oral uptake, many compounds provoke first signs of toxicity in the liver. This is mainly due to the location of the liver (first pass effect) and liver cell activation. Therefore, hepatotoxicity is an important target to study, particularly in the context of adverse xenobiotic effects. Hepatotoxicity is the result of various xenobiotic-induced underlying molecular mechanisms, which produce different liver toxic phenotypes, of which cholestasis, steatosis and necrosis are most frequently observed. Cholestasis is a chronic condition and is phenotypically characterized by bile accumulation as a result of changes in intra- or extracellular bile flow or bile composition[34]. Steatosis may occur chronically as well and is characterized as an increase in cellular lipid content due to an increase in *de novo* synthesis of fatty acids or reduced lipid secretion or oxidation[19]. Necrosis is an acute condition and is characterized by cell death due to oxidative stress[4,33].

Traditionally, these hepatotoxic properties of xenobiotics are determined using different *in vivo* and *in vitro* models. Detection of hepatotoxicity in *in vivo* studies is based on histopathology and clinical chemistry. However, these studies require high numbers of animals, interfere with animal welfare, and are associated with high costs and are not always predictive for the human situation. *In vitro* systems have limitations related to their reductionistic nature and to their loss of functionality compared to the liver *in vivo*[101]. In the effort to improve screening for hepatotoxicity regarding predictivity for humans and throughput and in the same time reduce animal experimentation, the development of alternative models has gained attention. As such, the zebrafish embryo is an alternative screening model with the potential to reduce animal experimentation. It combines the benefits of an *in vivo* model, namely complete biological complexity including interaction between tissues and cells[49,54,95], with the advantages of an *in vitro* model, that is reduced animal discomfort and the ability for median to high throughput testing. The structure and function of the adult zebrafish liver is similar to the mammalian liver[46,55], and fully functional liver tissue is present in the zebrafish embryo at 72 hours post fertilization (hpf), which is therefore a suitable time point to start hepatotoxicity testing. There is also high genetic conservation between humans and zebrafish, including genes functioning in biotransformation[46,55]. Previous studies showed that the zebrafish embryo could be used to identify human hepatotoxic responses using histopathology and gene expression analysis[149]. These studies have demonstrated that hepatotoxicity-associated gene expression remains detectable in the noise of other tissues and are distinct from developmental toxicity processes[149].

Although the above mentioned studies have shown promise for the zebrafish embryo as an alternative model, it still does not identify how comparable the obtained results are to the traditionally used models. Our anticipation is that the zebrafish embryo model shares commonalities with *in vivo* and *in vitro* models. To this end, we compared the ZFE to the *in vivo* mouse and rat liver, *in vitro* mouse and rat hepatocytes, and primary human hepatocytes using gene expression changes from existing experiments using a model compound for each hepatotoxic phenotype.

Three compounds, cyclosporine A (CsA), amiodarone (AMD), and acetaminophen (APAP), were chosen for the comparison because of their relevance to human toxicity and the availability of reference data in all of the selected models. The model compound CsA induces cholestasis. CsA competitively inhibits the bile salt export protein, which is the primary transporter involved in the biliary efflux of conjugated bile acids across the canalicular membrane[134,135]. AMD, an antiarrhythmic agent, induces steatosis in humans[137] by altering lipid homeostasis in the liver. Finally, necrosis is induced by APAP, an analgesic and antipyretic, which is considered safe at therapeutic doses. In this setting, APAP is inactivated by sulfation and glucuronidation. However, when the therapeutic doses are exceeded, APAP causes hepatic damage and may eventually lead to liver failure[1,138].

Although the zebrafish embryo model cannot distinguish between human hepatotoxicity phenotypes using transcriptomics or proteomics, mechanisms of general hepatotoxicity can be identified and these might overlap with those induced in the traditional models for which data is available (Fig. 1). Our current data suggest overlap in the activation of pathways of toxicity between ZFE and other models. Therefore, the zebrafish embryo may well serve as a preferred quick and accurate first round testing of new compounds.

Materials and methods

This study utilized data from multiple sources. In house (*in vivo* ZFE and mouse) and externally available data (*in vivo* rat and *in vitro* mouse, rat and human) were combined to assess the predictivity of the zebrafish embryo as a model for hepatotoxicity testing. In total, 161 treatment groups or conditions including a total of 161 Affymetrix CEL files with up to four replicates per conditions, were included in the analyses and an overview of each model is shown in Table 1 (Supplementary Table 1).

Zebrafish embryo model (ZFE). The studies on zebrafish embryos were conducted by the National Institute for Public Health and the Environment (RIVM) as described earlier[133]. Briefly, 72 hours old hatched embryos were randomly distributed over 48-well plates in a density of 5 embryos per well in 1 ml test or control medium. Following treatment, using previously described procedures[110,133,149], total RNA was isolated from the zebrafish embryo (1 sample consisted of 15 ZFE embryos) and used for gene expression analyses on

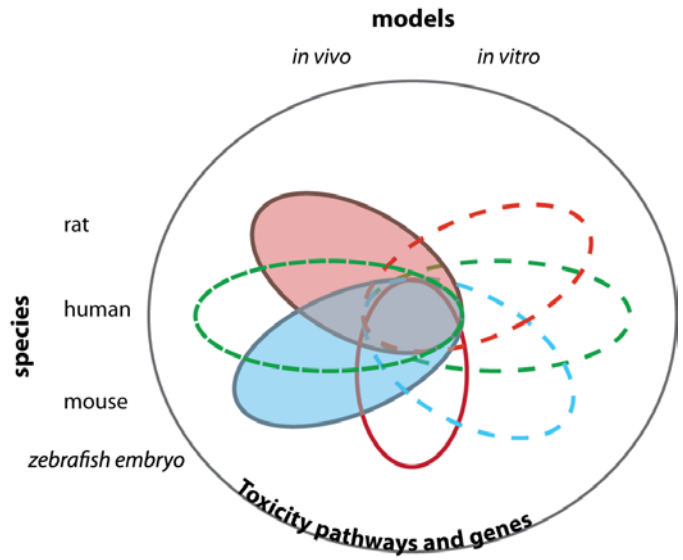

Figure 1 Concordance model for toxicogenomics-based extrapolation.
Central overlap represents species- and model-independent robust toxicity pathways or genes that are predictive for pathways/genes related to hepatotoxicity in humans. Solid red and blue lines, toxicity pathways/genes measured in *in vivo* models; large spaced dotted red, green, and blue lines, toxicity pathways/genes measured in *in vitro* models; small spaced dotted green line, the human *in vivo* toxicity pathways/genes to be predicted; red line, the zebrafish embryo toxicity pathways/gene contribution sharing similarity with *in vitro* as well as *in vivo* (adapted from Kienhuis *et al.*[5]).

Affymetrix Zebrafish Gene ST Array. At least 4 biological replicates were conducted. The expression data set is publicly available at the Gene Expression Omnibus (GEO) database, (http://www.ncbi.nlm.nih.gov/geo/), accession number GSE55618 (full dataset).

Mouse in vivo (MIV). The *in vivo* mouse liver studies were conducted by the RIVM as described previously[119,141,167]. Briefly, male C57BL/6Jlco mice, aged 10 weeks, were treated with a low, medium, and high dose of CsA and AMD for 1, 4, and 11 days, and for APAP, mice were given a single treatment at a low, medium, and high dose and assayed 1 and 2 days later. RNA from liver tissue was isolated and used for gene expression analysis by hybridizing to the Affymetrix HT Mouse Genome 430 PM Array. The expression data set is publicly available at the Gene Expression Omnibus (GEO) database, (http://www.ncbi.nlm.nih.gov/geo/), accession number GSE31540 (CsA), GSE48126 (AMD) and GSE51969 (APAP). At least 4 biological replicates were conducted.

Table 1 Model Description.

		Model						
Compound	**Dose**	MIV (mg/kg) 1, 2, 4, 11 days (RIVM, Kienhuis et al.)	MPH (µM) 24, 48 hours (UM, van Summeren et al.)	ZFE (µM) 48 hours (RIVM, Driessen et al)	HPH (µM) 2, 8, 24 hours (TG-Gates)	RIVS (mg/kg) 3, 6, 9, 24 hours (TG-Gates)	RIVR (mg/kg) 4, 8, 15, 29 days (TG-Gates)	RPH (µM) 2, 8, 24 hours (TG-Gates)
AMD	High	60	25	10	7	2000	200	7
	Medium	20	1	3.3	1.4	600	60	1.4
	Low	6.7	0	1.1	0.28	200	20	0.28
APAP	High	300	10000	660	5000	1000	1000	10000
	Medium	225	1000	220	1000	600	600	3000
	Low	168.75	0	73.3	200	300	300	1000
CsA	High	26.7	50	6	6	300	100	6
	Medium	8.9	10	3	1.2	100	30	1.2
	Low	3	0	1	0.24	30	10	0.24

Primary mouse hepatocytes (MPH). Samples were from a previous transcriptomics study from Maastricht University (UM) on mouse primary hepatocytes (MPH) treated with AMD, APAP and CsA[168]. In short, primary hepatocytes were isolated from adult male C57Bl/6 mice and brought into culture in a collagen-collagen sandwich formation. Following treatment, using previously published procedures[169], total RNA was isolated from cultured mouse hepatocytes and used for gene expression analyses on high-density oligonucleotide gene chips (Affymetrix Mouse Genome 430 2.0 GeneChip arrays). Three independent biological replicates were conducted.

Rat in vivo and in vitro rat and human. Experimental study designs for AMD, CsA and APAP for rat primary hepatocytes (RPH), rat *in vivo* repeated dosing (RIVR), rat *in vivo* single dosing (RIVS) and human primary hepatocytes (HPH) performed in the Japanese Toxicogenomics Project and Toxicogenomics Informatics Project (TGP) (Open TG-GATEs; http://toxico.nibio.go.jp)[170,171]. These studies can be obtained from ArrayExpress (https://www.ebi.ac.uk/arrayexpress/) under accession numbers E-MTAB-797 (rat primary hepatocytes), E-MTAB-798 (human primary hepatocytes), E-MTAB-799 (*in vivo* rat single dose) and E-MTAB-800 (*in vivo* rat repeated dose).

Data preprocessing and quality control. For all systems, the data was annotated with a MBNI custom CDF specifically designed for the chips (http://brainarray.mbni.med.umich.edu/Brainarray/Database/CustomCDF/CDF/)[118] and RMA normalized using the Robust Multichip Average algorithm[76]. RMA normalized data was Log_2 transformed and the quality of the micro array images was inspected visually (http://arrayanalysis.org, BiGCaT Maastricht University)[172].

Homolog conversion. The unique Entrez GeneIDs for each species was converted to human homologs by downloading the full HomoloGene data file from NCBI (ftp://ftp.ncbi.nlm.nih.gov/pub/HomoloGene/current) and matching the species GeneIDs to the human homologs using an Entrez ID conversion script in R in order to compare the model systems. Only the homologs present in all model species were used for further analysis which resulted in 7828, 7825, 7623 and 8855 Entrez ID for mouse, rat, human and zebrafish, respectively.

Gene expression analysis.

Single gene expression. To ensure that an equal number of genes were compared between the different treatment/condition groups, the top-500 ranked genes based on Log_2 fold-change (Log_2FC) were used. This analysis was performed because of differences in the power between the experimental designs.

Single gene overlap. Per model, the unique genes found above in the "Single gene expression" were compiled. Similarity between these lists was visualized by means of a heatmap as well as Principal Component Analysis (PCA).

Pathway analysis. Each of the lists compiled in the section "single gene overlap" were submitted to MetaCore from Thomsom Reuters and pathways having a p-value of < 0.05 were identified.

Biplot. Biplot representation of the pathway was done to display information on both the samples and the variables of the data matrix. In a biplot the samples are displayed as points, whereas the variables of the datamatrix are displayed as vectors. The biplot was generated using the "ade4" package in R (http://pbil.univ-lyon1.fr/ade4/home.php?lang=eng)[173,174] with an in-house R script based on the *ggplot2* R-package[175] function, with minor changes that helped improve graphical representation.

Results

Model-dependent gene expression changes. Changes in gene expression may be informative regarding how different models react to xenobiotic treatment. Therefore, to ensure equal numbers of differentially expressed genes (DEGs) for all 161 treatment conditions, we decided to use the top-500 ranked genes to determine the overlap between the conditions on single gene level and identify similarities between groups (Fig. 2, Supplementary Figure 1). Based on this stringent selection model dependent changes were observed; as expected the greatest amount of overlap was found within a model. Additionally, within a model, the different dose and time points of a given compound tend to overlap. Yet different compounds tend to overlap less within a model. Furthermore, when comparing a model to the other models, there is no difference in the overlap. Therefore, to identify whether common regulated genes were found across all models a gene overlap comparison was performed.

Gene overlap across models. Our goal was to determine the feasibility of the ZFE to pick relevant transcriptomics changes that mimic other more standard models. Therefore we determined the overlap at the single gene level between ZFE and all other models. Per model, we used the unique genes across the top-500 of each treatment/condition group; since per compound (AMD, APAP and CSA) we had several concentration/doses the total DEGs for the analysis typically 500 genes per model. Because conceptually the ZFE shares likely similarities with the *in vivo* models as well as with the *in vitro* models, a separation was made between *in vivo* and *in vitro*. More single DEGs were found to be in common across all the different *in vivo* models per compound (22 AMD, 14 APAP, 19 CsA) than in the *in vitro* model comparison (5 AMD, 11 APAP, 5 CsA) (Fig. 3A) (Supplementary Table 2). For both the *in vivo* and *in vitro* comparisons of AMD and CsA, ZFE shared most genes with the mouse model. Yet for APAP, there was not much difference in overlap between the pair-wise comparisons. Furthermore, to identify whether there were common genes altered across hepatotoxic states, the common genes identified from the above overlap were compared across compounds. Almost all compound specific changes across species were unique. Only one gene, CYP8B1, was found in common *in vivo* across AMD, APAP, and CsA, but no genes were found in common from the *in vitro* studies (Figure 3B).

Concordance identified at the pathway level. Next overrepresented pathways were determined using the unique top-500 ranked gene list for each model species to identify whether there were common pathways induced after reference compound exposure (Supplementary Table 3). Also here a separation between *in vivo* and *in vitro* models was made (see Fig. 4). Highest concordance for *in vivo* pathway activation was observed between rat and mouse; only several pathways overlapped between ZFE and rat and mouse, with mouse given the highest concordance with ZFE for CsA. Overlap for all the *in vivo* models was observed for only several pathways: for AMD one pathway that was shared between all models, which was the "Regulation of metabolism – Bile acids regulation of glucose and lipid metabolism via FXR". This pathway was also observed after exposure to APAP and CsA. Another pathway that was regulated after APAP exposure was the "Regulation of CFTR activity". For CsA, the pathways "Transcription – Transcription regulation of amino acid metabolism" and the pathway "Signal transduction – cAMP signaling" were enriched (Fig. 4).

For the *in vitro* comparison, at the pathway level ZFE correlated overall best with the mouse primary hepatocytes with respect to AMD and CsA. Overlapping pathways included the regulation of lipid metabolism (Supplementary Table 4). Interestingly, also *in vitro* APAP and CsA exposure resulted in the enrichment of the "Regulation of metabolism – bile acids regulation of glucose and lipid metabolism via FXR" pathway. After exposure

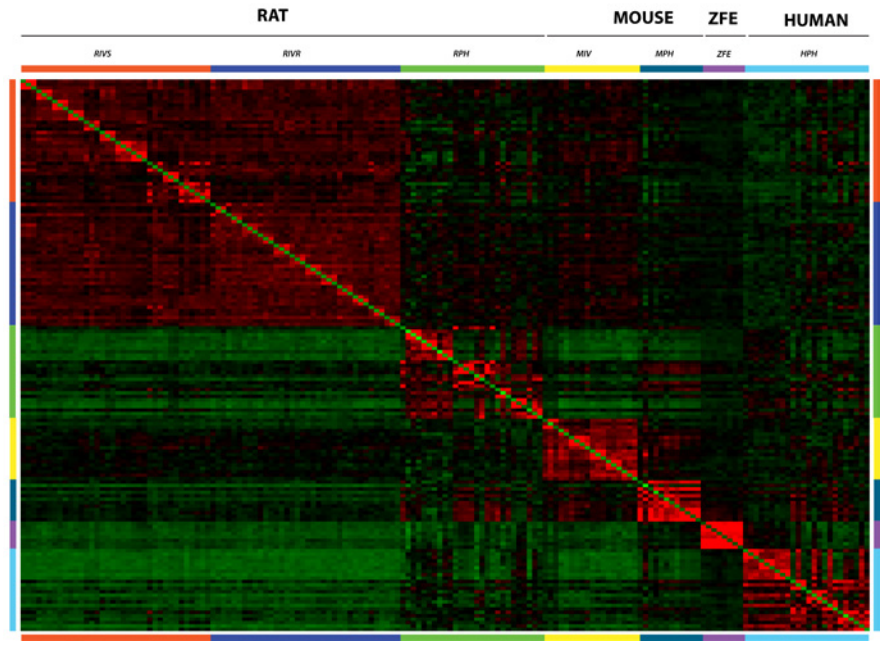

Figure 2 Single gene overlap between all conditions.
The top-500 ranked genes, for all 161 treatment conditions, were used to determine the overlap between the conditions on single gene level and identify similarities between groups. All conditions included in this study are color coded. RIVS is rat *in vivo* single dosing, RIVR is rat *in vivo* repeated dosing, RPH is rat primary hepatocytes, MIV is Mouse *in vivo* liver, MPH is mouse primary hepatocytes, ZFE is zebrafish embryos and PHH is human primary hepatocytes. Red color represents more overlap whereas green color represents less overlap.

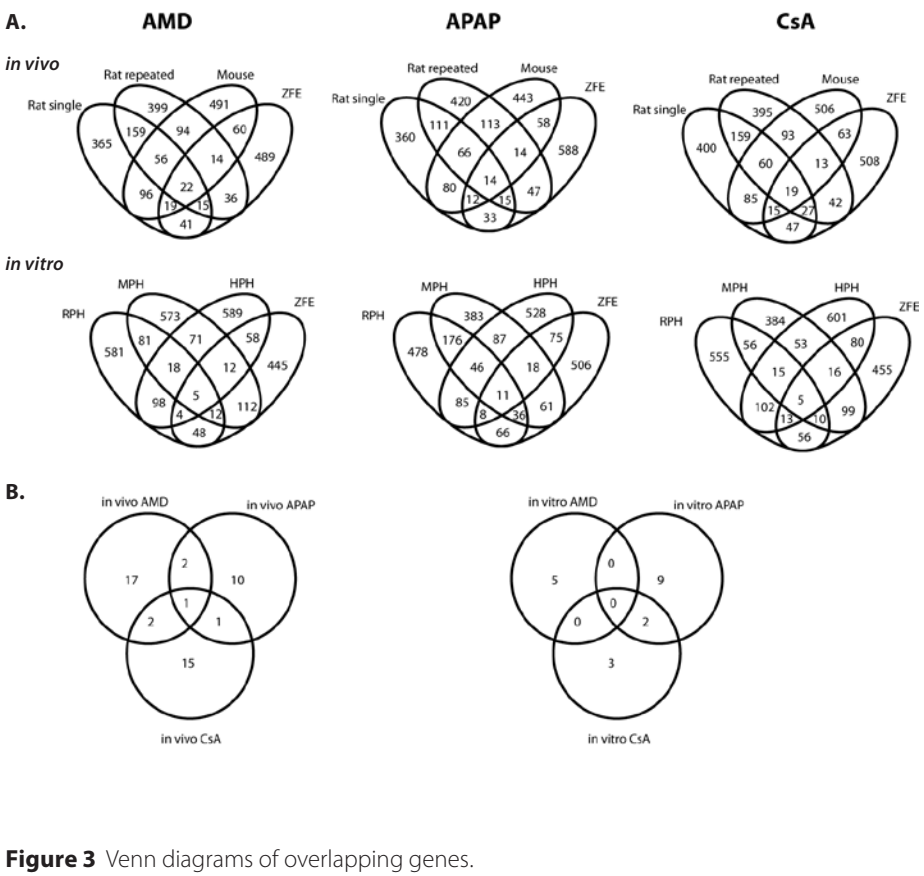

Figure 3 Venn diagrams of overlapping genes.
Unique top-500 genes for each model are compared between all species and overlap is presented in Venn diagrams. **A.** Gene overlap of compound dependent *in vivo* and *in vitro* models. **B.** Gene overlap of compound independent *in vivo* and *in vitro* models.

to AMD, this pathway was only observed in MPH, RPH and ZFE and not in HPH. However, HPH shared an enriched pathway with MPH and RPH, which was "Reproduction – Progesterone – mediated oocyte maturation" (Fig. 4) (Supplementary Table 3).

Species/model differences for genes within the enriched pathway. Overlap on single gene level resulted in one gene overlapping between the compounds in the *in vivo* models. This gene is part of the "Regulation of lipid metabolism_FXR-dependent negative-feedback regulation of bile acids concentration" pathway. For the *in vitro* models no overlap was found. However, pathway analysis resulted in one pathway enriched across most compounds and models being the "Regulation of metabolism – Bile acids regulation of glucose and lipid metabolism via FXR" pathway. To gain further insight into this specific

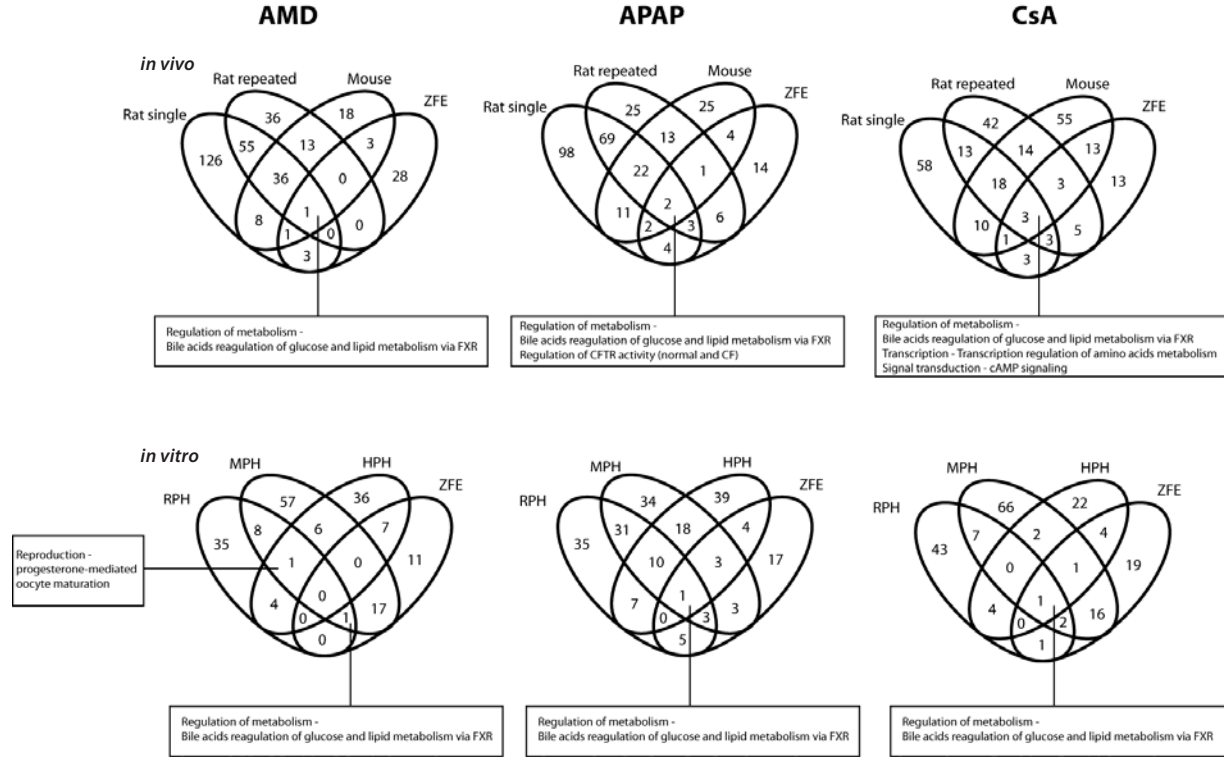

Figure 4 Venn diagrams of overlapping pathways.
Pathway overlap determined using venn diagrams. Pathways were based on the unique top-500 ranked genes per model and compound. Pathways were determined using MetaCore, a pathway was significant when $p < 0.05$.

pathway, a biplot was created to determine the effect of gene expression changes on each model (Fig. 5). It was observed that the genes APOE, LXR-α and HNF3-β had the lowest effect signified by their placement on the intersection of the axes. Genes were separated into the four different clusters: 1-topleft) SHP, PPAR-α, and ME1; 2-topright) MTP, APOB, HNF3-γ, F16P, HNF4-α, and FXR; 3-bottomleft) NIPK, SCD, ACACA, SREBP1 (nuclear), Insulin processed, GSK3-β, PLTP, HNF3-β, and FKHR; 4-bottomright) PPCKC and G6PT.
Models were also separated into the four different clusters: 1) RIVR_CsA, RIVR_AMD, HPH_APAP, HPH_AMD, RIVS_CsA, MPH_APAP and RIVS_APAP; 2) RIVS_AMD, RPH_AMD, ZFE_AMD, ZFE_APAP, ZFE_CsA, MIV_APAP; 3) HPH_CsA, RPH_CsA, MPH_AMD, MPH_CsA, RIVR_APAP, MIV_CsA and MIV_AMD; 4) RPH_APAP. Based on the gene expression changes, there was no separation between *in vivo* and *in vitro* models. The ZFE model treatments

Figure 5 Biplot of the "Regulation of metabolism – Bile acids regulation of glucose and lipid metabolism via FXR" pathway.

This pathway was found enriched across most compounds and models, and a biplot was created to determine the effect of gene expression changes on each model. Arrows represent the different conditions (model and compound). The arrow length indicates the strength of the effect.

were found in close proximity to each other on the biplot, and ZFE_AMD shared close similarity with AMD treated RPH *in vitro*, RIVS *in vivo*, and HPH *in vivo* models. These data indicate that although in all models an effect on the same pathway was observed, the components that were changed within the pathway were rather model dependent than compound dependent.

Discussion

Hepatotoxic potential of compounds to which humans are exposed are traditionally determined using rodent studies including mice and rats. However, these studies rely on long term exposure of the animals, and in light of the 3Rs, there is a need for new alternative testing models. The zebrafish embryo is a potential alternative testing model, which combines the benefits of an *in vivo* model, namely the complete biological complexity including the interactions between tissues and cells[49,54,95], with the advantages of an *in vitro* model, that is reduced animal discomfort and the ability for medium to high throughput testing. Here, we assessed the similarities of the zebrafish embryo model in relation to the traditionally used models including rat and mouse *in vivo* and *in vitro* to help in the identification of common hepatotoxic responses.

The changes on single gene level give information about how the different models respond to the xenobiotic treatment. Based on single gene overlap, the overlap within a species regardless of compound exposure was greater than between species. This might suggest that, within the limits of the data used for this analysis, every species produces a unique gene expression signature regardless of time, dose and compound. Also, comparing one model to the other models we found no difference in gene overlap suggesting that no two models are more similar to each other than the rest. When the DEGs were restricted to each individual model and compared across compounds, more DEGs were found in common for the *in vivo* comparison than for the *in vitro* comparison. This suggests that *in vivo* models may be more similar in the way they react to xenobiotic treatment than *in vitro* models. Alternatively the isolation procedure and culture procedures between mouse, rat and human hepatocytes affects the differentiation status of the cells preventing an equivocal comparison. Intriguingly, ZFE shared more genes with the mouse *in vivo* and *in vitro* models in the AMD and CsA comparison suggesting a strong similarity between the ZFE and mouse models.

CYP8B1 was identified in the *in vivo* models as a common gene altered in all hepatotoxic states. CYP8B1 is a cytochrome P450 family member that catalyzes numerous drug and lipid metabolizing reactions, and it is found in the pathway "Regulation of lipid metabolism_ FXR-dependent negative-feedback regulation of bile acids concentration". The expression of CYP8B1 is directly controlled by a combination of bile acids and the FXR receptor and indirectly by the PPAR-α receptor[176], supporting an important role of this gene in hepatotoxicity.

Inter- and intra-species comparison based on single genes is complicated because biological meaning is based on lists of differentially expressed genes. Instead, pathway analysis offers functional interpretation of these genes to a common, and therefore a more easy to compare endpoint[83]. Most importantly, in both *in vitro* (APAP and CsA) and *in vivo* (AMD, APAP and CsA) models, one pathway "Regulation of metabolism – Bile acids regulation of glucose and lipid metabolism via FXR" was found to be commonly regulated.

Bile acids are produced in the liver and aid in the adsorption of dietary lipids. Additionally, bile acids can activate various downstream signaling pathways including those of nuclear receptors, like the farnesoid X receptor (FXR), regulating bile acid and drug metabolism among others[34,177]. This pathway has been linked before to cholestatic liver diseases[164,178], and it has been regulated after exposure to AMD and APAP. After *in vivo* exposure of APAP, the pathway "Regulation of CFTR activity" was found in common. The cystic fibrosis transmembrane conductance regulator (CFTR), which is a member of the ATP-binding cassette (ABC) transporter family, is found in epithelial cells and acts as a glutathione channel among other functions. Furthermore, CFTR maintains water-salt homeostasis on the cell surface and normal function of epithelia lining airways, intestinal tract, and liver[80]. CFTR is significantly upregulated after APAP exposure in the mouse liver[179]. Since Kuppfer cells are suggested to play an important role in the upregulation of CFTR, this explains why this pathway is not observed in the *in vitro* models after APAP exposure because of their lack of Kupffer cells[180].

After *in vivo* exposure of CsA, the pathways "Transcription – Transcription regulation of amino acid metabolism" and "Signal transduction – cAMP signaling" were enriched. Amino acid metabolism is altered in the *in vivo* mouse model from CsA treatment[119], and cAMP signaling is important in many biological processes including the regulation of glycogen, sugar and lipid metabolism, which occurs in the liver[80]. From the AMD *in vitro* studies, the pathway "Reproduction – Progesterone – mediated oocyte maturation" was only observed in MPH, RPH and HPH and not in ZFE. Within HPH, this pathway contains genes that are generally responsible for cell growth, like p90RSK1 and PLK1, suggesting this pathway is important in liver cell function during xenobiotic exposure.

To gain more insight into how each model alters this particular pathway, a so-called biplot (Fig. 5) was made to identify the behavior of the genes, which resulted in their separation into five clusters. Additionally, the connection between the genes in each cluster was analyzed by plotting their location within the pathway (Fig. 6). In general, separation of the genes can be identified by their placement within the pathway. The genes within a particular cluster tend to have an interaction between them in a linear fashion then being scattered randomly. SHP and ME1 are found in cluster 1 where ME1 is controlled upstream by SHP in the regulation of lipogenesis. From cluster 2, HNF4-α is upstream of F16P in the modulation of gluconeogenesis and also upstream of MTP and APOB in the regulation of lipid transport. From cluster 3, NIPK and insulin processed are upstream of FKHR and GSK3β in the regulation of glycogenolysis and gluconeogenesis. Additionally, SREBP1 is upstream of ACACA and SCD in the regulation of lipogenesis, but is also separate from the cluster 1 genes in this regulation. From cluster 4, G6PT and PPCKC both modulate gluconeogenesis. Lastly, the genes found at the intersection of the axes (cluster 5 in Fig. 6), APOE, LXR-alpha and HNF3-beta, identify that the changes in gene expression are fairly similar among all models leading to these genes having the least effect and being randomly distributed throughout the pathway.

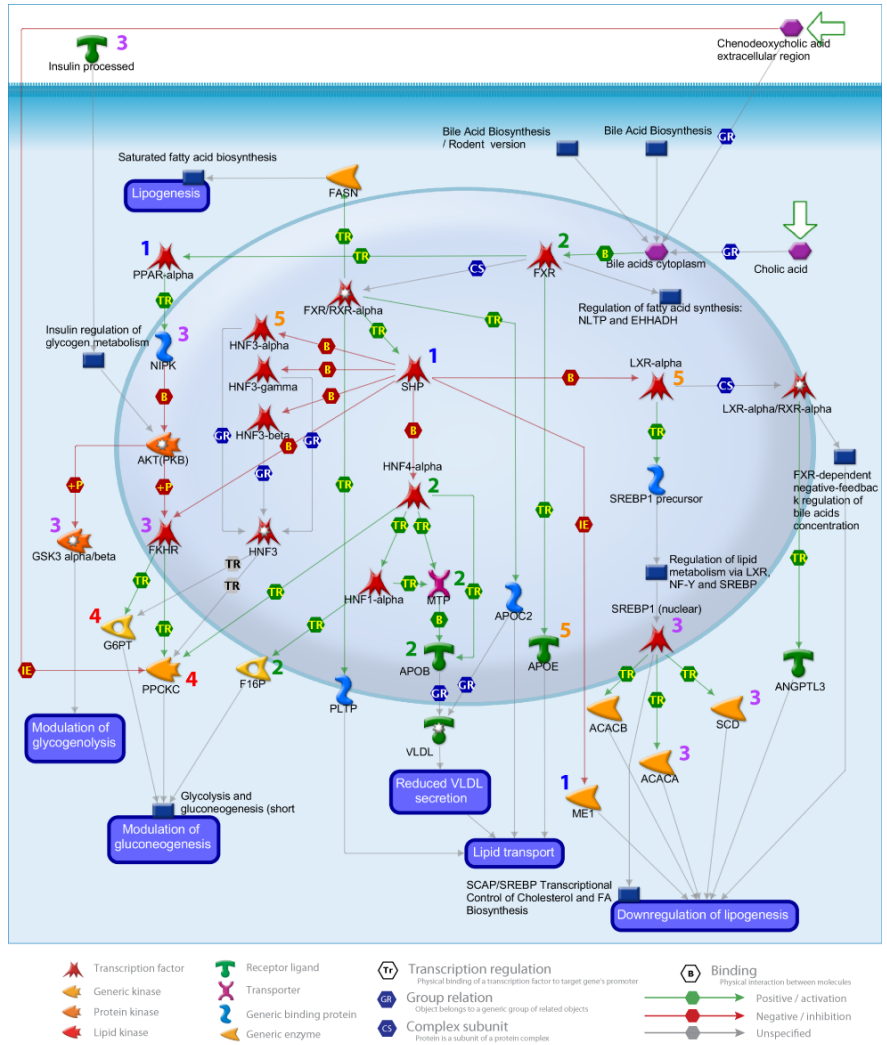

Figure 6 Diagram of the "Regulation of metabolism – Bile acids regulation of glucose and lipid metabolism via FXR" pathway from Metacore.

The relationship between the genes in each cluster from the biplot in Figure 5 was analyzed by plotting their location within the pathway (numbered genes on the figure correspond to the quadrants from Figure 5). In general, separation of the genes can be identified by their placement within the pathway.

In conclusion, the ZFE model shares similarity at the pathway level after xenobiotic exposure with both *in vivo* and *in vitro* models, using three reference compounds that cover a variety of hepatotoxic phenotypes. Concordance on the pathway level identified a single pathway to be altered across all hepatotoxic phenotypes, although with variations producing model and compound dependent clustering. Comparison at the single gene level showed that there were model specific changes and that outside of a model the overlap was fairly similar across models suggesting that on the gene level concordance cannot be readily identified. Therefore, the ZFE could be used as a prescreen for hepatotoxic compounds as it shares biological complexity with *in vivo* models and ease of testing found in *in vitro* models.

Acknowledgements

The authors wish to thank Paul Igor Costea PhD, of the European Molecular Biology Laboratory (EMBL), for helping to generate the biplot. In addition, we would like to thank Anke van Summeren and Edwin Mariman from Maastricht University (UM) for providing us with the mouse primary hepatocyte data. This work was supported by the Netherlands Genomics Initiative/Netherlands Organization for Scientific Research (NWO) grant number: 050-060-510.

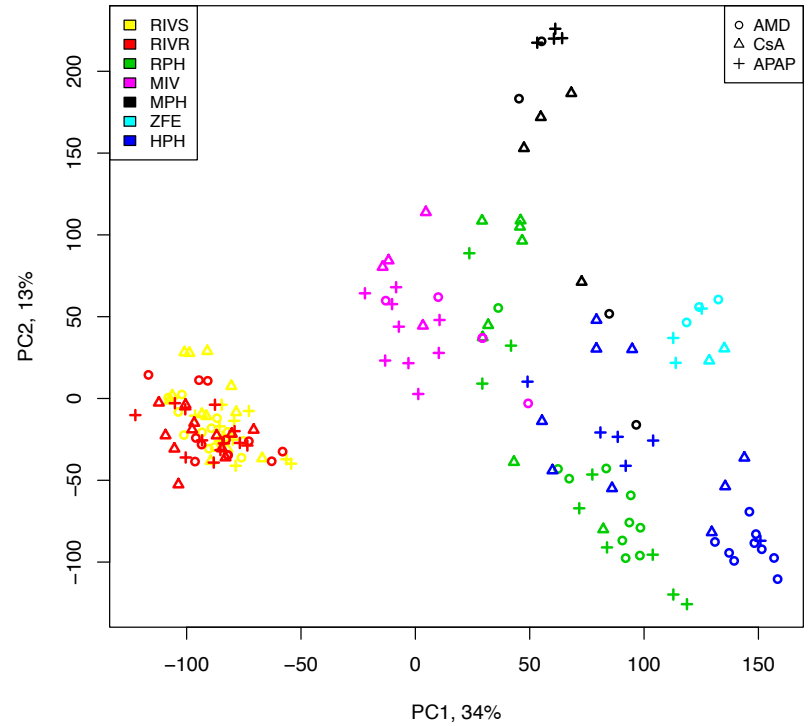

Supplementary Figure 1 PCA plot of the samples used within this study.
PCA plot of all the samples used within this study. PCA was based on a distance matrix using the overlap of the top-500 ranked genes between the samples. Samples are color-coded similar to as in Figure 2, and the different compounds are represented by the different shapes. Percentages on the x- and y-axis indicate the explained variances for the two first principal axes.

6

General Discussion

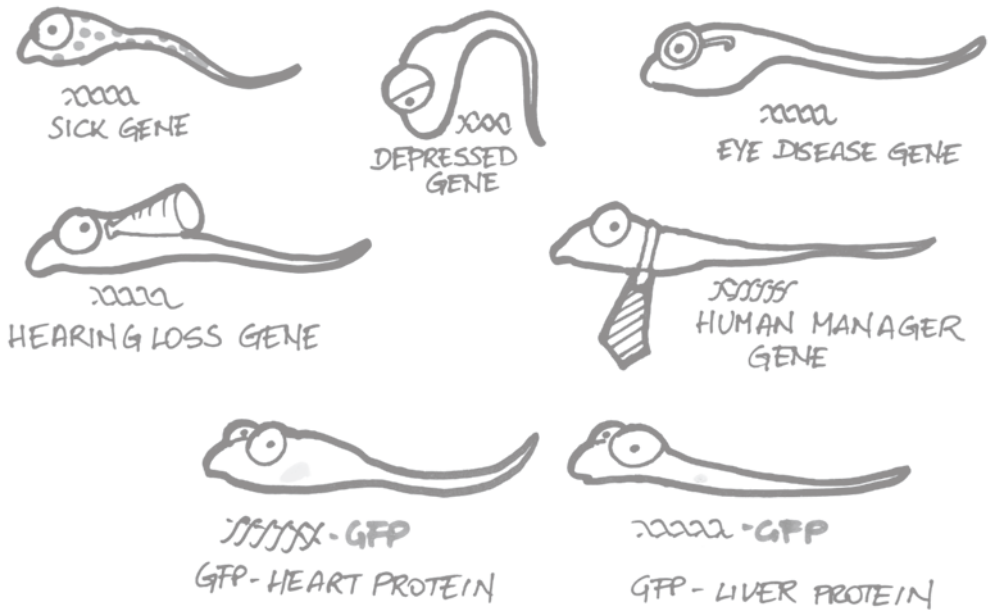

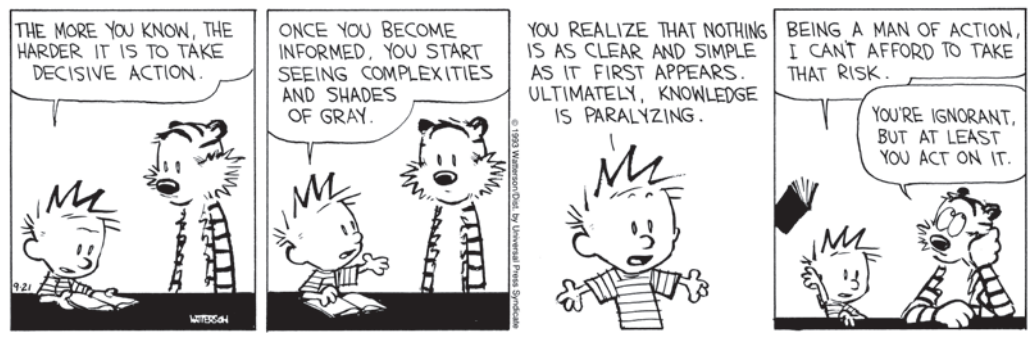

General Discussion

Hepatotoxicity-related pathologies as induced by drugs and industrial chemicals are traditionally measured in *in vivo* rat studies by histopathology and clinical chemistry. A disadvantage of *in vivo* studies is that they require enormous numbers of animals, which according to regulatory study protocols need to be exposed to high doses of compounds during extended periods of time. Apart from ethical and economical considerations, there is a scientific drawback because of the discordance between the hepatotoxic effects in rodents and humans, limiting the relevance of the outcome of *in vivo* studies regarding the prediction of human health risks. For these reasons, in recent years much effort was dedicated to the development of alternative test methods, and the zebrafish embryo is such a promising novel alternative test system. The general hypothesis of the work presented in this thesis is that the zebrafish embryo provides a simple and effective alternative animal model for hepatotoxicity testing, reproducing the complexity and functionality of the mammal liver *in vivo*. The main purpose of our studies was to develop and evaluate the zebrafish embryo model as an alternative system in a mechanism based way, using toxicogenomics approaches as a tool.

Through the mechanisms identified in our studies we provide evidence that the zebrafish embryo is a representative model to predict human hepatotoxicity, hence this discussion will focus on the critical factors related to hepatotoxicity testing in this model. First, the toxicokinetic properties of the zebrafish embryo will be discussed and how these differ from the human situation. Next, the histopathological changes as observed in the adult zebrafish liver and zebrafish embryo will be reviewed. Further, the additional value of toxicogenomic techniques presented in this thesis in identifying the underlying molecular mechanisms of hepatotoxicity will be discussed. Finally, further perspectives and applicability of the model will be considered.

Toxicokinetics in the zebrafish embryo

For a valid prediction of toxicity from fish to the mammal situation it is essential to take toxicokinetics in the zebrafish embryo toxicokinetics into account. Generally, toxicokinetics captures information on the administration and absorption, distribution, metabolism or biotransformation and excretion (ADME) of a toxic compound in an organism[181].

First, absorption of xenobiotic compounds greatly differs between mammals and zebrafish embryos. The difficulty to translate toxicity data from zebrafish embryos to humans starts with the xenobiotic characteristics, whereby water soluble compounds such as paracetamol may have completely different uptake and distribution patterns compared to more lipophilic compounds such as cyclosporine A. Lipophilicity may partly explain differences in absorption efficiency between fish and mammals, in view of the different surfaces through which absorption takes place. In fish, a major route of absorption of a compound is through the gills and skin, in addition to oral uptake[182,183], whereas in

humans most xenobiotic compounds are mainly orally ingested. Therefore, the zebrafish gills can be considered as an important first-pass organ in addition to the liver, which is the single first pass organ in mammals/humans. The importance of gills as a first pass organ is underlined by the presence of CYP450[184]. In addition, an important issue related to absorption difference between lipophilic and hydrophilic compounds in exposure studies in zebrafish embryos is the barrier that is formed by the chorion (egg shell). However, here we circumvented this problem by exposing after hatching of the embryo, which is a relevant timing for hepatotoxicity studies in view of the presence of functional liver tissue in the embryo.

After the administration and uptake of a compound, the distribution of a compound is responsible for inducing the toxicity in the target organs, and distribution modeling can therefore help to understand details of observed effects. In the zebrafish embryo, whole organism concentration studies are only beginning to emerge[185], while information regarding distribution is presently extremely limited, excluding direct comparison between relevant concentration in the fish versus plasma concentration in humans. Here, xenobiotic compounds dissolved in DMSO were added to the exposure medium, and were taken up by the zebrafish embryo presumably by passive diffusion, mainly through gills and skin[182]. The biotransformation capacity of the gills might influence the distribution of parent compound concentration and its metabolites at the site of the liver, and is a factor that needs to be taken into account when comparing liver toxicity profiles between ZFE and mammals. Furthermore, the distribution through the body might be influenced by the presence of the yolk sac, which is the internal food supply in the zebrafish embryo essential for initial development. However, the yolk is a lipid rich compartment allowing hydrophobic compounds to accumulated here. This accumulation could then lead to an overestimation for the effective concentrations required to induce organ toxicity[182].

Regarding the biotransformation of xenobiotic compounds, expression of most metabolizing enzymes is already present in early developmental stages[55,182]. Furthermore, enzymes that are part of the metabolizing process are highly conserved compared to mammals[182] and many orthologs are found in humans[55,182]. However, development of the ZFE is associated with stage dependent changes of expression levels of metabolizing enzymes, which might result in a different sensitivity to the xenobiotic compounds compared to mammals. This difference in sensitivity is further anticipated by the large evolutionary distance between humans and zebrafish, which is around 445 million years[186].

The final component in ADME is the excretion of the compound. However, excretion is not seen as a very important aspect in the zebrafish embryo model while the exposure is mainly static[182,187].

In future studies, it is imperative to improve characterization of the kinetic properties in fish to gain a better understanding of their influence on the development of hepatotoxicity. In this thesis, we have not measured the internal concentration of our compounds or their metabolites in the ZFE, but relied on the observed compound-induced phenotypic changes in the liver, which were suggestive for internal ZFE drug exposure.

Identification of hepatotoxicity using histopathology

Histopathology can be used to differentiate the three hepatotoxic phenotypes cholestasis, steatosis and necrosis. Cholestasis is a chronic condition and is phenotypically characterized by bile accumulation as a result of changes in intra- or extracellular bile flow or bile composition[34]. Steatosis may occur chronically as well and is characterized as an increase in cellular lipid content due to an increase in *de novo* synthesis of fatty acids or reduced lipid secretion or oxidation[19]. Necrosis is an acute condition and is characterized by cell death due to oxidative stress and/or mitochondrial damage leading to loss of cellular ATP levels[4,33]. The model compounds CsA, EE2 and CPZ induce cholestasis. AMD, TET and VPA induce steatosis in humans[137]. Finally, necrosis is induced by APAP, PQ and TAA[1,4].

In **chapter 2**, we showed that the zebrafish embryo demonstrates clear histopathological changes after xenobiotic exposure, but failed to display the classical cholestatic and necrotic phenotypes as observed in humans. To verify whether this difference was life stage dependent or represents a response difference between fish and mammals, the adult zebrafish was also exposed to the same reference hepatotoxicants. The adult zebrafish liver was found particularly sensitive to the development of cholestasis and displayed a phenotype similar to humans. Cholestasis could not be identified in the zebrafish embryo probably due to the underdevelopment of bile production mechanisms, in line with the observation that genes involved in the formation of bile ducts are first expressed at 48-hpf [126] and that onset of fully operational bile production in the embryo is only from 5-dpf onwards[44]. The observed steatosis in both zebrafish life stages was consistent with the nominal phenotype as observed in mammals. The necrotic phenotype was represented in both life stages as hepatocellular vacuoles, but no apparent apoptosis or necrosis was induced.

The onset of necrosis typically involves lipid peroxidation, which is especially the case for acetaminophen. Lipid peroxidation is generally coupled to the formation of reactive oxygen species (ROS) and is a result of oxidative stress in cells. The Nrf2 transcription factor plays a very important role in the defense against oxidative stress[188]. In the zebrafish embryos, the Nrf2 pathway was not identified as a critical reporter for most of our hepatotoxicants. The Nrf2 pathway is conserved between humans and zebrafish and is even present in the zebrafish embryos. However, it has been shown that the *nrf2* mutant zebrafish embryo is not sensitive to all ROS productions as is the case within the mammalian systems[189], suggesting that alternative defense mechanisms are active. This explains why this pathway has not been found as critical in the zebrafish embryo. Overall, there are apparently species and life stage dependent apical phenotypes, suggesting that toxicity pathways diverge between life stages and species. This is in line with the conclusion that our toxicogenomic methods could not distinguish the nominal pathological classes represented in our set of model compounds in the zebrafish embryo.

Identification of hepatotoxicity using gene expression profiling

Histopathology is the classical method to verify toxic events, but it does not provide information about the underlying molecular mechanisms leading to hepatotoxicity, and thus may limit full comparison of effects between testing models. Our working hypothesis was that the underlying molecular mechanisms leading to a toxic phenotype might be conserved between humans and zebrafish embryos, and therefore be more informative than histopathology regarding the translation of effects. In case of zebrafish, toxicogenomics techniques, including transcriptomics and proteomics, were already applied mostly in the area of developmental and ecotoxicological toxicity in the zebrafish embryo[53,66–70,187]. However, the implementation of transcriptomics or proteomics in the zebrafish embryo for predicting hepatotoxicity had not been applied, and our initial results described in **chapter 1** indeed supported that the application of toxicogenomics in hepatotoxicity appeared to be of great added value regarding better understanding of the underlying molecular mechanisms of toxicant induced effects.

Defining liver-associated transcripts

In rodent experiments, the liver is dissected and subjected to RNA isolation for the determination of gene expression changes, but the zebrafish embryo is too small for liver dissection. Although sophisticated procedures such as micro-dissection can be applied to collect small amounts of liver material, this will hamper the throughput and robustness of the testing system. Therefore, we first determined whether liver-associated gene expression can be detected in the whole zebrafish embryo using whole body homogenates. In the zebrafish embryo, the liver accounts for only approximately 20% of the total body weight, and this relatively small proportion might limit the detectability of liver specific signals. Therefore, to ensure that we were able to determine liver-specific gene expression, whole embryo homogenates were compared to isolated adult zebrafish livers. This comparison was complicated by the necessity to use pools of 15 zebrafish embryos per sample meaning that the specific signal of the individual embryo is diluted, but on the other hand, the observed gene expression changes are more robust[106]. In this comparison we used next-generation sequencing, which is a relatively new technique, which can be used for mapping as well as quantifying transcriptomes. The advantage over the use of the traditional RNA arrays is that this technique provides a more sensitive and precise measure of transcript levels resulting from the relative low background signal and the absence of an upper limit of detection[64]. The results in **chapter 2** support theadditional value of this still developing technique for toxicity testing. Furthermore, we confirmed through next generation sequencing that liver-associated gene expression is present in the whole zebrafish embryo and that hepatotoxicity-associated signals are detectable over the noise of other tissues, and that the whole zebrafish embryo can therefore be used as a proxy for the assessment of hepatotoxicity. Building on this premise, a detailed analysis of mechanisms of hepatotoxicity was conducted using RNA arrays as shown in **chapter 3**. This resulted in a better description of hepatotoxic responses and to the development of expression markers predictive for hepatotoxicity in humans. To assess the liver-specificity of the found markers, we assessed their location using *in situ* hydrization (data not shown), and could thus confirm liver specificity of eight marker genes . This supports that the small proportion of the liver and the pooling of the samples did not influence the liver associated gene expression.

Analysis of gene expression resulted in markers for general hepatotoxicity, but specific phenotypes were not reflected, possibly due to suboptimal exposure concentrations and durations. Additional efforts to discriminate between nominal phenotypes using proteomics (**chapter 4**) produced a similar result, *i.e.* identification of general markers for hepatotoxicity but not for specific phenotypes. Furthermore, we observed that most of the expressed proteins were linked to a more general hepatotoxic stress response, possibly also related to the used concentrations and exposure durations. On the other hand, we did not observe interference of yolk sac related proteins, which is a general problem in proteomics studies with zebrafish embryos, supporting robustness of the liver specific protein signals. This suggests that deyolking of a 5-dpf old whole zebrafish embryo is not necessary which improves the throughput of the system when applying proteomics.

Determination of hepatotoxic classes

The reference compounds used in this thesis were selected to represent three different histopathological endpoints (cholestasis, steatosis or necrosis), but as described in **chapter 1**, within each class, individual compounds have unique underlying molecular mechanisms for these histopathological changes. In **chapter 3 and 4**, we identified markers for general hepatotoxicity, while the applied zebrafish toxicogenomics strategy was unable to discriminate between the hepatotoxic classes of interest. This is either due to species dependent differences in liver physiology or to experimental conditions. With regard to the latter, the selected exposure concentrations were based on the maximum tolerable concentration inducing no teratological deviations or death. It might be that this single concentration of the compounds was not optimal for unducing the specific hepatotoxic phenotypes; moreover, the exposure period might be too short to induce the specific phenotype. Alternatively, zebrafish specific responsiveness to xenobiotics could be in line with deviating responses in other models, such as hepatoma-derived cell lines which strongly differ from the whole liver gene expression profile[64,101]. It should be noted that we only tested a set of nine compounds, and a more comprehensive range of compounds will probably generate more robust results. A first attempt was made to validate our markers by using an additional set of seven hepatotoxic compounds (not shown). Zebrafish embryos were exposed to this new set of model hepatotoxicants and compared to three old reference hepatotoxicants. After exposure, the expression of the markers genes obtained in **chapter 2 and 3**, were determined using qPCR. Most of the additional hepatotoxicants had similar expression patterns as the original set of hepato-

toxicants, confirming the validity of our markers. However, this additional exercise was not designed to improve class distinction, and only a larger drug library screen in a more high-through put setting including more hepatotoxicants and non-hepatotoxicants may provide a better estimate whether the zebrafish embryo is able to discriminate between classes.

Interspecies extrapolation

As mentioned above, the zebrafish embryos were able to determine the hepatotoxic potential of xenobiotic compounds. It is important to extrapolate the observations to mammalian species and where possible even to the human situation, to underpin major added value of the zebrafish embryos. Therefore, in **chapter 2 and 5**, we compared the zebrafish embryo to the *in vivo* mouse and rat liver, *in vitro* mouse and rat hepatocytes, and primary human hepatocytes using gene expression changes from experiments using a model compound for each hepatotoxic phenotype to identify commonalities. Three compounds, CsA, AMD, and APAP, were chosen for the comparison because of their relevance to human toxicity and the availability of reference data in the selected models. This comparison revealed that the zebrafish embryo shares similarities at the pathway level after xenobiotic exposure with both *in vivo* and *in vitro* models, with the highest concordance to the mouse model. One pathway which was shared between all models was the pathway "Regulation of metabolism – bile acids regulation of glucose and lipid metabolism via FXR". While bile acids are important in the regulation of the normal liver, they also activate various signaling pathways including those of nuclear receptors[34,177]. In this particular pathway, it was observed that each species targeted a specific part suggesting species differences. Still, the common regulation of this particular pathway between all included species indicates its robustness. This supports that the zebrafish embryo model has a similar response to the hepatotoxicants as the traditionally used models and therefore, the zebrafish embryo could be used as a prescreen for hepatotoxic compounds.

Optimization of the zebrafish embryo screening for high throughput

The studies presented in this thesis have shown the promise and applicability of the embryo model for the detection of hepatoxic potential of compounds. In the current work, the model was not optimized for high throughput screening. Optimization of the model can be achieved in multiple ways. First, the experimental setup including handling of the zebrafish embryos and the distribution of the xenobiotic compound of interest can be improved. The handling of the embryos can be automated by using an embryo sorting machine, for example the COPAS XL[59,190]. The distribution of the xenobiotic compound to the well plates can be improved by either using a multichannel pipette or automated by the use of a robotic liquid-handling machine[59]. Furthermore, the whole genome sequencing or the microarray technologies that we applied here provide highly detailed information, but are rather time consuming. Dedicated arrays or selected qPCR with marker genes for hepatotoxicity could improve the throughput of the screening. A drawback of these methods is that these still require time consuming RNA extraction, and have no informationt on the tissue distribution, *i.e.* liver expression, of marker genes. To overcome these drawbacks, another optimization could be to generate transgenic reporter zebrafish, which allows screening in high throughput manner. The technique of generation reporters is well developed for zebrafish, and could be applied for the markers from **chapter 2** and **3**. For this purpose, DNA constructs enabling the expression of a fluorescent protein after induction of the marker of hepatotoxicity should be designed and injected in wild type one cell stage zebrafish embryos. Selected of embryos which show the intended presence of the fluorescent protein are further raised to adulthood and paired to produce fluorescent embryos which can subsequently be used for screening purposes[191]. With the use of transgenic zebrafish embryos for hepatotoxicity testing, large drugs screens can be tested in a more high-throughput manner using COPAS or confocal microscopy which has been shown to be a valid approach for developmental toxicity screening[192–194]. Preliminary testing with one such a reporter fish, *fabp10*[195,196], has been initiated.

Implementation of the zebrafish embryo in drug discovery process

The zebrafish embryo testing model fits into multiple stages of the drug discovery pipeline, ranging from lead and target identification to lead optimization and ADME studies[193,197]. Application of this model is attractive because it is relatively cheap, it contributes to reduction of animal experimentation, and relatively small amounts of the xenobiotic compounds are needed. The model can be incorporated easily into the existing tiered approach for the prediction of hepatotoxicity. Combining multiple *in vitro* screening models in a tiered approach could overcome the limitations of each individual *in vitro* model in the prediction of toxicity, and a in a series of models, they can complement each other for information regarding toxicity[164,197]. Presently, the earliest test models in such a tiered approach for hepatotoxicity are typically the *in vitro* hepatoma cell lines, for example HepG2 or HepaRG. Next, primary hepatocytes from either rat or human origin would be tested, to ensure incorporation of drug metabolism and transport capabilities as well as bioenergetics that are closer to the *in vivo* situation. Precision cut tissue slices, which provide an intact architecture similar to the organ of interest, provide an alternative method that can used next in the line of *in vitro* models[164,197]. Although all these models are suitable for the detection of hepatotoxic potential of compounds, the zebrafish embryo offers biological complexitity similar to *in vivo* models with the ease of testing as is possible with *in vitro* models. Therefore, the zebrafish embryo can be used to prioritize the compounds, which should be tested in an *in vivo* set-up, thereby contributing to the reduction and refinement of animal experimentation.

Current and future application of the zebrafish embryo

The implementation of the zebrafish embryo as a model for hepatotoxicity testing requires a number of steps. Firstly, as mentioned above, the toxicokinetic parameters, which limit assessment of particular compounds in the zebrafish embryo model, should be characterized better. As discussed, a clear example in this respect is the yolk sac which might cause underestimation of the results obtained by the more lipophilic xenobiotics compounds.

Here, we tested only nine compounds which are known to induce hepatotoxicity in humans. To validate the model further and determine the predictability of the model, a large screen of many hepatotoxicants needs to be performed. For practical reasons, we had to limit our studies to a single sub-lethal concentration of each compound, but obviously confirmation of concentration-dependent responses would improve robustness of the identified markers. As indicated, improvement of the throughput of testing could be achieved through the development of transgenic zebrafish. In addition, humanized transgenic fish that would express relevant biotransformation enzymes could further strengthen the zebrafish embryo system.

The zebrafish embryo can be of added value to elucidate the underlying molecular mechanisms by using morpholino techniques to establish a knock down of genes of interest. Morpholinos allow the temporary knockdown of genes thus identifying their role in the involved toxic mechanism of hepatotoxicity. For example genes that were induced by any of our model compounds in the present study could be interrogated for involvement in the onset of the phenotypic hepatotoxic changes in the liver. In particular those genes that would then be functionally associated with the onset of hepatotoxicity and have translational relevance would be of the highest interest to serve as marker for hepatotoxicity liabilities of novel chemical entities.

Conclusion

In this thesis we showed the applicability of the zebrafish embryo as an alternative model for hepatotoxicity testing using analysis of mechanisms through toxicogenomics. By applying a variety of toxicogenomics techniques, we were able to characterize specific responses. NGS revealed that hepatotoxicity-associated gene expression remains detectable even in non-tissue specific analysis in whole body zebrafish embryo homogenates. Gene and protein expression profiling resulted in the identification of a set of marker genes that could be linked to pathways and processes, which are associated with a general hepatotoxic response. Application of such markers will increase the throughput of the system. Finally, we showed that the zebrafish embryo model shares similarities with *in vivo* and *in vitro* models for hepatotoxicity, where the model has more commonality with the mouse *in vivo* and *in vitro* models than with the other models.

Overall, the model has the advantages of the *in vitro* models with the biological complexicity of an *in vivo* response, and we thus anticipate that the zebrafish embryo can contribute to the 3R strategy by reducing, refining and replacing animal studies. Our observations support that this model can have added value in a tiered approach as a pre-screen for the detection of hepatotoxic potential of compounds.

7

English Summary

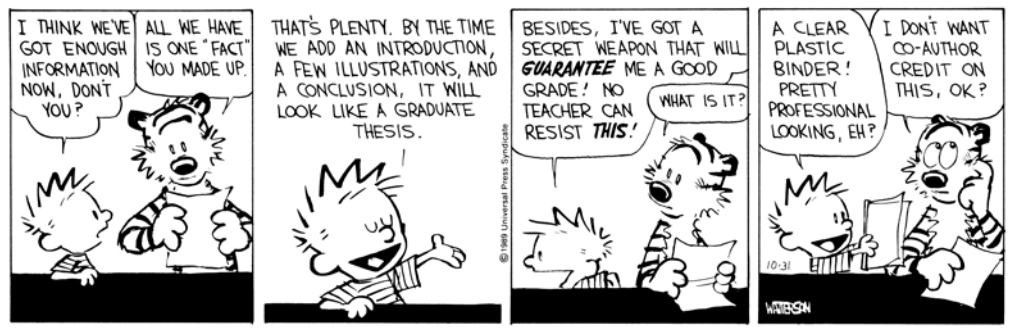

English Summary

This thesis aims to establish whether the zebrafish embryo is a suitable alternative testing method for the prediction of hepatotoxic potential of compounds, thereby using toxicogenomic techniques. The goal was to establish improved alternative models to better predict human hepatotoxicity, thereby directly contributing to the reduction, refinement and replacement (3Rs) of animal experimentation.

In **chapter 1**, liver toxicity was introduced as an important target to study adverse drug effects. Especially, in mammals and particularly for xenobiotics that rely on oral uptake, many compounds provoke the first sign of toxicity in the liver. This is due to its function as a first pass organ in metabolism of toxic compounds, resulting in exposure of liver cells, mainly hepatocytes, to potentially toxic parent compounds and reactive metabolites. Hepatotoxicity is the result of various underlying molecular mechanisms arising from different xenobiotic-induced toxic phenotypes, of which cholestasis, steatosis and necrosis are most frequently observed. Cholestasis is a chronic condition and is phenotypically characterized by bile accumulation as a result of changes in intra- or extracellular bile flow or bile composition[34]. Steatosis may occur chronically as well and is characterized as an increase in cellular lipid content due to an increase in *de novo* synthesis of fatty acids or reduced lipid secretion or oxidation[19]. Necrosis is an acute condition and is characterized by cell death due to oxidative stress[4,33]. Traditionally, the hepatotoxic potential of compounds is tested using rodent studies. The aim of this thesis is to investigate whether the zebrafish embryo model combined with toxicogenomic techniques can be proposed as a promising alternative high-throughput method for hepatotoxicity testing.

In **chapter 2,** the applicability of the whole ZFE for hepatotoxicity testing was further underpinned by combining histopathology and next generation sequencing-based gene expression profiling. To this end, whole ZFE and adult zebrafish were exposed to a set of hepatotoxic reference compounds. Histopathology revealed compound and life-stage specific effects indicative of toxic injury in livers of whole ZFE and adult zebrafish. Next generation sequencing (NGS) was used to compare transcript profiles in pooled RNA samples of whole ZFE and livers of adult zebrafish. This revealed that hepatotoxicity-associated expression can be detected above the overall transcription noise in the whole embryo supporting the applicability of the whole ZFE model for compound-induced hepatotoxicity screening.

In **chapter 3,** we hypothesized that the detailed analysis of underlying mechanisms of hepatotoxicity in ZFE contributes to the improved identification of hepatotoxic properties of new compounds and to the reduction of the number of rodents used for chemical safety assessment. ZFEs were exposed to nine reference hepatotoxicants, targeted at

induction of cholestasis, steatosis and necrosis, and two non-hepatotoxic controls. Histopathology revealed various specific morphological changes in the ZFE hepatocytes indicative of cell injury. Gene expression profiles of the individual compounds were generated using microarrays. Regulation of single genes and of pathways could be linked to hepatotoxic responses in general, but phenotype-specific responses could not be distinguished. Hepatotoxicity-associated pathways included xenobiotic metabolism and oxidoreduction related pathways. Overall analysis of gene expression identified a small set of potential biomarkers specific for a common hepatotoxicity response.

To allow for verification of the histopathology, we applied another -omics technique, which was proteomics. Proteomics identified multiple markers for hepatotoxicity using the whole zebrafish embryo. Furthermore, we compared the gene expression results with the obtained proteomics results in **chapter 4**. Proteomics results showed that it is possible to identify markers after exposure to hepatotoxicants. These markers can be linked to enriched biological processes which are associated with hepatotoxicity. Furthermore, as observed in **chapter 3**, the zebrafish embryo is so far in our hands only able to distinguished general hepatotoxicity and not phenotype-specific hepatotoxicity.

In **chapter 5,** the zebrafish embryo was compared with the traditionally used models, including mice and rats. The ZFE model shares similarity at the pathway level after xenobiotic exposure with both *in vivo* and *in vitro* models. Concordance on the pathway level identified a single pathway to be altered across all hepatotoxic phenotypes. This analysis also suggest that pathways are better suited as hepatotoxicity markers than single genes as each model was found to effect different genes within the same pathway. Comparing at the single gene level showed that there were model specific changes and that outside of a model the overlap was fairly similar across models suggesting that on the gene level concordance cannot be readily identified. The advantage of the ZFE is that is can be used as a pre-screen to determine hepatotoxic potential of compounds, providing a quick and easy high-throughput testing model.

In **chapter 6**, we provided a general discussion of the obtained results including the assessment of the toxicokinetics parameters. Further, we addressed the limitations and strengths of this model. In addition, we provided the future perspectives of this model for the use in hepatotoxicity testing.

Nederlandse samenvatting
References
Curriculum vitae
List of publications

Nederlandse Samenvatting

Korte introductie

Mensen worden gedurende hun hele leven blootgesteld aan een veelheid van schadelijke stoffen, via zowel natuurlijke als artificiële wegen. Soms vindt blootstelling aan deze schadelijke stoffen onbewust plaats, zoals blootstelling via voedsel, door inademing of door opname via de huid, of bewust wanneer men bijvoorbeeld een medicijn inneemt. Het gebruik van medicijnen kan leiden tot schade aan het lichaam, zeker wanneer er een te hoge dosering wordt ingenomen. Door middel van toxicologisch onderzoek probeert men de risico's in te schatten van deze schadelijke stoffen.

Bij toxicologisch onderzoek is de lever een belangrijk orgaan. Dit komt onder andere door de rol die de lever in het menselijk lichaam heeft. De lever komt als eerste in aanraking met giftige stoffen, nadat deze door de darm zijn opgenomen. Verder speelt de lever een rol in het omzetten van giftige stoffen naar mindere giftige stoffen die gemakkelijk door het lichaam zijn uit te scheiden. Dit proces verloopt normaal gesproken zonder problemen, maar soms kan deze omzetting van stoffen juist tot een giftiger product leiden waardoor de lever schade oploopt.

Leverschade kan resulteren in een verscheidenheid aan histopathologische veranderingen, waarbij cholestase, steatose en necrose de drie belangrijkste afwijkingen zijn. Cholestase is te zien in de levercel als geel-oranje druppeltjes. Steatose wordt gekenmerkt door ophoping van vet in de levercel en wordt zichtbaar door middel van histopathologische kleuringen. Bij necrose is er sprake van versterf van levercellen, wat afhankelijk van het stadium zichtbaar is als verkleuring of verval van levercellen. Alle vormen van leverschade kunnen uiteindelijk resulteren in leverfalen.

Om te kunnen voorspellen welke giftige stoffen tot leverschade leiden, wordt er gebruik gemaakt van zowel *in vitro* als *in vivo* modellen. Bij *in vitro* modellen analyseert men de effecten van schadelijke stoffen op cellijnen, schijfjes lever en primaire lever cellen. *In vivo* modellen richten zich op het testen van stoffen in dieren, en daarbij worden er voornamelijk muizen en ratten gebruikt. Aan deze *in vivo* dierstudies kleven een aantal ethische, economische en wetenschappelijke bezwaren. Er worden veel dieren gebruikt die voor langere tijd aan hoge doseringen van de giftige stoffen worden blootgesteld. Het belangrijkste bezwaar is echter dat de resultaten die met deze dierstudies worden behaald, lang niet altijd de situatie in de mens goed voorspellen. Dit wordt ook wel aangeduid als vals positieve of vals negatieve resultaten. Daardoor heeft het onderzoek de afgelopen jaren zich voornamelijk gefocust op de ontwikkeling van alternatieve testmethoden die de situatie in de mens beter kunnen voorspellen.

Een mogelijk goed alternatief model is het zebravis embryo model. Dit model combineert verschillende voordelen, waarvan er één is dat deze embryo's nog zo'n primitief zenuwstelsel hebben dat niet wordt verwacht dat ze pijn of ongerief kunnen ervaren. Zebravis embryo's worden daarom niet gezien als proefdier en het model draagt op die manier bij

aan de drie V strategie (Vermindering, Vervanging en Verfijning van proefdiergebruik).
Normaal gesproken word het effect van de giftige stoffen bepaald door het bekijken van histopathologische veranderingen en meten van leverenzymen. Deze methoden geven echter geen informatie over het mechanisme dat leidt tot leverschade, terwijl juist dit moleculaire mechanisme mogelijkheden geeft om leverschade goed te voorspellen. Om dit onderliggende mechanisme te kunnen begrijpen, wordt er gebruik gemaakt van verschillende moleculaire technieken, gericht op analyse van met name gen- en eiwitexpressie.
Dit proefschrift beschrijft hoe het zebravis embryo model in combinatie met gen-expressie analyse-technieken het beste gebruikt kan worden om leverschade in de mens te kunnen voorspellen.

Samenvatting van de studies beschreven in dit proefschrift

Hoofdstuk 2 beschrijft twee technieken die gebruikt zijn om te bepalen of het zebravis embryo als alternatief model gebruikt kan worden bij de voorspelling van leverschade. Hierbij hebben we veranderingen in extracten van het gehele embryo vergeleken met veranderingen in de lever van de volwassen zebravis, om de vraag te beantwoorden of effecten op de lever wel in het zebravis embryo gemeten kunnen worden. Allereerst hebben we met behulp van histologie gekeken of er daadwerkelijk morfologische veranderingen in de lever van zowel de volwassen zebravis als de embryo waargenomen kunnen worden. Hieruit kwam naar voren dat er leeftijd- en stofspecifieke veranderingen optraden in beide modellen. Daarna hebben we met behulp van next generation sequencing onderzocht of we in staat waren om genexpressie veranderingen in het embryo te kunnen waarnemen, omdat de lever maar in geringe plaats inneemt in het embryo. Na analyse kwam naar voren dat we in staat zijn om leverspecifieke veranderingen waar te nemen in het gehele embryo.
Omdat we in staat waren lever- geassocieerde genexpressie te kunnen bepalen in het gehele embryo, hebben we in **hoofdstuk 3** geanalyseeerd of het mogelijk is om op basis van genexpressie profielen (transcriptomics) onderscheid te maken tussen de verschillende typen leverschade. Voor deze studie hebben we gebruik gemaakt van dezelfde stoffen als in **hoofdstuk 2**, maar zijn de genexpressie profielen op een andere manier geanalyseerd, namelijk met behulp van microarrays. Het bleek dat in het zebravis embryo model op die manier de verschillende klassen van leverschade niet te onderscheiden zijn, omdat de genexpressie profielen van alle klassen veel overlappen. Wel bleek het mogelijk om genexpressie markers te identificeren die leverschade zouden kunnen voorspellen in de mens.
Omdat met genexpressie geen onderscheid gemaakt kon worden tussen de verschillende typen leverschade hebben we in **hoofdstuk 4** gebruik gemaakt van een andere techniek, namelijk het meten van eiwitexpressie veranderingen (proteomics). Maar ook met deze techniek bleek het niet mogelijk om in het zebravis embryo model onderscheid te maken tussen de verschillende typen klassen van leverschade. Daarentegen waren we wel in staat om een kleine lijst met markers te selecteren die leverschade in de mens zouden kunnen voorspellen.
Om echt de voorspellende waarde van het zebravis embryo model te kunnen definiëren, hebben we in **hoofdstuk 5** een overkoepelende analyse uitgevoerd die de genexpressie profielen van de verschillende testmodellen voor leverschade vergelijkt. In plaats van alleen te kijken naar veranderingen in expressie van alleen genen, hebben we bestudeerd of groepen van genen, de zogenaamde pathways, veranderde na blootstelling. Uit deze vergelijking bleek dat het zebravis embryo model met betrekking tot gereguleerde pathways overlap heeft met zowel de *in vivo* als de *in vitro* modellen. Wanneer we alle modellen met elkaar vergelijken, zowel *in vivo* als *in vitro,* komt er één pathway naar voren die in alle modellen gereguleerd is.
In de afsluitende discussie (**hoofdstuk 6**) van het proefschrift worden de voor- en nadelen van de gebruikte technieken beschouwd, en besproken welke aanvullende studies nodig zijn om het zebravisembryo model daadwerkelijk in te zetten voor het voorspellen van leverschade door chemische stoffen in de mens. Als slotconclusie wordt geconcludeerd dat het zebravis embryo model gebruikt kan worden als alternatief voor dierproeven bij het voorspellen van leverschade in de mens.

References

1. Zimmerman, H. J. Hepatotoxicity: the adverse effects of drugs and other chemicals on the liver. (1999).
2. Olson, H. *et al.* Concordance of the toxicity of pharmaceuticals in humans and in animals. *Regul Toxicol Pharmacol* **32,** 56–67 (2000).
3. Niesink, R. J. M., De Vries, J. & Hollinger, M. A. *Toxicology*. (CRC Pressl Llc, 1996).
4. Jaeschke, H. *et al.* Mechanisms of hepatotoxicity. *Toxicol. Sci. Off. J. Soc. Toxicol.* **65,** 166–176 (2002).
5. Kienhuis, A. S. *et al.* Application of toxicogenomics in hepatic systems toxicology for risk assessment: Acetaminophen as a case study. *Toxicol. Appl. Pharmacol.* **250,** 96–107 (2011).
6. Lee, W. M. Drug-induced hepatotoxicity. *N. Engl. J. Med.* **349,** 474–485 (2003).
7. Godoy, P. *et al.* Recent advances in 2D and 3D in vitro systems using primary hepatocytes, alternative hepatocyte sources and non-parenchymal liver cells and their use in investigating mechanisms of hepatotoxicity, cell signaling and ADME. *Arch. Toxicol.* **87,** 1315–1530 (2013).
8. Laskin, D. L. Sinusoidal Lining Cells and Hepatotoxicity. *Toxicol. Pathol.* **24,** 112–118 (1996).
9. Kolios, G., Valatas, V., Kouroumalis, E. & others. Role of Kupffer cells in the pathogenesis of liver disease. *World J. Gastroenterol.* **12,** 7413 (2006).
10. Roberts, R. A. *et al.* Role of the Kupffer Cell in Mediating Hepatic Toxicity and Carcinogenesis. *Toxicol. Sci.* **96,** 2–15 (2007).
11. Sahu, S. C. Hepatotoxicity: From Genomics to in vitro and in vivo Models. (2008).
12. Wagner, M., Zollner, G. & Trauner, M. Nuclear receptor regulation of the adaptive response of bile acid transporters in cholestasis. *Semin. Liver Dis.* **30,** 160–177 (2010).
13. Zollner, G. & Trauner, M. Mechanisms of cholestasis. *Clin. Liver Dis.* **12,** 1–26– vii (2008).
14. Zollner, G. & Trauner, M. Molecular mechanisms of cholestasis. *Wien. Med. Wochenschr. 1946* **156,** 380–385 (2006).
15. Yamamoto, Y. *et al.* Estrogen receptor alpha mediates 17alpha-ethynylestradiol causing hepatotoxicity. *J. Biol. Chem.* **281,** 16625–16631 (2006).
16. Anthérieu, S. *et al.* Oxidative stress plays a major role in chlorpromazine-induced cholestasis in human HepaRG cells. *Hepatology* **57,** 1518–1529 (2013).
17. Van Summeren, A. *et al.* Screening for drug-induced hepatotoxicity in primary mouse hepatocytes using acetaminophen, amiodarone, and cyclosporin a as model compounds: an omics-guided approach. *Omics J. Integr. Biol.* **17,** 71–83 (2013).
18. Jansen, P. L., Müller, M. & Sturm, E. Genes and cholestasis. *Hepatol. Baltim. Md* **34,** 1067–1074 (2001).
19. Anderson, N. & Borlak, J. Molecular mechanisms and therapeutic targets in steatosis and steatohepatitis. *Pharmacol. Rev.* **60,** 311–357 (2008).
20. McCarthy, T. C., Pollak, P. T., Hanniman, E. A. & Sinal, C. J. Disruption of hepatic lipid homeostasis in mice after amiodarone treatment is associated with peroxisome proliferator-activated receptor-alpha target gene activation. *J. Pharmacol. Exp. Ther.* **311,** 864–873 (2004).
21. Anthérieu, S., Rogue, A., Fromenty, B., Guillouzo, A. & Robin, M.-A. Induction of vesicular steatosis by amiodarone and tetracycline is associated with up-regulation of lipogenic genes in HepaRG cells. *Hepatol. Baltim. Md* **53,** 1895–1905 (2011).
22. Yin, H.-Q. *et al.* Hepatic gene expression profiling and lipid homeostasis in mice exposed to steatogenic drug, tetracycline. *Toxicol. Sci. Off. J. Soc. Toxicol.* **94,** 206–216 (2006).
23. Silva, M. F. B. *et al.* Valproic acid metabolism and its effects on mitochondrial fatty acid oxidation: a review. *J. Inherit. Metab. Dis.* **31,** 205–216 (2008).
24. Lee, M.-H. *et al.* Subchronic effects of valproic acid on gene expression profiles for lipid metabolism in mouse liver. *Toxicol. Appl. Pharmacol.* **226,** 271–284 (2008).
25. Lee, M.-H. *et al.* Gene expression profiles of murine fatty liver induced by the administration of valproic acid. *Toxicol. Appl. Pharmacol.* **220,** 45–59 (2007).
26. Matsuzaka, T. & Shimano, H. Molecular mechanisms involved in hepatic steatosis and insulin resistance. *J. Diabetes Investig.* **2,** 170–175 (2011).
27. Kim, J.-S., He, L. & Lemasters, J. J. Mitochondrial permeability transition: a common pathway to necrosis and apoptosis. *Biochem. Biophys. Res. Commun.* **304,** 463–470 (2003).

53. Yang, L. *et al.* Transcriptional profiling reveals barcode-like toxicogenomic responses in the zebrafish embryo. *Genome Biol* **8,** R227 (2007).
54. Sukardi, H., Chng, H. T., Chan, E. C. Y., Gong, Z. & Lam, S. H. Zebrafish for drug toxicity screening: bridging the in vitro cell-based models and in vivo mammalian models. *Expert Opin. Drug Metab. Toxicol.* **7,** 579–589 (2011).
55. Goldstone, J. V. *et al.* Identification and developmental expression of the full complement of Cytochrome P450 genes in Zebrafish. *BMC Genomics* **11,** 643 (2010).
56. McGrath, P. & Li, C.-Q. Zebrafish: a predictive model for assessing drug-induced toxicity. *Drug Discov. Today* **13,** 394–401 (2008).
57. Amali, A. A. *et al.* Thioacetamide induced liver damage in zebrafish embryo as a disease model for steatohepatitis. *J. Biomed. Sci.* **13,** 225–232 (2006).
58. Sawle, A. D., Wit, E., Whale, G. & Cossins, A. R. An Information-Rich Alternative, Chemicals Testing Strategy Using a High Definition Toxicogenomics and Zebrafish (Danio rerio) Embryos. *Toxicol. Sci.* **118,** 128–139 (2010).
59. Delvecchio, C., Tiefenbach, J. & Krause, H. M. The Zebrafish: A Powerful Platform for *In Vivo* , HTS Drug Discovery. *ASSAY Drug Dev. Technol.* **9,** 354–361 (2011).
60. Soldatow, V. Y., LeCluyse, E. L., Griffith, L. G. & Rusyn, I. In vitro models for liver toxicity testing. *Toxicol. Res.* **2,** 23 (2013).
61. Blomme, E. A. G., Yang, Y. & Waring, J. F. Use of toxicogenomics to understand mechanisms of drug-induced hepatotoxicity during drug discovery and development. *Toxicol. Lett.* **186,** 22–31 (2009).
62. Aubrecht, J., Schomaker, S. J. & Amacher, D. E. Emerging hepatotoxicity biomarkers and their potential to improve understanding and management of drug-induced liver injury. *Genome Med.* **5,** 85 (2013).
63. Zhang, M., Chen, M. & Tong, W. Is Toxicogenomics a More Reliable and Sensitive Biomarker than Conventional Indicators from Rats To Predict Drug-Induced Liver Injury in Humans? *Chem. Res. Toxicol.* **25,** 122–129 (2012).
64. Chen, M., Zhang, M., Borlak, J. & Tong, W. A decade of toxicogenomic research and its contribution to toxicological science. *Toxicol. Sci.* kfs223 (2012).
65. Chen, M. *et al.* Toward predictive models for drug-induced liver injury in humans: are we there yet? *Biomark. Med.* **8,** 201–213 (2014).
66. Hermsen, S. A., van den Brandhof, E. J., van der Ven, L. T. & Piersma, A. H. Relative embryotoxicity of two classes of chemicals in a modified zebrafish embryotoxicity test and comparison with their in vivo potencies. *Toxicol Vitro* **25,** 745–753 (2011).
67. Hermsen, S. A. B., Pronk, T. E., van den Brandhof, E.-J., van der Ven, L. T. M. & Piersma, A. H. Transcriptomic analysis in the developing zebrafish embryo after compound exposure: individual gene expression and pathway regulation. *Toxicol. Appl. Pharmacol.* **272,** 161–171 (2013).
68. Hermsen, S. A. B., Pronk, T. E., van den Brandhof, E.-J., van der Ven, L. T. M. & Piersma, A. H. Concentration-response analysis of differential gene expression in the zebrafish embryotoxicity test following flusilazole exposure. *Toxicol. Sci. Off. J. Soc. Toxicol.* **127,** 303–312 (2012).
69. Hermsen, S. A. B., Pronk, T. E., van den Brandhof, E.-J., van der Ven, L. T. M. & Piersma, A. H. Triazole-induced gene expression changes in the zebrafish embryo. *Reprod. Toxicol. Elmsford N* **34,** 216–224 (2012).
70. Hermsen, S. A. B., Pronk, T. E., van den Brandhof, E.-J., van der Ven, L. T. M. & Piersma, A. H. Chemical class-specific gene expression changes in the zebrafish embryo after exposure to glycol ether alkoxy acids and 1,2,4-triazole antifungals. *Reprod. Toxicol. Elmsford N* **32,** 245–252 (2011).
71. Van Summeren, A., Renes, J., van Delft, J. H. M., Kleinjans, J. C. S. & Mariman, E. C. M. Proteomics in the search for mechanisms and biomarkers of drug-induced hepatotoxicity. *Toxicol Vitro* **26,** 373–385 (2012).
72. Van Summeren, A. *et al.* Proteomics investigations of drug-induced hepatotoxicity in HepG2 cells. *Toxicol. Sci. Off. J. Soc. Toxicol.* **120,** 109–122 (2011).
73. Voelker, D. *et al.* Differential gene expression as a toxicant-sensitive endpoint in zebrafish embryos and larvae. *Aquat. Toxicol.* **81,** 355–364 (2007).
74. Quackenbush, J. Microarray data normalization and transformation. *Nat. Genet.* **32,** 496–501 (2002).
75. Irizarry, R. A. *et al.* Exploration, normalization, and summaries of high density oligonucleotide array probe level data. *Biostat. Oxf. Engl.* **4,** 249–264 (2003).
76. Irizarry, R. A. *et al.* Summaries of Affymetrix GeneChip probe level data. *Nucleic Acids Res* **31,** e15 (2003).
77. Ashburner, M. *et al.* Gene ontology: tool for the unification of biology. The Gene Ontology Consortium. *Nat. Genet.* **25,** 25–29 (2000).

28. McGill, M. R. *et al.* The mechanism underlying acetaminophen-induced hepatotoxicity in humans and mice involves mitochondrial damage and nuclear DNA fragmentation. *J. Clin. Invest.* **122,** 1574–1583 (2012).
29. McGill, M. R. & Jaeschke, H. Mechanistic biomarkers in acetaminophen-induced hepatotoxicity and acute liver failure: from preclinical models to patients. *Expert Opin. Drug Metab. Toxicol.* **10,** 1005–1017 (2014).
30. Bus, J. S. & Gibson, J. E. Paraquat: model for oxidant-initiated toxicity. *Environ. Health Perspect.* **55,** 37–46 (1984).
31. Hunter, A., Holscher, M. & Neal, R. Thioacetamide-induced hepatic necrosis I. Involvement of the mixed-function oxidase enzyme system. (1976).
32. Hinson, J. A., Roberts, D. W. & James, L. P. Mechanisms of acetaminophen-induced liver necrosis. *Handb. Exp. Pharmacol.* 369–405 (2010). doi:10.1007/978-3-642-00663-0_12
33. Jaeschke, H., McGill, M. R. & Ramachandran, A. Oxidant stress, mitochondria, and cell death mechanisms in drug-induced liver injury: lessons learned from acetaminophen hepatotoxicity. *Drug Metab. Rev.* **44,** 88–106 (2012).
34. Wagner, M., Zollner, G. & Trauner, M. New molecular insights into the mechanisms of cholestasis. *J. Hepatol.* **51,** 565–580 (2009).
35. McGill, M. R., Williams, C. D., Xie, Y., Ramachandran, A. & Jaeschke, H. Acetaminophen-induced liver injury in rats and mice: comparison of protein adducts, mitochondrial dysfunction, and oxidative stress in the mechanism of toxicity. *Toxicol. Appl. Pharmacol.* **264,** 387–394 (2012).
36. Burk, R. F., Lawrence, R. A. & Lane, J. M. Liver necrosis and lipid peroxidation in the rat as the result of paraquat and diquat administration: Effect of selenium deficiency. *J. Clin. Invest.* **65,** 1024 (1980).
37. Guillouzo, A. Liver cell models in in vitro toxicology. *Environ. Health Perspect.* **106 Suppl 2,** 511–532 (1998).
38. Tolosa, L., Donato, M. T., Pérez-Cataldo, G., Castell, J. V. & Gómez-Lechón, M. J. Upgrading cytochrome P450 activity in HepG2 cells co-transfected with adenoviral vectors for drug hepatotoxicity assessment. *Toxicol. In Vitro* **26,** 1272–1277 (2012).
39. Aninat, C. *et al.* Expression of cytochromes P450, conjugating enzymes and nuclear receptors in human hepatoma HepaRG cells. *Drug Metab. Dispos. Biol. Fate Chem.* **34,** 75–83 (2006).
40. Guillouzo, A. *et al.* The human hepatoma HepaRG cells: a highly differentiated model for studies of liver metabolism and toxicity of xenobiotics. *Chem Biol Interact* **168,** 66–73 (2007).
41. McGill, M. R. *et al.* HepaRG cells: A human model to study mechanisms of acetaminophen hepatotoxicity. *Hepatol. Baltim. Md* **53,** 974–982 (2011).
42. Ramaiahgari, S. C. *et al.* A 3D in vitro model of differentiated HepG2 cell spheroids with improved liver-like properties for repeated dose high-throughput toxicity studies. *Arch. Toxicol.* (2014). doi:10.1007/s00204-014-1215-9
43. Farkas, D. & Tannenbaum, S. R. In vitro methods to study chemically-induced hepatotoxicity: a literature review. *Curr. Drug Metab.* **6,** 111–125 (2005).
44. Chu, J. & Sadler, K. C. New school in liver development: Lessons from zebrafish. *Hepatol. Baltim. Md* **50,** 1656–1663 (2009).
45. Crawford, A. D., Esguerra, C. V. & de Witte, P. A. M. Fishing for drugs from nature: zebrafish as a technology platform for natural product discovery. *Planta Med.* **74,** 624–632 (2008).
46. Hill, A., Mesens, N., Steemans, M., Xu, J. J. & Aleo, M. D. Comparisons between in vitro whole cell imaging and in vivo zebrafish-based approaches for identifying potential human hepatotoxicants earlier in pharmaceutical development. *Drug Metab. Rev.* **44,** 127–140 (2012).
47. Hill, A. J., Teraoka, H., Heideman, W. & Peterson, R. E. Zebrafish as a model vertebrate for investigating chemical toxicity. *Toxicol. Sci. Off. J. Soc. Toxicol.* **86,** 6–19 (2005).
48. Hölttä Vuori, M. *et al.* Zebrafish: gaining popularity in lipid research. *Biochem. J.* **429,** 235–242 (2010).
49. Jones, M., Ball, J. S., Dodd, A. & Hill, A. J. Comparison between zebrafish and Hep G2 assays for the predictive identification of hepatotoxins. *Toxicology* (2009).
50. Barros, T. P., Alderton, W. K., Reynolds, H. M., Roach, A. G. & Berghmans, S. Zebrafish: an emerging technology for in vivo pharmacological assessment to identify potential safety liabilities in early drug discovery. *Br. J. Pharmacol.* **154,** 1400–1413 (2008).
51. Kimmel, C. B., Ballard, W. W., Kimmel, S. R., Ullmann, B. & Schilling, T. F. Stages of embryonic development of the zebrafish. *Dev. Dyn.* **203,** 253–310 (2005).
52. Streisinger, G., Walker, C., Dower, N., Knauber, D. & Singer, F. Production of clones of homozygous diploid zebra fish (Brachydanio rerio). *Nature* **291,** 293–296 (1981).

104. EFSA. Opinion of the Scientific Panel on Animal Health and Welfare on a request from the Commission related to 'Aspects of the biology and welfare of animals used for experimental and other scientific purposes'. *EFSA J.* **292,** 1–46 (2005).
105. Alderton, W. *et al.* Accumulation and metabolism of drugs and CYP probe substrates in zebrafish larvae. *Xenobiotica* **40,** 547–557 (2010).
106. Pronk, T. E., van der Veen, J. W., Ezendam, J., Van Loveren, H. & Pennings, J. L. A. Effects of pooling RNA from samples treated with different compounds for determining class specific biomarkers and processes in toxicogenomics. *Toxicol. In Vitro* **25,** 1841–1847 (2011).
107. 't Hoen, P. A. *et al.* Deep sequencing-based expression analysis shows major advances in robustness, resolution and inter-lab portability over five microarray platforms. *Nucleic Acids Res* **36,** e141 (2008).
108. Sabaliauskas, N. A. *et al.* High-throughput zebrafish histology. *Methods San Diego Calif* **39,** 246–254 (2006).
109. Tsao-Wu, G. S., Weber, C. H., Budgeon, L. R. & Cheng, K. C. *Agarose-embedded tissue arrays for histologic and genetic analysis.* 614–618 (1998).
110. De Jong, M. *et al.* RNA isolation method for single embryo transcriptome analysis in zebrafish. *BMC Res Notes* **3,** 73 (2010).
111. Mortazavi, A., Williams, B. A., McCue, K., Schaeffer, L. & Wold, B. Mapping and quantifying mammalian transcriptomes by RNA-Seq. *Nat Methods* **5,** 621–628 (2008).
112. Hegedűs, Z. *et al.* Deep sequencing of the zebrafish transcriptome response to mycobacterium infection. *Mol. Immunol.* **46,** 2918–2930 (2009).
113. Ordas, A. *et al.* Deep sequencing of the innate immune transcriptomic response of zebrafish embryos to Salmonella infection. *Fish Amp Shellfish Immunol.* **31,** 716–724 (2011).
114. Stockhammer, O. W. *et al.* Transcriptome analysis of Traf6 function in the innate immune response of zebrafish embryos. *Mol. Immunol.* **48,** 179–190 (2010).
115. Jelier, R. *et al.* Anni 2.0: a multipurpose text-mining tool for the life sciences. *Genome Biol* **9,** R96 (2008).
116. Van Iersel, M. P. *et al.* Presenting and exploring biological pathways with PathVisio. *BMC Bioinformatics* (2008). doi:10.1186/1471-2105-9-399
117. Barbazuk, W. B. *et al.* The syntenic relationship of the zebrafish and human genomes. *Genome Res* **10,** 1351–1358 (2000).
118. Dai, M. *et al.* Evolving gene/transcript definitions significantly alter the interpretation of GeneChip data. *Nucleic Acids Res.* **33,** e175–e175 (2005).
119. Kienhuis, A. S. *et al.* Cyclosporine A treated in vitro models induce cholestasis response through comparison of phenotype-directed gene expression analysis of in vivo Cyclosporine A-induced cholestasis. *Toxicol. Lett.* **221,** 225–236 (2013).
120. Jennen, D. G. J. *et al.* Comparison of HepG2 and HepaRG by Whole-Genome Gene Expression Analysis for the Purpose of Chemical Hazard Identification. *Toxicol. Sci.* **115,** 66–79 (2010).
121. Liberzon, A. *et al.* Molecular signatures database (MSigDB) 3.0. *Bioinformatics* **27,** 1740
122. Rozen, S. & Skaletsky, H. Primer3 on the WWW for general users and for biologist programmers. *Methods Mol Biol* **132,** 365–386 (2000).
123. Flynn, E. J., Trent, C. M. & Rawls, J. F. Ontogeny and nutritional control of adipogenesis in zebrafish (Danio rerio). *J. Lipid Res.* **50,** 1641–1652 (2009).
124. Thisse, C. & Thisse, B. High-resolution in situ hybridization to whole-mount zebrafish embryos. *Nat Protoc* **3,** 59–69 (2008).
125. Hibiya, T. *et al. An Atlas of Fish HistologyNormal and Pathological Features.* (Kodansha LTD, 21-21 Otowa 2-chome, Bunkyo-ku, Tokyo 112, Japan, 1982).
126. Tao, T. & Peng, J. Liver development in zebrafish (Danio rerio). *J. Genet. Genomics* **36,** 325–334 (2009).
127. Strmac, M. & Braunbeck, T. Effects of Triphenyltin Acetate on Survival, Hatching Success, and Liver Ultrastructure of Early Life Stages of Zebrafish (Danio rerio). *Ecotoxicol. Environ. Saf.* **44,** 25–39 (1999).
128. Reynaud, S., Raveton, M. & Ravanel, P. Interactions between immune and biotransformation systems in fish: a review. *Aquat Toxicol* **87,** 139–145 (2008).
129. JONSSON, M., Orrego, R., WOODIN, B., GOLDSTONE, J. & STEGEMAN, J. Basal and 3,3',4,4',5-pentachlorobiphenyl-induced expression of cytochrome P450 1A, 1B and 1C genes in zebrafish. *Toxicol. Appl. Pharmacol.* **221,** 29–41 (2007).

78. Apweiler, R. *et al.* UniProt: the Universal Protein knowledgebase. *Nucleic Acids Res.* **32,** D115–119 (2004).
79. Magrane, M. & Consortium, U. UniProt Knowledgebase: a hub of integrated protein data. *Database J. Biol. Databases Curation* **2011,** bar009 (2011).
80. NCBI Resource Coordinators. Database resources of the National Center for Biotechnology Information. *Nucleic Acids Res.* **42,** D7–17 (2014).
81. Davis, A. P. *et al.* The Comparative Toxicogenomics Database: update 2013. *Nucleic Acids Res.* **41,** D1104–1114 (2013).
82. Bradford, Y. *et al.* ZFIN: enhancements and updates to the zebrafish model organism database. *Nucleic Acids Res* **1,** D822–D829 (2011).
83. Boorsma, A., Foat, B. C., Vis, D., Klis, F. & Bussemaker, H. J. T-profiler: scoring the activity of predefined groups of genes using gene expression data. *Nucleic Acids Res.* **33,** W592–5 (2005).
84. Da Wei Huang, Sherman, B. T. & Lempicki, R. A. Systematic and integrative analysis of large gene lists using DAVID bioinformatics resources. *Nat. Protoc.* **4,** 44–57 (2008).
85. Huang, D. W., Sherman, B. T. & Lempicki, R. A. Bioinformatics enrichment tools: paths toward the comprehensive functional analysis of large gene lists. *Nucleic Acids Res* **37,** 1–13 (2009).
86. Kanehisa, M. & Goto, S. KEGG: kyoto encyclopedia of genes and genomes. *Nucleic Acids Res.* **28,** 27–30 (2000).
87. Kanehisa, M. *et al.* Data, information, knowledge and principle: back to metabolism in KEGG. *Nucleic Acids Res* **42,** D199–205 (2014).
88. Kelder, T. *et al.* WikiPathways: building research communities on biological pathways. *Nucleic Acids Res* **40,** D1301–7 (2012).
89. Kelder, T. *et al.* Mining biological pathways using WikiPathways web services. *PLoS ONE* **4,** e6447 (2009).
90. Keller, A., Eng, J., Zhang, N., Li, X. & Aebersold, R. A uniform proteomics MS/MS analysis platform utilizing open XML file formats. *Mol. Syst. Biol.* **1,** 2005.0017 (2005).
91. Kuhn, M. *et al.* STITCH 4: integration of protein-chemical interactions with user data. *Nucleic Acids Res.* **42,** D401–407 (2014).
92. Kuhn, M. *et al.* STITCH 3: zooming in on protein-chemical interactions. *Nucleic Acids Res.* **40,** D876–880 (2012).
93. Kuhn, M. *et al.* STITCH 2: an interaction network database for small molecules and proteins. *Nucleic Acids Res.* **38,** D552–556 (2010).
94. Kuhn, M., von Mering, C., Campillos, M., Jensen, L. J. & Bork, P. STITCH: interaction networks of chemicals and proteins. *Nucleic Acids Res.* **36,** D684–688 (2008).
95. Peterson, R. T. & Macrae, C. A. Systematic approaches to toxicology in the zebrafish. *Annu. Rev. Pharmacol. Toxicol.* **52,** 433–453 (2012).
96. ELFERINK, M. *et al.* Microarray analysis in rat liver slices correctly predicts in vivo hepatotoxicity. *Toxicol. Appl. Pharmacol.* **229,** 300–309 (2008).
97. Kienhuis, A. S. *et al.* A toxicogenomics-based parallelogram approach to evaluate the relevance of coumarin-induced responses in primary human hepatocytes in vitro for humans in vivo. *Toxicol Vitro* **23,** 1163–1169 (2009).
98. Kienhuis, A. S. *et al.* Parallelogram approach using rat-human in vitro and rat in vivo toxicogenomics predicts acetaminophen-induced hepatotoxicity in humans. *Toxicol. Sci. Off. J. Soc. Toxicol.* **107,** 544–552 (2009).
99. Schoonen, W. G., de Roos, J. A., Westerink, W. M. & Debiton, E. Cytotoxic effects of 110 reference compounds on HepG2 cells and for 60 compounds on HeLa, ECC-1 and CHO cells. II mechanistic assays on NAD(P)H, ATP and DNA contents. *Toxicol Vitro* **19,** 491–503 (2005).
100. Schoonen, W. G. E. J., Westerink, W. M. A., de Roos, J. A. D. M. & Débiton, E. Cytotoxic effects of 100 reference compounds on Hep G2 and HeLa cells and of 60 compounds on ECC-1 and CHO cells. I Mechanistic assays on ROS, glutathione depletion and calcein uptake. *Toxicol. In Vitro* **19,** 505–516 (2005).
101. Boess, F. *et al.* Gene expression in two hepatic cell lines, cultured primary hepatocytes, and liver slices compared to the in vivo liver gene expression in rats: possible implications for toxicogenomics use of in vitro systems. *Toxicol. Sci. Off. J. Soc. Toxicol.* **73,** 386–402 (2003).
102. Dooley, K., Dooley, K. & Zon, L. I. Zebrafish: a model system for the study of human disease. *Curr Opin Genet Dev* **10,** 252–256 (2000).
103. Zon, L. I. & Peterson, R. T. In vivo drug discovery in the zebrafish. *Nat Rev Drug Discov* **4,** 35–44 (2005).

130. Ryu, J. *et al.* Molecular cloning of cytochrome P4501A cDNA of medaka (Oryzias latipes) and messenger ribonucleic acid regulation by environmental pollutants. *Env. Toxicol Chem* **23,** 1004–1011 (2004).
131. Sharma, M. K. *et al.* Hierarchical subfunctionalization of fabp1a, fabp1b and fabp10 tissue-specific expression may account for retention of these duplicated genes in the zebrafish (Danio rerio) genome. *FEBS J.* **273,** 3216–3229 (2006).
132. Vaziri, N. D., Liang, K. & Azad, H. Effect of cyclosporine on HMG-CoA reductase, cholesterol 7alpha-hydroxylase, LDL receptor, HDL receptor, VLDL receptor, and lipoprotein lipase expressions. *J Pharmacol Exp Ther* **294,** 778–783 (2000).
133. Driessen, M. *et al.* Exploring the zebrafish embryo as an alternative model for the evaluation of liver toxicity by histopathology and expression profiling. *Arch. Toxicol.* **87,** 807–823 (2013).
134. Ansede, J. H., Smith, W. R., Perry, C. H., St Claire, R. L. & Brouwer, K. R. An in vitro assay to assess transporter-based cholestatic hepatotoxicity using sandwich-cultured rat hepatocytes. *Drug Metab. Dispos. Biol. Fate Chem.* **38,** 276–280 (2010).
135. Bohan, A. & Boyer, J. L. Mechanisms of hepatic transport of drugs: implications for cholestatic drug reactions. *Semin. Liver Dis.* **22,** 123–136 (2002).
136. Leitner, J. M., Graninger, W. & Thalhammer, F. Hepatotoxicity of antibacterials: Pathomechanisms and clinical. *Infection* **38,** 3–11 (2010).
137. Santangeli, P. *et al.* Examining the safety of amiodarone. *Expert Opin. Drug Saf.* **11,** 191–214 (2012).
138. Jaeschke, H., Knight, T. R. & Bajt, M. L. The role of oxidant stress and reactive nitrogen species in acetaminophen hepatotoxicity. *Toxicol. Lett.* **144,** 279–288 (2003).
139. DeLeve, L. D. & Kaplowitz, N. Glutathione metabolism and its role in hepatotoxicity. *Pharmacol. Amp Ther.* **52,** 287–305 (1991).
140. Ellinger-Ziegelbauer, H. *et al.* The enhanced value of combining conventional and "omics" analyses in early assessment of drug-induced hepatobiliary injury. *Toxicol. Appl. Pharmacol.* **252,** 97–111 (2011).
141. Vitins, A. P. *et al.* Mechanisms of amiodarone and valproic acid induced liver steatosis in mouse in vivo act as a template for other hepatotoxicity models. *Arch. Toxicol.* 1–16 (2014). doi:10.1007/s00204-014-1211-0
142. Nciri, R. *et al.* Lipid peroxidation, antioxidant activities and stress protein (HSP72/73, GRP94) expression in kidney and liver of rats under lithium treatment. *J. Physiol. Biochem.* **68,** 11–18 (2012).
143. Siddik, Z. H. Cisplatin: mode of cytotoxic action and molecular basis of resistance. *Oncogene* **22,** 7265–7279 (2003).
144. Serviddio, G. *et al.* Mitochondrial oxidative stress and respiratory chain dysfunction account for liver toxicity during amiodarone but not dronedarone administration. *Free Radic. Biol. Amp Med.* **51,** 2234–2242 (2011).
145. Tsukamoto, M., Tampo, Y., Sawada, M. & Yonaha, M. Paraquat-induced oxidative stress and dysfunction of the glutathione redox cycle in pulmonary microvascular endothelial cells. *Toxicol Appl Pharmacol* **178,** 82–92 (2002).
146. Zidek, N., Hellmann, J., Kramer, P.-J. & Hewitt, P. G. Acute hepatotoxicity: a predictive model based on focused illumina microarrays. *Toxicol. Sci. Off. J. Soc. Toxicol.* **99,** 289–302 (2007).
147. Chang, C. *et al.* liver-enriched gene 1a and 1b encode novel secretory proteins essential for normal liver development in zebrafish. *PLoS ONE* **6,** e22910 (2011).
148. Baginsky, S., Hennig, L., Zimmermann, P. & Gruissem, W. Gene Expression Analysis, Proteomics, and Network Discovery. *Plant Physiol.* **152,** 402–410 (2010).
149. Driessen, M. *et al.* Gene expression markers in the zebrafish embryo reflect a hepatotoxic response in animal models and humans. *Toxicol. Lett.* doi:10.1016/j.toxlet.2014.06.844
150. Van der Plas-Duivesteijn, S. J. *et al.* Identifying Proteins in Zebrafish Embryos Using Spectral Libraries Generated from Dissected Adult Organs and Tissues. *J. Proteome Res.*
151. Pedrioli, P. G. A. *et al.* A common open representation of mass spectrometry data and its application to proteomics research. *Nat. Biotechnol.* **22,** 1459–1466 (2004).
152. Deutsch, E. W. *et al.* A guided tour of the Trans-Proteomic Pipeline. *Proteomics* **10,** 1150–1159 (2010).
153. Craig, R. & Beavis, R. C. TANDEM: matching proteins with tandem mass spectra. *Bioinformatics* (2004). doi:10.1093/bioinformatics/bth092
154. Keller, A., Nesvizhskii, A. I., Kolker, E. & Aebersold, R. Empirical statistical model to estimate the accuracy of peptide identifications made by MS/MS and database search. *Anal. Chem.* **74,** 5383–5392 (2002).
155. Shteynberg, D. *et al.* iProphet: multi-level integrative analysis of shotgun proteomic data improves peptide and protein identification rates and error estimates. *Mol. Cell. Proteomics MCP* **10,** M111.007690 (2011).
156. Palmblad, M. *et al.* Parallel deep transcriptome and proteome analysis of zebrafish larvae. *BMC Res Notes* **6,** 428 (2013).
157. Paschen, W., Proud, C. G. & Mies, G. Shut-down of translation, a global neuronal stress response: mechanisms and pathological relevance. *Curr. Pharm. Des.* **13,** 1887–1902 (2007).
158. Fribley, A., Zhang, K. & Kaufman, R. J. Regulation of Apoptosis by the Unfolded Protein Response. *Methods Mol. Biol. Clifton NJ* **559,** 191–204 (2009).
159. Fredriksson, L. *et al.* Drug-induced endoplasmic reticulum and oxidative stress responses independently sensitize toward TNFα-mediated hepatotoxicity. *Toxicol. Sci. Off. J. Soc. Toxicol.* **140,** 144–159 (2014).
160. Hanisch, K. *et al.* Proteomic Signatures of the Zebrafish (*Danio rerio*) Embryo: Sensitivity and Specificity in Toxicity Assessment of Chemicals. *Int. J. Proteomics* **2010,** e630134 (2010).
161. Shi, X., Liu, C., Wu, G. & Zhou, B. Waterborne exposure to PFOS causes disruption of the hypothalamus-pituitary-thyroid axis in zebrafish larvae. *Chemosphere* **77,** 1010–1018 (2009).
162. Hu, Z. *et al.* Quantitative liver-specific protein fingerprint in blood: a signature for hepatotoxicity. *Theranostics* **4,** 215–228 (2014).
163. Ponnudurai, R. P. *et al.* Proteomic analysis of zebrafish (Danio rerio) embryos exposed to cyclosporine A. *J. Proteomics* **75,** 1004–1017 (2012).
164. Szalowska, E., Stoopen, G., Groot, M. J., Hendriksen, P. J. & Peijnenburg, A. A. Treatment of mouse liver slices with cholestatic hepatotoxicants results in down-regulation of Fxr and its target genes. *BMC Med. Genomics* **6,** 39 (2013).
165. Locatelli, I. *et al.* Endogenous annexin A1 is a novel protective determinant in nonalcoholic steatohepatitis in mice. *Hepatol. Baltim. Md* **60,** 531–544 (2014).
166. Greenbaum, D., Colangelo, C., Williams, K. & Gerstein, M. Comparing protein abundance and mRNA expression levels on a genomic scale. *Genome Biol.* **4,** 117 (2003).
167. Vitins, A. P., Kienhuis, A. S., Speksnijder, E. N., Roodbergen, M. & der Ven, L. T. M. van. A mouse in vivo study of liver necrosis inducing chemical compounds acetaminophen, paraquat, and isoniazid identifies robust markers for the onset and progression of disease.
168. Van Summeren, A., Renes, J., Lizarraga, D., Bouwman, F. G., Noben, J.-P., van Delft, J. H. M., et al. (2013). Screening for drug-induced hepatotoxicity in primary mouse hepatocytes using acetaminophen, amiodarone, and cyclosporin a as model compounds: an omics-guided approach. *Omics : a Journal of Integrative Biology*, **17(2),** 71–83. doi:10.1089/omi.2012.0079.
169. Mathijs, K. *et al.* Assessing the metabolic competence of sandwich-cultured mouse primary hepatocytes. *Drug Metab. Dispos. Biol. Fate Chem.* (2009). doi:10.1124/dmd.108.025775
170. Noriyuki, N. *et al.* Evaluation of DNA microarray results in the Toxicogenomics Project (TGP) consortium in Japan. *J. Toxicol. Sci.* **37,** 791–801 (2012).
171. Uehara, T. *et al.* The Japanese toxicogenomics project: Application of toxicogenomics. *Mol. Nutr. Amp Food Res.* **54,** 218–227 (2010).
172. User-friendly solutions for microarray quality control and pre-processing on ArrayAnalysis.org. *Nucleic Acids Res* **41,** W71–6 (2013).
173. Chessel, D., Dufour, A. B. & Dray, S. *ade4: Analysis of Ecological Data: Exploratory and Euclidean methods in Multivariate data analysis and graphical display.* (R package version, 2007).
174. Dray, S. & Dufour, A. B. The ade4 package: implementing the duality diagram for ecologists. *J. Stat. Softw.* (2007).
175. Wickham, H. *ggplot2: elegant graphics for data analysis.* (2009).
176. Tomaszewski, P., Kubiak-Tomaszewska, G. & Pachecka, J. Cytochrome P450 polymorphism--molecular, metabolic, and pharmacogenetic aspects. II. Participation of CYP isoenzymes in the metabolism of endogenous substances and drugs. *Acta Pol. Pharm.* **65,** 307–318 (2008).
177. Li, L. *et al.* Farnesoid X receptor up-regulates expression of lipid transfer inhibitor protein in liver cells and mice. *Biochem. Biophys. Res. Commun.* **441,** 880–885 (2013).
178. Jonker, J. W., Liddle, C. & Downes, M. FXR and PXR: potential therapeutic targets in cholestasis. *J. Steroid Biochem. Mol. Biol.* **130,** 147–158 (2012).
179. Campion, S. N. *et al.* Hepatic Mrp4 induction following acetaminophen exposure is dependent on Kupffer cell function. *Am. J. Physiol. Gastrointest. Liver Physiol.* **295,** G294–304 (2008).

180. Groneberg, D. A., Grosse-Siestrup, C. & Fischer, A. In Vitro Models to Study Hepatotoxicity. *Toxicol. Pathol.* **30,** 394–399 (2002).
181. Stadnicka, J., Schirmer, K. & Ashauer, R. Predicting concentrations of organic chemicals in fish by using toxicokinetic models. *Environ. Sci. Technol.* **46,** 3273–3280 (2012).
182. Diekmann, H. & Hill, A. ADMETox in zebrafish. *Drug Discov. Today Dis. Models* **10,** e31–e35 (2013).
183. Stadnicka-Michalak, J., Tanneberger, K., Schirmer, K. & Ashauer, R. Measured and modeled toxicokinetics in cultured fish cells and application to in vitro-in vivo toxicity extrapolation. *PloS One* **9,** e92303 (2014).
184. Uno, T., Ishizuka, M. & Itakura, T. Cytochrome P450 (CYP) in fish. *Environ. Toxicol. Pharmacol.* **34,** 1–13 (2012).
185. De Koning, C. *et al.* Zebrafish embryotoxicity test (ZET): the importance of internal exposure analyses. in (2014).
186. Shaukat Ali, H. G. J. van M. Large-scale assessment of the zebrafish embryo as a possible predictive model in toxicity testing. *PloS One* **6,** e21076 (2011).
187. Scholz, S. Zebrafish embryos as an alternative model for screening of drug-induced organ toxicity. *Arch. Toxicol.* (2013). doi:10.1007/s00204-013-1044-2
188. Aleksunes, L. M. & Manautou, J. E. Emerging role of Nrf2 in protecting against hepatic and gastrointestinal disease. *Toxicol. Pathol.* **35,** 459–473 (2007).
189. Mukaigasa, K. *et al.* Genetic evidence of an evolutionarily conserved role for Nrf2 in the protection against oxidative stress. *Mol. Cell. Biol.* **32,** 4455–4461 (2012).
190. Bugel, S. M., Tanguay, R. L. & Planchart, A. Zebrafish: A Marvel of High-Throughput Biology for 21st Century Toxicology. *Curr. Environ. Health Rep.* **1,** 341–352 (2014).
191. Higashijima, S. Transgenic zebrafish expressing fluorescent proteins in central nervous system neurons. *Dev. Growth Differ.* **50,** 407–413 (2008).
192. Leet, J. K. *et al.* High-content screening in zebrafish embryos identifies butafenacil as a potent inducer of anemia. *PloS One* **9,** e104190 (2014).
193. Sipes, N. S., Padilla, S. & Knudsen, T. B. Zebrafish: as an integrative model for twenty-first century toxicity testing. *Birth Defects Res. Part C Embryo Today Rev.* **93,** 256–267 (2011).
194. Truong, L., Mandrell, D., Mandrell, R., Simonich, M. & Tanguay, R. L. A rapid throughput approach identifies cognitive deficits in adult zebrafish from developmental exposure to polybrominated flame retardants. *Neurotoxicology* **43,** 134–142 (2014).
195. Her, G. M., Chiang, C.-C., Chen, W.-Y. & Wu, J.-L. In vivo studies of liver-type fatty acid binding protein (L-FABP) gene expression in liver of transgenic zebrafish (Danio rerio). *FEBS Lett.* **538,** 125–133 (2003).
196. Zhang, X., Li, C. & Gong, Z. Development of a Convenient In Vivo Hepatotoxin Assay Using a Transgenic Zebrafish Line with Liver-Specific DsRed Expression. *PLoS ONE* **9,** e91874 (2014).
197. McKim, J. M. Building a Tiered Approach to In Vitro Predictive Toxicity Screening: A Focus on Assays with In Vivo Relevance. *Comb. Chem. High Throughput Screen.* **13,** 188–206 (2010).

Curriculum Vitae

Marja Driessen was born on January 23, 1985 in Breda, The Netherlands. After graduating from secondary school at Stedelijk Lyceum in Roermond in 2003, she started her study in Health Sciences at the University of Maastricht with a major in Bioregulation & Health and a minor in Movement Sciences. During her studies, she completed several internships. Her Bachelor internship was conducted at the Academic Hospital Pharmacy in Maastricht under the supervision of Dr. Leo Stolk and Dr. Joyce Pullen. Her Master internship was performed at the Department of Tumor Immunology, Maastricht University under the supervision of Dr. Michel van Gelder and Peter Frings. After obtaining her Master degree in 2007, she applied for a second Master in Bio-Informatics at the Catholic University of Leuven, Belgium. There she conducted her internship in the Department of Electrical Engineering (ESAT) under the supervision of Prof. Dr. Bart de Moor and Tunde Adeshoyla Adefoyie. After graduating in 2009, she started her PhD study on the applicability of the zebrafish embryo as a screening model for hepatotoxicity under the direct scientific supervision of Dr. Leo T.M. van der Ven and Dr. Anne. S. Kienhuis (RIVM, Laboratory for Health Protection Research). Since February 2014, Marja has a position as a postdoctoral fellow in the Structural Computational Biology Department of the European Molecular Biology Laboratory (EMBL) Heidelberg, Germany.

List of publications

Articles

Driessen M, Duijvesteijn – van der Plas S, Vitins AP, Kienhuis AS, Pennings JL, van den Brandhof EJ, Roodbergen M, van de Water B, Spaink HP, Palmblad NM, van der Ven LTM. *Toxicogenomics approach in the zebrafish embryo to assess hepatotoxicity: combination of protein and gene expression changes*. In preparation

Driessen M, Vitins AP, Pennings JL, Kienhuis AS, van de Water B, van der Ven LTM. *A transcriptomics-based hepatotoxicity comparison between the zebrafish embryo and established human and rodent in vitro and in vivo models using cyclosporine A, amiodarone and acetaminophen*. Revisions in Toxicology Letters

Driessen M, Kienhuis AS, Vitins AP, Pennings JL, Pronk TE, van den Brandhof EJ, Roodbergen M, van de Water B, van der Ven LTM. *Gene expression markers in the zebrafish embryo reflect a hepatotoxic response in animal models and humans*. Toxicology Letters, 2014 Jul 24;230(1):48-56

Driessen M, Kienhuis AS, Pennings JL, Pronk TE, van den Brandhof EJ, Roodbergen M, Spaink HP, van de Water B, van der Ven LTM. *Exploring the zebrafish embryo as an alternative model for the evaluation of liver toxicity by histopathology and expression profiling*. Archives of Toxicology 2013 May;87(5):807-23

Kienhuis AS, Bessems JG, Pennings JL, Driessen M, Luijten M, van Delft JH, Peijnenburg AA, van der LTM. *Application of toxicogenomics in hepatic sytems toxicology for risk assessment: acetaminophen as a case study*. Toxicology and Applied Pharmacology. 2011 Jan 15;250(2):96-107

Pullen J, Driessen M, Stolk LM, Degraeuwe PL, van Tiel FH, Neef C and Zimmermann LJ. *Amoxicillin pharmacokinetics in (pre)term infants aged 10 to 52 days: effect of postnatal age*. Therapeutic Drugs Monitoring 2007 Jun;29(3):376-80

Book chapter

Driessen M and van der Ven, LTM. Chapter in Toxicogenomics-Based Cellular Methods, *Alternatives to Animal Testing for Safety Assessment*, 1st Edition. *Academic Press*, 2014 March 7 ISBN: 9780123978622

Patent

Driessen, M and van der Ven LTM. *Hepatotoxicity testing in zebrafish embryo*. Patent application number EP13165649.8 (European)

Supplementary Table 1

Concept	Sum	Cholestasis	Necrosis	Steatosis	Max
DLAT	0,105669253	0,075439912	0,005487761	0,024741581	0,075439912
ABCC2	0,077013887	0,059428233	0,005082565	0,012503092	0,059428233
CYP7A1	0,089591041	0,058404153	0,007123153	0,024063732	0,058404153
CASP7	0,068513878	0,008636802	0,051599174	0,008277902	0,051599174
hmgb1	0,060479209	0,005607468	0,047319817	0,007551923	0,047319817
NR1H4	0,059509341	0,046385944	0,003026804	0,010096595	0,046385944
ADIPOQ	0,062472939	0,009134896	0,007845505	0,045492538	0,045492538
BCL2	0,061035451	0,008593643	0,044535566	0,007906242	0,044535566
SLCO1C1	0,054385055	0,04260197	0,002904114	0,008878971	0,04260197
SREBF1	0,0620065	0,013704743	0,005960525	0,042341229	0,042341229
SLC10A2	0,050060485	0,041890794	0,002339994	0,005829697	0,041890794
slc10a1	0,048767049	0,040859258	0,002002404	0,005905387	0,040859258
MTTP	0,055873889	0,010500532	0,004744735	0,040628622	0,040628622
FAS	0,057379473	0,009123832	0,03891766	0,009337983	0,03891766
CASP9	0,051490605	0,00653371	0,037912443	0,007044452	0,037912443
ANXA5	0,050925869	0,006237081	0,037873741	0,006815049	0,037873741
CYP8B1	0,047159228	0,035887965	0,002677058	0,008594205	0,035887965
AGXT2	0,062399663	0,018095136	0,008463845	0,035840681	0,035840681
FASLG	0,050953589	0,008522448	0,034139986	0,008291154	0,034139986
PPARA	0,057423495	0,015419781	0,007888278	0,034115437	0,034115437
CASP8	0,046544049	0,006266749	0,033743194	0,006534107	0,033743194
TNFSF10	0,047283791	0,006461546	0,032733891	0,008088356	0,032733891
BCL2L1	0,045185164	0,006388873	0,032475919	0,006320371	0,032475919
ADIPOR2	0,039930321	0,004846609	0,002866152	0,032217559	0,032217559
JAG1	0,039694384	0,03195867	0,002512847	0,005222866	0,03195867
DNTT	0,044375997	0,006255758	0,031688804	0,006431436	0,031688804
ABCC4	0,041712489	0,031682357	0,003264796	0,006765335	0,031682357
GGT1	0,058739889	0,031172252	0,005695994	0,021871642	0,031172252
FABP6	0,038181286	0,030617575	0,002039491	0,005524218	0,030617575
ADIPOR1	0,037684642	0,004346629	0,002950362	0,030387653	0,030387653
VPS33B	0,03448106	0,030334381	0,001184143	0,002962535	0,030334381
ACOX1	0,041716449	0,009044701	0,003520968	0,029150779	0,029150779
HBP1	0,036433827	0,003363358	0,028806382	0,004264088	0,028806382
GPATCH3	0,043840192	0,028778959	0,002853069	0,012208163	0,028778959
CIRH1A	0,034875907	0,028750676	0,001859005	0,004266228	0,028750676
UGT1A1	0,045257438	0,028064319	0,004773295	0,012419822	0,028064319
SFPQ	0,048192773	0,015613025	0,004788	0,027791747	0,027791747
ABCG5	0,042074256	0,027521077	0,003103841	0,011449339	0,027521077
ADFP	0,033044651	0,003688654	0,00266236	0,026693638	0,026693638
FASN	0,041606337	0,010148192	0,00521373	0,026244416	0,026244416
ABCG8	0,038630858	0,026150254	0,002783493	0,009697112	0,026150254
AIFM1	0,034080546	0,003527898	0,025849619	0,00470303	0,025849619
PPARG	0,04306988	0,008887263	0,008552227	0,025630391	0,025630391
PARP1	0,034437459	0,004169373	0,025604269	0,004663819	0,025604269
CYP3A4	0,055940114	0,021053389	0,00944177	0,025444956	0,025444956
CASP2	0,033359248	0,004090021	0,025314556	0,003954672	0,025314556
DGAT2	0,032043066	0,005136488	0,002244031	0,024662545	0,024662545
GPT2	0,045966722	0,014927394	0,006657721	0,024381608	0,024381608

Supplementary Table 1 Continued

Concept	Sum	Cholestasis	Necrosis	Steatosis	Max
XIAP	0,032255523	0,004228349	0,023416213	0,004610962	0,023416213
CYP1A1	0,049911678	0,017936408	0,00858312	0,02339215	0,02339215
jag1a	0,027385078	0,023124695	0,001624401	0,002635983	0,023124695
APAF1	0,030219667	0,003756397	0,022798733	0,003664537	0,022798733
GPT	0,041659337	0,01239166	0,006703541	0,022564135	0,022564135
SCD	0,032475173	0,007002905	0,00295036	0,02252191	0,02252191
CASP10	0,031575859	0,004469684	0,022499723	0,004606452	0,022499723
DIABLO	0,031049399	0,003709918	0,022362359	0,004977122	0,022362359
CFLAR	0,031918153	0,004809873	0,021988189	0,005120092	0,021988189
dgat1	0,028060596	0,004171592	0,002479491	0,021409514	0,021409514
CASP6	0,028183853	0,00381928	0,02132523	0,003039344	0,02132523
MCL1	0,032170791	0,006030846	0,021251496	0,004888448	0,021251496
VIPR1	0,031439044	0,006466684	0,003761836	0,021210522	0,021210522
UCP2	0,035706505	0,006824117	0,00767204	0,02121035	0,02121035
FADD	0,030821892	0,005090054	0,021062072	0,004669766	0,021062072
NR1I2	0,037313148	0,020762435	0,005245015	0,011305696	0,020762435
XRCC5	0,048392344	0,01924159	0,008398013	0,020752742	0,020752742
TNFRSF1A	0,036860697	0,006620295	0,020456534	0,009783869	0,020456534
tnfb	0,044520594	0,007519054	0,020302272	0,016699269	0,020302272
HNF1A	0,048218399	0,019955347	0,008419686	0,019843366	0,019955347
AQP8	0,027445087	0,019715747	0,002881121	0,00484822	0,019715747
FABP1	0,034598611	0,011019209	0,00391388	0,019665524	0,019665524
NR1H3	0,038704947	0,014066209	0,005043181	0,019595555	0,019595555
zgc:158371	0,030945756	0,008310882	0,003057135	0,019577738	0,019577738
RBP4	0,031877313	0,007494911	0,004879188	0,019503214	0,019503214
RIPK1	0,025423696	0,002608761	0,019347206	0,00346773	0,019347206
CTGF	0,033212196	0,008016778	0,005851786	0,019343631	0,019343631
LPIN1	0,025058595	0,003857077	0,00187868	0,019322839	0,019322839
APOB	0,037570022	0,011408326	0,006972171	0,019189526	0,019189526
adipoql2	0,024932278	0,004123997	0,001853973	0,018954308	0,018954308
ifn3	0,031407136	0,009136916	0,003346376	0,018923844	0,018923844
KLHL20	0,025708759	0,002857364	0,018885973	0,003965421	0,018885973
BLVRB	0,027435131	0,018821862	0,003161966	0,005451304	0,018821862
CIDEC	0,023659833	0,002490126	0,00235765	0,018812056	0,018812056
PEMT	0,02801092	0,006710683	0,002700171	0,018600066	0,018600066
LDHA	0,043637305	0,011814404	0,018361333	0,013461568	0,018361333
atp7b	0,033615317	0,011889859	0,003828626	0,017896832	0,017896832
TMEM30A	0,022028193	0,017752279	0,001752175	0,002523738	0,017752279
HNF4A	0,041129429	0,015616528	0,00785573	0,017657171	0,017657171
PRSS1	0,03302978	0,017508695	0,009131679	0,006389406	0,017508695
BIRC2	0,024949275	0,003646871	0,017405748	0,003896657	0,017405748
PNPLA2	0,022414861	0,002911551	0,002238363	0,017264946	0,017264946
FGF19	0,027127514	0,017255177	0,001887887	0,007984449	0,017255177
ACADL	0,023819951	0,004163025	0,002457517	0,01719941	0,01719941
ALDH2	0,028506346	0,00620342	0,005104705	0,017198221	0,017198221
HMGB2	0,023257989	0,003421158	0,017075146	0,002761686	0,017075146
DFFB	0,023612443	0,003317844	0,01691659	0,003378008	0,01691659
BLVRA	0,023062713	0,01687457	0,002087081	0,004101064	0,01687457

Supplementary Table 1 Continued

Concept	Sum	Cholestasis	Necrosis	Steatosis	Max
GNPAT	0,023393609	0,004263772	0,002335872	0,016793964	0,016793964
MAPK8	0,031920541	0,007347827	0,01660703	0,007965685	0,01660703
G6PC	0,030762972	0,009994931	0,004217285	0,016550757	0,016550757
PDHX	0,022350101	0,016546109	0,001617638	0,004186353	0,016546109
BAX	0,023386002	0,003407412	0,016497386	0,003481202	0,016497386
Cyp2b10	0,031427596	0,016436847	0,003478998	0,011511752	0,016436847
SQSTM1	0,033328641	0,005772629	0,016417256	0,011138758	0,016417256
PSME3	0,020864666	0,001998459	0,002495453	0,016370753	0,016370753
BCS1L	0,022746054	0,016334401	0,001825698	0,004585956	0,016334401
TGFB1	0,034526296	0,009064811	0,009154524	0,016306962	0,016306962
GOT1	0,030751588	0,009404703	0,005074093	0,016272791	0,016272791
ENTPD2	0,021686478	0,016172193	0,002182854	0,003331431	0,016172193
CD81	0,02492677	0,005359821	0,003475744	0,016091206	0,016091206
CYB5A	0,03473004	0,013363705	0,005395612	0,015970723	0,015970723
MGC92741	0,029027721	0,009795703	0,003330093	0,015901925	0,015901925
BNIP3	0,022055592	0,003227175	0,015794465	0,003033953	0,015794465
KRT18	0,037396435	0,010717558	0,010888772	0,015790104	0,015790104
HNF1B	0,038111903	0,015772928	0,006786002	0,015552973	0,015772928
VEGFA	0,032956634	0,009097955	0,015749989	0,00810869	0,015749989
TAT	0,03454319	0,012827191	0,005981295	0,015734704	0,015734704
ONECUT1	0,03052704	0,015676341	0,003968638	0,010882061	0,015676341
HIF1A	0,029163299	0,00800684	0,015662777	0,005493682	0,015662777
TP53	0,035636984	0,011853149	0,015628177	0,008155658	0,015628177
PCK1	0,031706557	0,010997188	0,005163926	0,015545441	0,015545441
FECH	0,028193304	0,015301908	0,003130973	0,009760423	0,015301908
PPARGC1A	0,028814338	0,007493079	0,006074304	0,015246955	0,015246955
TFR2	0,024453809	0,006236985	0,002998946	0,015217877	0,015217877
MIB1	0,028292784	0,006619989	0,015216871	0,006455925	0,015216871
HMOX1	0,041445717	0,015163179	0,013389433	0,012893107	0,015163179
BMPER	0,020479662	0,003626294	0,001703037	0,015150331	0,015150331
LEPR	0,0253284	0,004935588	0,005291006	0,015101806	0,015101806
TMEM30B	0,017649939	0,014935248	0,001120503	0,001594189	0,014935248
AHR	0,031836182	0,010715636	0,006185695	0,014934851	0,014934851
RATCERP	0,0336731	0,013174264	0,00564872	0,014850115	0,014850115
XPR1	0,022100756	0,014750975	0,001548462	0,005801318	0,014750975
SLC17A5	0,025975481	0,007172962	0,004123068	0,014679451	0,014679451
ACACA	0,021395484	0,004392912	0,002381212	0,01462136	0,01462136
ACADM	0,021878643	0,004075392	0,003258889	0,014544361	0,014544361
NFS1	0,021899361	0,004464439	0,003054629	0,014380294	0,014380294
ENDOG	0,019517068	0,00211346	0,014328009	0,003075599	0,014328009
cdkn1a	0,02839379	0,007771789	0,014297138	0,006324864	0,014297138
MAPK14	0,031152397	0,008763671	0,014289556	0,008099171	0,014289556
AGFG1	0,019824354	0,002580235	0,014250232	0,002993888	0,014250232
CEBPA	0,030453065	0,009797923	0,006407595	0,014247547	0,014247547
MAP2K4	0,026101328	0,00586159	0,014159399	0,00608034	0,014159399
KRAS	0,030957714	0,009369169	0,014141153	0,007447392	0,014141153
LPL	0,030910455	0,008934553	0,007899185	0,014076717	0,014076717
HFE2	0,021908689	0,005368965	0,002572366	0,013967358	0,013967358

Supplementary Table 1 Continued

Concept	Sum	Cholestasis	Necrosis	Steatosis	Max
mapk8	0,027983427	0,006004318	0,013945263	0,008033846	0,013945263
MLYCD	0,01773577	0,002179631	0,001714337	0,013841802	0,013841802
PIK3CG	0,031432491	0,009305946	0,013794655	0,008331888	0,013794655
Oct-01	0,022415508	0,013731853	0,003222523	0,00546113	0,013731853
HGF	0,033095926	0,012791373	0,006613493	0,013691059	0,013691059
PPARD	0,02097626	0,003482133	0,003820982	0,013673146	0,013673146
LIPC	0,029702909	0,010502266	0,005543574	0,013657069	0,013657069
MYC	0,029281709	0,008713666	0,013643687	0,006924356	0,013643687
ACLY	0,022523088	0,005979786	0,002933711	0,013609591	0,013609591
SLCO4A1	0,016806575	0,013362893	0,001299644	0,002144038	0,013362893
ADH5	0,023087617	0,006043346	0,003731309	0,013312962	0,013312962
CRK	0,025748551	0,006500926	0,013275154	0,00597247	0,013275154
DmelCG3861	0,027328024	0,007669253	0,013178549	0,006480223	0,013178549
RAF1	0,026557527	0,006484465	0,006931248	0,013141815	0,013141815
tjp1	0,015545474	0,013027028	0,001011238	0,001507209	0,013027028
MDM2	0,029093042	0,009109273	0,012982607	0,007001163	0,012982607
FOXO1	0,025163382	0,006291558	0,005901	0,012970823	0,012970823
ATG5	0,017572628	0,002202801	0,012941201	0,002428627	0,012941201
PRKRIR	0,015710823	0,001632279	0,00114529	0,012933254	0,012933254
MAP1LC3A	0,018914178	0,002765334	0,01286324	0,003285605	0,01286324
MAPK1	0,032464631	0,01046966	0,012845321	0,009149651	0,012845321
GFER	0,027299328	0,008619265	0,005840884	0,012839179	0,012839179
SLC23A1	0,016969826	0,012802857	0,001644121	0,002522848	0,012802857
RXRB	0,024259202	0,012783087	0,003669822	0,007806293	0,012783087
RXRA	0,027782276	0,012761163	0,003819636	0,011201478	0,012761163
SLC22A7	0,021758072	0,012754619	0,002439743	0,006563711	0,012754619
MAPK11	0,027976003	0,007853746	0,012743211	0,007379047	0,012743211
HADHB	0,023525519	0,008007959	0,002869872	0,012647688	0,012647688
ASPSCR1	0,021471515	0,0125962	0,005902733	0,002972582	0,0125962
HMOX2	0,024094654	0,012448587	0,00563486	0,006011207	0,012448587
POR	0,028214144	0,009718726	0,00606595	0,012429467	0,012429467
MTHFR	0,02562429	0,00581557	0,00740474	0,01240398	0,01240398
CD36	0,025321567	0,007080521	0,005910512	0,012330534	0,012330534
GHR	0,029211026	0,010487233	0,006411711	0,012312081	0,012312081
SERPINE1	0,024628581	0,005979443	0,006378766	0,012270373	0,012270373
API5	0,016351219	0,012257269	0,002029005	0,002064946	0,012257269
TRAIL	0,021770967	0,003489736	0,012175872	0,006105358	0,012175872
IL10	0,029994518	0,008696327	0,012144284	0,009153906	0,012144284
SEPSECS	0,024295079	0,012085529	0,002514439	0,009695112	0,012085529
APOA1	0,0207518	0,004711499	0,00399787	0,012042432	0,012042432
LIPE	0,018377451	0,003182043	0,003192937	0,012002471	0,012002471
GNMT	0,021026932	0,006332406	0,002700348	0,011994178	0,011994178
SCARB1	0,027560173	0,011876814	0,00496066	0,010722697	0,011876814
RELA	0,025274077	0,006750236	0,011872988	0,006650853	0,011872988
NFKBIA	0,023749791	0,005797198	0,011863844	0,00608875	0,011863844
MAT1A	0,021962637	0,007120771	0,002995166	0,0118467	0,0118467
RNF7	0,01884741	0,002692109	0,011846173	0,004309129	0,011846173
C9orf3	0,015491753	0,002286068	0,001385057	0,011820628	0,011820628

Supplementary Table 1 Continued

Concept	Sum	Cholestasis	Necrosis	Steatosis	Max
COL1A1	0,024066279	0,007663363	0,004724976	0,01167794	0,01167794
SOD2	0,02739279	0,006341274	0,011615956	0,009435559	0,011615956
CAST	0,020438122	0,004497664	0,011609449	0,004331008	0,011609449
ABCG2	0,020177564	0,01158277	0,004630657	0,003964137	0,01158277
ABCA1	0,028468257	0,010925477	0,006062501	0,011480279	0,011480279
VIM	0,026992368	0,007930084	0,011457288	0,007604996	0,011457288
FOXA2	0,025602154	0,00980739	0,004358126	0,011436638	0,011436638
EHHADH	0,020967282	0,006625546	0,002924709	0,011417027	0,011417027
SMAD2	0,023918748	0,006454806	0,006070317	0,011393625	0,011393625
WDR26	0,025986934	0,01137865	0,006387496	0,008220789	0,01137865
FOXE3	0,026381619	0,010293738	0,004722645	0,011365237	0,011365237
SHBG	0,027700087	0,008172066	0,008173291	0,01135473	0,01135473
SOCS1	0,020077337	0,004351029	0,004374156	0,011352152	0,011352152
SMAD7	0,02269466	0,006279146	0,00507803	0,011337484	0,011337484
HLA-DRB1	0,02612205	0,00745553	0,011322855	0,007343666	0,011322855
UCP3	0,02187326	0,004323154	0,006233111	0,011316994	0,011316994
HSD3B7	0,015171532	0,011298706	7,82E-04	0,003091293	0,011298706
CCDC6	0,020314105	0,011269399	0,004839968	0,004204737	0,011269399
SIRT1	0,021563865	0,004282773	0,006027154	0,011253938	0,011253938
NOTCH2	0,017253086	0,011232573	0,003118563	0,002901949	0,011232573
fgf21	0,018556805	0,005386142	0,001972406	0,011198258	0,011198258
ABHD5	0,014097907	0,00172406	0,001187289	0,011186558	0,011186558
mat2a	0,020196145	0,006057636	0,002959666	0,011178844	0,011178844
ACADS	0,017703975	0,004517278	0,002133949	0,011052748	0,011052748
CDC2	0,025367407	0,008024441	0,011049162	0,006293806	0,011049162
SOCS7	0,015677366	0,002342825	0,002308094	0,011026448	0,011026448
ELOVL6	0,015407526	0,002998615	0,001385874	0,011023037	0,011023037
OCLN	0,018720072	0,011016652	0,004121236	0,003582184	0,011016652
INS	0,025144149	0,006420076	0,007750246	0,010973826	0,010973826
IGFBP1	0,026227554	0,00907476	0,006222358	0,010930435	0,010930435
JUN	0,025010629	0,007635969	0,010907425	0,006467235	0,010907425
UROD	0,01971429	0,006031759	0,002777734	0,010904798	0,010904798
rxrga	0,022707826	0,010859312	0,003126233	0,00872228	0,010859312
ATG7	0,015807344	0,002102256	0,010844933	0,002860155	0,010844933
PPARGC1B	0,01855463	0,0050136	0,002703208	0,010837823	0,010837823
ACADVL	0,016470009	0,003538457	0,002166314	0,010765238	0,010765238
HADHA	0,022723211	0,010018039	0,001995165	0,010710007	0,010710007
NR5A2	0,020822095	0,010706359	0,005255265	0,00486047	0,010706359
MBD2	0,024617489	0,009620801	0,004296141	0,010700547	0,010700547
DDC	0,030310558	0,010085961	0,010689252	0,009535345	0,010689252
abcb3l2	0,014051754	0,010675858	0,001145562	0,002230335	0,010675858
MAPK3	0,028548514	0,009496857	0,010657417	0,00839424	0,010657417
G6PD	0,020211326	0,010644634	0,005010072	0,00455662	0,010644634
GPC3	0,02011111	0,00509334	0,004463585	0,010554185	0,010554185
ADRA2B	0,016404252	0,003594533	0,002260285	0,010549436	0,010549436
MAP2K1	0,026280683	0,008172674	0,010545855	0,007562153	0,010545855
CPT2	0,019630326	0,006059116	0,003065126	0,010506085	0,010506085
SDAD1	0,019355072	0,010487013	0,001943135	0,006924922	0,010487013

Supplementary Table 1 Continued

Concept	Sum	Cholestasis	Necrosis	Steatosis	Max
SLCO3A1	0,013669365	0,010459238	0,001304136	0,001905991	0,010459238
KRT8	0,025367884	0,010456328	0,005198249	0,009713307	0,010456328
PPP1R3C	0,022853142	0,010392411	0,006787655	0,005673075	0,010392411
CEBPB	0,026209027	0,008805877	0,007062452	0,010340697	0,010340697
ERBB2	0,02883878	0,010340378	0,010201171	0,008297231	0,010340378
CDKN1B	0,0248792	0,007998035	0,010322264	0,006558901	0,010322264
FLT1	0,022246571	0,006310704	0,010303729	0,005632139	0,010303729
or126-1	0,022517679	0,005152976	0,010299297	0,007065406	0,010299297
TP73	0,021288596	0,006283781	0,010298626	0,004706189	0,010298626
ADD1	0,023682488	0,009257686	0,004136428	0,010288375	0,010288375
TNNC1	0,019872447	0,004934718	0,010275212	0,004662518	0,010275212
itga2b	0,023629891	0,010255006	0,006998573	0,006376312	0,010255006
ADAM17	0,019318532	0,003539303	0,010218241	0,005560987	0,010218241
AGT	0,02728812	0,010209682	0,00865866	0,008419779	0,010209682
CD68	0,023753181	0,005981891	0,010183056	0,007588235	0,010183056
CDK2	0,025480891	0,008452711	0,010170162	0,006858018	0,010170162
EPHX1	0,022888599	0,00826272	0,004458632	0,010167248	0,010167248
Pnp1	0,024196813	0,009133171	0,004898556	0,010165086	0,010165086
KDR	0,022250498	0,006675374	0,010121336	0,005453788	0,010121336
KIT	0,020301972	0,005275846	0,010114	0,004912126	0,010114
ABCG1	0,021244468	0,007480102	0,003696286	0,010068079	0,010068079
GRAP2	0,022504104	0,006559567	0,010037411	0,005907126	0,010037411
PTGS2	0,025359506	0,008330947	0,010008347	0,007020213	0,010008347
DPAGT1	0,017164266	0,004266203	0,00289536	0,010002703	0,010002703

Supplementary Table 2

Concept	Sum	Brain	Eye	Heart	Max
PAX6	0,178321943	0,022913222	0,140569324	0,0148394	0,140569324
SIX3	0,141870365	0,01567154	0,116627347	0,009571472	0,116627347
six3b	0,133513004	0,01326474	0,114330692	0,005917569	0,114330692
NKX2-5	0,131155327	0,006951189	0,014265265	0,109938867	0,109938867
GATA4	0,119178429	0,006391891	0,010700367	0,102086171	0,102086171
six6a	0,117921859	0,01256135	0,101633277	0,003727231	0,101633277
TBX5	0,11584647	0,005487368	0,027726691	0,08263241	0,08263241
GATA6	0,088820197	0,005249717	0,00959564	0,073974836	0,073974836
ZFPM2	0,088794149	0,00335001	0,013068723	0,072375416	0,072375416
EYA1	0,08824259	0,006215983	0,068925288	0,013101321	0,068925288
SIX1	0,089750901	0,008327516	0,068836522	0,012586864	0,068836522
VAX2	0,090695895	0,004744419	0,068345736	0,017605737	0,068345736
TBX20	0,085233591	0,003792624	0,013351319	0,068089651	0,068089651
GATA5	0,077895351	0,003146774	0,007228061	0,067520514	0,067520514
VAX1	0,079889186	0,007381369	0,059493494	0,013014324	0,059493494
DAB1	0,074998029	0,059293475	0,010185451	0,005519101	0,059293475
DACH1	0,077562876	0,012655557	0,059247098	0,005660218	0,059247098
VSX2	0,076123282	0,008164224	0,058703932	0,009255126	0,058703932
RELN	0,077823713	0,058193578	0,012041848	0,007588284	0,058193578
MYL7	0,062604882	0,003154815	0,005332639	0,054117424	0,054117424
MEF2C	0,069035895	0,008002068	0,007215631	0,053818199	0,053818199
RAX	0,066668369	0,005990172	0,052369375	0,008308824	0,052369375
SIX4	0,066366047	0,005530024	0,051422338	0,009413684	0,051422338
EAF2	0,055084154	0,001100045	0,051024867	0,00295924	0,051024867
MITF	0,06393414	0,005255749	0,048964265	0,009714129	0,048964265
IRX4	0,059788555	0,003167061	0,008632615	0,047988879	0,047988879
OTX2	0,094262525	0,02878294	0,046866905	0,01861268	0,046866905
EYA3	0,054065339	0,002812763	0,046522075	0,004730502	0,046522075
mef2ca	0,056918621	0,005001749	0,005485586	0,046431288	0,046431288
PROX1	0,069144674	0,011860002	0,046077012	0,011207656	0,046077012
CRYAA	0,053587563	0,004484663	0,044179551	0,00492335	0,044179551
SRF	0,057598684	0,005425971	0,008297033	0,043875681	0,043875681
MYL2	0,052577663	0,004240988	0,00454675	0,043789927	0,043789927
DMBX1	0,067832008	0,017208477	0,043393016	0,007230513	0,043393016
wnt11	0,070198424	0,005844284	0,021064411	0,043289726	0,043289726
WNT11	0,070253387	0,00585135	0,021113247	0,04328879	0,04328879
TBX3	0,068560131	0,004006329	0,021442098	0,043111701	0,043111701
wnt11	0,070103385	0,005952562	0,021061623	0,043089204	0,043089204
CDK5	0,055067398	0,043061133	0,006038619	0,005967648	0,043061133
SOX1	0,075169489	0,01233842	0,042511489	0,020319583	0,042511489
MYH6	0,054092713	0,006164146	0,006078841	0,041849726	0,041849726
AES	0,052372187	0,004985748	0,041345441	0,006040997	0,041345441
nppa	0,052520875	0,002180919	0,009267298	0,041072659	0,041072659
LRRC10	0,044885568	0,001325308	0,002594433	0,040965827	0,040965827
DACH2	0,052785467	0,006090651	0,040520912	0,006173904	0,040520912
PITX2	0,07998991	0,007150433	0,039893058	0,032946416	0,039893058
hopx	0,045636944	0,001978416	0,003982008	0,03967652	0,03967652
SOX2	0,076029941	0,011762438	0,039673298	0,024594208	0,039673298

Supplementary Table 2 Continued

Concept	Sum	Brain	Eye	Heart	Max
six2	0,05517618	0,004621344	0,039425987	0,011128848	0,039425987
SIX2	0,05517618	0,004621344	0,039425987	0,011128848	0,039425987
CDK5R2	0,045541085	0,038721235	0,003440829	0,003379022	0,038721235
CTCF	0,047221705	0,004501128	0,038721193	0,003999385	0,038721193
pax2a	0,063120492	0,012553503	0,038562609	0,012004382	0,038562609
MAF	0,04994427	0,00505733	0,038482288	0,006404654	0,038482288
MEF2D	0,055798467	0,009617308	0,00784199	0,03833917	0,03833917
PITX3	0,055921994	0,008077445	0,038269354	0,009575194	0,038269354
otx1l	0,06698294	0,037639449	0,020088836	0,009254652	0,037639449
eya4	0,04538827	0,003412652	0,037568666	0,004406954	0,037568666
NKX2-2	0,063139036	0,012279124	0,037403122	0,013456793	0,037403122
EOMES	0,060267769	0,013516373	0,037321223	0,009430175	0,037321223
MYEF2	0,055019524	0,008953787	0,008966454	0,037099285	0,037099285
ISL1	0,077418409	0,009697639	0,031026876	0,036693894	0,036693894
OLFM3	0,044368021	0,004928045	0,036399123	0,003040856	0,036399123
mef2b	0,044603784	0,005991912	0,002782786	0,035829087	0,035829087
TBX18	0,051387899	0,003048582	0,012655642	0,035683673	0,035683673
BFSP2	0,043155961	0,003528312	0,035635648	0,003992001	0,035635648
FOXC1	0,063333727	0,012053639	0,035447269	0,01583282	0,035447269
EAF1	0,038386859	0,001111476	0,035410508	0,001864875	0,035410508
NKX2-3	0,045547318	0,00303399	0,007121174	0,035392151	0,035392151
MAB21L2	0,046415213	0,00532077	0,035342341	0,005752102	0,035342341
BMP2	0,074442334	0,008676405	0,030556471	0,035209456	0,035209456
EMX2	0,066138677	0,019494217	0,035163632	0,011480829	0,035163632
SHH	0,07605724	0,017809118	0,035152873	0,023095253	0,035152873
ELP4	0,048270274	0,010565259	0,035148573	0,002556442	0,035148573
TBX4	0,052892078	0,003972127	0,014202544	0,034717405	0,034717405
DBX1	0,0493926	0,008270895	0,034697068	0,006424637	0,034697068
CDK5R1	0,041871481	0,034050861	0,004114853	0,003705767	0,034050861
gsh2	0,04946842	0,008919284	0,034032437	0,006516698	0,034032437
dyrk1aa	0,040136397	0,033909927	0,002974366	0,003252102	0,033909927
BDNF	0,050921854	0,033133779	0,009176592	0,008611482	0,033133779
EMX1	0,067901835	0,025410886	0,033115316	0,009375636	0,033115316
map1b	0,041389551	0,033070242	0,004212758	0,004106549	0,033070242
slc8a1a	0,03906348	0,003132934	0,003020789	0,032909758	0,032909758
CNKSR2	0,038777225	0,003942589	0,0328765	0,001958135	0,0328765
bmp7a	0,06064434	0,005086783	0,032789459	0,022768099	0,032789459
MECP2	0,044530712	0,032737361	0,006551348	0,005242004	0,032737361
ISL2	0,058784898	0,006464186	0,032696817	0,019623896	0,032696817
ATOH7	0,04434729	0,005779851	0,032416155	0,006151283	0,032416155
ALDH1A3	0,049356967	0,004982705	0,032254044	0,012120218	0,032254044
MYLPF	0,037528805	0,002634016	0,002693603	0,032201188	0,032201188
BMP4	0,072191142	0,009958062	0,030106348	0,032126728	0,032126728
GJA5	0,044666402	0,005254206	0,007305357	0,03210684	0,03210684
mesp1	0,04332763	0,003057487	0,008281343	0,0319888	0,0319888
OTX1	0,071658097	0,028336401	0,031592966	0,011728727	0,031592966
rc3	0,037628155	0,03134258	0,003386031	0,002899542	0,03134258
MEF2A	0,045554403	0,007263368	0,00696501	0,031326027	0,031326027

Supplementary Table 2 Continued

Concept	Sum	Brain	Eye	Heart	Max
WNT7B	0,063460559	0,008227264	0,03118088	0,024052415	0,03118088
MIP26	0,037572999	0,002932955	0,031060736	0,003579308	0,031060736
ZFPM1	0,045669008	0,003030051	0,011592472	0,031046486	0,031046486
BARHL2	0,039026093	0,003503176	0,031041031	0,004481884	0,031041031
POU5F1	0,059299685	0,012491451	0,015791289	0,031016944	0,031016944
TBX1	0,051753845	0,00899995	0,012006022	0,030747875	0,030747875
GFAP	0,050052516	0,03035348	0,011980851	0,007718185	0,03035348
NRL	0,040873673	0,004896084	0,030012292	0,005965297	0,030012292
FGF8	0,074985333	0,016159748	0,029844517	0,028981069	0,029844517
dbx2	0,044370908	0,009551957	0,029763821	0,005055131	0,029763821
NKX6-1	0,047607213	0,008105194	0,029690779	0,009811242	0,029690779
BMP7	0,064983256	0,007817911	0,029592777	0,027572565	0,029592777
BMP10	0,04093951	0,002080864	0,009294992	0,029563652	0,029563652
QSOX1	0,050521735	0,007846194	0,029502586	0,013172955	0,029502586
ELL	0,032946594	0,001846564	0,029262511	0,001837519	0,029262511
MYH7	0,038419295	0,004272257	0,004950251	0,029196788	0,029196788
MEIS2	0,047619447	0,006859206	0,02907285	0,01168739	0,02907285
HMX1	0,039346017	0,004099694	0,028858175	0,006388147	0,028858175
SMO	0,05328599	0,009916445	0,02856085	0,014808696	0,02856085
ZIC2	0,049256913	0,012437338	0,02829927	0,008520305	0,02829927
FBLIM1	0,032188959	0,001365398	0,002535972	0,028287591	0,028287591
cmlc1	0,031222668	0,001151086	0,001845259	0,028226322	0,028226322
GLI1	0,051256716	0,010014968	0,027898233	0,013343517	0,027898233
disc1	0,03634996	0,027724347	0,00469909	0,003926522	0,027724347
FGFR1	0,058377851	0,009416889	0,021312542	0,027648422	0,027648422
DLX1	0,056612384	0,013838526	0,027593378	0,015180481	0,027593378
GBX2	0,058807906	0,016732653	0,027584914	0,01449034	0,027584914
PLP1	0,03692067	0,027554902	0,00493995	0,00442582	0,027554902
cxcl12a	0,044893011	0,012436565	0,00490571	0,027550738	0,027550738
FZD5	0,044416055	0,004986577	0,027543419	0,01188606	0,027543419
MEIS1	0,040830385	0,004958775	0,027391298	0,008480311	0,027391298
FOXE3	0,043705333	0,004926329	0,02739064	0,011388364	0,02739064
VLDLR	0,034854352	0,027235883	0,00381426	0,003804211	0,027235883
CRYBB2	0,032442637	0,00270538	0,02720431	0,002532945	0,02720431
SOX7	0,036506724	0,002653695	0,006656682	0,027196346	0,027196346
GLI3	0,053298395	0,012226133	0,027126459	0,013945804	0,027126459
TGIF1	0,045431446	0,011387736	0,027106441	0,00693727	0,027106441
GJA3	0,046109647	0,005238436	0,026928989	0,013942222	0,026928989
wnt2	0,060179651	0,008064431	0,025197949	0,02691727	0,02691727
GFM2	0,033138629	0,003685707	0,00256539	0,026887532	0,026887532
WNT1	0,061392847	0,014224196	0,02676771	0,02040094	0,02676771
BFSP1	0,034378961	0,004007753	0,026674243	0,003696967	0,026674243
PAFAH1B1	0,035960585	0,026474292	0,004688761	0,004797533	0,026474292
FGFR2	0,058963306	0,00985375	0,022727918	0,026381639	0,026381639
TNNT2	0,032926798	0,003472916	0,003143604	0,026310279	0,026310279
EN1	0,0576239	0,016632098	0,026278517	0,014713286	0,026278517
jarid2a	0,030356819	0,002452832	0,001778801	0,026125185	0,026125185
sox17	0,040689476	0,004891027	0,009704305	0,026094144	0,026094144

Supplementary Table 2 Continued

Concept	Sum	Brain	Eye	Heart	Max
KERA	0,034869812	0,003642897	0,025988516	0,005238399	0,025988516
ST8SIA2	0,037097566	0,025876889	0,006068415	0,005152261	0,025876889
TBR1	0,053038184	0,018898884	0,025826156	0,008313144	0,025826156
SOX3	0,042719733	0,008054777	0,025788568	0,008876388	0,025788568
NKX2-1	0,046325054	0,00894093	0,01169997	0,025684153	0,025684153
LHX2	0,054539438	0,009577774	0,025657777	0,019303887	0,025657777
MBP	0,035998113	0,025597471	0,005371406	0,005029237	0,025597471
TNNC1	0,032461237	0,003756149	0,003321753	0,025383335	0,025383335
FGF16	0,037439812	0,005542275	0,006594595	0,025302943	0,025302943
FXR1	0,038347255	0,025299991	0,008200328	0,004846936	0,025299991
FMR1	0,037486117	0,02523618	0,007881047	0,004368888	0,02523618
USP9X	0,035733059	0,006609781	0,025174655	0,003948622	0,025174655
WNT5B	0,053338371	0,006776334	0,025162138	0,021399901	0,025162138
MOGAT2	0,031827275	0,003459433	0,025136205	0,003231636	0,025136205
RYBP	0,029893968	0,002490263	0,025073768	0,002329938	0,025073768
wnt2b	0,049035594	0,006226124	0,025038552	0,017770917	0,025038552
HES1	0,055086743	0,01207773	0,024948425	0,018060589	0,024948425
RFX4	0,032660566	0,024928018	0,004694026	0,003038522	0,024928018
BARHL1	0,036062241	0,005752957	0,024912561	0,005396722	0,024912561
JARID2	0,038222723	0,006833288	0,006517717	0,024871717	0,024871717
IRX3	0,044584271	0,007712609	0,024821637	0,012050024	0,024821637
Mnpepl	0,029616041	0,024731512	0,00260208	0,00228245	0,024731512
LHX5	0,038766783	0,006216482	0,024697323	0,007852977	0,024697323
MOV10L1	0,02943725	0,001653069	0,00311855	0,02466563	0,02466563
WNT5A	0,053680688	0,007518694	0,024657597	0,021504396	0,024657597
SHOX2	0,037456013	0,004567843	0,008233335	0,024654836	0,024654836
QRSL1	0,030455885	0,002176684	0,003682479	0,024596723	0,024596723
BMP2K	0,030476553	0,001799168	0,024548864	0,004128521	0,024548864
HEY2	0,044127516	0,005736743	0,013861591	0,024529182	0,024529182
acta1b	0,027575837	0,001039336	0,002050466	0,024486035	0,024486035
NOTCH1	0,056757666	0,013034332	0,024459129	0,019264205	0,024459129
CUGBP2	0,034336235	0,003782853	0,006127221	0,02442616	0,02442616
MSI2	0,039115552	0,009795312	0,024186608	0,00513363	0,024186608
CRYAB	0,037196208	0,006379911	0,024152212	0,006664084	0,024152212
NES	0,056818299	0,024117543	0,016765688	0,015935069	0,024117543
wnt3l	0,048337616	0,005633234	0,018602809	0,024101573	0,024101573
ik:tdsubc_2b12	0,042899556	0,004967245	0,013859455	0,024072857	0,024072857
GJA1	0,047220107	0,00789789	0,015263161	0,024059056	0,024059056
RCVRN	0,033371031	0,005393403	0,02402826	0,003949369	0,02402826
FAM82A2	0,027533328	0,001613726	0,024018743	0,00190086	0,024018743
FGF19	0,042887799	0,006769323	0,024001575	0,012116902	0,024001575
NTF3	0,046850536	0,023985725	0,009189357	0,013675452	0,023985725
WRB	0,02851413	0,00117694	0,003353637	0,023983553	0,023983553
ROS1	0,031588215	0,003161279	0,023890754	0,004536182	0,023890754
CRYBA4	0,028498895	0,002622936	0,023858195	0,002017763	0,023858195
MSX2	0,050886989	0,006521304	0,023827489	0,020538197	0,023827489
lhx9	0,044708923	0,008117174	0,012774229	0,02381752	0,02381752
GJA8	0,034679476	0,003037003	0,023749851	0,007892623	0,023749851

Supplementary Table 2 Continued

Concept	Sum	Brain	Eye	Heart	Max
SALL4	0,038861264	0,003949093	0,011175396	0,023736773	0,023736773
C10orf97	0,028556654	0,002700439	0,002125974	0,023730242	0,023730242
MSX1	0,053728081	0,007533196	0,023686059	0,022508826	0,023686059
NLK	0,036519263	0,004439509	0,023604308	0,008475446	0,023604308
NKX2-8	0,044484258	0,004155898	0,016890421	0,023437938	0,023437938
hesx1	0,049895227	0,009634887	0,023432597	0,016827745	0,023432597
ASCL1	0,054272223	0,015907495	0,023428644	0,014936083	0,023428644
SIK1	0,028957779	0,001949921	0,003585171	0,023422686	0,023422686
fgf2	0,051920965	0,01423993	0,014392997	0,023288038	0,023288038
cyp26b1	0,039859537	0,007192183	0,023199149	0,009468207	0,023199149
CXCR4	0,040120531	0,010955157	0,005987118	0,023178255	0,023178255
BMPR2	0,047159161	0,004501385	0,019636406	0,023021369	0,023021369
GRIN1	0,037281398	0,023003917	0,005519285	0,008758196	0,023003917
cyp1b1	0,033091258	0,004410882	0,022927461	0,005752914	0,022927461
ST8SIA4	0,031684294	0,022918701	0,004507717	0,004257877	0,022918701
CDON	0,036375858	0,007605392	0,022785506	0,005984959	0,022785506
SMAD1	0,04817846	0,005973095	0,019450217	0,022755147	0,022755147
EP300	0,044398893	0,006472839	0,015262833	0,02266322	0,02266322
CYP26B1	0,039906535	0,00726112	0,022637604	0,010007811	0,022637604
NR2F2	0,045781989	0,00479003	0,022618656	0,018373304	0,022618656
RCN1	0,034977473	0,003663671	0,022615608	0,008698193	0,022615608
SOX9	0,047367927	0,008909498	0,022601361	0,015857067	0,022601361
CYP1B1	0,032787576	0,004458903	0,022561952	0,005766722	0,022561952
POSTN	0,031442791	0,003515699	0,005390816	0,022536277	0,022536277
GAP43	0,034558035	0,022516441	0,0067539	0,005287693	0,022516441
LIM2	0,030111955	0,002737294	0,022446238	0,004928424	0,022446238
PDLIM2	0,028293736	0,001371684	0,004512483	0,02240957	0,02240957
PAX3	0,052264906	0,008103669	0,022362836	0,0217984	0,022362836
EGFR	0,036054131	0,006920896	0,022316275	0,006816961	0,022316275
crx	0,031049853	0,005144442	0,02225418	0,003651232	0,02225418
WNT2B	0,042936482	0,005863449	0,022241546	0,014831487	0,022241546
ATE1	0,02794145	0,001395948	0,004307426	0,022238076	0,022238076
ALDH1A2	0,050024379	0,006788738	0,021075317	0,022160324	0,022160324
LHX1	0,045076795	0,007393114	0,022150259	0,015533422	0,022150259
ATP2A2	0,031287681	0,00442642	0,004721118	0,022140142	0,022140142
GLI2	0,041967671	0,007866989	0,022085879	0,012014804	0,022085879
zscn5a	0,025616581	0,001651678	0,001897557	0,022067346	0,022067346
mylk3	0,024548538	8,61E-04	0,001638854	0,022048549	0,022048549
WNT8A	0,04474207	0,005800274	0,01690616	0,022035637	0,022035637
EN2	0,052092474	0,019805849	0,022010936	0,010275689	0,022010936
WNT3	0,049606014	0,007756128	0,019855111	0,021994776	0,021994776
IHH	0,043540005	0,007312392	0,021968678	0,014258934	0,021968678
MOCS3	0,027472891	0,002833089	0,02193768	0,00270212	0,02193768
NEUROD1	0,035579193	0,006998828	0,021879413	0,006700952	0,021879413
MYL9	0,028713042	0,003295566	0,003542504	0,021874973	0,021874973
FABP7	0,04393116	0,016084607	0,021820116	0,006026438	0,021820116
TTN	0,027050497	0,002192772	0,003052867	0,021804857	0,021804857
mitfa	0,030560462	0,002279493	0,021784979	0,006495989	0,021784979

Supplementary Table 2 Continued

Concept	Sum	Brain	Eye	Heart	Max
GJB1	0,041288603	0,008516785	0,011018864	0,021752955	0,021752955
FGF10	0,048042748	0,007855693	0,018463977	0,021723081	0,021723081
actc1a	0,024923079	0,001307192	0,001893343	0,021722544	0,021722544
DKK1	0,040483549	0,005834496	0,013023512	0,021625543	0,021625543
MYOC	0,028429329	0,003958834	0,021593544	0,002876952	0,021593544
BMPR1A	0,045165718	0,004900517	0,018672443	0,021592756	0,021592756
NOTCH2	0,048108365	0,010510799	0,021589355	0,016008212	0,021589355
WNT8B	0,045234382	0,007471677	0,021581803	0,016180902	0,021581803
WT1	0,048053455	0,006406316	0,021545574	0,020101564	0,021545574
PDX1	0,043724023	0,008593513	0,021540211	0,013590298	0,021540211
PAFAH1B3	0,02403738	0,021491927	0,001461668	0,001083786	0,021491927
TLL1	0,033280242	0,004300124	0,007508491	0,021471625	0,021471625
FERMT2	0,026723983	0,002299919	0,003019597	0,021404467	0,021404467
GPR143	0,026142489	0,002720293	0,021347794	0,002074402	0,021347794
NTRK2	0,037401538	0,021343136	0,007148148	0,008910254	0,021343136
MAG	0,031912714	0,021315108	0,005646596	0,004951011	0,021315108
TBX6	0,040322423	0,005429581	0,013598496	0,021294348	0,021294348
PCDH21	0,029890001	0,001902653	0,006696494	0,021290853	0,021290853
NEUROG1	0,048326306	0,01491267	0,021272069	0,012141568	0,021272069
RBM15	0,030828165	0,001661747	0,021236146	0,007930271	0,021236146
MOV10	0,032241687	0,005406248	0,005600735	0,021234703	0,021234703
pbx2	0,031616744	0,004367194	0,021230006	0,006019545	0,021230006
HMGN3	0,026601138	0,002712062	0,021149996	0,002739079	0,021149996
PKNOX1	0,030171281	0,004406209	0,021051145	0,004713927	0,021051145
lrp6	0,045641918	0,008234733	0,016391866	0,021015318	0,021015318
APP	0,036498643	0,020971099	0,008429689	0,007097855	0,020971099
GNL3	0,025157336	0,0031654	0,02094908	0,001042857	0,02094908
CREBBP	0,041858677	0,005662455	0,015293505	0,020902715	0,020902715
TCF7L1	0,036089927	0,006045029	0,020689138	0,009355762	0,020689138
SOX11	0,039279487	0,009959121	0,02053006	0,008790307	0,02053006
s100b	0,027917126	0,020511336	0,003311971	0,004093819	0,020511336
BARX1	0,040349282	0,004263926	0,020510331	0,015575026	0,020510331
NDEL1	0,027513713	0,020468984	0,003855482	0,003189246	0,020468984
DKK2	0,0377452	0,003732664	0,020443763	0,013568773	0,020443763
nr2f5	0,040116522	0,004223669	0,020428028	0,015464826	0,020428028
PAFAH1B2	0,022537149	0,020394135	0,00114892	9,94E-04	0,020394135
LBX1	0,03728091	0,004705756	0,012200593	0,020374562	0,020374562
TCF3	0,045556389	0,010763823	0,014420898	0,020371667	0,020371667
ptc1	0,036177151	0,007233932	0,020331102	0,008612116	0,020331102
RGR	0,02499561	0,002294843	0,020307384	0,002393382	0,020307384
MSI1	0,040877145	0,012406702	0,020264287	0,008206157	0,020264287
IRX2	0,034057893	0,003929339	0,009864995	0,020263559	0,020263559
CTNNBL1	0,040574796	0,020213373	0,013535398	0,006826025	0,020213373
hes5	0,047472879	0,012523353	0,020162611	0,014786914	0,020162611
TFE3	0,027610516	0,002449294	0,020161509	0,004999714	0,020161509
HAND2	0,032965384	0,007185623	0,005703633	0,020076128	0,020076128
CHRD	0,046179812	0,006559904	0,019549224	0,020070686	0,020070686
SPON1	0,027971201	0,005251834	0,020061544	0,002657822	0,020061544

Supplementary Table 2 Continued

Concept	Sum	Brain	Eye	Heart	Max
HOMER3	0,028946461	0,006612483	0,020036593	0,002297385	0,020036593
SIAH2	0,027553787	0,002860683	0,020034364	0,00465874	0,020034364
RRH	0,022913512	0,001262244	0,02002279	0,001628478	0,02002279
AKR1B1	0,027673084	0,004139197	0,019984997	0,003548891	0,019984997
STRA6	0,031129818	0,003968036	0,019962034	0,007199748	0,019962034
Stra6	0,031129818	0,003968036	0,019962034	0,007199748	0,019962034
NEUROD2	0,032629546	0,019908753	0,007159667	0,005561124	0,019908753
NEUROD6	0,042239882	0,019870948	0,017678084	0,004690851	0,019870948
OLIG2	0,047951449	0,017439818	0,019830989	0,010680641	0,019830989
SCN1B	0,026604047	0,003850269	0,00298971	0,019764069	0,019764069
APLP2	0,033040363	0,019749105	0,007269941	0,006021316	0,019749105
OPN3	0,023138495	0,001908903	0,019747189	0,001482404	0,019747189
smad4	0,036347397	0,005640531	0,01099182	0,019715047	0,019715047
col18a1	0,026350018	0,003363547	0,019621445	0,003365026	0,019621445
RBPJ	0,039283674	0,006625412	0,019607717	0,013050544	0,019607717
WNT9A	0,042610437	0,004724476	0,019603079	0,018282881	0,019603079
CNKSR1	0,023457309	0,001683891	0,019553595	0,002219823	0,019553595
CDH2	0,043976985	0,00889714	0,015540349	0,019539495	0,019539495
FGFR4	0,047205739	0,008374338	0,0193252	0,019506201	0,019506201
WNT9B	0,041080143	0,005060593	0,019500227	0,016519322	0,019500227
MBNL1	0,041813411	0,003155207	0,019162123	0,019496081	0,019496081
pax2b	0,02850662	0,004228995	0,019492304	0,004785322	0,019492304
NUDT6	0,036553536	0,007955809	0,009109222	0,019488507	0,019488507
tbx6	0,03478289	0,004518766	0,010822453	0,01944167	0,01944167
NFATC1	0,032435082	0,005097486	0,007911894	0,019425702	0,019425702
fgf6a	0,045286931	0,007654507	0,018220379	0,019412045	0,019412045
SMAD4	0,036019776	0,005716284	0,010894592	0,0194089	0,0194089
WNT7A	0,045386795	0,007780789	0,019393143	0,018212861	0,019393143
LIFR	0,03461219	0,008033181	0,007215912	0,019363098	0,019363098
vcana	0,025733801	0,002339732	0,004043683	0,019350385	0,019350385
LHX3	0,039165303	0,006853398	0,019348466	0,012963441	0,019348466
CA4	0,02732351	0,019343049	0,003956516	0,004023946	0,019343049
SMYD1	0,040899627	0,003120169	0,01844253	0,019336926	0,019336926
DDC	0,03094116	0,019311999	0,006511254	0,005117909	0,019311999
bmp2a	0,038129434	0,003374986	0,01547545	0,019278999	0,019278999
fabp7a	0,038585715	0,014187615	0,019277694	0,005120405	0,019277694
MBNL3	0,029036237	0,001570699	0,019249557	0,008215981	0,019249557
MBNL2	0,029553423	0,001730771	0,01923841	0,008584242	0,01923841
WNT16	0,039581712	0,004942751	0,019186898	0,015452062	0,019186898
PLA2G7	0,0262738	0,019133144	0,003717397	0,003423258	0,019133144
nf1	0,035512049	0,009675354	0,006758718	0,019077978	0,019077978
PAX7	0,039025705	0,007060136	0,019052784	0,012912785	0,019052784
UTP6	0,022339279	0,001997804	0,00130654	0,019034935	0,019034935
hdac9b	0,025769532	0,002295088	0,004449755	0,019024689	0,019024689
hsf4	0,031734128	0,003040359	0,018972305	0,009721465	0,018972305
SMAD5	0,040730748	0,004291857	0,017468861	0,018970029	0,018970029
FKBP8	0,026642211	0,003350663	0,018967311	0,004324237	0,018967311
SNAI1	0,030459296	0,003514196	0,00798651	0,01895859	0,01895859

Supplementary Table 2 Continued

Concept	Sum	Brain	Eye	Heart	Max
RHO	0,0262239	0,003989129	0,01889785	0,003336922	0,01889785
GPR177	0,029663064	0,003224814	0,018894684	0,007543566	0,018894684
IGF1	0,03518175	0,018833438	0,006922584	0,009425729	0,018833438
SFRP2	0,037814047	0,005078703	0,018820071	0,013915272	0,018820071
OPTN	0,024622945	0,003207808	0,018814484	0,002600653	0,018814484
IRX5	0,033662569	0,003544987	0,011315394	0,018802188	0,018802188
HOXD4	0,033558287	0,005435137	0,01872565	0,009397501	0,01872565
ZEB2	0,031630773	0,004659844	0,008248496	0,018722435	0,018722435
TYRP1	0,028174592	0,003910425	0,018619237	0,005644929	0,018619237
KLF13	0,026842875	0,003053665	0,005176788	0,018612421	0,018612421
DTH	0,032772422	0,018565816	0,007943048	0,006263557	0,018565816
GDF6	0,03007577	0,00287334	0,018549187	0,008653243	0,018549187
OPN1LW	0,027268264	0,004462638	0,018543143	0,004262483	0,018543143
OPN1SW	0,025112189	0,003038872	0,018482902	0,003590415	0,018482902
SERPINF1	0,026187284	0,00337362	0,018467836	0,004345829	0,018467836
Choline acetylase	0,029375819	0,018466671	0,005648566	0,005260582	0,018466671
SATB2	0,031406388	0,007364576	0,018396017	0,005645794	0,018396017
wnt4a	0,033107743	0,004285261	0,018378763	0,010443718	0,018378763
BCAN	0,027115548	0,018345413	0,003535383	0,005234753	0,018345413
SMARCD3	0,027041711	0,003228566	0,005486916	0,01832623	0,01832623
HEY1	0,038651209	0,005225367	0,015105512	0,018320331	0,018320331
HEXIM1	0,023411497	0,002333456	0,002789239	0,018288803	0,018288803
FGF4	0,042261239	0,007174217	0,016802565	0,018284459	0,018284459
MYF5	0,037655018	0,007367682	0,012012752	0,018274585	0,018274585
SLC1A3	0,031689681	0,018266988	0,008276386	0,005146305	0,018266988
PLOD1	0,029539671	0,002367537	0,00890676	0,018265374	0,018265374
TAF15	0,023547957	0,003006751	0,018213704	0,002327502	0,018213704
DISP1	0,028158344	0,004789024	0,018158989	0,005210331	0,018158989
SYP	0,030561646	0,018158566	0,006757078	0,005646003	0,018158566
TBX15	0,028938714	0,002727619	0,008082073	0,018129022	0,018129022
wu:fc26c12	0,026800072	0,002485418	0,006198619	0,018116034	0,018116034
WDR5	0,035008095	0,003371911	0,013529398	0,018106788	0,018106788
HHIP	0,031413261	0,005447593	0,018094265	0,007871403	0,018094265
REST	0,03722759	0,008999273	0,018070311	0,010158006	0,018070311
GATA2	0,032912023	0,005543733	0,009367362	0,018000928	0,018000928
SLC8A1	0,022510771	0,001817217	0,002696897	0,017996656	0,017996656
GMNN	0,026835611	0,003031444	0,017958531	0,005845637	0,017958531
HTR1A	0,028134517	0,017956831	0,005270921	0,004906766	0,017956831
SFRS2	0,025862589	0,004167447	0,003757627	0,017937515	0,017937515
HOXB1	0,045214772	0,011115123	0,017937484	0,016162166	0,017937484
WNT10A	0,040485099	0,005235283	0,017352946	0,01789687	0,01789687
LHX6	0,034284171	0,00778266	0,017895922	0,008605588	0,017895922
FOXD3	0,038368028	0,005635334	0,014840214	0,01789248	0,01789248
PRPH2	0,026125636	0,00481883	0,01788964	0,003417165	0,01788964
LMX1B	0,035238206	0,008025343	0,017884083	0,009328779	0,017884083
SIP1	0,030403502	0,005208097	0,007333815	0,017861591	0,017861591
DCT	0,028093373	0,00403126	0,017852634	0,00620948	0,017852634
HMX3	0,032545973	0,004918173	0,017848912	0,009778887	0,017848912

Supplementary Table 2 Continued

Concept	Sum	Brain	Eye	Heart	Max
MYOG	0,035915717	0,007607698	0,010494675	0,017813344	0,017813344
NR4A3	0,027671095	0,006023973	0,017806312	0,00384081	0,017806312
FOXA2	0,036871966	0,006115178	0,012971281	0,017785506	0,017785506
TEAD1	0,025981484	0,003266837	0,004956739	0,017757908	0,017757908
DMAP1	0,022455761	0,001700591	0,017753863	0,003001306	0,017753863
Imx1b	0,034592327	0,007934612	0,017724352	0,008933361	0,017724352
BMP6	0,040415749	0,005353805	0,017347771	0,017714173	0,017714173
HSF2	0,03604297	0,006627713	0,011874769	0,017540487	0,017540487
SH3BGR	0,0204858	0,001525809	0,001424721	0,01753527	0,01753527
CRYBA2	0,022028303	0,002095886	0,017534441	0,002397975	0,017534441
CRIM1	0,023863098	0,00233609	0,017512414	0,004014593	0,017512414
NDRG4	0,032772548	0,010784803	0,004493768	0,017493977	0,017493977
FSTL3	0,02443908	0,002019652	0,004979007	0,017440421	0,017440421
RRBP1	0,021628475	0,001230671	0,002968061	0,017429743	0,017429743
ABAT	0,027868891	0,006297938	0,004182428	0,017388524	0,017388524
TFAP2A	0,033082996	0,005058646	0,017382235	0,010642115	0,017382235
C21orf33	0,033242159	0,005870156	0,017337438	0,010034564	0,017337438
SUFU	0,029701259	0,004836745	0,017335427	0,007529085	0,017335427
RORA	0,029929241	0,017334212	0,006157314	0,006437716	0,017334212
CITED2	0,030051166	0,003678972	0,00905381	0,017318385	0,017318385
SIK2	0,020864479	0,001129033	0,002451603	0,017283844	0,017283844
ADNP	0,036654517	0,017229578	0,006957201	0,01246774	0,017229578
GATA1	0,034144912	0,006430553	0,010489445	0,017224914	0,017224914
CAPN2	0,026927872	0,00471981	0,017205957	0,005002104	0,017205957
FOXL1	0,031560492	0,003992111	0,017189129	0,010379251	0,017189129
STAU2	0,023395022	0,003652158	0,017166938	0,002575926	0,017166938
FGF1	0,041954368	0,010068872	0,014771551	0,017113945	0,017113945
FGFR3	0,04164803	0,007493715	0,017105214	0,017049101	0,017105214
DLL1	0,043078557	0,009297848	0,016703363	0,017077346	0,017077346
CDH10	0,02237862	0,002806724	0,002523753	0,017048142	0,017048142
sox10	0,043510582	0,009680961	0,017013929	0,016815692	0,017013929
AGRN	0,032423157	0,009712216	0,016950836	0,005760106	0,016950836
NR2E3	0,026827853	0,005458677	0,016934511	0,004434664	0,016934511
PAX9	0,034347594	0,004990829	0,016932707	0,01242406	0,016932707
TYR	0,027361494	0,005284308	0,016928488	0,005148698	0,016928488
PRDX5	0,024428666	0,016889743	0,004256174	0,003282748	0,016889743
VEGFA	0,035975493	0,00736562	0,01173971	0,016870163	0,016870163
PSEN1	0,033355143	0,016851356	0,009233229	0,007270559	0,016851356
HOXA2	0,03780115	0,007770806	0,016832604	0,01319774	0,016832604
PAX1	0,033455823	0,004793974	0,01679441	0,011867437	0,01679441
SMARCA5	0,02704465	0,005594725	0,016771124	0,004678802	0,016771124
SEMA5A	0,037018549	0,009020081	0,016762271	0,011236198	0,016762271
htra1	0,024147389	0,004102218	0,016761044	0,003284126	0,016761044
NEUROD4	0,034431938	0,009919189	0,01674384	0,00776891	0,01674384
CDH6	0,033029556	0,006503333	0,016739894	0,009786331	0,016739894
cdh4	0,026430035	0,007962693	0,016734322	0,001733021	0,016734322
TRIM71	0,02620095	0,004451265	0,016670834	0,005078851	0,016670834
GRIA3	0,02558055	0,016659248	0,004417847	0,004503455	0,016659248

Supplementary Table 2 Continued

Concept	Sum	Brain	Eye	Heart	Max
UBE3C	0,022779178	0,002301598	0,00382996	0,01664762	0,01664762
GCM2	0,030937014	0,00437185	0,016630741	0,009934424	0,016630741
FZD8	0,033254877	0,005388604	0,016608278	0,011257996	0,016608278
PBX1	0,031933341	0,007220792	0,016599524	0,008113024	0,016599524
AGTPBP1	0,023945466	0,016584575	0,003973869	0,003387022	0,016584575
ror2	0,036457341	0,007957316	0,011925195	0,016574829	0,016574829
PDLIM1	0,021480916	0,001911543	0,003013647	0,016555725	0,016555725
JAG2	0,03663655	0,008263698	0,016551223	0,011821631	0,016551223
RGD1564874	0,025852228	0,004233568	0,016546538	0,005072122	0,016546538
NR2F1	0,034935329	0,006819474	0,016466304	0,01164955	0,016466304
VPS35	0,021668181	0,001944739	0,016459442	0,003264	0,016459442
RAX1	0,022780515	0,002583072	0,016456775	0,003740669	0,016456775
ZEB1	0,0293293	0,004879171	0,008001665	0,016448463	0,016448463
TLX1	0,035822429	0,004822973	0,014557193	0,016442262	0,016442262
TEK	0,028507879	0,005471453	0,006604484	0,016431941	0,016431941
ARX	0,025134906	0,016424782	0,004608551	0,004101573	0,016424782
S1PR1	0,027875559	0,006830073	0,004624784	0,016420702	0,016420702
GSK3B	0,038137432	0,012679706	0,009057949	0,016399777	0,016399777
dhh	0,028949333	0,005373812	0,016396522	0,007178999	0,016396522
HMGA1	0,023489391	0,002835158	0,004268177	0,016386057	0,016386057
DPYSL2	0,025818106	0,016380666	0,005084177	0,004353262	0,016380666
OPTC	0,021771511	0,001355217	0,016346772	0,004069523	0,016346772
SLC1A2	0,025853058	0,016337583	0,005574121	0,003941353	0,016337583
DLX5	0,039950721	0,009324478	0,014297298	0,016328947	0,016328947
CYP26A1	0,035233378	0,006220052	0,016311999	0,012701329	0,016311999
RCBTB1	0,026976412	0,004580154	0,00612142	0,016274839	0,016274839
MARCKS	0,023865871	0,016250152	0,0041315	0,003484219	0,016250152
couptf2	0,026613163	0,001755174	0,01624682	0,008611168	0,01624682
FBLN2	0,022096397	0,002725323	0,003127944	0,01624313	0,01624313
VSX1	0,02356755	0,003490475	0,016217204	0,00385987	0,016217204
CRIP2	0,020943526	0,001853887	0,002874339	0,0162153	0,0162153
klf4	0,031755593	0,005179514	0,010372138	0,016203941	0,016203941
CASP7	0,03252209	0,01616028	0,007923226	0,008438585	0,01616028
CRB1	0,022819938	0,003596754	0,01615378	0,003069405	0,01615378
GTF2A2	0,021201454	0,00343208	0,016137987	0,001631389	0,016137987
SIAH1	0,024883492	0,005402516	0,016134753	0,003346223	0,016134753
OLFML3	0,023403399	0,002346699	0,016083825	0,004972875	0,016083825
VANGL2	0,033708833	0,007632115	0,010003525	0,016073191	0,016073191
GAD1	0,027546477	0,016063257	0,006345623	0,005137597	0,016063257
NR2E1	0,037826721	0,016031435	0,016055693	0,005739594	0,016055693
GRIN2C	0,025719907	0,016027502	0,003926394	0,005766011	0,016027502
IRX1	0,032361884	0,004857722	0,011537533	0,015966628	0,015966628
JAG1	0,037655137	0,006485921	0,015956381	0,015212836	0,015956381
SLIT1	0,032865286	0,008679417	0,015911901	0,008273967	0,015911901
KLF4	0,031152926	0,005131635	0,010162172	0,01585912	0,01585912
EPHA7	0,030652264	0,007727077	0,015855166	0,007070022	0,015855166
NR5A2	0,032770127	0,006807629	0,01011076	0,01585174	0,01585174
BMPR1B	0,034774542	0,003957066	0,014993968	0,015823506	0,015823506

Supplementary Table 2 Continued

Concept	Sum	Brain	Eye	Heart	Max
PUM1	0,021061277	0,002710784	0,015820677	0,002529816	0,015820677
KIF7	0,02750233	0,004470164	0,01581176	0,007220406	0,01581176
PAX5	0,030613441	0,00688433	0,015810675	0,007918437	0,015810675
GATA3	0,031424776	0,006182012	0,009434126	0,015808638	0,015808638
WNT10B	0,035224374	0,005550469	0,015795552	0,013878355	0,015795552
COL15A1	0,020685846	0,00199672	0,015783168	0,002905957	0,015783168
FZD7	0,034988135	0,005061746	0,014145608	0,015780782	0,015780782
ATOH1	0,036266804	0,011134793	0,015745212	0,009386799	0,015745212
FRS2	0,036817517	0,006285037	0,015726012	0,01480647	0,015726012
AMH	0,027866181	0,006254137	0,005924802	0,015687242	0,015687242
FKBP1B	0,019860722	0,002350536	0,001823874	0,015686313	0,015686313
PDLIM5	0,021685233	0,002943723	0,003062631	0,015678881	0,015678881
CDH1	0,033298288	0,006741844	0,010895949	0,015660495	0,015660495
ID2	0,032632519	0,006541388	0,010458304	0,015632826	0,015632826
GRID2	0,022821186	0,015624526	0,003551426	0,003645234	0,015624526
PAX8	0,038313802	0,010195236	0,015563558	0,012555008	0,015563558
BMP5	0,034297388	0,004124276	0,014611974	0,015561138	0,015561138
SALL1	0,032592662	0,004181384	0,015539107	0,012872171	0,015539107
fgf8b	0,037987906	0,007986483	0,014479774	0,015521648	0,015521648
INVS	0,026709612	0,003867739	0,007352423	0,015489451	0,015489451
HMGN2	0,021236913	0,001856999	0,015472668	0,003907246	0,015472668
TSHR	0,023641333	0,015466246	0,003649649	0,004525438	0,015466246
SH3GL1	0,020463135	0,002015736	0,015422841	0,003024559	0,015422841
DPYSL3	0,027475325	0,01541293	0,008214423	0,003847972	0,01541293
RGD1562983	0,029274942	0,002952577	0,015404973	0,010917392	0,015404973
SLC8A3	0,023240611	0,005564627	0,002275715	0,015400268	0,015400268
cb85	0,035432674	0,006197253	0,013900258	0,015335165	0,015335165
tnni1	0,020021997	0,002142216	0,002545112	0,015334668	0,015334668
SFRS2IP	0,024176199	0,003310998	0,005537722	0,015327479	0,015327479
map-1	0,019812824	0,015320323	0,002756283	0,001736218	0,015320323
KDR	0,032817278	0,007154919	0,010355203	0,015307156	0,015307156
Hmx1	0,026897589	0,004362637	0,015301032	0,00723392	0,015301032
RS1	0,020335892	0,002999156	0,015278143	0,002058594	0,015278143
THOC4	0,03110561	0,004847798	0,011005467	0,015252344	0,015252344
SFRP1	0,034310289	0,005155457	0,015249536	0,013905295	0,015249536
ACVR1	0,033604175	0,003650241	0,015203028	0,014750907	0,015203028
HTT	0,030699525	0,015197397	0,009212536	0,006289592	0,015197397
jag1a	0,031741768	0,004791794	0,011783989	0,015165986	0,015165986
LRP5	0,033320662	0,00535752	0,015163559	0,012799583	0,015163559
PITX1	0,03411565	0,004622824	0,015136412	0,014356415	0,015136412
PUM2	0,023206649	0,003275648	0,01513148	0,00479952	0,01513148
UNC5C	0,028032605	0,008748188	0,015122823	0,004161594	0,015122823
CDX1	0,032780159	0,005327413	0,012331695	0,015121049	0,015121049
POU4F2	0,027431095	0,005184559	0,015089367	0,00715717	0,015089367
CABIN1	0,020668205	0,003462116	0,002143284	0,015062804	0,015062804
CRYBB1	0,018851593	0,001428558	0,015039532	0,002383503	0,015039532
SFRP5	0,029741278	0,003656108	0,01105785	0,015027319	0,015027319
SILV	0,021558011	0,003468896	0,015013504	0,003075612	0,015013504

Supplementary Table 2 Continued

Concept	Sum	Brain	Eye	Heart	Max
cb717	0,02261195	0,015009001	0,003072111	0,004530837	0,015009001
SMAD2	0,031090442	0,006140311	0,009954046	0,014996086	0,014996086
TFDP2	0,026963552	0,005000449	0,014982353	0,006980751	0,014982353
THRB	0,02945058	0,014958903	0,006260844	0,008230833	0,014958903
neurog3	0,030462997	0,006490286	0,014941471	0,009031239	0,014941471
LFNG	0,032872897	0,005027521	0,012913328	0,014932047	0,014932047
INHA	0,024257999	0,00523666	0,004092456	0,014928884	0,014928884
msi2b	0,02160823	0,004348342	0,014911721	0,002348168	0,014911721
rsp-4	0,024087558	0,004538281	0,004678965	0,01487031	0,01487031
NEFL	0,024356782	0,014868271	0,00538225	0,004106261	0,014868271
TAL1	0,031043317	0,006428419	0,009792597	0,014822301	0,014822301
FGF3	0,035463195	0,00652805	0,014794961	0,014140182	0,014794961
LEF1	0,036064152	0,007543026	0,01375417	0,014766954	0,014766954
zgc:92533	0,018685322	0,001930664	0,014745576	0,002009083	0,014745576
SMAD9	0,032157689	0,004119986	0,013319974	0,014717731	0,014717731
AHI1	0,021415832	0,014689419	0,003977914	0,002748497	0,014689419
wu:fc44a10	0,016965613	0,014687767	0,001213199	0,001064647	0,014687767
ZIC3	0,028039221	0,006010002	0,007350128	0,01467909	0,01467909
ric-4	0,023904586	0,014675458	0,005972588	0,003256539	0,014675458
PDXP	0,020160688	0,014671074	0,002745152	0,002744461	0,014671074
fyna	0,024556547	0,014668664	0,005273151	0,004614732	0,014668664
ALDOC	0,022663083	0,01466651	0,004210532	0,003786041	0,01466651
FGF7	0,035786059	0,00697851	0,014142133	0,014665414	0,014665414
Mcph1	0,019552499	0,014647883	0,002935203	0,001969413	0,014647883
crmp1	0,026006045	0,014638954	0,008306967	0,003060123	0,014638954
NGFR	0,027806574	0,01463879	0,006328964	0,006838821	0,01463879
GDNF	0,032394651	0,014635764	0,008997806	0,008761082	0,014635764
SEMA3A	0,03446313	0,014597205	0,009345179	0,010520745	0,014597205
FOXA3	0,022376288	0,002294042	0,00549563	0,014586617	0,014586617
CAPN3	0,026586853	0,002897632	0,014555245	0,009133977	0,014555245
NRG1	0,034913935	0,014551393	0,007147504	0,013215038	0,014551393
GAS1	0,024913676	0,004416236	0,014550937	0,005946503	0,014550937
SEMA6D	0,023202876	0,004513826	0,004171366	0,014517684	0,014517684
FOXG1	0,036280058	0,014516241	0,013260201	0,008503618	0,014516241
DYX1C1	0,019258969	0,014506509	0,002462406	0,002290054	0,014506509
DLG4	0,028168149	0,014476212	0,0081077	0,005584236	0,014476212
MEOX1	0,029061187	0,003440336	0,011172006	0,014448846	0,014448846
GPC4	0,031007295	0,014440415	0,009824303	0,006742578	0,014440415
MYL1	0,023054525	0,004752896	0,003873348	0,014428282	0,014428282
SNAP25	0,023838209	0,014412381	0,006064345	0,003361482	0,014412381
ARID4A	0,029966604	0,006499487	0,014395202	0,009071915	0,014395202
ETV1	0,026549919	0,005310648	0,014377884	0,006861387	0,014377884
FGF17	0,037167415	0,009342097	0,014360442	0,013464874	0,014360442
FOXP2	0,026262127	0,014348163	0,0063031	0,005610864	0,014348163
RUNX2	0,034668908	0,007565932	0,012793302	0,014309673	0,014309673
HCCS	0,024103709	0,001594409	0,00821048	0,01429882	0,01429882
CASD1	0,033131715	0,014281432	0,009332016	0,009518267	0,014281432
hsd3b	0,017926365	0,002046974	0,001623037	0,014256354	0,014256354

Supplementary Table 2 Continued

Concept	Sum	Brain	Eye	Heart	Max
DmelCG3861	0,036623374	0,009144784	0,013233503	0,014245087	0,014245087
BCKDHA	0,031827446	0,006955553	0,010632626	0,014239266	0,014239266
ASPM	0,019257573	0,014238895	0,003121394	0,001897286	0,014238895
HOXB5	0,032435112	0,005816368	0,01422852	0,012390224	0,01422852
sp8	0,030514419	0,008808886	0,014221653	0,00748388	0,014221653
JAM3	0,01767919	0,001714975	0,001742896	0,014221319	0,014221319
MAP3K3	0,019563753	0,002396552	0,00295149	0,014215711	0,014215711
Tnni2	0,018558858	0,001569089	0,00277795	0,014211819	0,014211819
LDB2	0,02649118	0,006209168	0,014190123	0,006091889	0,014190123
ybx1	0,026997792	0,008391784	0,004454804	0,014151205	0,014151205
SSR1	0,016846482	9,35E-04	0,001791314	0,014120314	0,014120314
FOS	0,031926282	0,014105567	0,008723301	0,009097416	0,014105567
RCAN1	0,023239369	0,006044106	0,003098494	0,014096768	0,014096768
TSC1	0,023438169	0,01409649	0,005824009	0,00351767	0,01409649
DCLK2	0,0190232	0,014093827	0,002383787	0,002545586	0,014093827
CSPG5	0,019794161	0,014070826	0,003200477	0,002522858	0,014070826
LUM	0,023654597	0,003906079	0,014052294	0,005696224	0,014052294
HES7	0,030119652	0,004286637	0,011786764	0,014046251	0,014046251
espl1	0,017473839	0,002466491	0,014030217	9,77E-04	0,014030217
HOXB6	0,030157553	0,005004209	0,014029088	0,011124256	0,014029088
INA	0,023379466	0,014020409	0,004825931	0,004533126	0,014020409
MAPK11	0,029773451	0,006764405	0,008990746	0,0140183	0,0140183
DLX6	0,033073124	0,008101313	0,010955147	0,014016664	0,014016664
frs2	0,033008941	0,005421648	0,013588333	0,013998961	0,013998961
S1PR2	0,022910045	0,005923903	0,002987187	0,013998956	0,013998956
ADRB1	0,021563575	0,003940655	0,003631527	0,013991393	0,013991393
HDAC4	0,020912757	0,003571735	0,003351678	0,013989345	0,013989345
MAPK14	0,031442191	0,007768661	0,009689124	0,013984405	0,013984405
cxcr4b	0,024290346	0,007226576	0,003101283	0,013962486	0,013962486
UNC5D	0,020226229	0,002652042	0,013942295	0,003631892	0,013942295
CPSF1	0,019836921	0,002604228	0,013938131	0,003294563	0,013938131
NPY	0,025144322	0,013920032	0,005814601	0,00540969	0,013920032
kdrl	0,028219357	0,006204035	0,008096629	0,013918693	0,013918693
GUCA1A	0,019695366	0,002805581	0,013912618	0,002977167	0,013912618
JMJD6	0,027201146	0,00202956	0,013902266	0,011269321	0,013902266
CDKL5	0,017617343	0,013893267	0,002090945	0,00163313	0,013893267
HOXB3	0,033053149	0,006431458	0,01386565	0,012756042	0,01386565
GRM1	0,021868473	0,013860768	0,003865248	0,004142458	0,013860768
ACVR2B	0,029473878	0,003387066	0,012232498	0,013854313	0,013854313
SP8	0,029903481	0,008692846	0,013840897	0,007369737	0,013840897
NRP1	0,033755403	0,010000843	0,009919253	0,013835308	0,013835308
MAB21L1	0,020500623	0,003479882	0,013823251	0,003197489	0,013823251
TAZ	0,0216686	0,00262303	0,013797378	0,005248191	0,013797378
HOXC6	0,029639676	0,0051094	0,013786235	0,010744041	0,013786235
ANGPT1	0,024791243	0,00480195	0,006205525	0,013783769	0,013783769
SEMA3C	0,033777244	0,006431435	0,013780337	0,013565473	0,013780337
E2F4	0,031565811	0,004777089	0,013761921	0,013026801	0,013761921
SFRS6	0,020353969	0,002697091	0,013761628	0,003895251	0,013761628

Supplementary Table 2 Continued

Concept	Sum	Brain	Eye	Heart	Max
CAMK2D	0,028858004	0,013706957	0,004778958	0,01037209	0,013706957
dab2	0,025440838	0,007294283	0,004441216	0,013705339	0,013705339
POU1F1	0,02751256	0,005243496	0,0136757	0,008593363	0,0136757
S100A1	0,02675426	0,009474046	0,003621861	0,013658353	0,013658353
FGF13	0,026146835	0,004796659	0,00769419	0,013655986	0,013655986
SMN	0,027462391	0,007930878	0,005888869	0,013642645	0,013642645
OCA2	0,019317685	0,002907387	0,013630069	0,002780228	0,013630069
SLC6A4	0,023962582	0,013626723	0,005759888	0,004575971	0,013626723
HSBP1	0,017838143	0,001823732	0,002409294	0,013605117	0,013605117
tfdp1	0,023875052	0,004180703	0,013597736	0,006096613	0,013597736
bmp1l	0,023061883	0,003425075	0,006051973	0,013584835	0,013584835
NUP155	0,019336769	0,002457127	0,013584566	0,003295077	0,013584566
DAB2	0,025306646	0,007390721	0,004336545	0,01357938	0,01357938
NKX3-2	0,029275129	0,00422223	0,011474904	0,013577996	0,013577996
EDN1	0,025691936	0,007062256	0,005058684	0,013570995	0,013570995
YY1	0,030087028	0,00455155	0,011967094	0,013568384	0,013568384
NDE1	0,017984258	0,013511463	0,002611888	0,001860906	0,013511463
HAS2	0,023289099	0,003306234	0,006476222	0,013506644	0,013506644
itpr3	0,020613879	0,001505994	0,005607498	0,013500386	0,013500386
MYOD1	0,026549457	0,005073984	0,00797536	0,013500112	0,013500112
SNAI2	0,029230297	0,005917116	0,009823906	0,013489275	0,013489275
PLS3	0,018136524	0,002171563	0,002478261	0,013486701	0,013486701
SP1	0,038106542	0,011464289	0,01347939	0,013162864	0,01347939
NOTCH3	0,029576397	0,007958272	0,013472552	0,008145572	0,013472552
JUN	0,031887095	0,007722368	0,010697273	0,013467453	0,013467453
tie1	0,021322558	0,003122476	0,004762748	0,013437333	0,013437333
ORAOV1	0,019127788	0,002292237	0,01343102	0,003404531	0,01343102
celsr3	0,029330978	0,013425452	0,007334842	0,008570683	0,013425452
celsr3	0,029330978	0,013425452	0,007334842	0,008570683	0,013425452
celsr3	0,029330978	0,013425452	0,007334842	0,008570683	0,013425452
IL6ST	0,025257755	0,005317484	0,006522339	0,013417932	0,013417932
STMN2	0,024590461	0,013407189	0,006153248	0,005030024	0,013407189
tnk2	0,020296764	0,013402266	0,003916809	0,002977688	0,013402266
PENK	0,02355504	0,013393764	0,005311193	0,004850085	0,013393764
MED12	0,022571838	0,005911142	0,013384626	0,003276069	0,013384626
RGL2	0,015781119	0,001051815	0,0133751	0,001354204	0,0133751
FBXW11	0,024825152	0,002892048	0,008563286	0,013369817	0,013369817
ETS1	0,026420418	0,004872913	0,008182867	0,013364638	0,013364638
TSC2	0,022531915	0,013361098	0,005085997	0,00408482	0,013361098
SCUBE2	0,018664571	0,001745898	0,013360276	0,003558396	0,013360276
HOXB4	0,031432685	0,006308527	0,011770285	0,013353873	0,013353873
egln1	0,01880216	0,003095153	0,002355293	0,013351715	0,013351715
RYK	0,033170372	0,007915219	0,013345683	0,011909471	0,013345683
FZD6	0,031941235	0,005760419	0,012835619	0,013345197	0,013345197
TFEC	0,01697777	0,0012284	0,013340035	0,002409335	0,013340035
HOXA1	0,03774805	0,013339927	0,012049295	0,012358826	0,013339927
SP4	0,025235513	0,006926743	0,004983618	0,013325153	0,013325153
FRZB	0,029798804	0,004198779	0,012292622	0,013307403	0,013307403

Supplementary Table 2 Continued

Concept	Sum	Brain	Eye	Heart	Max
DLL4	0,028079109	0,005324418	0,013279188	0,009475503	0,013279188
ALX4	0,02721924	0,004496201	0,013242791	0,009480249	0,013242791
LGSN	0,01844871	0,002072159	0,013235728	0,003140823	0,013235728
MYF6	0,027188977	0,004969757	0,008987451	0,013231769	0,013231769
FGF5	0,030902153	0,007080872	0,010640495	0,013180787	0,013180787
fzd10	0,02885174	0,005202943	0,013170234	0,010478564	0,013170234
CDT1	0,02220824	0,003146442	0,013161163	0,005900634	0,013161163
GDF7	0,023986097	0,003962819	0,013148184	0,006875095	0,013148184
FKTN	0,028619407	0,013142884	0,011609862	0,00386666	0,013142884
CNR1	0,020948699	0,013141536	0,003937376	0,003869786	0,013141536
FAF2	0,019875679	0,003489319	0,013134783	0,003251577	0,013134783
JUND	0,029466948	0,006505588	0,009835285	0,013126074	0,013126074
HIPK	0,022266088	0,004349268	0,013123476	0,004793343	0,013123476
HOXA13	0,030927008	0,006745349	0,013122489	0,011059171	0,013122489
HOXB7	0,029397763	0,005604667	0,013117663	0,010675433	0,013117663
IGFBP3	0,024781941	0,013117563	0,005124583	0,006539794	0,013117563
SMARCC1	0,023223152	0,013116916	0,004503919	0,005602318	0,013116916
SDC3	0,02356687	0,013097456	0,005105342	0,005364072	0,013097456
HMX2	0,02578089	0,004480037	0,013091681	0,008209173	0,013091681
FOSL2	0,021558952	0,003359932	0,01307747	0,005121551	0,01307747
KRAS	0,028609158	0,007694819	0,013053861	0,007860477	0,013053861
STAT3	0,032978207	0,007975871	0,01195048	0,013051857	0,013051857
PTN	0,024999058	0,013048065	0,005045979	0,006905014	0,013048065
KCND3	0,020675426	0,004591034	0,003038382	0,013046009	0,013046009
FLT1	0,027778957	0,006096534	0,008638455	0,013043968	0,013043968
DTX2	0,019339906	0,00255377	0,003765972	0,013020164	0,013020164
RTN1	0,028184287	0,012998228	0,0122654	0,002920659	0,012998228
STRN3	0,023178918	0,004553798	0,012979166	0,005645956	0,012979166
CUGBP1	0,022177629	0,003115355	0,006106529	0,012955744	0,012955744
SNTB1	0,019077947	0,002313275	0,01295098	0,003813692	0,01295098
ID1	0,028792636	0,005301036	0,010542097	0,012949503	0,012949503
OSR1	0,022635961	0,002766791	0,006940863	0,012928307	0,012928307
CAV3	0,019920174	0,003467359	0,003548463	0,012904353	0,012904353
dlc	0,022586869	0,004100046	0,005583416	0,012903408	0,012903408
SF1	0,026885195	0,005911376	0,00809032	0,012883499	0,012883499
TEF	0,025440948	0,006714763	0,005854281	0,012871905	0,012871905
fzd4	0,028716121	0,004678906	0,012860806	0,011176409	0,012860806
FHL2	0,019974228	0,002799867	0,004319644	0,012854718	0,012854718
SLC1A1	0,02187714	0,012846806	0,00535715	0,003673184	0,012846806
HMGA2	0,022776568	0,004107226	0,005824548	0,012844794	0,012844794
sox32	0,02151243	0,002985537	0,005683467	0,012843425	0,012843425
chad	0,018749543	0,001420793	0,004505531	0,012823218	0,012823218
HOXC8	0,030066898	0,006152252	0,012821128	0,011093517	0,012821128
ABRA	0,01605108	0,001454125	0,001782578	0,012814378	0,012814378
BEGAIN	0,017170172	0,01279256	0,003019998	0,001357615	0,01279256
odz4	0,018836502	0,003286083	0,012790965	0,002759454	0,012790965
HRSP12	0,017577918	0,003122024	0,012776389	0,001679504	0,012776389
WHSC2	0,016979417	0,002202141	0,002022517	0,01275476	0,01275476

Supplementary Table 2 Continued

Concept	Sum	Brain	Eye	Heart	Max
DRD2	0,022625184	0,012750722	0,00514065	0,004733812	0,012750722
TNC	0,028940432	0,00973233	0,006459798	0,012748304	0,012748304
NPR1	0,021250155	0,005042643	0,00347201	0,012735502	0,012735502
CDCA8	0,017981922	0,002348663	0,012734928	0,002898331	0,012734928
NOS1	0,023464534	0,012719828	0,005239613	0,005505093	0,012719828
MNX1	0,027422892	0,004681666	0,012693227	0,010048	0,012693227
SUZ12	0,02429188	0,004135777	0,007469423	0,01268668	0,01268668
BRUNOL4	0,018882571	0,002350539	0,003864352	0,01266768	0,01266768
KREMEN1	0,025226932	0,003592675	0,008969501	0,012664756	0,012664756
TBP	0,027931949	0,005232677	0,012660854	0,010038417	0,012660854
CDKN1C	0,031315155	0,008640643	0,012637526	0,010036986	0,012637526
NTRK1	0,025776831	0,012622953	0,006113362	0,007040516	0,012622953
JARID1C	0,022139974	0,012605106	0,003525241	0,006009627	0,012605106
ttf1	0,02182566	0,004332988	0,004891559	0,012601112	0,012601112
IGF1R	0,027501607	0,012582544	0,006803157	0,008115906	0,012582544
FEZ1	0,018929569	0,012581108	0,004177292	0,002171169	0,012581108
cxcr7	0,019728253	0,004918344	0,002236262	0,012573646	0,012573646
PBRM1	0,016762489	0,001859647	0,002339449	0,012563395	0,012563395
RGMA	0,019796047	0,002367097	0,01256149	0,004867459	0,01256149
fzd1	0,027238887	0,00508779	0,012559214	0,009591883	0,012559214
CALB1	0,021450944	0,012555632	0,005565157	0,003330155	0,012555632
DPYSL4	0,018551696	0,012551013	0,003215898	0,002784786	0,012551013
AQP4	0,025367374	0,012512331	0,008958562	0,003896481	0,012512331
thraa	0,0273272	0,012506755	0,004533028	0,010287418	0,012506755
CSRP3	0,022693003	0,003333288	0,006853189	0,012506525	0,012506525
GRIA2	0,021231804	0,012486351	0,004325589	0,004419866	0,012486351
B4GALT5	0,016996898	0,012463482	0,001754443	0,002778974	0,012463482
AXIN2	0,026795482	0,004686981	0,012458041	0,009650461	0,012458041
KCNQ1	0,021531066	0,004011982	0,005063225	0,012455859	0,012455859
ANKRD6	0,029043391	0,012454745	0,008076714	0,008511931	0,012454745
pdlim5	0,017581822	0,003248719	0,00188087	0,012452234	0,012452234
dab2ip	0,016099431	0,01245168	0,002320641	0,001327108	0,01245168
RTN4R	0,02097645	0,012425605	0,004693355	0,003857491	0,012425605
RXRA	0,023740586	0,003429689	0,012419671	0,007891225	0,012419671
HAPLN1	0,020967258	0,002953961	0,005602944	0,012410353	0,012410353
rdh5	0,016418457	0,001619581	0,012404072	0,002394804	0,012404072
MNAT1	0,020102356	0,012402695	0,004082029	0,00361763	0,012402695
NCOA6	0,027954236	0,003406503	0,012169469	0,012378263	0,012378263
FXR2	0,021534301	0,012367086	0,004962718	0,004204499	0,012367086
INHBA	0,026336057	0,005298851	0,008692531	0,012344675	0,012344675
CUL3	0,017927017	0,002548388	0,012330941	0,003047688	0,012330941
COL4A3BP	0,017381536	0,012329287	0,002418381	0,002633868	0,012329287
FGF20	0,027237153	0,004540041	0,010368519	0,012328592	0,012328592
HIF1A	0,029449396	0,008547682	0,00858015	0,012321564	0,012321564
OLIG1	0,032094527	0,012320993	0,012265993	0,007507541	0,012320993
GRSF1	0,018730681	0,012307075	0,002702353	0,003721254	0,012307075
FZD2	0,029627211	0,005158773	0,012294533	0,012173905	0,012294533
SYN2	0,021289611	0,006491005	0,012269783	0,002528824	0,012269783

Supplementary Table 2 Continued

Concept	Sum	Brain	Eye	Heart	Max
EGR1	0,033352427	0,011525875	0,012264174	0,009562379	0,012264174
EFHC1	0,016217604	0,012237656	0,001791013	0,002188936	0,012237656
NRCAM	0,025463898	0,01223696	0,007625617	0,005601321	0,01223696
POFUT1	0,026915599	0,003329966	0,011353225	0,012232407	0,012232407
wnt7	0,026505115	0,002912177	0,011410101	0,012182836	0,012182836
LECT1	0,019100199	0,002395584	0,012166083	0,004538531	0,012166083
WIF1	0,027539851	0,004881425	0,012150585	0,010507841	0,012150585
TCF21	0,0236059	0,003050771	0,008428642	0,012126487	0,012126487
ALDH8A1	0,021037577	0,002431559	0,012122727	0,006483291	0,012122727
FOXA1	0,028132938	0,004938465	0,011077486	0,012116987	0,012116987
si:ch211-251g8.3	0,026906988	0,00361504	0,012109617	0,011182331	0,012109617
WWTR1	0,019648496	0,0022222	0,005325384	0,012100912	0,012100912
rxrbb	0,03001425	0,006782646	0,012098746	0,011132859	0,012098746
ETS2	0,023399334	0,004580226	0,006720514	0,012098593	0,012098593
ST8SIA3	0,016377861	0,01209308	0,002250302	0,002034479	0,01209308
B4GALT7	0,016405363	0,001511919	0,012078188	0,002815254	0,012078188
si:rp71-1f1.4	0,016801817	0,002286308	0,002441903	0,012073607	0,012073607
BMP3	0,026950864	0,002985256	0,011892677	0,01207293	0,01207293
PES1	0,022324812	0,006631584	0,012069649	0,003623579	0,012069649
KCND2	0,022462411	0,006835218	0,003563014	0,012064179	0,012064179
TNNI2	0,019725714	0,001683393	0,005984104	0,012058217	0,012058217
Sep-06	0,017653491	0,003518623	0,002076802	0,012058067	0,012058067
TGFBR1	0,022790259	0,004215968	0,00652744	0,012046851	0,012046851
MAOB	0,019965474	0,012044987	0,004182639	0,003737848	0,012044987
zgc:111879	0,0270721	0,003746467	0,012031493	0,01129414	0,012031493
UBE3A	0,021492414	0,012029309	0,004860605	0,004602499	0,012029309
ACVR2A	0,026313435	0,003886923	0,01041008	0,012016433	0,012016433
MAF1	0,016181411	0,001303353	0,012016298	0,002861761	0,012016298
EVX1	0,0297828	0,00577837	0,012007727	0,011996704	0,012007727
ELK4	0,020955987	0,003487631	0,005462835	0,012005521	0,012005521
ACVRL1	0,023142371	0,002229172	0,008922367	0,011990832	0,011990832
FBLN1	0,01908052	0,003365323	0,003731949	0,011983248	0,011983248
GINS2	0,01482001	0,001100057	0,011967501	0,001752452	0,011967501
RUNX1	0,028094005	0,005240671	0,011965125	0,010888208	0,011965125
FOXF1	0,028732453	0,005381271	0,011400802	0,011950379	0,011950379
sox8	0,030116592	0,006747425	0,011420126	0,011949042	0,011949042
MAPK1	0,032518253	0,009185283	0,011411195	0,011921776	0,011921776
SPRY1	0,025441699	0,004695326	0,008829241	0,011917131	0,011917131
COL8A2	0,015595082	0,001670392	0,011911413	0,002013278	0,011911413
NDUFS3	0,015418398	0,001458236	0,002050252	0,01190991	0,01190991
DVL2	0,027590407	0,006177828	0,00950432	0,01190826	0,01190826
GREM2	0,021774625	0,002618048	0,011892759	0,007263818	0,011892759
CAMK4	0,023255365	0,011890912	0,004144514	0,00721994	0,011890912
IGF2	0,029472457	0,011886984	0,007125702	0,01045977	0,011886984
PTF1A	0,028809046	0,006380484	0,010549088	0,011879474	0,011879474
PSEN2	0,024744043	0,011876749	0,007399545	0,00546775	0,011876749
e2f5	0,02646165	0,004992279	0,011872484	0,009596886	0,011872484
CXCR7	0,019098772	0,004799192	0,002429124	0,011870456	0,011870456

Supplementary Table 2 Continued

Concept	Sum	Brain	Eye	Heart	Max
ELF3	0,019090069	0,002686205	0,01186149	0,004542375	0,01186149
IGFBP1	0,023045633	0,011858264	0,005079665	0,006107704	0,011858264
STAT1	0,030756373	0,007324194	0,011852513	0,011579667	0,011852513
igfbp5a	0,022025153	0,011848204	0,004148253	0,006028696	0,011848204
SLC45A2	0,015211837	0,001385514	0,011841472	0,001984851	0,011841472
SP3	0,029970556	0,009022091	0,009109033	0,011839432	0,011839432
G3BP1	0,015769241	0,002285369	0,011829966	0,001653908	0,011829966
nkx2.1a	0,022990908	0,004341044	0,006853727	0,011796138	0,011796138
DRD3	0,019311575	0,011789444	0,0041631	0,00335903	0,011789444
DRD1	0,020322526	0,011777631	0,004521411	0,004023484	0,011777631
GRIA4	0,021983063	0,011768375	0,006071991	0,004142698	0,011768375
col15a1	0,015126006	0,001205967	0,011761891	0,002158147	0,011761891
ZIC1	0,029825179	0,011749265	0,009523488	0,008552426	0,011749265
WNK1	0,016821906	0,002488704	0,002587784	0,011745418	0,011745418
GRIK1	0,018149827	0,011738543	0,003128287	0,003282997	0,011738543
igfbp5	0,023831867	0,011733324	0,005985801	0,006112741	0,011733324
VIM	0,032025564	0,011715782	0,009033917	0,011275866	0,011715782
IDH1	0,02110433	0,002143266	0,011710007	0,007251057	0,011710007
MSTN	0,021291915	0,003434619	0,006155927	0,01170137	0,01170137
ADCYAP1	0,022265378	0,011691582	0,005256859	0,005316938	0,011691582
MYOZ1	0,015169119	0,00145435	0,002024139	0,01169063	0,01169063
MYCN	0,023800751	0,005765296	0,006344897	0,011690558	0,011690558
MAFB	0,031107293	0,008891026	0,011686402	0,010529865	0,011686402
BMP1	0,025259797	0,005732143	0,007842976	0,011684676	0,011684676
SUMO3	0,017804723	0,002296445	0,00382483	0,011683448	0,011683448
POU3F1	0,024512034	0,011681798	0,006467603	0,006362633	0,011681798
ERBB4	0,030699907	0,009081923	0,009936379	0,011681605	0,011681605
YWHAE	0,021634424	0,011680358	0,003831961	0,006122106	0,011680358
CDC2	0,030075682	0,011679228	0,010008704	0,008387751	0,011679228
GJD2	0,030187918	0,009847653	0,008661267	0,011678998	0,011678998
NUMB	0,024463698	0,006972192	0,011675021	0,005816485	0,011675021
Sep-02	0,015958214	0,002463649	0,00182506	0,011669506	0,011669506
SMYD2	0,016603341	0,001223181	0,003720794	0,011659367	0,011659367
arpp19b	0,013933877	0,011658436	0,001117634	0,001157806	0,011658436
ENO2	0,022991421	0,011653886	0,005917678	0,005419857	0,011653886
SLC26A5	0,019210577	0,003995389	0,011650956	0,003564232	0,011650956
ACTN2	0,019777933	0,005506837	0,002627426	0,011643671	0,011643671
ERBB2	0,028687511	0,009590258	0,011639825	0,007457427	0,011639825
HOXA11	0,025496678	0,004272185	0,011636368	0,009588126	0,011636368
DNAJC5	0,018600238	0,00506813	0,011635893	0,001896216	0,011635893
VANGL1	0,028685778	0,007055359	0,010003632	0,011626787	0,011626787
myhz1	0,022538608	0,002622744	0,008289385	0,011626478	0,011626478
mbp	0,017758362	0,011621123	0,003277539	0,002859699	0,011621123
AGT	0,025434235	0,007836647	0,005978355	0,011619232	0,011619232
CLDN11	0,018889353	0,011618506	0,002887344	0,004383502	0,011618506
TRH	0,021743553	0,011614918	0,005103466	0,005025167	0,011614918
GJB6	0,022542806	0,006134848	0,004813332	0,011594627	0,011594627
DCDC2	0,015696645	0,011594283	0,002100576	0,002001787	0,011594283

Supplementary Table 2 Continued

Concept	Sum	Brain	Eye	Heart	Max
PURA	0,020694524	0,011592613	0,003620117	0,005481794	0,011592613
GBX1	0,025626857	0,006098072	0,011591109	0,007937675	0,011591109
tfap2c	0,021514937	0,002275156	0,00765601	0,011583771	0,011583771
IGFBP2	0,022761183	0,011583738	0,004539007	0,006638437	0,011583738
cyp19a1b	0,024594855	0,01157569	0,005734116	0,007285048	0,01157569
SORBS3	0,017407494	0,001472511	0,004362819	0,011572164	0,011572164
TSPAN3	0,013725227	0,011562628	0,00106423	0,001098368	0,011562628
POU3F2	0,027748229	0,007762995	0,011550419	0,008434814	0,011550419
foxi1	0,021074278	0,003327285	0,011529833	0,006217161	0,011529833
IFT88	0,02356036	0,003925902	0,008121098	0,011513359	0,011513359
SOX5	0,024781005	0,004260216	0,01148247	0,009038319	0,01148247
CASQ2	0,015649283	0,001797996	0,002374364	0,011476923	0,011476923
ABLIM1	0,019591548	0,003546614	0,011475618	0,004569315	0,011475618
ACVR1B	0,023477152	0,003524012	0,008486668	0,011466472	0,011466472
POLA1	0,015918037	0,002500403	0,011458636	0,001958998	0,011458636
AHR	0,02682594	0,00645542	0,008916561	0,011453959	0,011453959
FGF18	0,028451322	0,005869244	0,011138273	0,011443805	0,011443805
TRDN	0,013934673	0,001209298	0,001290911	0,011434463	0,011434463
MT-1	0,018340591	0,011413642	0,003671249	0,0032557	0,011413642
CACNB2	0,01543266	0,001834074	0,00218599	0,011412595	0,011412595
m17	0,020678351	0,004657541	0,004610199	0,01141061	0,01141061
th2	0,027946135	0,009422041	0,007114259	0,011409836	0,011409836
pld1a	0,018233869	0,003897059	0,002944136	0,011392675	0,011392675
CYP19A1	0,024097512	0,011378011	0,006154307	0,006565195	0,011378011
zgc:171463	0,021030108	0,011374061	0,004864787	0,00479126	0,011374061
tnnt1	0,014785297	0,001430213	0,002004563	0,011350521	0,011350521
BBS5	0,015835902	0,001300451	0,011346893	0,003188558	0,011346893
BBS5	0,015835902	0,001300451	0,011346893	0,003188558	0,011346893
SOX6	0,025990961	0,004851758	0,011345433	0,009793769	0,011345433
HSF1	0,024492584	0,005740338	0,007425329	0,011326918	0,011326918
SP7	0,025147876	0,004185982	0,009655778	0,011306116	0,011306116
NR2F6	0,025216129	0,003093144	0,011303599	0,010819386	0,011303599
HNF1A	0,027529277	0,005937436	0,010303909	0,011287932	0,011287932
HCN2	0,019400531	0,005390371	0,002728457	0,011281702	0,011281702
ROBO2	0,029855415	0,009311443	0,009267137	0,011276835	0,011276835
NCAM1	0,025020501	0,007932664	0,005815191	0,011272647	0,011272647
PRDM1	0,021840006	0,003750222	0,01126909	0,006820695	0,01126909
KIAA0712	0,016869577	0,011267795	0,002913654	0,002688126	0,011267795
TGFB1	0,026090164	0,007485843	0,007340909	0,011263411	0,011263411
FOXH1	0,022558298	0,003004644	0,008302626	0,011251029	0,011251029
PLXNA1	0,024201237	0,006900161	0,006062925	0,011238151	0,011238151
COL2A1	0,023807982	0,005207506	0,011228832	0,007371645	0,011228832
BHLHE40	0,020322725	0,003283826	0,011226484	0,005812416	0,011226484
MOBKL3	0,02340967	0,001778817	0,011220734	0,010410119	0,011220734
dkk3	0,024561878	0,003632248	0,011219018	0,009710613	0,011219018
NEGR1	0,018849356	0,011215153	0,005372308	0,002261896	0,011215153
gdf5	0,025170237	0,00371275	0,011214849	0,010242638	0,011214849
DTNBP1	0,017993564	0,011209527	0,002918474	0,003865564	0,011209527

Supplementary Table 2 Continued

Concept	Sum	Brain	Eye	Heart	Max
PAH	0,01963564	0,011194037	0,004717222	0,003724381	0,011194037
NR4A2	0,026823627	0,011180746	0,008370427	0,007272453	0,011180746
CASP9	0,024798874	0,011178628	0,006661987	0,006958258	0,011178628
DYNC1H1	0,022432288	0,011172893	0,009250736	0,002008659	0,011172893
EGR2	0,031703524	0,011167363	0,009903363	0,010632798	0,011167363
SLC2A3	0,022996781	0,011153606	0,004986665	0,006856509	0,011153606
LAMA1	0,025599806	0,003608608	0,011142091	0,010849107	0,011142091
CKM	0,019269627	0,003318912	0,004814912	0,011135803	0,011135803
LDB1	0,028085334	0,006184399	0,010768679	0,011132257	0,011132257
HTR2C	0,019371163	0,011106766	0,004274588	0,003989809	0,011106766
TGFBR2	0,022036517	0,004570047	0,006364066	0,011102405	0,011102405
ANGPT2	0,021169093	0,004244511	0,005827526	0,011097057	0,011097057
DYRK2	0,022145012	0,011071575	0,004476258	0,00659718	0,011071575
DLX3	0,026172755	0,004387285	0,010715709	0,011069761	0,011069761
MAPK7	0,021845844	0,00585645	0,004920088	0,011069305	0,011069305
NR1H3	0,021882486	0,004605759	0,011060539	0,006216188	0,011060539
HLF	0,017516773	0,011057135	0,003431388	0,00302825	0,011057135
TGFB3	0,022951346	0,005148163	0,006766232	0,011036951	0,011036951
HOXA10	0,025449008	0,005240739	0,011031882	0,009176387	0,011031882
EHF	0,015400069	0,001673769	0,01103033	0,00269597	0,01103033
CDK2	0,029502016	0,010283798	0,011029515	0,008188702	0,011029515
DIO2	0,024957422	0,009766858	0,00416136	0,011029205	0,011029205
PLK2	0,017624861	0,003097519	0,011021727	0,003505614	0,011021727
PRICKLE2	0,028202863	0,008849234	0,008360162	0,010993468	0,010993468
CHRNA7	0,019228347	0,010988195	0,004020162	0,00421999	0,010988195
BMPER	0,021018596	0,002721925	0,007314935	0,010981737	0,010981737
PHOX2B	0,025862986	0,006533439	0,008354096	0,010975452	0,010975452
VRK1	0,016240073	0,001905882	0,003362578	0,010971613	0,010971613
ACP1	0,015326801	0,002742138	0,010965659	0,001619005	0,010965659
BACE1	0,018756788	0,010939894	0,004103211	0,003713683	0,010939894
TGFB2	0,025844857	0,004870738	0,010932367	0,010041752	0,010932367
DZIP1	0,018121487	0,00263238	0,010915131	0,004573976	0,010915131
SEMA3D	0,017649869	0,003135654	0,003600154	0,010914061	0,010914061
GRIK4	0,01696069	0,010907918	0,002612213	0,003440559	0,010907918
WFDC1	0,014746926	0,001127825	0,010901903	0,002717197	0,010901903
DACT2	0,022516709	0,003183476	0,008447649	0,010885584	0,010885584
ACTA2	0,015657233	0,00162739	0,00314618	0,010883664	0,010883664
SLC2A1	0,026026735	0,009822871	0,005320816	0,010883048	0,010883048
MAP2K1	0,028599216	0,007696963	0,010868666	0,010033587	0,010868666
DLGAP1	0,018698346	0,010839235	0,004907831	0,00295128	0,010839235
TNR	0,021560866	0,010834058	0,004445893	0,006280916	0,010834058
SMAD7	0,02298218	0,00433423	0,00781447	0,01083348	0,01083348
SIM2	0,022629229	0,01082384	0,006520514	0,005284875	0,01082384
PSMA6	0,02219975	0,0042959	0,007107464	0,010796386	0,010796386
RPL15	0,015105269	0,001421602	0,002895624	0,010788042	0,010788042
GMFB	0,017264787	0,010787338	0,004166591	0,002310859	0,010787338
TNMD	0,016472537	0,001586909	0,010784575	0,004101053	0,010784575
MLC1	0,024634434	0,010776517	0,003241122	0,010616795	0,010776517

Supplementary Table 2 Continued

Concept	Sum	Brain	Eye	Heart	Max
SLC1A6	0,019518673	0,010772222	0,006076378	0,002670072	0,010772222
PTPN11	0,026504502	0,005995029	0,010757795	0,009751677	0,010757795
MYT1	0,022656487	0,006709289	0,010752483	0,005194715	0,010752483
TSC22D1	0,023430377	0,00947229	0,010750663	0,003207423	0,010750663
STK11	0,019337757	0,003651616	0,010749324	0,004936817	0,010749324
HOXB9	0,024995033	0,004876613	0,010744512	0,009373907	0,010744512
MYC	0,029243855	0,008346933	0,010738471	0,010158451	0,010738471
HOXD12	0,021809865	0,003811043	0,010735887	0,007262935	0,010735887
SOX21	0,020010134	0,004541848	0,010730659	0,004737627	0,010730659
CTF4	0,028085219	0,007341555	0,010014155	0,010729509	0,010729509
FOXI1	0,021207333	0,003387112	0,010702886	0,007117336	0,010702886
rdh10b	0,01847749	0,010690546	0,004189322	0,003597621	0,010690546
foxd1	0,022358369	0,004190183	0,010687631	0,007480555	0,010687631
NRP2	0,028461004	0,009122972	0,008653774	0,010684258	0,010684258
PIK3CG	0,030581363	0,00935734	0,010543412	0,010680611	0,010680611
HRC	0,013590302	0,001395599	0,001515931	0,010678772	0,010678772
PTK2	0,026489791	0,008283154	0,007530077	0,010676559	0,010676559
FOXM1	0,022615703	0,004740977	0,007200429	0,010674296	0,010674296
IFT20	0,016044006	0,002216495	0,003155757	0,010671754	0,010671754
RBL1	0,024263646	0,005821131	0,010656111	0,007786404	0,010656111
id3	0,024634747	0,005509242	0,008477814	0,010647691	0,010647691
PCTK1	0,01432375	0,010647633	0,002143833	0,001532284	0,010647633
RAB23	0,020173553	0,004147874	0,010645035	0,005380646	0,010645035
SEMA3F	0,02727071	0,01063462	0,006471369	0,010164722	0,01063462
HNF4A	0,027400419	0,006232531	0,01054153	0,010626358	0,010626358
NKX6-2	0,026366962	0,008738926	0,010617754	0,007010281	0,010617754
KLF2	0,019475274	0,003154055	0,005728361	0,010592858	0,010592858
ROR1	0,025423301	0,010589206	0,007156205	0,007677892	0,010589206
gys1	0,013261279	0,001601791	0,001074197	0,010585291	0,010585291
ADCYAP1R1	0,01862699	0,010579362	0,003957714	0,004089914	0,010579362
CDC25B	0,021109341	0,004536255	0,010577149	0,005995936	0,010577149
CAMKK1	0,0149774	0,010566498	0,002512593	0,00189831	0,010566498
nr4a2b	0,026002729	0,010554458	0,007733877	0,007714393	0,010554458
MAPK3	0,02984681	0,009115186	0,010178811	0,010552813	0,010552813
GRB2	0,023775905	0,006095263	0,010544382	0,007136261	0,010544382
PROM1	0,026743777	0,00854675	0,007652776	0,01054425	0,01054425
MYL6	0,017845755	0,003577768	0,003729943	0,010538045	0,010538045
DICER1	0,024951741	0,003963124	0,010460372	0,010528244	0,010528244
SPAG5	0,018324845	0,002859844	0,010507771	0,004957228	0,010507771
UNCX	0,019503018	0,003104448	0,005904962	0,010493608	0,010493608
bmp3	0,022840263	0,002459429	0,009892813	0,01048802	0,01048802
B3GAT1	0,025095861	0,007925735	0,006695847	0,01047428	0,01047428
SCRIB	0,020245533	0,003270928	0,006500852	0,010473754	0,010473754
NKD1	0,02512805	0,004291694	0,010467272	0,010369084	0,010467272
CNTN2	0,023950806	0,010452344	0,008229627	0,005268836	0,010452344
MET	0,023005784	0,00549722	0,007062747	0,010445817	0,010445817
PLXNB3	0,018442458	0,010440651	0,00285767	0,005144137	0,010440651
POU2F1	0,023712747	0,004824847	0,008448933	0,010438967	0,010438967

Supplementary Table 2 Continued

Concept	Sum	Brain	Eye	Heart	Max
TSHZ1	0,017668152	0,0030529	0,01043788	0,004177372	0,01043788
ALCAM	0,018618267	0,00405588	0,004141824	0,010420563	0,010420563
NCAPG	0,015957067	0,001904431	0,003632796	0,01041984	0,01041984
NXNL1	0,012692794	7,86E-04	0,010411536	0,00149526	0,010411536
GSK3A	0,022142041	0,008212884	0,003518555	0,010410604	0,010410604
MAGI2	0,019859364	0,005413611	0,010403762	0,004041991	0,010403762
prkar1a	0,015374902	0,002136062	0,002835218	0,010403622	0,010403622
PLK4	0,015597959	0,001931649	0,003265386	0,010400924	0,010400924
NPC2	0,022236453	0,006455311	0,010388397	0,005392745	0,010388397
MAPK8	0,027404157	0,007758571	0,010381517	0,00926407	0,010381517
DYRK3	0,014588271	0,010364504	0,002044579	0,002179189	0,010364504
SPARC	0,024571795	0,004231037	0,010364107	0,009976652	0,010364107
SPARCL1	0,022986814	0,004450919	0,008174353	0,010361542	0,010361542
STAR	0,020861112	0,005615819	0,004884723	0,010360571	0,010360571
CCND2	0,026303662	0,007196867	0,008759859	0,010346936	0,010346936
mbd1	0,019527487	0,010343633	0,005301421	0,003882434	0,010343633
FAT1	0,019893762	0,005464042	0,010322406	0,004107313	0,010322406
GIPC3	0,021377692	0,003209758	0,010322404	0,00784553	0,010322404
dclk1	0,015150169	0,0103159	0,002203284	0,002630985	0,0103159
GDF2	0,02284239	0,002587446	0,009939726	0,010315218	0,010315218
MYG	0,020355692	0,005493263	0,00455009	0,01031234	0,01031234
CEBPB	0,025337679	0,005931802	0,009094568	0,010311309	0,010311309
FZD3	0,029970258	0,009379516	0,010284593	0,010306149	0,010306149
PPP5C	0,016451316	0,004051986	0,002099357	0,010299973	0,010299973
FABP1	0,020200295	0,005058439	0,004850589	0,010291267	0,010291267
FYN	0,019499611	0,010287933	0,004812593	0,004399086	0,010287933
PAXIP1	0,016621273	0,002400834	0,010279773	0,003940665	0,010279773
PDGFA	0,026347516	0,006640857	0,010260097	0,009446561	0,010260097
twist2	0,021246029	0,002891863	0,008097658	0,010256507	0,010256507
otx5	0,021491261	0,005379558	0,010252162	0,005859542	0,010252162
TNNC2	0,015430113	0,002575921	0,002602623	0,010251568	0,010251568
phox2a	0,022316368	0,005265228	0,006802252	0,010248889	0,010248889
DMRT1	0,023483692	0,004908331	0,008339282	0,010236078	0,010236078
GRK1	0,014809219	0,001788721	0,010230248	0,00279025	0,010230248
HDAC6	0,019175863	0,004334256	0,004616028	0,010225579	0,010225579
RGS5	0,018754421	0,00299991	0,005534122	0,010220388	0,010220388
HOXB8	0,023306273	0,004355024	0,010211311	0,008739938	0,010211311
DLG3	0,017987119	0,010209955	0,004478328	0,003298835	0,010209955
lin28	0,023005994	0,004079864	0,008717823	0,010208307	0,010208307
DKK3	0,023535099	0,003842817	0,010208278	0,009484004	0,010208278
DNAJB9	0,013781803	0,001812618	0,001774216	0,010194968	0,010194968
XRCC5	0,024417987	0,005441897	0,008787648	0,010188441	0,010188441
L1CAM	0,018919507	0,010173927	0,004518682	0,004226897	0,010173927
F11R	0,017068934	0,003289243	0,010161594	0,003618095	0,010161594
tcf3	0,024634151	0,005993428	0,008492455	0,010148269	0,010148269
SOSTDC1	0,021549366	0,002809158	0,010143472	0,008596735	0,010143472
CDX4	0,023610182	0,004156285	0,009311346	0,010142552	0,010142552
ADSSL1	0,013238929	0,001321552	0,001781843	0,010135534	0,010135534

Supplementary Table 2 Continued

Concept	Sum	Brain	Eye	Heart	Max
NPAS4	0,013785467	0,010133391	0,001671966	0,001980111	0,010133391
MMP2	0,022435257	0,006559132	0,005759762	0,010116363	0,010116363
ELAVL4	0,019894816	0,010115225	0,005851009	0,003928581	0,010115225
ihhb	0,018336684	0,003450368	0,010106972	0,004779343	0,010106972
APLNR	0,016909763	0,002458544	0,004348863	0,010102356	0,010102356
SPI1	0,025301853	0,005968076	0,009236389	0,010097389	0,010097389
FZD9	0,023770584	0,005320288	0,010081746	0,008368551	0,010081746
ITGB1	0,025427431	0,008076439	0,007276592	0,0100744	0,0100744
nedd8	0,015012197	0,002011081	0,010073671	0,002927445	0,010073671
SLC32A1	0,020012105	0,010066601	0,006719578	0,003225925	0,010066601
SMARCA2	0,021933643	0,004976143	0,010066156	0,006891344	0,010066156
FOXO3	0,020970454	0,004706187	0,006203481	0,010060787	0,010060787
GARS	0,022024408	0,003235361	0,008748321	0,010040726	0,010040726
mchr2	0,012919294	0,001858224	0,001024445	0,010036625	0,010036625
col9a1	0,014241372	0,0019612	0,010031328	0,002248844	0,010031328
EFNA5	0,025266789	0,009901202	0,01002959	0,005335998	0,01002959
TUBA1A	0,020413084	0,010028994	0,006165692	0,004218399	0,010028994
ATXN1	0,022125777	0,007886863	0,010023311	0,004215603	0,010023311
GPX4	0,018180132	0,010016657	0,004549958	0,003613517	0,010016657
CDK4	0,027606985	0,009785376	0,010012372	0,007809238	0,010012372
ENO3	0,015005909	0,002476247	0,002521595	0,010008067	0,010008067
zgc:110164	0,018886177	0,002967048	0,005912496	0,010006633	0,010006633

Supplementary Table 3

Feature.ID	Expression.values.ZF	Expression.values.ZFE	Sum	Cholestasis	Necrosis	Steatosis	Max
ABCC2	44,82557696	14,92890273	0,077013887	0,059428233	0,005082565	0,012503092	0,059428233
ABCC4	9,324918909	17,31227095	0,041712489	0,031682357	0,003264796	0,006765335	0,031682357
ABCG5	8,227333663	5,889999226	0,042074256	0,027521077	0,003103841	0,011449339	0,027521077
ABCG8	16,73607996	3,416021008	0,038630858	0,026150254	0,002783493	0,009697112	0,026150254
ACADM	239,4903964	125,8165362	0,021878643	0,004075392	0,003258889	0,014544361	0,014544361
ACADS	38,37813334	22,95076745	0,017703975	0,004517278	0,002133949	0,011052748	0,011052748
ACADVL	115,2226426	65,60680926	0,016470009	0,003538457	0,002166314	0,010765238	0,010765238
ACOX1	91,44284995	39,90439619	0,041716449	0,009044701	0,003520968	0,029150779	0,029150779
ADD1	8,890479253	23,21992742	0,023682488	0,009257686	0,004136428	0,010288375	0,010288375
ADH5	185,9726784	107,3427021	0,023087617	0,006043346	0,003731309	0,013312962	0,013312962
ADIPOR2	23,90921391	45,77604023	0,039930321	0,004846609	0,002866152	0,032217559	0,032217559
ADRA2B	1,104650512	3,951360682	0,016404252	0,003594533	0,002260285	0,010549436	0,010549436
AGT	377,0012398	23,61386123	0,02728812	0,010209682	0,00865866	0,008419779	0,010209682
APAF1	2,803194208	6,435978406	0,030219667	0,003756397	0,022798733	0,003664537	0,022798733
API5	8,339437574	33,9956096	0,016351219	0,012257269	0,002029005	0,002064946	0,012257269
APOA1	5368,123544	1268,492767	0,0207518	0,004711499	0,00399787	0,012042432	0,012042432
APOB	242,1716426	21,39642033	0,037570022	0,011408326	0,006972171	0,019189526	0,019189526
ATG5	6,09118839	10,65827261	0,017572628	0,002202801	0,012941201	0,002428627	0,012941201
ATG7	1,196703827	4,049285585	0,015807344	0,002102256	0,010844933	0,002860155	0,010844933
BCL2	0,95678364	4,442045097	0,061035451	0,008593643	0,044535566	0,007906242	0,044535566
BCS1L	1,547084928	6,643677531	0,022746054	0,016334401	0,001825698	0,004585956	0,016334401
BIRC2	12,10309739	33,45166888	0,024949275	0,003646871	0,017405748	0,003896657	0,017405748
BLVRB	27,27104596	22,4778521	0,027435131	0,018821862	0,003161966	0,005451304	0,018821862
BMPER	0,001	9,227547986	0,020479662	0,003626294	0,001703037	0,015150331	0,015150331
CASP2	1,175373738	6,300164642	0,033359248	0,004090021	0,025314556	0,003954672	0,025314556
CASP6	4,056175271	4,350155253	0,028183853	0,00381928	0,02132523	0,003039344	0,02132523
CASP8	3,032239959	4,281990814	0,046544049	0,006266749	0,033743194	0,006534107	0,033743194
CASP9	1,419193514	6,323288363	0,051490605	0,00653371	0,037912443	0,007044452	0,037912443
CAST	10,31751332	52,29798187	0,020438122	0,004497664	0,011609449	0,004331008	0,011609449
CD36	6,288256716	70,46346231	0,025321567	0,007080521	0,005910512	0,012330534	0,012330534
CD81	9,528793203	238,5779886	0,02492677	0,005359821	0,003475744	0,016091206	0,016091206
CDK2	2,543544816	8,979739389	0,025480891	0,008452711	0,010170162	0,006858018	0,010170162
CDKN1B	11,38727393	37,18383469	0,0248792	0,007998035	0,010322264	0,006558901	0,010322264
CEBPA	9,121480044	16,98361489	0,030453065	0,009797923	0,006407595	0,014247547	0,014247547
CEBPB	63,04305331	31,99001321	0,026209027	0,008805877	0,007062452	0,010340697	0,010340697
CFLAR	2,992572402	5,853770503	0,031918153	0,004809873	0,021988189	0,005120092	0,021988189
CIRH1A	12,00911533	12,02633604	0,034875907	0,028750676	0,001859005	0,004266228	0,028750676
CPT2	19,76413574	14,01319778	0,019630326	0,006059116	0,003065126	0,010506085	0,010506085
CRK	7,209310662	22,65269365	0,025748551	0,006500926	0,013275154	0,00597247	0,013275154
CTGF	1,922007197	39,38037706	0,033212196	0,008016778	0,005851786	0,019343631	0,019343631
CYB5A	263,4268918	107,6954326	0,03473004	0,013363705	0,005395612	0,015970723	0,015970723
DDC	4,963320937	10,3268003	0,030310558	0,010085961	0,010689252	0,009535345	0,010689252
DFFB	1,657687715	3,782372125	0,023612443	0,003317844	0,01691659	0,003378008	0,01691659
DGAT2	58,74214147	23,9670907	0,032043066	0,005136488	0,002244031	0,024662545	0,024662545
DLAT	3,921573888	14,09515255	0,105669253	0,075439912	0,005487761	0,024741581	0,075439912
DPAGT1	11,02363831	9,546879365	0,017164266	0,004266203	0,00289536	0,010002703	0,010002703
EHHADH	65,05138954	7,170441641	0,020967282	0,006625546	0,002924709	0,011417027	0,011417027

Supplementary Table 3 Continued

Feature.ID	Expression.values.ZF	Expression.values.ZFE	Sum	Cholestasis	Necrosis	Steatosis	Max
ELOVL6	57,89943202	20,70040554	0,015407526	0,002998615	0,001385874	0,011023037	0,011023037
EPHX1	75,45824173	12,00644431	0,022888599	0,00826272	0,004458632	0,010167248	0,010167248
ERBB2	6,951416382	4,742550064	0,02883878	0,010340378	0,010201171	0,008297231	0,010340378
FABP6	0,001	149,7185745	0,038181286	0,030617575	0,002039491	0,005524218	0,030617575
FADD	6,167302297	7,595666486	0,030821892	0,005090054	0,021062072	0,004669766	0,021062072
FAS	0,681434485	1,359948928	0,057379473	0,009123832	0,03891766	0,009337983	0,03891766
FASLG	0,117812232	0,001	0,050953589	0,008522448	0,034139986	0,008291154	0,034139986
FASN	4,02739947	10,76606294	0,041606337	0,010148192	0,00521373	0,026244416	0,026244416
FECH	1,458594967	2,816107342	0,028193304	0,015301908	0,003130973	0,009760423	0,015301908
FGF19	0,122142023	0,968768834	0,027127514	0,017255177	0,001887887	0,007984449	0,017255177
FLT1	1,839201017	1,309551888	0,022246571	0,006310704	0,010303729	0,005632139	0,010303729
FOXA2	22,79098457	4,506487217	0,025602154	0,00980739	0,004358126	0,011436638	0,011436638
FOXE3	0,327230763	2,447602834	0,026381619	0,010293738	0,004722645	0,011365237	0,011365237
GFER	4,937207523	8,49887181	0,027299328	0,008619265	0,005840884	0,012839179	0,012839179
GGT1	0,001	0,721100276	0,058739889	0,031172252	0,005695994	0,021871642	0,031172252
GNMT	143,4323997	34,16008257	0,021026932	0,006332406	0,002700348	0,011994178	0,011994178
GNPAT	1,470753512	4,688973719	0,023393609	0,004263772	0,002335872	0,016793964	0,016793964
GOT1	63,8266418	99,22935225	0,030751588	0,009404703	0,005074093	0,016272791	0,016272791
GPC3	0,001	2,571735874	0,02011111	0,00509334	0,004463585	0,010554185	0,010554185
GPT2	0,393747944	6,62471783	0,045966722	0,014927394	0,006657721	0,024381608	0,024381608
HADHA	51,25144087	13,961273	0,022723211	0,010018039	0,001995165	0,010710007	0,010710007
HFE2	3,229190927	2,303597352	0,021908689	0,005368965	0,002572366	0,013967358	0,013967358
HMGB2	31,96692829	272,4247087	0,023257989	0,003421158	0,017075146	0,002761686	0,017075146
HMOX1	16,95985439	12,15940931	0,041445717	0,015163179	0,013389433	0,012893107	0,015163179
HNF1A	7,886318781	2,902018634	0,048218399	0,019955347	0,008419686	0,019843366	0,019955347
HNF4A	49,06556047	9,954180886	0,041129429	0,015616528	0,00785573	0,017657171	0,017657171
HSD3B7	74,68288492	14,37781683	0,015171532	0,011298706	0,000782	0,003091293	0,011298706
IL10	0,001	0,001	0,029994518	0,008696327	0,012144284	0,009153906	0,012144284
INS	0,657444807	3,746820763	0,025144149	0,006420076	0,007750246	0,010973826	0,010973826
JUN	13,79269365	45,61784692	0,025010629	0,007635969	0,010907425	0,006467235	0,010907425
KDR	1,813695297	2,362934557	0,022250498	0,006675374	0,010121336	0,005453788	0,010121336
KLHL20	1,881012559	7,321126624	0,025708759	0,002857364	0,018885973	0,003965421	0,018885973
KRAS	3,488570042	20,34409521	0,030957714	0,009369169	0,014141153	0,007447392	0,014141153
KRT18	466,5976757	165,3483625	0,037396435	0,010717558	0,010888772	0,015790104	0,015790104
KRT8	493,6805144	404,8514515	0,025367884	0,010456328	0,005198249	0,009713307	0,010456328
LDHA	9,142657629	181,3878948	0,043637305	0,011814404	0,018361333	0,013461568	0,018361333
LEPR	2,558063202	3,550204497	0,0253284	0,004935588	0,005291006	0,015101806	0,015101806
LIPC	212,95974	0,418143157	0,029702909	0,010502266	0,005543574	0,013657069	0,013657069
LPIN1	30,20772955	49,16458362	0,025058595	0,003857077	0,00187868	0,019322839	0,019322839
MAP1LC3A	32,32884316	52,73154608	0,018914178	0,002765334	0,01286324	0,003285605	0,01286324
MAP2K1	7,707091218	19,34897855	0,026280683	0,008172674	0,010545855	0,007562153	0,010545855
MAP2K4	1,793811449	4,584121875	0,026101328	0,00586159	0,014159399	0,00608034	0,014159399
MAPK1	3,283224037	16,69665826	0,032464631	0,01046966	0,012845321	0,009149651	0,012845321
MAPK3	2,849759018	3,166575029	0,028548514	0,009496857	0,010657417	0,00839424	0,010657417
MAT1A	598,328758	101,9681742	0,021962637	0,007120771	0,002995166	0,0118467	0,0118467
MBD2	4,184226714	4,011231641	0,024617489	0,009620801	0,004296141	0,010700547	0,010700547
MDM2	5,878038889	15,71224445	0,029093042	0,009109273	0,012982607	0,007001163	0,012982607

Supplementary Table 3 Continued

Feature.ID	Expression.values.ZF	Expression.values.ZFE	Sum	Cholestasis	Necrosis	Steatosis	Max
NFS1	8,652978931	13,47661614	0,021899361	0,004464439	0,003054629	0,014380294	0,014380294
NOTCH2	3,837263455	9,710167419	0,017253086	0,011232573	0,003118563	0,002901949	0,011232573
NR1H4	16,04568011	2,659726401	0,059509341	0,046385944	0,003026804	0,010096595	0,046385944
NR1I2	12,29845316	8,184744036	0,037313148	0,020762435	0,005245015	0,011305696	0,020762435
NR5A2	14,93647739	3,599706097	0,020822095	0,010706359	0,005255265	0,00486047	0,010706359
ONECUT1	0,083673889	0,425580115	0,03052704	0,015676341	0,003968638	0,010882061	0,015676341
PARP1	2,485717839	17,6605449	0,034437459	0,004169373	0,025604269	0,004663819	0,025604269
PCK1	27,91625839	76,34542805	0,031706557	0,010997188	0,005163926	0,015545441	0,015545441
POR	3,2356716	21,55966249	0,028214144	0,009718726	0,00606595	0,012429467	0,012429467
PPARG	24613,6446	2528,198403	0,04306988	0,008887263	0,008552227	0,025630391	0,025630391
PPARGC1B	5,678718194	8,483471535	0,01855463	0,0050136	0,002703208	0,010837823	0,010837823
PRKRIR	1,766266266	7,581362174	0,015710823	0,001632279	0,00114529	0,012933254	0,012933254
PSME3	8,507929815	17,98376848	0,020864666	0,001998459	0,002495453	0,016370753	0,016370753
RBP4	3275,754367	699,926721	0,031877313	0,007494911	0,004879188	0,019503214	0,019503214
RNF7	21,242118	60,80971782	0,01884741	0,002692109	0,011846173	0,004309129	0,011846173
SCARB1	1,997037262	12,62886017	0,027560173	0,011876814	0,00496066	0,010722697	0,011876814
SCD	2,431507673	0,925601328	0,032475173	0,007002905	0,00295036	0,02252191	0,02252191
SDAD1	25,92869434	17,45438429	0,019355072	0,010487013	0,001943135	0,006924922	0,010487013
SEPSECS	8,730270026	3,24451775	0,024295079	0,012085529	0,002514439	0,009695112	0,012085529
SERPINE1	19,67664234	7,190450593	0,024628581	0,005979443	0,006378766	0,012270373	0,012270373
SFPQ	15,74344349	74,80480799	0,048192773	0,015613025	0,004788	0,027791747	0,027791747
SHBG	346,884657	11,77683501	0,027700087	0,008172066	0,008173291	0,01135473	0,01135473
SLC10A2	0,169245438	6,529313252	0,050060485	0,041890794	0,002339994	0,005829697	0,041890794
SLC23A1	1,509281158	4,692434969	0,016969826	0,012802857	0,001644121	0,002522848	0,012802857
SLCO1C1	0,142235827	3,09574504	0,054385055	0,04260197	0,002904114	0,008878971	0,04260197
SLCO3A1	0,475099028	4,620845608	0,013669365	0,010459238	0,001304136	0,001905991	0,010459238
SLCO4A1	0,001	3,835557912	0,016806575	0,013362893	0,001299644	0,002144038	0,013362893
SMAD2	3,781409926	12,28375512	0,023918748	0,006454806	0,006070317	0,011393625	0,011393625
SMAD7	5,847674514	10,21192594	0,02269466	0,006279146	0,00507803	0,011337484	0,011337484
SOCS1	3,334390683	4,271036601	0,020077337	0,004351029	0,004374156	0,011352152	0,011352152
SOCS7	0,093646613	7,137940767	0,015677366	0,002342825	0,002308094	0,011026448	0,011026448
SOD2	71,26165447	77,20095537	0,02739279	0,006341274	0,011615956	0,009435559	0,011615956
SQSTM1	55,56137115	31,03552352	0,033328641	0,005772629	0,016417256	0,011138758	0,016417256
SREBF1	11,27778401	12,00100437	0,0620065	0,013704743	0,005960525	0,042341229	0,042341229
TAT	306,6853912	30,86567388	0,03454319	0,012827191	0,005981295	0,015734704	0,015734704
TFR2	81,72260335	2,871331277	0,024453809	0,006236985	0,002998946	0,015217877	0,015217877
TMEM30A	9,237611566	25,5132471	0,022028193	0,017752279	0,001752175	0,002523738	0,017752279
TNFRSF1A	1,072399556	0,664767203	0,036860697	0,006620295	0,020456534	0,009783869	0,020456534
TNNC1	0,001	5,181196031	0,019872447	0,004934718	0,010275212	0,004662518	0,010275212
TP53	5,843986963	15,30868189	0,035636984	0,011853149	0,015628177	0,008155658	0,015628177
TP73	0,001	0,789306777	0,021288596	0,006283781	0,010298626	0,004706189	0,010298626
UROD	5,269735587	9,671257507	0,01971429	0,006031759	0,002777734	0,010904798	0,010904798
VIM	0,21470073	64,53292452	0,026992368	0,007930084	0,011457288	0,007604996	0,011457288
VIPR1	0,001	1,06088157	0,031439044	0,006466684	0,003761836	0,021210522	0,021210522
VPS33B	3,15450443	4,810771849	0,03448106	0,030334381	0,001184143	0,002962535	0,030334381
XIAP	9,660739561	19,05401865	0,032255523	0,004228349	0,023416213	0,004610962	0,023416213
XRCC5	2,220057407	5,065974978	0,048392344	0,01924159	0,008398013	0,020752742	0,020752742

Supplementary Table 4

Feature.ID	Expression.values.ZF	Expression.values.ZFE	Sum	Brain	Eye	Heart	Max
ABAT	49,94653841	67,90229578	0,027868891	0,006297938	0,004182428	0,017388524	0,017388524
ACP1	0,001	0,274059831	0,015326801	0,002742138	0,010965659	0,001619005	0,010965659
ACTA2	9,814040215	138,769799	0,015657233	0,00162739	0,00314618	0,010883664	0,010883664
ACTN2	0,001	12,21774858	0,019777933	0,005506837	0,002627426	0,011643671	0,011643671
ACVR1B	1,215293162	20,78808439	0,023477152	0,003524012	0,008486668	0,011466472	0,011466472
ACVR2A	2,971192873	16,41577059	0,026313435	0,003886923	0,01041008	0,012016433	0,012016433
ACVRL1	1,265737226	7,08665736	0,023142371	0,002229172	0,008922367	0,011990832	0,011990832
ADCYAP1R1	0,001	7,752555621	0,01862699	0,010579362	0,003957714	0,004089914	0,010579362
ADNP	0,001	8,445057708	0,036654517	0,017229578	0,006957201	0,01246774	0,017229578
ADRB1	0,001	2,674851847	0,021563575	0,003940655	0,003631527	0,013991393	0,013991393
ADSSL1	0,058174225	22,44692468	0,013238929	0,001321552	0,001781843	0,010135534	0,010135534
AES	1,728698297	13,14584342	0,052372187	0,004985748	0,041345441	0,006040997	0,041345441
AGT	377,0012398	23,61386123	0,025434235	0,007836647	0,005978355	0,011619232	0,011619232
AHI1	0,287226245	5,254688115	0,021415832	0,014689419	0,003977914	0,002748497	0,014689419
AKR1B1	33,88513639	52,01606334	0,027673084	0,004139197	0,019984997	0,003548891	0,019984997
ALDH1A2	1,951904822	27,46067055	0,050024379	0,006788738	0,021075317	0,022160324	0,022160324
ALDH8A1	28,34145823	7,460762201	0,021037577	0,002431559	0,012122727	0,006483291	0,012122727
ALX4	0,001	3,334935908	0,02721924	0,004496201	0,013242791	0,009480249	0,013242791
AMH	0,187191618	0,001	0,027866181	0,006254137	0,005924802	0,015687242	0,015687242
ANGPT1	0,289918028	2,364037525	0,024791243	0,00480195	0,006205525	0,013783769	0,013783769
ANGPT2	0,001	0,349517717	0,021169093	0,004244511	0,005827526	0,011097057	0,011097057
ANKRD6	2,133676261	10,30558677	0,029043391	0,012454745	0,008076714	0,008511931	0,012454745
APLP2	8,616560571	51,41967469	0,033040363	0,019749105	0,007269941	0,006021316	0,019749105
AQP4	0,001	3,205675511	0,025367374	0,012512331	0,008958562	0,003896481	0,012512331
ARX	0,001	6,385849508	0,025134906	0,016424782	0,004608551	0,004101573	0,016424782
ASPM	1,1778774	4,58924719	0,019257573	0,014238895	0,003121394	0,001897286	0,014238895
ATOH7	0,001	3,418239995	0,04434729	0,005779851	0,032416155	0,006151283	0,032416155
AXIN2	1,971469813	12,05349415	0,026795482	0,004686981	0,012458041	0,009650461	0,012458041
B4GALT5	0,112959246	1,087069606	0,016996898	0,012463482	0,001754443	0,002778974	0,012463482
B4GALT7	2,949424538	3,752006922	0,016405363	0,001511919	0,012078188	0,002815254	0,012078188
BARHL2	0,001	15,010992	0,039026093	0,003503176	0,031041031	0,004481884	0,031041031
BARX1	0,001	2,703660868	0,040349282	0,004263926	0,020510331	0,015575026	0,020510331
BBS5	0,635307302	7,179673433	0,015835902	0,001300451	0,011346893	0,003188558	0,011346893
BBS5	0,635307302	7,179673433	0,015835902	0,001300451	0,011346893	0,003188558	0,011346893
BCAN	0,001	7,774925379	0,027115548	0,018345413	0,003535383	0,005234753	0,018345413
BCKDHA	17,66933571	32,74910796	0,031827446	0,006955553	0,010632626	0,014239266	0,014239266
BDNF	0,331162461	10,40999382	0,050921854	0,033133779	0,009176592	0,008611482	0,033133779
BHLHE40	17,33660929	94,11987701	0,020322725	0,003283826	0,011226484	0,005812416	0,011226484
BMP10	0,453083965	0,001	0,04093951	0,002080864	0,009294992	0,029563652	0,029563652
BMP2K	3,948499941	11,12759943	0,030476553	0,001799168	0,024548864	0,004128521	0,024548864
BMP3	0,21721407	10,41946676	0,026950864	0,002985256	0,011892677	0,01207293	0,01207293
BMP4	0,234683699	7,735018164	0,072191142	0,009958062	0,030106348	0,032126728	0,032126728
BMP6	3,672384019	1,871512289	0,040415749	0,005353805	0,017347771	0,017714173	0,017714173
BMPER	0,001	9,227547986	0,021018596	0,002721925	0,007314935	0,010981737	0,010981737
CALB1	0,001	10,25326012	0,021450944	0,012555632	0,005565157	0,003330155	0,012555632
CAMK4	0,066337339	14,42950007	0,023255365	0,011890912	0,004144514	0,00721994	0,011890912
CAMKK1	1,041088599	3,932922904	0,0149774	0,010566498	0,002512593	0,00189831	0,010566498

Supplementary Table 4 Continued

Feature.ID	Expression. values.ZF	Expression. values.ZFE	Sum	Brain	Eye	Heart	Max
CASD1	1,365759923	11,76528472	0,033131715	0,014281432	0,009332016	0,009518267	0,014281432
CASP9	1,419193514	6,323288363	0,024798874	0,011178628	0,006661987	0,006958258	0,011178628
CASQ2	0,001	45,3296218	0,015649283	0,001797996	0,002374364	0,011476923	0,011476923
CAV3	0,001	44,62854274	0,019920174	0,003467359	0,003548463	0,012904353	0,012904353
CDCA8	0,61201068	3,487563479	0,017981922	0,002348663	0,012734928	0,002898331	0,012734928
CDH1	36,16465206	25,14712463	0,033298288	0,006741844	0,010895949	0,015660495	0,015660495
CDH10	0,05673588	4,898837338	0,02237862	0,002806724	0,002523753	0,017048142	0,017048142
CDH2	33,66852547	48,25474004	0,043976985	0,00889714	0,015540349	0,019539495	0,019539495
CDH6	0,001	16,22155486	0,033029556	0,006503333	0,016739894	0,009786331	0,016739894
CDK2	2,543544816	8,979739389	0,029502016	0,010283798	0,011029515	0,008188702	0,011029515
CDK5	1,657295872	8,842439896	0,055067398	0,043061133	0,006038619	0,005967648	0,043061133
CDKL5	0,045562833	6,332708518	0,017617343	0,013893267	0,002090945	0,00163313	0,013893267
CDKN1C	0,132513771	13,28391133	0,031315155	0,008640643	0,012637526	0,010036986	0,012637526
CDON	2,763599212	17,03908584	0,036375858	0,007605392	0,022785506	0,005984959	0,022785506
CDT1	0,615924279	3,966051746	0,02220824	0,003146442	0,013161163	0,005900634	0,013161163
CDX4	0,001	0,333015931	0,023610182	0,004156285	0,009311346	0,010142552	0,010142552
CEBPB	63,04305331	31,99001321	0,025337679	0,005931802	0,009094568	0,010311309	0,010311309
CHRNA7	0,090515201	0,818269985	0,019228347	0,010988195	0,004020162	0,00421999	0,010988195
CLDN11	0,682326183	4,80773387	0,018889353	0,011618506	0,002887344	0,004383502	0,011618506
CNKSR1	0,182236597	4,091742696	0,023457309	0,001683891	0,019553595	0,002219823	0,019553595
CNKSR2	0,001	2,395869013	0,038777225	0,003942589	0,0328765	0,001958135	0,0328765
CNR1	0,001	3,105092844	0,020948699	0,013141536	0,003937376	0,003869786	0,013141536
COL15A1	0,720588156	2,683672135	0,020685846	0,00199672	0,015783168	0,002905957	0,015783168
CPSF1	2,604800977	10,41073765	0,019836921	0,002604228	0,013938131	0,003294563	0,013938131
CRB1	0,001	4,356881023	0,022819938	0,003596754	0,01615378	0,003069405	0,01615378
CRIM1	0,391860267	6,413216078	0,023863098	0,00233609	0,017512414	0,004014593	0,017512414
CRIP2	0,915333839	16,56622343	0,020943526	0,001853887	0,002874339	0,0162153	0,0162153
CRYAA	0,222656688	33,58203991	0,053587563	0,004484663	0,044179551	0,00492335	0,044179551
CRYBA4	0,001	873,3472541	0,028498895	0,002622936	0,023858195	0,002017763	0,023858195
CRYBB1	0,330277781	1509,347559	0,018851593	0,001428558	0,015039532	0,002383503	0,015039532
CRYBB2	0,001	0,184757245	0,032442637	0,00270538	0,02720431	0,002532945	0,02720431
CSPG5	0,001	74,63589159	0,019794161	0,014070826	0,003200477	0,002522858	0,014070826
CSRP3	0,147852854	0,58758264	0,022693003	0,003333288	0,006853189	0,012506525	0,012506525
CTCF	10,11250724	37,69599009	0,047221705	0,004501128	0,038721193	0,003999385	0,038721193
CUGBP1	10,07415721	24,7189911	0,022177629	0,003115355	0,006106529	0,012955744	0,012955744
CUGBP2	0,842112033	41,037351	0,034336235	0,003782853	0,006127221	0,02442616	0,02442616
CUL3	7,634667507	25,09951872	0,017927017	0,002548388	0,012330941	0,003047688	0,012330941
CYP1B1	0,001	1,036466106	0,032787576	0,004458903	0,022561952	0,005766722	0,022561952
CYP26A1	0,001	4,45059342	0,035233378	0,006220052	0,016311999	0,012701329	0,016311999
CYP26B1	0,324580077	14,64047465	0,039906535	0,00726112	0,022637604	0,010007811	0,022637604
DAB1	0,087556021	6,816930358	0,074998029	0,059293475	0,010185451	0,005519101	0,059293475
DAB2	1,569110337	11,72857576	0,025306646	0,007390721	0,004336545	0,01357938	0,01357938
DACT2	0,151399561	1,831855475	0,022516709	0,003183476	0,008447649	0,010885584	0,010885584
DCLK2	0,001	3,938997655	0,0190232	0,014093827	0,002383787	0,002545586	0,014093827
DCT	0,001	19,88847528	0,028093373	0,00403126	0,017852634	0,00620948	0,017852634
DDC	4,963320937	10,3268003	0,03094116	0,019311999	0,006511254	0,005117909	0,019311999
DICER1	3,743504156	9,510715699	0,024951741	0,003963124	0,010460372	0,010528244	0,010528244

Supplementary Table 4 Continued

Feature.ID	Expression. values.ZF	Expression. values.ZFE	Sum	Brain	Eye	Heart	Max
DIO2	270,7054943	1,319378666	0,024957422	0,009766858	0,00416136	0,011029205	0,011029205
DISP1	0,865648237	2,46793803	0,028158344	0,004789024	0,018158989	0,005210331	0,018158989
DKK3	4,607867364	9,260588444	0,023535099	0,003842817	0,010208278	0,009484004	0,010208278
DLG3	5,356590917	31,7419335	0,017987119	0,010209955	0,004478328	0,003298835	0,010209955
DLGAP1	0,001	2,780908147	0,018698346	0,010839235	0,004907831	0,00295128	0,010839235
DLL4	2,789265568	6,394114685	0,028079109	0,005324418	0,013279188	0,009475503	0,013279188
DMAP1	1,88124798	9,237368686	0,022455761	0,001700591	0,017753863	0,003001306	0,017753863
DMRT1	0,040508252	0,001	0,023483692	0,004908331	0,008339282	0,010236078	0,010236078
DPYSL2	0,301720605	55,83895573	0,025818106	0,016380666	0,005084177	0,004353262	0,016380666
DPYSL3	0,475004642	71,45944774	0,027475325	0,01541293	0,008214423	0,003847972	0,01541293
DPYSL4	0,001	15,28542067	0,018551696	0,012551013	0,003215898	0,002784786	0,012551013
DRD1	0,001	0,043903674	0,020322526	0,011777631	0,004521411	0,004023484	0,011777631
DRD3	0,001	2,567957457	0,019311575	0,011789444	0,0041631	0,00335903	0,011789444
DVL2	1,751265935	4,673075863	0,027590407	0,006177828	0,00950432	0,01190826	0,01190826
DYNC1H1	15,40278886	42,22917477	0,022432288	0,011172893	0,009250736	0,002008659	0,011172893
DYRK2	2,235686376	14,90825081	0,022145012	0,011071575	0,004476258	0,00659718	0,011071575
DYX1C1	0,110798488	0,502227768	0,019258969	0,014506509	0,002462406	0,002290054	0,014506509
DZIP1	0,048571411	5,348626062	0,018121487	0,00263238	0,010915131	0,004573976	0,010915131
E2F4	2,887628002	11,48898586	0,031565811	0,004777089	0,013761921	0,013026801	0,013761921
EAF1	3,712922451	15,01463299	0,038386859	0,001111476	0,035410508	0,001864875	0,035410508
EAF2	5,93317924	11,74774063	0,055084154	0,001100045	0,051024867	0,00295924	0,051024867
EDN1	0,257013475	2,484479166	0,025691936	0,007062256	0,005058684	0,013570995	0,013570995
EFHC1	0,171014483	2,814407825	0,016217604	0,012237656	0,001791013	0,002188936	0,012237656
EGFR	0,721681364	4,759598308	0,036054131	0,006920896	0,022316275	0,006816961	0,022316275
EGR1	32,65271858	34,0689472	0,033352427	0,011525875	0,012264174	0,009562379	0,012264174
EHF	0,315126963	1,434982918	0,015400069	0,001673769	0,01103033	0,00269597	0,01103033
ELAVL4	0,001	71,26329942	0,019894816	0,010115225	0,005851009	0,003928581	0,010115225
ELF3	6,880102229	11,13006945	0,019090069	0,002686205	0,01186149	0,004542375	0,01186149
ELK4	0,820818431	1,527527181	0,020955987	0,003487631	0,005462835	0,012005521	0,012005521
ELL	7,421488733	7,405358387	0,032946594	0,001846564	0,029262511	0,001837519	0,029262511
ELP4	0,902220837	4,743590017	0,048270274	0,010565259	0,035148573	0,002556442	0,035148573
EMX1	0,001	2,591705592	0,067901835	0,025410886	0,033115316	0,009375636	0,033115316
EMX2	0,001	3,328183919	0,066138677	0,019494217	0,035163632	0,011480829	0,035163632
ENO2	0,001	80,45595729	0,022991421	0,011653886	0,005917678	0,005419857	0,011653886
ENO3	370,6639876	181,557777	0,015005909	0,002476247	0,002521595	0,010008067	0,010008067
EPHA7	0,571327048	2,550290641	0,030652264	0,007727077	0,015855166	0,007070022	0,015855166
ERBB2	6,951416382	4,742550064	0,028687511	0,009590258	0,011639825	0,007457427	0,011639825
ETS2	10,79508164	16,11005405	0,023399334	0,004580226	0,006720514	0,012098593	0,012098593
ETV1	0,001	4,50100164	0,026549919	0,005310648	0,014377884	0,006861387	0,014377884
EVX1	0,001	1,148655723	0,0297828	0,00577837	0,012007727	0,011996704	0,012007727
EYA1	0,001	9,464126139	0,08824259	0,006215983	0,068925288	0,013101321	0,068925288
EYA3	2,780171117	7,527101699	0,054065339	0,002812763	0,046522075	0,004730502	0,046522075
F11R	20,13999102	38,22290299	0,017068934	0,003289243	0,010161594	0,003618095	0,010161594
FAM82A2	5,183820784	10,35201675	0,027533328	0,001613726	0,024018743	0,00190086	0,024018743
FAT1	4,641989719	12,38838643	0,019893762	0,005464042	0,010322406	0,004107313	0,010322406
FBLN1	0,718050189	12,54872242	0,01908052	0,003365323	0,003731949	0,011983248	0,011983248
FBLN2	2,019849116	8,741177099	0,022096397	0,002725323	0,003127944	0,01624313	0,01624313

Supplementary Table 4 Continued

Feature.ID	Expression. values.ZF	Expression. values.ZFE	Sum	Brain	Eye	Heart	Max
FERMT2	8,516861912	7,658143561	0,026723983	0,002299919	0,003019597	0,021404467	0,021404467
FEZ1	0,001	67,17791161	0,018929569	0,012581108	0,004177292	0,002171169	0,012581108
FGF1	0,001	1,995420087	0,041954368	0,010068872	0,014771551	0,017113945	0,017113945
FGF13	1,232944541	9,798715242	0,026146835	0,004796659	0,00769419	0,013655986	0,013655986
FGF16	0,001	1,290003027	0,037439812	0,005542275	0,006594595	0,025302943	0,025302943
FGF17	0,039268083	0,088346493	0,037167415	0,009342097	0,014360442	0,013464874	0,014360442
FGF19	0,122142023	0,968768834	0,042887799	0,006769323	0,024001575	0,012116902	0,024001575
FGF3	0,001	0,114686389	0,035463195	0,00652805	0,014794961	0,014140182	0,014794961
FGF4	0,001	0,446217554	0,042261239	0,007174217	0,016802565	0,018284459	0,018284459
FGF5	0,001	0,001	0,030902153	0,007080872	0,010640495	0,013180787	0,013180787
FGF7	0,001	0,32384422	0,035786059	0,00697851	0,014142133	0,014665414	0,014665414
FGFR3	0,001	9,766216293	0,04164803	0,007493715	0,017105214	0,017049101	0,017105214
FGFR4	19,43235693	12,71319867	0,047205739	0,008374338	0,0193252	0,019506201	0,019506201
FKBP8	8,783768151	2,434637716	0,026642211	0,003350663	0,018967311	0,004324237	0,018967311
FKTN	3,07489347	7,708860268	0,028619407	0,013142884	0,011609862	0,00386666	0,013142884
FLT1	1,839201017	1,309551888	0,027778957	0,006096534	0,008638455	0,013043968	0,013043968
FMR1	4,767917567	18,60426765	0,037486117	0,02523618	0,007881047	0,004368888	0,02523618
FOS	16,33840179	26,30186985	0,031926282	0,014105567	0,008723301	0,009097416	0,014105567
FOXA1	17,40991629	5,003019215	0,028132938	0,004938465	0,011077486	0,012116987	0,012116987
FOXA2	22,79098457	4,506487217	0,036871966	0,006115178	0,012971281	0,017785506	0,017785506
FOXA3	17,82174628	5,111711684	0,022376288	0,002294042	0,00549563	0,014586617	0,014586617
FOXD3	0,001	7,951313457	0,038368028	0,005635334	0,014840214	0,01789248	0,01789248
FOXE3	0,327230763	2,447602834	0,043705333	0,004926329	0,02739064	0,011388364	0,02739064
FOXF1	0,508435863	6,578017807	0,028732453	0,005381271	0,011400802	0,011950379	0,011950379
FOXH1	0,146187226	0,884702139	0,022558298	0,003004644	0,008302626	0,011251029	0,011251029
FOXI1	0,001	0,391060675	0,021207333	0,003387112	0,010702886	0,007117336	0,010702886
FOXL1	0,578164034	4,611797732	0,031560492	0,003992111	0,017189129	0,010379251	0,017189129
FOXP2	1,079462835	13,47316067	0,026262127	0,014348163	0,0063031	0,005610864	0,014348163
FRS2	3,867193339	9,233402394	0,036817517	0,006285037	0,015726012	0,01480647	0,015726012
FRZB	0,119205529	5,835486962	0,029798804	0,004198779	0,012292622	0,013307403	0,013307403
FXR1	7,578846921	32,18782634	0,038347255	0,025299991	0,008200328	0,004846936	0,025299991
FZD2	2,514349456	19,85591956	0,029627211	0,005158773	0,012294533	0,012173905	0,012294533
FZD3	0,186837642	9,544880002	0,029970258	0,009379516	0,010284593	0,010306149	0,010306149
FZD9	0,001	7,581459957	0,023770584	0,005320288	0,010081746	0,008368551	0,010081746
G3BP1	13,64505635	41,23903146	0,015769241	0,002285369	0,011829966	0,001653908	0,011829966
GAD1	0,024837381	103,8669596	0,027546477	0,016063257	0,006345623	0,005137597	0,016063257
GATA3	0,120959457	32,24167861	0,031424776	0,006182012	0,009434126	0,015808638	0,015808638
GATA4	14,79096764	2,962223171	0,119178429	0,006391891	0,010700367	0,102086171	0,102086171
GATA5	1,703895059	6,941785532	0,077895351	0,003146774	0,007228061	0,067520514	0,067520514
GBX1	0,001	4,325944368	0,025626857	0,006098072	0,011591109	0,007937675	0,011591109
GBX2	0,001	6,267840267	0,058807906	0,016732653	0,027584914	0,01449034	0,027584914
GCM2	0,001	3,92058267	0,030937014	0,00437185	0,016630741	0,009934424	0,016630741
GDF7	0,001	0,484503106	0,023986097	0,003962819	0,013148184	0,006875095	0,013148184
GDNF	0,001	1,667391746	0,032394651	0,014635764	0,008997806	0,008761082	0,014635764
GFAP	0,061571011	123,9791003	0,050052516	0,03035348	0,011980851	0,007718185	0,03035348
GINS2	0,937634664	6,093897237	0,01482001	0,001100057	0,011967501	0,001752452	0,011967501
GLI3	0,06485703	1,148804816	0,053298395	0,012226133	0,027126459	0,013945804	0,027126459

Supplementary Table 4 Continued

Feature.ID	Expression. values.ZF	Expression. values.ZFE	Sum	Brain	Eye	Heart	Max
GMFB	0,642704794	17,16527008	0,017264787	0,010787338	0,004166591	0,002310859	0,010787338
GMNN	2,733159614	5,197771099	0,026835611	0,003031444	0,017958531	0,005845637	0,017958531
GNL3	15,66153159	25,22773242	0,025157336	0,0031654	0,02094908	0,001042857	0,02094908
GPC4	10,41296405	18,52245953	0,031007295	0,014440415	0,009824303	0,006742578	0,014440415
GPR143	0,050233361	4,383610293	0,026142489	0,002720293	0,021347794	0,002074402	0,021347794
GPR177	5,570758805	26,22975168	0,029663064	0,003224814	0,018894684	0,007543566	0,018894684
GRB2	11,3887493	34,29655007	0,023775905	0,006095263	0,010544382	0,007136261	0,010544382
GREM2	0,177561017	1,310745605	0,021774625	0,002618048	0,011892759	0,007263818	0,011892759
GRID2	2,265890141	7,063026065	0,022821186	0,015624526	0,003551426	0,003645234	0,015624526
GRIK4	0,001	2,825551332	0,01696069	0,010907918	0,002612213	0,003440559	0,010907918
GRIN2C	5,527925391	2,770178948	0,025719907	0,016027502	0,003926394	0,005766011	0,016027502
GRSF1	11,45004981	12,31858483	0,018730681	0,012307075	0,002702353	0,003721254	0,012307075
GSK3A	8,460724304	39,2923593	0,022142041	0,008212884	0,003518555	0,010410604	0,010410604
GSK3B	8,508615284	21,1665384	0,038137432	0,012679706	0,009057949	0,016399777	0,016399777
GUCA1A	0,149461422	0,678723241	0,019695366	0,002805581	0,013912618	0,002977167	0,013912618
HAND2	2,442204284	7,501800013	0,032965384	0,007185623	0,005703633	0,020076128	0,020076128
HAS2	0,001	0,806569937	0,023289099	0,003306234	0,006476222	0,013506644	0,013506644
HCCS	7,909060535	15,0427202	0,024103709	0,001594409	0,00821048	0,01429882	0,01429882
HCN2	0,001	6,090658057	0,019400531	0,005390371	0,002728457	0,011281702	0,011281702
HDAC4	0,669858295	4,29746294	0,020912757	0,003571735	0,003351678	0,013989345	0,013989345
HDAC6	1,699251951	4,232109283	0,019175863	0,004334256	0,004616028	0,010225579	0,010225579
HEY1	0,187135214	12,34825105	0,038651209	0,005225367	0,015105512	0,018320331	0,018320331
HEY2	0,001	2,679518409	0,044127516	0,005736743	0,013861591	0,024529182	0,024529182
HHIP	23,45351308	13,98703503	0,031413261	0,005447593	0,018094265	0,007871403	0,018094265
HMGA2	1,416742718	16,02344623	0,022776568	0,004107226	0,005824548	0,012844794	0,012844794
HMGN3	8,518741552	111,1314753	0,026601138	0,002712062	0,021149996	0,002739079	0,021149996
HMX1	0,001	5,885777072	0,039346017	0,004099694	0,028858175	0,006388147	0,028858175
HMX2	0,001	4,428895589	0,02578089	0,004480037	0,013091681	0,008209173	0,013091681
HMX3	0,001	5,272990866	0,032545973	0,004918173	0,017848912	0,009778887	0,017848912
HNF1A	7,886318781	2,902018634	0,027529277	0,005937436	0,010303909	0,011287932	0,011287932
HNF4A	49,06556047	9,954180886	0,027400419	0,006232531	0,01054153	0,010626358	0,010626358
HRC	0,001	70,09602787	0,013590302	0,001395599	0,001515931	0,010678772	0,010678772
HSBP1	19,72095685	80,94110001	0,017838143	0,001823732	0,002409294	0,013605117	0,013605117
HSF1	2,698800278	6,424773977	0,024492584	0,005740338	0,007425329	0,011326918	0,011326918
HSF2	4,813000703	30,76293422	0,03604297	0,006627713	0,011874769	0,017540487	0,017540487
HTT	3,099221506	7,48572182	0,030699525	0,015197397	0,009212536	0,006289592	0,015197397
ID1	26,76364573	172,5041557	0,028792636	0,005301036	0,010542097	0,012949503	0,012949503
IDH1	59,95124959	102,4082866	0,02110433	0,002143266	0,011710007	0,007251057	0,011710007
IFT20	3,779374182	6,116270177	0,016044006	0,002216495	0,003155757	0,010671754	0,010671754
IFT88	1,009135963	5,238938382	0,02356036	0,003925902	0,008121098	0,011513359	0,011513359
IGF1	43,10004265	1,473651308	0,03518175	0,018833438	0,006922584	0,009425729	0,018833438
IGFBP3	3,462869268	6,745648165	0,024781941	0,013117563	0,005124583	0,006539794	0,013117563
IL6ST	10,33603071	7,954064431	0,025257755	0,005317484	0,006522339	0,013417932	0,013417932
INVS	4,120526088	1,789820528	0,026709612	0,003867739	0,007352423	0,015489451	0,015489451
ISL1	0,001	28,11875357	0,077418409	0,009697639	0,031026876	0,036693894	0,036693894
JAG2	0,438992148	5,193054873	0,03663655	0,008263698	0,016551223	0,011821631	0,016551223
JAM3	1,888920597	11,99808963	0,01767919	0,001714975	0,001742896	0,014221319	0,014221319

Supplementary Table 4 Continued

Feature.ID	Expression. values.ZF	Expression. values.ZFE	Sum	Brain	Eye	Heart	Max
JMJD6	2,685939265	4,470756489	0,027201146	0,00202956	0,013902266	0,011269321	0,013902266
JUN	13,79269365	45,61784692	0,031887095	0,007722368	0,010697273	0,013467453	0,013467453
JUND	0,001	0,001	0,029466948	0,006505588	0,009835285	0,013126074	0,013126074
KCND2	0,001	5,464793076	0,022462411	0,006835218	0,003563014	0,012064179	0,012064179
KCND3	0,001	6,561966164	0,020675426	0,004591034	0,003038382	0,013046009	0,013046009
KCNQ1	0,063063873	0,425980392	0,021531066	0,004011982	0,005063225	0,012455859	0,012455859
KDR	1,813695297	2,362934557	0,032817278	0,007154919	0,010355203	0,015307156	0,015307156
KERA	0,001	10,41581553	0,034869812	0,003642897	0,025988516	0,005238399	0,025988516
KIF7	0,995773766	1,479006404	0,02750233	0,004470164	0,01581176	0,007220406	0,01581176
KLF4	0,096408748	3,9208502	0,031152926	0,005131635	0,010162172	0,01585912	0,01585912
KRAS	3,488570042	20,34409521	0,028609158	0,007694819	0,013053861	0,007860477	0,013053861
LAMA1	0,027598803	1,245585434	0,025599806	0,003608608	0,011142091	0,010849107	0,011142091
LECT1	0,001	110,0453689	0,019100199	0,002395584	0,012166083	0,004538531	0,012166083
LEF1	0,222098359	12,71198919	0,036064152	0,007543026	0,01375417	0,014766954	0,014766954
LFNG	2,93029436	24,07676481	0,032872897	0,005027521	0,012913328	0,014932047	0,014932047
LGSN	0,034436675	22,62954074	0,01844871	0,002072159	0,013235728	0,003140823	0,013235728
LHX2	0,001	8,104327194	0,054539438	0,009577774	0,025657777	0,019303887	0,025657777
LHX3	0,001	5,437823662	0,039165303	0,006853398	0,019348466	0,012963441	0,019348466
LHX5	0,001	11,61808359	0,038766783	0,006216482	0,024697323	0,007852977	0,024697323
LHX6	0,329022146	4,894335471	0,034284171	0,00778266	0,017895922	0,008605588	0,017895922
LRP5	9,55827004	8,08270374	0,033320662	0,00535752	0,015163559	0,012799583	0,015163559
LRRC10	0,001	0,181168974	0,044885568	0,001325308	0,002594433	0,040965827	0,040965827
LUM	0,001	33,73023464	0,023654597	0,003906079	0,014052294	0,005696224	0,014052294
MAB21L1	0,001	0,23349922	0,020500623	0,003479882	0,013823251	0,003197489	0,013823251
MAB21L2	0,001	0,290919093	0,046415213	0,00532077	0,035342341	0,005752102	0,035342341
MAF	1,67006787	8,265438618	0,04994427	0,00505733	0,038482288	0,006404654	0,038482288
MAF1	3,725801822	21,30770996	0,016181411	0,001303353	0,012016298	0,002861761	0,012016298
MAG	0,001	14,6543759	0,031912714	0,021315108	0,005646596	0,004951011	0,021315108
MAGI2	0,181715394	3,392510188	0,019859364	0,005413611	0,010403762	0,004041991	0,010403762
MAP2K1	7,707091218	19,34897855	0,028599216	0,007696963	0,010868666	0,010033587	0,010868666
MAP3K3	0,875014708	3,533687292	0,019563753	0,002396552	0,00295149	0,014215711	0,014215711
MAPK1	3,283224037	16,69665826	0,032518253	0,009185283	0,011411195	0,011921776	0,011921776
MAPK3	2,849759018	3,166575029	0,02984681	0,009115186	0,010178811	0,010552813	0,010552813
MAPK7	0,801969157	4,266808397	0,021845844	0,00585645	0,004920088	0,011069305	0,011069305
MBNL2	7,167607765	17,80839704	0,029553423	0,001730771	0,01923841	0,008584242	0,01923841
MBNL3	8,215643286	4,459002991	0,029036237	0,001570699	0,019249557	0,008215981	0,019249557
MBP	0,001	62,57889193	0,035998113	0,025597471	0,005371406	0,005029237	0,025597471
MECP2	1,253996463	3,867230228	0,044530712	0,032737361	0,006551348	0,005242004	0,032737361
MED12	3,904928007	12,22696921	0,022571838	0,005911142	0,013384626	0,003276069	0,013384626
MEF2A	3,250976505	9,03906792	0,045554403	0,007263368	0,00696501	0,031326027	0,031326027
MEF2D	2,957955635	20,81839889	0,055798467	0,009617308	0,00784199	0,03833917	0,03833917
MEIS1	3,484331406	60,29355779	0,040830385	0,004958775	0,027391298	0,008480311	0,027391298
MEOX1	0,001	4,792653921	0,029061187	0,003440336	0,011172006	0,014448846	0,014448846
MET	3,796023275	1,621460949	0,023005784	0,00549722	0,007062747	0,010445817	0,010445817
MLC1	0,001	4,947088759	0,024634434	0,010776517	0,003241122	0,010616795	0,010776517
MMP2	3,024165567	53,50840358	0,022435257	0,006559132	0,005759762	0,010116363	0,010116363
MNAT1	1,457300888	3,614034042	0,020102356	0,012402695	0,004082029	0,00361763	0,012402695

Supplementary Table 4 Continued

Feature.ID	Expression. values.ZF	Expression. values.ZFE	Sum	Brain	Eye	Heart	Max
MNX1	0,001	1,194358827	0,027422892	0,004681666	0,012693227	0,010048	0,012693227
MOBKL3	17,01411059	53,21555707	0,02340967	0,001778817	0,011220734	0,010410119	0,011220734
MOCS3	1,250627725	2,633857247	0,027472891	0,002833089	0,02193768	0,00270212	0,02193768
MOGAT2	1,419869861	20,13636617	0,031827275	0,003459433	0,025136205	0,003231636	0,025136205
MSI1	0,036656473	26,57337253	0,040877145	0,012406702	0,020264287	0,008206157	0,020264287
MYCN	0,064764253	28,30876927	0,023800751	0,005765296	0,006344897	0,011690558	0,011690558
MYEF2	10,25744045	52,67398706	0,055019524	0,008953787	0,008966454	0,037099285	0,037099285
MYF5	0,10955695	2,72658096	0,037655018	0,007367682	0,012012752	0,018274585	0,018274585
MYF6	0,001	2,801001021	0,027188977	0,004969757	0,008987451	0,013231769	0,013231769
MYH6	0,001	1,211217357	0,054092713	0,006164146	0,006078841	0,041849726	0,041849726
MYL2	0,043362958	1,93486003	0,052577663	0,004240988	0,00454675	0,043789927	0,043789927
MYL7	0,001	23,23823196	0,062604882	0,003154815	0,005332639	0,054117424	0,054117424
MYOD1	0,001	7,565919954	0,026549457	0,005073984	0,00797536	0,013500112	0,013500112
MYOG	0,001	10,16171058	0,035915717	0,007607698	0,010494675	0,017813344	0,017813344
NCAM1	0,42564454	30,4676532	0,025020501	0,007932664	0,005815191	0,011272647	0,011272647
NCAPG	0,442910486	7,439837955	0,015957067	0,001904431	0,003632796	0,01041984	0,01041984
NCOA6	3,578061935	12,07585777	0,027954236	0,003406503	0,012169469	0,012378263	0,012378263
NDRG4	0,151694655	69,66701908	0,032772548	0,010784803	0,004493768	0,017493977	0,017493977
NDUFS3	36,72588929	81,96022945	0,015418398	0,001458236	0,002050252	0,01190991	0,01190991
NEFL	0,452379996	17,07970738	0,024356782	0,014868271	0,00538225	0,004106261	0,014868271
NEGR1	1,378089596	28,1468591	0,018849356	0,011215153	0,005372308	0,002261896	0,011215153
NES	0,1223334	2,862736052	0,056818299	0,024117543	0,016765688	0,015935069	0,024117543
NEUROD2	0,001	4,86428368	0,032629546	0,019908753	0,007159667	0,005561124	0,019908753
NEUROD4	0,001	24,0383338	0,034431938	0,009919189	0,01674384	0,00776891	0,01674384
NEUROG1	0,001	4,690995108	0,048326306	0,01491267	0,021272069	0,012141568	0,021272069
NFATC1	0,078189992	2,702508522	0,032435082	0,005097486	0,007911894	0,019425702	0,019425702
NGFR	0,001	3,049183357	0,027806574	0,01463879	0,006328964	0,006838821	0,01463879
NKD1	0,001	8,81418349	0,02512805	0,004291694	0,010467272	0,010369084	0,010467272
NOS1	0,492681508	4,025648746	0,023464534	0,012719828	0,005239613	0,005505093	0,012719828
NOTCH2	3,837263455	9,710167419	0,048108365	0,010510799	0,021589355	0,016008212	0,021589355
NOTCH3	3,249245705	13,43488182	0,029576397	0,007958272	0,013472552	0,008145572	0,013472552
NPAS4	0,001	11,95693855	0,013785467	0,010133391	0,001671966	0,001980111	0,010133391
NPC2	81,17849944	41,06881673	0,022236453	0,006455311	0,010388397	0,005392745	0,010388397
NPY	0,001	7,958421715	0,025144322	0,013920032	0,005814601	0,00540969	0,013920032
NR2E1	0,11474164	3,570693686	0,037826721	0,016031435	0,016055693	0,005739594	0,016055693
NR2E3	0,001	4,345278425	0,026827853	0,005458677	0,016934511	0,004434664	0,016934511
NR2F2	18,55433771	44,00904835	0,045781989	0,00479003	0,022618656	0,018373304	0,022618656
NR4A3	0,238701645	6,391050771	0,027671095	0,006023973	0,017806312	0,00384081	0,017806312
NR5A2	14,93647739	3,599706097	0,032770127	0,006807629	0,01011076	0,01585174	0,01585174
NRG1	0,117149781	3,944520793	0,034913935	0,014551393	0,007147504	0,013215038	0,014551393
NRL	0,001	0,856143472	0,040873673	0,004896084	0,030012292	0,005965297	0,030012292
NTF3	0,001	2,355433772	0,046850536	0,023985725	0,009189357	0,013675452	0,023985725
NTRK1	0,037434555	1,082099313	0,025776831	0,012622953	0,006113362	0,007040516	0,012622953
NUMB	1,856799246	2,936364249	0,024463698	0,006972192	0,011675021	0,005816485	0,011675021
NUP155	5,290005652	10,65871139	0,019336769	0,002457127	0,013584566	0,003295077	0,013584566
NXNL1	0,001	4,344629007	0,012692794	0,000786	0,010411536	0,00149526	0,010411536
OCA2	0,001	2,004478991	0,019317685	0,002907387	0,013630069	0,002780228	0,013630069

Supplementary Table 4 Continued

Feature.ID	Expression. values.ZF	Expression. values.ZFE	Sum	Brain	Eye	Heart	Max
OLFM3	0,001	5,638382535	0,044368021	0,004928045	0,036399123	0,003040856	0,036399123
OLIG1	0,001	2,600853564	0,032094527	0,012320993	0,012265993	0,007507541	0,012320993
OLIG2	0,557215154	6,401674055	0,047951449	0,017439818	0,019830989	0,010680641	0,019830989
OPN3	0,001	3,914704221	0,023138495	0,001908903	0,019747189	0,001482404	0,019747189
OPTC	0,001	0,001	0,021771511	0,001355217	0,016346772	0,004069523	0,016346772
OPTN	7,478053422	8,676961721	0,024622945	0,003207808	0,018814484	0,002600653	0,018814484
ORAOV1	1,053110171	2,882716357	0,019127788	0,002292237	0,01343102	0,003404531	0,01343102
OSR1	0,266146292	3,733027177	0,022635961	0,002766791	0,006940863	0,012928307	0,012928307
OTX2	0,001	23,93195857	0,094262525	0,02878294	0,046866905	0,01861268	0,046866905
PAFAH1B3	9,116063963	22,16129442	0,02403738	0,021491927	0,001461668	0,001083786	0,021491927
PAH	507,7014651	42,56210369	0,01963564	0,011194037	0,004717222	0,003724381	0,011194037
PAX5	0,001	0,733615452	0,030613441	0,00688433	0,015810675	0,007918437	0,015810675
PAX8	0,001	3,292288362	0,038313802	0,010195236	0,015563558	0,012555008	0,015563558
PAX9	0,001	6,126981808	0,034347594	0,004990829	0,016932707	0,01242406	0,016932707
PAXIP1	1,782323531	8,179981453	0,016621273	0,002400834	0,010279773	0,003940665	0,010279773
PBRM1	1,230900385	8,884419937	0,016762489	0,001859647	0,002339449	0,012563395	0,012563395
PCDH21	0,182236597	8,113540291	0,029890001	0,001902653	0,006696494	0,021290853	0,021290853
PDLIM1	9,965596329	20,70394949	0,021480916	0,001911543	0,003013647	0,016555725	0,016555725
PDLIM2	26,68166231	16,99931986	0,028293736	0,001371684	0,004512483	0,02240957	0,02240957
PDX1	0,139635456	6,250570635	0,043724023	0,008593513	0,021540211	0,013590298	0,021540211
PENK	7,944316847	9,257787946	0,02355504	0,013393764	0,005311193	0,004850085	0,013393764
PHOX2B	0,001	10,92146759	0,025862986	0,006533439	0,008354096	0,010975452	0,010975452
PITX1	0,001	10,2876001	0,03411565	0,004622824	0,015136412	0,014356415	0,015136412
PITX2	0,001	9,860184943	0,07998991	0,007150433	0,039893058	0,032946416	0,039893058
PITX3	0,001	6,356020296	0,055921994	0,008077445	0,038269354	0,009575194	0,038269354
PLK2	3,43145351	11,74596059	0,017624861	0,003097519	0,011021727	0,003505614	0,011021727
PLK4	0,233810071	2,843917862	0,015597959	0,001931649	0,003265386	0,010400924	0,010400924
PLS3	40,68621325	35,06912035	0,018136524	0,002171563	0,002478261	0,013486701	0,013486701
POFUT1	5,693431882	6,347539421	0,026915599	0,003329966	0,011353225	0,012232407	0,012232407
POLA1	0,730106156	5,975395653	0,015918037	0,002500403	0,011458636	0,001958998	0,011458636
POSTN	1,856635792	214,1122089	0,031442791	0,003515699	0,005390816	0,022536277	0,022536277
POU1F1	0,001	0,150832831	0,02751256	0,005243496	0,0136757	0,008593363	0,0136757
POU3F1	0,001	24,80016068	0,024512034	0,011681798	0,006467603	0,006362633	0,011681798
POU3F2	0,001	23,30705718	0,027748229	0,007762995	0,011550419	0,008434814	0,011550419
POU4F2	0,001	15,91107889	0,027431095	0,005184559	0,015089367	0,00715717	0,015089367
POU5F1	0,001	0,111208138	0,059299685	0,012491451	0,015791289	0,031016944	0,031016944
PRDX5	37,48983175	93,13832513	0,024428666	0,016889743	0,004256174	0,003282748	0,016889743
PRICKLE2	0,914281671	7,02797009	0,028202863	0,008849234	0,008360162	0,010993468	0,010993468
PROX1	32,75766565	13,91109147	0,069144674	0,011860002	0,046077012	0,011207656	0,046077012
PSEN1	5,430928045	17,80768748	0,033355143	0,016851356	0,009233229	0,007270559	0,016851356
PSEN2	8,020869628	13,51203063	0,024744043	0,011876749	0,007399545	0,00546775	0,011876749
PTF1A	0,065271165	1,17458602	0,028809046	0,006380484	0,010549088	0,011879474	0,011879474
PTN	0,001	35,5017142	0,024999058	0,013048065	0,005045979	0,006905014	0,013048065
PTPN11	0,061475624	0,346087425	0,026504502	0,005995029	0,010757795	0,009751677	0,010757795
PUM1	12,75417588	39,544775	0,021061277	0,002710784	0,015820677	0,002529816	0,015820677
PURA	0,001	0,001	0,020694524	0,011592613	0,003620117	0,005481794	0,011592613
QRSL1	1,089904194	2,983494717	0,030455885	0,002176684	0,003682479	0,024596723	0,024596723

Supplementary Table 4 Continued

Feature.ID	Expression. values.ZF	Expression. values.ZFE	Sum	Brain	Eye	Heart	Max
RAB23	3,08124102	7,435013515	0,020173553	0,004147874	0,010645035	0,005380646	0,010645035
RBL1	1,028628259	4,080218423	0,024263646	0,005821131	0,010656111	0,007786404	0,010656111
RBM15	3,329692971	17,3997476	0,030828165	0,001661747	0,021236146	0,007930271	0,021236146
RCAN1	0,043503621	13,72848991	0,023239369	0,006044106	0,003098494	0,014096768	0,014096768
RCBTB1	1,062292223	5,515120587	0,026976412	0,004580154	0,00612142	0,016274839	0,016274839
RCN1	4,10902954	10,38872864	0,034977473	0,003663671	0,022615608	0,008698193	0,022615608
RELN	2,238880025	8,541471341	0,077823713	0,058193578	0,012041848	0,007588284	0,058193578
REST	4,139456395	4,137689017	0,03722759	0,008999273	0,018070311	0,010158006	0,018070311
RFX4	0,001	6,102626111	0,032660566	0,024928018	0,004694026	0,003038522	0,024928018
RGL2	2,359018848	2,999628095	0,015781119	0,001051815	0,0133751	0,001354204	0,0133751
RGMA	0,15932258	33,18677561	0,019796047	0,002367097	0,01256149	0,004867459	0,01256149
RGR	1,428584433	25,82418704	0,02499561	0,002294843	0,020307384	0,002393382	0,020307384
RHO	0,001	1047,52691	0,0262239	0,003989129	0,01889785	0,003336922	0,01889785
ROS1	0,694632567	2,411795481	0,031588215	0,003161279	0,023890754	0,004536182	0,023890754
RPL15	1412,099778	1342,087686	0,015105269	0,001421602	0,002895624	0,010788042	0,010788042
RRBP1	96,93814099	22,43625128	0,021628475	0,001230671	0,002968061	0,017429743	0,017429743
RRH	0,001	1,773128579	0,022913512	0,001262244	0,02002279	0,001628478	0,02002279
RS1	0,001	94,43785667	0,020335892	0,002999156	0,015278143	0,002058594	0,015278143
RTN4R	0,091304577	4,690212659	0,02097645	0,012425605	0,004693355	0,003857491	0,012425605
RUNX1	0,318536093	0,589877869	0,028094005	0,005240671	0,011965125	0,010888208	0,011965125
S100A1	0,001	1,271321824	0,02675426	0,009474046	0,003621861	0,013658353	0,013658353
S1PR1	1,633738998	37,37989561	0,027875559	0,006830073	0,004624784	0,016420702	0,016420702
S1PR2	1,038016607	6,251304975	0,022910045	0,005923903	0,002987187	0,013998956	0,013998956
SALL4	0,230608498	1,756664512	0,038861264	0,003949093	0,011175396	0,023736773	0,023736773
SATB2	0,276942668	4,199908065	0,031406388	0,007364576	0,018396017	0,005645794	0,018396017
SCRIB	10,22669764	16,59987184	0,020245533	0,003270928	0,006500852	0,010473754	0,010473754
SCUBE2	3,178426123	5,40696092	0,018664571	0,001745898	0,013360276	0,003558396	0,013360276
SEMA3C	0,467232552	3,86748743	0,033777244	0,006431435	0,013780337	0,013565473	0,013780337
SEMA3D	0,001	10,19122866	0,017649869	0,003135654	0,003600154	0,010914061	0,010914061
SEMA5A	0,153187667	12,77637655	0,037018549	0,009020081	0,016762271	0,011236198	0,016762271
SEMA6D	1,004676231	5,728200858	0,023202876	0,004513826	0,004171366	0,014517684	0,014517684
Sep-02	8,727769305	38,8715866	0,015958214	0,002463649	0,00182506	0,011669506	0,011669506
Sep-06	21,46827776	47,80612654	0,017653491	0,003518623	0,002076802	0,012058067	0,012058067
SF1	19,05672221	49,25518657	0,026885195	0,005911376	0,00809032	0,012883499	0,012883499
SFRP2	0,001	24,90187974	0,037814047	0,005078703	0,018820071	0,013915272	0,018820071
SFRP5	1,128184834	7,231419816	0,029741278	0,003656108	0,01105785	0,015027319	0,015027319
SFRS2	34,60406492	80,86499094	0,025862589	0,004167447	0,003757627	0,017937515	0,017937515
SFRS2IP	6,316398757	14,25617269	0,024176199	0,003310998	0,005537722	0,015327479	0,015327479
SHOX2	0,001	4,33424422	0,037456013	0,004567843	0,008233335	0,024654836	0,024654836
SIAH1	2,527028041	12,62700467	0,024883492	0,005402516	0,016134753	0,003346223	0,016134753
SIM2	0,001	0,282452037	0,022629229	0,01082384	0,006520514	0,005284875	0,01082384
SIP1	4,713807975	17,90121079	0,030403502	0,005208097	0,007333815	0,017861591	0,017861591
SLC1A2	0,172055774	241,5271847	0,025853058	0,016337583	0,005574121	0,003941353	0,016337583
SLC1A6	0,001	10,46189849	0,019518673	0,010772222	0,006076378	0,002670072	0,010772222
SLC26A5	14,98929245	11,22948514	0,019210577	0,003995389	0,011650956	0,003564232	0,011650956
SLC2A3	0,001	36,30970074	0,022996781	0,011153606	0,004986665	0,006856509	0,011153606
SLC32A1	0,001	50,17296399	0,020012105	0,010066601	0,006719578	0,003225925	0,010066601

Supplementary Table 4 Continued

Feature.ID	Expression. values.ZF	Expression. values.ZFE	Sum	Brain	Eye	Heart	Max
SLC45A2	0,001	10,39871153	0,015211837	0,001385514	0,011841472	0,001984851	0,011841472
SLC8A3	0,001	2,133080683	0,023240611	0,005564627	0,002275715	0,015400268	0,015400268
SMAD1	3,194402753	11,49029548	0,04817846	0,005973095	0,019450217	0,022755147	0,022755147
SMAD2	3,781409926	12,28375512	0,031090442	0,006140311	0,009954046	0,014996086	0,014996086
SMAD5	6,383774208	11,06490054	0,040730748	0,004291857	0,017468861	0,018970029	0,018970029
SMAD7	5,847674514	10,21192594	0,02298218	0,00433423	0,00781447	0,01083348	0,01083348
SMAD9	2,330748508	4,565295856	0,032157689	0,004119986	0,013319974	0,014717731	0,014717731
SMARCA2	7,768984464	8,388147115	0,021933643	0,004976143	0,010066156	0,006891344	0,010066156
SMARCA5	2,897241825	28,1819187	0,02704465	0,005594725	0,016771124	0,004678802	0,016771124
SMARCC1	3,885395849	19,43207653	0,023223152	0,013116916	0,004503919	0,005602318	0,013116916
SMO	0,347805332	5,998736907	0,05328599	0,009916445	0,02856085	0,014808696	0,02856085
SNAI2	0,411716805	10,89893469	0,029230297	0,005917116	0,009823906	0,013489275	0,013489275
SORBS3	1,24368577	6,054329134	0,017407494	0,001472511	0,004362819	0,011572164	0,011572164
SOSTDC1	0,001	0,001	0,021549366	0,002809158	0,010143472	0,008596735	0,010143472
SOX2	0,037960559	40,24171434	0,076029941	0,011762438	0,039673298	0,024594208	0,039673298
SOX3	0,001	22,65939335	0,042719733	0,008054777	0,025788568	0,008876388	0,025788568
SOX5	6,032395148	17,42892397	0,024781005	0,004260216	0,01148247	0,009038319	0,01148247
SOX6	2,115175793	8,634271029	0,025990961	0,004851758	0,011345433	0,009793769	0,011345433
SOX7	0,173670959	7,055741389	0,036506724	0,002653695	0,006656682	0,027196346	0,027196346
SP1	4,863155092	6,988514653	0,038106542	0,011464289	0,01347939	0,013162864	0,01347939
SP3	1,339982609	2,965527186	0,029970556	0,009022091	0,009109033	0,011839432	0,011839432
SP4	1,508305026	10,00945883	0,025235513	0,006926743	0,004983618	0,013325153	0,013325153
SP7	1,088875956	1,366685927	0,025147876	0,004185982	0,009655778	0,011306116	0,011306116
SPARC	7,497442469	529,6407661	0,024571795	0,004231037	0,010364107	0,009976652	0,010364107
SPI1	2,394115247	2,134695372	0,025301853	0,005968076	0,009236389	0,010097389	0,010097389
SPRY1	0,593166866	6,556330739	0,025441699	0,004695326	0,008829241	0,011917131	0,011917131
SRF	2,058957854	3,945499817	0,057598684	0,005425971	0,008297033	0,043875681	0,043875681
SSR1	134,6232472	77,65727204	0,016846482	0,000935	0,001791314	0,014120314	0,014120314
ST8SIA2	0,001	0,605758643	0,037097566	0,025876889	0,006068415	0,005152261	0,025876889
ST8SIA3	0,085819484	1,114197534	0,016377861	0,01209308	0,002250302	0,002034479	0,01209308
ST8SIA4	0,394133768	2,733758396	0,031684294	0,022918701	0,004507717	0,004257877	0,022918701
STAR	0,001	4,56693969	0,020861112	0,005615819	0,004884723	0,010360571	0,010360571
STAT3	3,445328055	4,748615111	0,032978207	0,007975871	0,01195048	0,013051857	0,013051857
STAU2	30,77129316	108,643707	0,023395022	0,003652158	0,017166938	0,002575926	0,017166938
STRA6	0,054317628	11,37966192	0,031129818	0,003968036	0,019962034	0,007199748	0,019962034
STRN3	13,76889506	22,86182805	0,023178918	0,004553798	0,012979166	0,005645956	0,012979166
SUFU	5,143628754	10,04846901	0,029701259	0,004836745	0,017335427	0,007529085	0,017335427
SUMO3	10,43117861	37,87540994	0,017804723	0,002296445	0,00382483	0,011683448	0,011683448
TAL1	0,93478775	11,02413075	0,031043317	0,006428419	0,009792597	0,014822301	0,014822301
TAZ	13,53667548	15,19936429	0,0216686	0,00262303	0,013797378	0,005248191	0,013797378
TBP	3,599107253	10,64701691	0,027931949	0,005232677	0,012660854	0,010038417	0,012660854
TBX1	0,001	6,881548583	0,051753845	0,00899995	0,012006022	0,030747875	0,030747875
TBX15	0,051880452	7,665850066	0,028938714	0,002727619	0,008082073	0,018129022	0,018129022
TBX18	0,034162367	2,23393616	0,051387899	0,003048582	0,012655642	0,035683673	0,035683673
TBX20	0,001	1,74161118	0,085233591	0,003792624	0,013351319	0,068089651	0,068089651
TBX4	0,001	1,140360811	0,052892078	0,003972127	0,014202544	0,034717405	0,034717405
TBX5	0,001	0,687391589	0,11584647	0,005487368	0,027726691	0,08263241	0,08263241

Supplementary Table 4 Continued

Feature.ID	Expression. values.ZF	Expression. values.ZFE	Sum	Brain	Eye	Heart	Max
TBX6	0,001	0,58596379	0,040322423	0,005429581	0,013598496	0,021294348	0,021294348
TCF21	1,084782349	0,495744342	0,0236059	0,003050771	0,008428642	0,012126487	0,012126487
TEF	14,44398893	129,9691718	0,025440948	0,006714763	0,005854281	0,012871905	0,012871905
TFAP2A	0,001	39,6120371	0,033082996	0,005058646	0,017382235	0,010642115	0,017382235
TFDP2	0,588786039	10,78982381	0,026963552	0,005000449	0,014982353	0,006980751	0,014982353
TFEC	0,54340143	1,053321681	0,01697777	0,0012284	0,013340035	0,002409335	0,013340035
TGFB3	2,913512847	23,69910341	0,022951346	0,005148163	0,006766232	0,011036951	0,011036951
TGFBR2	4,30011566	12,85094577	0,022036517	0,004570047	0,006364066	0,011102405	0,011102405
TGIF1	1,623360955	15,82300163	0,045431446	0,011387736	0,027106441	0,00693727	0,027106441
THRB	6,744940035	10,09017565	0,02945058	0,014958903	0,006260844	0,008230833	0,014958903
TLL1	0,183353651	1,268579925	0,033280242	0,004300124	0,007508491	0,021471625	0,021471625
TLX1	0,035549727	0,35586723	0,035822429	0,004822973	0,014557193	0,016442262	0,016442262
TNC	0,177467401	25,53137032	0,028940432	0,00973233	0,006459798	0,012748304	0,012748304
TNNC1	0,001	5,181196031	0,032461237	0,003756149	0,003321753	0,025383335	0,025383335
TNR	0,60820812	7,446018094	0,021560866	0,010834058	0,004445893	0,006280916	0,010834058
TRH	0,044392114	8,271010384	0,021743553	0,011614918	0,005103466	0,005025167	0,011614918
TRIM71	1,462774004	7,091027754	0,02620095	0,004451265	0,016670834	0,005078851	0,016670834
TSC2	5,298525091	12,20748343	0,022531915	0,013361098	0,005085997	0,00408482	0,013361098
TSC22D1	3,025131377	101,2552853	0,023430377	0,00947229	0,010750663	0,003207423	0,010750663
TSHZ1	1,425642173	13,80279004	0,017668152	0,0030529	0,01043788	0,004177372	0,01043788
TYR	0,001	9,869129137	0,027361494	0,005284308	0,016928488	0,005148698	0,016928488
UBE3A	5,14766264	13,12516435	0,021492414	0,012029309	0,004860605	0,004602499	0,012029309
UBE3C	2,489172886	7,371468954	0,022779178	0,002301598	0,00382996	0,01664762	0,01664762
UNCX	0,084755772	6,070700188	0,019503018	0,003104448	0,005904962	0,010493608	0,010493608
UTP6	3,903721448	11,84939882	0,022339279	0,001997804	0,00130654	0,019034935	0,019034935
VANGL1	0,92226061	12,72827737	0,028685778	0,007055359	0,010003632	0,011626787	0,011626787
VAX1	0,001	5,181228213	0,079889186	0,007381369	0,059493494	0,013014324	0,059493494
VAX2	0,001	1,139340336	0,090695895	0,004744419	0,068345736	0,017605737	0,068345736
VIM	0,21470073	64,53292452	0,032025564	0,011715782	0,009033917	0,011275866	0,011715782
VLDLR	4,505635922	22,57418871	0,034854352	0,027235883	0,00381426	0,003804211	0,027235883
VPS35	10,75184581	33,54539121	0,021668181	0,001944739	0,016459442	0,003264	0,016459442
VRK1	0,253644877	2,480634771	0,016240073	0,001905882	0,003362578	0,010971613	0,010971613
VSX1	0,099340643	30,97668351	0,02356755	0,003490475	0,016217204	0,00385987	0,016217204
VSX2	0,001	7,527211602	0,076123282	0,008164224	0,058703932	0,009255126	0,058703932
WDR5	4,044860306	22,84207463	0,035008095	0,003371911	0,013529398	0,018106788	0,018106788
WIF1	1,523094039	14,13239473	0,027539851	0,004881425	0,012150585	0,010507841	0,012150585
WNT1	0,139012655	2,127333835	0,061392847	0,014224196	0,02676771	0,02040094	0,02676771
WNT10A	0,001	0,546100783	0,040485099	0,005235283	0,017352946	0,01789687	0,01789687
WNT10B	0,155328284	0,705505338	0,035224374	0,005550469	0,015795552	0,013878355	0,015795552
WNT11	0,001	0,576577337	0,070253387	0,00585135	0,021113247	0,04328879	0,04328879
WNT16	0,001	2,964726318	0,039581712	0,004942751	0,019186898	0,015452062	0,019186898
WNT3	0,001	1,002739496	0,049606014	0,007756128	0,019855111	0,021994776	0,021994776
WNT5A	0,001	0,664529189	0,053680688	0,007518694	0,024657597	0,021504396	0,024657597
WNT5B	1,420832097	6,685050361	0,053338371	0,006776334	0,025162138	0,021399901	0,025162138
WNT7A	0,001	8,515785713	0,045386795	0,007780789	0,019393143	0,018212861	0,019393143
WNT8A	0,046716692	0,105347864	0,04474207	0,005800274	0,01690616	0,022035637	0,022035637
WNT8B	0,001	1,278948113	0,045234382	0,007471677	0,021581803	0,016180902	0,021581803

Supplementary Table 4 Continued

Feature.ID	Expression. values.ZF	Expression. values.ZFE	Sum	Brain	Eye	Heart	Max
WNT9B	0,001	1,751351269	0,041080143	0,005060593	0,019500227	0,016519322	0,019500227
WRB	0,160509953	0,820179494	0,02851413	0,00117694	0,003353637	0,023983553	0,023983553
WWTR1	4,989699404	6,757915227	0,019648496	0,0022222	0,005325384	0,012100912	0,012100912
XRCC5	2,220057407	5,065974978	0,024417987	0,005441897	0,008787648	0,010188441	0,010188441
ZEB1	1,914216382	7,031041044	0,0293293	0,004879171	0,008001665	0,016448463	0,016448463
ZFPM1	2,914772039	2,836054324	0,045669008	0,003030051	0,011592472	0,031046486	0,031046486
ZIC1	0,001	31,34187397	0,029825179	0,011749265	0,009523488	0,008552426	0,011749265
ZIC3	0,001	20,73239204	0,028039221	0,006010002	0,007350128	0,01467909	0,01467909

Supplementary Table 5

GeneSymbool obtained from DeepSequence	EntrezGeneID of Affymetrix	Position in Deep sequence
rpl23	336812	45
rpl14	323365	109
itln3	555334	452
cox7a2	554103	846
zgc:63667	553543	1551
mhc1ze	378479	1721
zgc:103738	541319	2502
cyp46a1	553543	2797
LOC559001	335859	3581
LOC563036	378479	3914
fuca1	335494	4003
zgc:158252	790940	4017
LOC100150150	378479	4049
phka1	572183	4767
gtpbp1	378721	4990
ruvbl1	317679	5939
fasn	335859	6007
trnt1	415249	6554
sgsm3	406635	7150
zgc:100963	445222	7551
LOC571647	378479	7553
neu3.3	445250	7624
zgc:175195	334455	7863
glmna	492774	8113
numb	692064	9048
rrm2	30733	9846
zgc:158270	791213	9956
f13a1	561287	10055
asb13	436801	10420
loxl1	560115	10801
neu3.5	445250	11981
dck	474325	12103
cldnd	81583	12653
lrrn1	568527	13047
neu3.1	780844	14174
tmem41ab	406356	14550
zgc:86764	797431	14795
neu3.2	445250	15894
LOC100149324	100149324	16212
lgals2a	326706	53541

Supplementary Table 6

TranscriptID	ZFE_GeneID	Mouse_GeneID	ZFE_CsA_C1	ZFE_CsA_C2	ZFE_CsA_C3	ZFE_CsA_C4	ZFE_CsA_C5	aZFL	CsA_01_C_1	CsA_02_C_1	CsA_03_C_1	CsA_04_C_1	CsA_05_C_1	CsA_06_L_1	CsA_07_L_1	CsA_08_L_1	CsA_09_L_1	CsA_11_M_1	CsA_12_M_1
13003871	30144	22423	-0,202392	-0,493617	-0,273244	-0,441142	-0,549005	-0,2591235	0,05785765	-0,070105384	-0,02482802	-0,058569144	0,0956449	-0,11211123	-0,204823182	0,226364881	-0,243634359	-0,161159569	-0,124452085
13110453	81583	54419	0,487805	0,404225	0,333043	0,481648	0,5112	0,5093255	0,097709111	0,08557761	-0,257492765	-0,02452872	0,098734765	-0,072154986	-0,084545279	0,014350783	0,164960844	-0,176130954	0,185512104
13305252	335494	71665	0,442363	0,752296	0,490159	0,698706	0,629938	-0,5890005	-0,04894975	-0,135289724	0,096880546	0,028683856	0,058675074	0,137923491	0,0331383	-0,006888815	0,10290374	0,09102672	0,058386681
13283206	378479	14964	-0,885064	-2,230631	-1,254029	-0,868238	-2,064966	1,621455	0,049809716	-0,067085749	0,047055869	-0,077510196	0,047730364	-0,007823771	-0,076723975	-0,080796104	-0,041924024	-0,093989402	-0,03999117
13284362	378479	14964	-0,885064	-2,230631	-1,254029	-0,868238	-2,064966	1,621455	0,049809716	-0,067085749	0,047055869	-0,077510196	0,047730364	-0,007823771	-0,076723975	-0,080796104	-0,041924024	-0,093989402	-0,03999117
13131516	393530	53311	0,277255	0,90484	0,318033	0,60422	0,46505	0,1722305	0,133226438	-0,110572775	-0,065327684	-0,015469041	0,05814306	0,36726267	0,150882345	0,071098812	-0,010114565	-0,205090277	-0,321149351
13113617	474325	13178	-0,769185	-0,647585	-0,584364	-0,427937	-0,211119	-0,8417785	0,006415477	0,213422855	-0,18143595	-0,027181145	-0,011221234	-0,029985388	0,155250114	-0,006269627	0,095971617	-0,143079255	0,111932904
13079367	492774	170823	-0,545197	-0,554926	-0,560557	-0,322014	-0,227127	-0,1797875	-0,343282882	0,268232408	-0,070971749	0,060530668	0,085491555	-0,15581164	0,307495422	0,012041558	0,075822933	0,068981869	0,064959225
13152298	494036	68016	0,519397	0,630466	0,266743	0,47097	0,371837	0,042008	0,021765976	-0,104013536	0,155591137	-0,132758499	0,059414922	0,125169028	-0,067554712	0,107473727	0,063286819	0,063424844	-0,008199632
13283630	541319	12925	0,302382	0,227114	0,422399	0,675729	0,47825	-0,566397	0,158298699	-0,055555703	-0,131418506	0,057179309	-0,028503798	0,1334611	0,150253636	-0,01797534	0,053101131	0,220579812	0,278965952
12964078	550569	59310	0,5278415	0,5549205	0,3810315	0,5798515	0,4631605	0,2599035	-0,076866388	0,023078722	0,00464142	0,027506075	0,021640172	0,166621496	0,026009635	0,054300439	0,124728591	0,062610762	-0,08368925
13081404	553336	216152	-0,542924	-0,253451	-0,222699	-0,496319	-0,542862	0,218988	0,143722456	-0,159833206	0,178925696	-0,160208258	-0,002606686	0,074255895	-0,241782959	-0,053825948	-0,573462787	-0,201999448	-0,286741647
13094209	553543	13116	0,651351	0,475638	0,46391	0,277795	0,512897	-0,089556	-0,090739756	0,256577711	-0,076123095	0,07851136	-0,168226218	-0,093847028	-0,052872915	0,161554135	0,145364621	0,27893755	0,397020063
13054773	554103	12866	0,114273	0,555591	0,593705	0,565034	0,4568	0,2138275	0,093935222	0,061228918	-0,083962775	-0,014613019	-0,056588344	-0,01969527	0,03913283	-0,016484962	-0,005032954	-0,000608767	-0,055950227
13065823	560115	16949	0,3747515	0,5145025	0,2590325	0,7679475	0,6953505	0,612996	-0,10974215	0,000151601	0,104562581	0,040953897	-0,03592593	0,393897824	0,13269258	0,189655728	0,178145359	0,036719525	0,095163394
13234461	561287	74145	-0,716307	-0,486624	-0,716973	-0,390164	-0,462106	-0,0347705	0,088718511	0,054273573	0,06937364	-0,156973604	-0,055392123	0,025583168	0,213170478	-0,002428126	0,105550504	0,117710344	-0,113731088
12956364	564383	242022	0,637787	0,846888	0,966453	0,940433	1,008885	-0,2860905	-0,180045345	0,035064788	-0,033463053	-0,027508924	0,205952534	-0,013494376	0,041260754	0,103369928	0,167292988	-0,034436963	0,074865097
13034897	571184	211482	-0,4095035	-0,6042265	-0,5993245	-0,4424615	-0,5817115	0,416319	0,080248436	-0,11758983	0,139712736	-0,213206384	0,110835045	-0,092359177	-0,09099233	0,019104596	-0,152705464	-0,131350561	0,212793186
13278988	572183	18679	0,695956	0,791756	0,412596	1,072473	0,74914	0,5758485	-0,162442578	-0,365774945	-0,041421461	0,130750238	0,438888743	-0,129190989	-0,029980187	0,098469188	0,136730984	0,097130934	0,126341895
13200912	791610	14080	0,3503155	0,1684505	0,4078565	0,4850535	0,6159035	-0,24775	0,112201991	0,123962595	-0,056796215	-0,013352734	-0,166015639	0,123997812	-0,067713854	0,068349878	0,062001673	0,036622376	-0,05518621
13036819	100000322	64177	0,606221	1,709899	0,866182	0,897898	1,1636	0,0754655	0,00800186	-0,113134733	-0,088581121	0,206396816	-0,012682824	0,378908977	0,001649315	-0,019161991	0,015930079	-0,067503353	-0,159106499
13166102	100073335	104582	-0,728183	-0,30249	-0,556249	-0,390703	-0,676573	0,145974	0,199352026	-0,135980628	-0,036530967	-0,012591086	-0,014249347	0,000851151	-0,278886106	-0,287220766	0,024982295	-0,007552102	0,314738212
13153157	100124599	140781	0,472492	0,868807	0,551368	0,84333	0,705466	0,511235	-0,003978496	-0,090197946	0,047347165	-0,048554405	0,09538368	0,223690476	0,309768815	0,05984867	0,028800351	0,039573917	-0,027257332
12992494	335859	14104	-0,362356	-0,386481	-0,245179	-0,432966	-0,797939	-0,762153	-0,155701714	0,632349574	-0,187089602	-0,331663222	0,042104964	0,41527505	0,002420435	0,427500973	-0,136222067	0,434612428	0,359951077
13176029	378721	14904	-1,735606	-1,550183	-0,983129	-1,081322	-1,488407	-0,207051	0,28558547	-0,154642735	-0,103740343	0,050854572	-0,078056962	-0,069946453	-0,179598063	-0,225703554	-0,085705375	-0,112211797	-0,097590947
13223058	568527	16979	0,3188675	0,3381485	0,5973935	0,6809075	0,2986065	0,451721	-0,107922143	-0,206606119	0,042578086	0,072956347	0,198993827	0,251892772	0,032754733	-0,041763045	-0,010725167	0,146046759	-0,045752585
13048660	692064	18222	-0,4332075	-0,4268095	-0,5583265	-0,6322795	-0,9201365	0,188312	-0,070668404	0,01639467	-0,137190833	0,151170106	0,040294462	0,001622771	0,137008951	-0,030055983	0,057825435	0,215391278	0,081224135
13109885	445250	50877	0,248273	0,802071	0,406888	0,76368	0,56946	-0,161587	0,015963268	0,171750559	-0,149673178	0,017744907	-0,055785553	-0,193409926	-0,183691322	0,072051957	0,001443024	0,043333052	-0,082686564
13109885	555206	50877	0,248273	0,802071	0,406888	0,76368	0,56946	-0,161587	0,015963268	0,171750559	-0,149673178	0,017744907	-0,055785553	-0,193409926	-0,183691322	0,072051957	0,001443024	0,043333052	-0,082686564
13109885	780844	50877	0,248273	0,802071	0,406888	0,76368	0,56946	-0,161587	0,015963268	0,171750559	-0,149673178	0,017744907	-0,055785553	-0,193409926	-0,183691322	0,072051957	0,001443024	0,043333052	-0,082686564
13109885	793046	50877	0,248273	0,802071	0,406888	0,76368	0,56946	-0,161587	0,015963268	0,171750559	-0,149673178	0,017744907	-0,055785553	-0,193409926	-0,183691322	0,072051957	0,001443024	0,043333052	-0,082686564
13109885	100000684	50877	0,248273	0,802071	0,406888	0,76368	0,56946	-0,161587	0,015963268	0,171750559	-0,149673178	0,017744907	-0,055785553	-0,193409926	-0,183691322	0,072051957	0,001443024	0,043333052	-0,082686564
13176029	336812	65019	-1,735606	-1,550183	-0,983129	-1,081322	-1,488407	-0,207051	0,185409436	0,004815352	-0,115888967	-0,014999102	-0,059336721	0,087282394	0,065256562	0,149181891	0,192255059	-0,021108689	-0,180489467
13071605	100329433	67469	0,249227	0,525937	0,471702	0,692404	0,333244	-0,1663795	0,464090666	-0,209510726	-0,113299373	-0,189302122	0,048021556	-0,063462165	-0,206707265	-0,292406594	-0,027325752	0,144966046	-0,031522546
13223058	415249	70047	0,3188675	0,3381485	0,5973935	0,6809075	0,2986065	0,451721	0,055943212	0,183071305	0,183309912	-0,184552983	-0,23777145	-0,036974576	0,132478092	-0,083765087	-0,006137339	0,045032576	0,007532754
13071605	791138	72415	0,249227	0,525937	0,471702	0,692404	0,333244	-0,1663795	-0,087878505	0,047875138	-0,000156118	0,015546277	0,024613207	0,925317376	-0,116905208	-0,243395965	-0,05272336	-0,041977181	-0,258775052
13176029	437026	73293	-1,735606	-1,550183	-0,983129	-1,081322	-1,488407	-0,207051	-0,070269865	-0,059057439	0,031780539	-0,076429815	0,173976577	-0,177198324	-0,162405798	-0,110859522	-0,037022612	0,030510034	0,005857277
13280104	553445	75732	0,468533	0,85854	0,530088	0,415316	0,493642	-0,023891	-0,037042149	-0,097650597	0,090938921	0,020957711	0,022796112	-0,008266259	-0,16841699	-0,131382576	-0,05701402	-0,086985819	0,097216356
13048660	334455	97827	-0,4332075	-0,4268095	-0,5583265	-0,6322795	-0,9201365	0,188312	-0,066951612	0,161990191	0,026308407	-0,036532137	-0,084814847	-0,193533585	-0,204369965	-0,406486719	-0,279886058	-0,004351111	-0,150364283
13176029	406635	105835	-1,735606	-1,550183	-0,983129	-1,081322	-1,488407	-0,207051	-0,122940173	0,125104756	-0,25706693	0,170941157	0,083961193	0,372616121	0,165512173	0,44876172	0,299608778	0,160841526	0,214886847
13223058	100333566	232288	0,3188675	0,3381485	0,5973935	0,6809075	0,2986065	0,451721	-0,438945095	0,365219773	-0,123193366	0,359205296	-0,162286608	0,433364362	-0,083558715	-0,262970333	0,018402715	0,773399373	0,699980364
13071605	323365	100040970	0,249227	0,525937	0,471702	0,692404	0,333244	-0,1663795											
13103533	30733		-1,1732018	-0,513069	-0,460112	-0,581411	-0,32109	-0,055904											
13149335	100124621		-0,832527	-0,758598	-0,487658	-0,686713	-0,400825	-0,2117805											
13108001	100136851		-0,286971	-0,410512	-0,484425	-0,503558	-0,455494	-0,1578735											
13168252	100137108		1,152169	1,109029	0,480781	0,421349	1,184601	-0,0900815											
13300520	100148409		0,462583	0,859696	0,918119	0,376967	0,625568	0,635497											
13024318	100149324		-0,7624145	-0,3170415	-0,6865215	-0,2739085	-0,6383935	-0,2770055											
13106669	100150294		-0,343677	-0,461186	-0,344101	-0,626498	-0,87161	-0,565908											
12988489	100538165		0,549699	0,828137	0,623532	0,503771	0,534346	0,0921685											
13287022	100004883		-0,356771	-0,433107	-0,511798	-0,391137	-0,504585	-0,5943025											
13271005	100005575		-0,4704265	-0,8449595	-0,7157095	-0,4854985	-0,9459795	0,318522											
13115203	797431		-0,78794	-0,700089	-0,433847	-0,248362	-0,690636	-0,400418											
13031162	798527		0,535675	0,57285	0,615937	0,714429	0,857358	0,25629											
13282574	326706		-0,5447785	-0,4771905	-0,6040745	-0,6536435	-0,2378195	-0,03969											
13284122	326706		-0,5447785	-0,4771905	-0,6040745	-0,6536435	-0,2378195	-0,03969											
13218627	790940		0,305683	0,476406	0,376756	0,400269	0,602545	0,435753											
12976741	791213		-0,128711	-0,641837	-0,340338	-0,425044	-0,498207	-0,6748915											
13043707	560526		-0,247932	-0,394274	-0,587718	-0,571003	-0,46077	-0,168377											
13008652	555334		-0,301029	-0,758465	-0,867434	-1,36513	-1,363258	0,8606725											
13049400	559427		0,526567	0,482467	0,324405	0,675258	0,324929	-0,053496											
13092976	550371		0,379921	0,597878	0,422762	0,394646	0,537735	0,1737675											
13181059	436801		0,568796	0,948333	0,461188	0,370841	0,244328	0,2117265											
13261534	445222		-0,26093	-0,616846	-0,509804	-0,678381	-0,789329	-0,460568											
13078348	336038		0,292775	0,627167	0,235366	0,498335	0,654735	-0,2044905											
12971056	393511		-1,681193	-2,156234	-1,996144	-2,488381	-2,022008	0,4283755											
13008742	403309	269295	-1,024995	-0,98147	-1,137205	-1,096485	-1,448919	-0,0996135											
12947809	406356		0,834604	1,208438	0,844445	0,952509	0,726933	0,621199											
13305278	415164	238880	0,599933	0,700872	0,549721	0,273886	0,465054	0,0395105											
13222673	317679	56505	-0,4126645	-0,4162045	-0,3595775	-0,7144065	-0,3729105	-0,8789725											

Supplementary Table 6 Continued

TranscriptID	CsA_13_M_1	CsA_14_M_1	CsA_15_M_1	CsA_16_H_1	CsA_17_H_1	CsA_18_H_1	CsA_19_H_1	CsA_20_H_1	CsA_21_C_4	CsA_22_C_4	CsA_23_C_4	CsA_24_C_4	CsA_25_C_4	CsA_26_L_4	CsA_27_L_4	CsA_28_L_4	CsA_29_L_4	CsA_30_L_4	CsA_31_M_4
13003871	-0,323863642	0,526362124	0,015000589	-0,104037329	-0,229771238	-0,102618564	-0,186216621	-0,067123135	-0,259025487	0,140559897	0,070359565	0,044977517	0,003128507	0,115907704	0,032494581	0,061528135	0,041198908	0,007969002	0,095547223
13110453	-0,107033825	-0,038495439	0,030327319	-0,209580832	0,088718592	-0,074896852	-0,216604483	0,184687038	-0,100953089	0,288516786	0,056769776	0,075451623	-0,319785099	-0,000888231	-0,07368912	-0,218607616	-0,147105088	-0,198139835	0,052732434
13305252	0,142626991	0,316669067	-0,118102007	0,070168854	0,047535366	0,103871182	-0,098331859	-0,021268456	0,187303047	-0,116552809	-0,046073306	-0,006183433	-0,018493497	0,040428339	-0,0291998	-0,107911865	-0,201851379	0,067263159	-0,060414336
13283206	0,077342187	-0,053470937	-0,046110266	-0,06244859	-0,025146649	0,083333108	-0,025709178	-0,022394159	-0,070567177	0,020879525	-0,072337078	0,108831473	0,013193257	0,075978556	0,126497524	0,223801539	0,075807937	0,069000229	0,060985954
13284362	0,077342187	-0,053470937	-0,046110266	-0,06244859	-0,025146649	0,083333108	-0,025709178	-0,022394159	-0,070567177	0,020879525	-0,072337078	0,108831473	0,013193257	0,075978556	0,126497524	0,223801539	0,075807937	0,069000229	0,060985954
13131516	-0,188862198	-0,030581978	0,072054858	-0,236273149	-0,252013248	0,416796937	0,11920216	-0,194530244	0,335861408	0,285072196	-0,206216252	-0,184880103	-0,229837247	0,387907119	-0,061928731	0,203194933	0,258721912	0,149652036	0,234266157
13113617	-0,014072525	-0,131290646	0,167184013	0,029472631	-0,102049995	0,278848273	-0,002872492	0,053422142	0,007713454	-0,117758816	0,156070539	0,134410673	-0,180435852	0,013501609	-0,065754487	0,138723727	-0,053151325	0,024495848	0,050912013
13079367	0,48556273	-0,437707368	-0,010434878	0,096267295	-0,038030543	0,128605865	0,125935761	-0,082382946	0,248140533	-0,18538293	0,106020065	-0,124985868	-0,043791798	0,288858676	-0,257966781	-0,205242964	0,168231691	0,106932473	0,17571276
13152298	0,032912023	0,093579952	0,143556992	-0,05793123	-0,202791042	0,052042938	0,185629957	-0,025129314	-0,010809036	0,067098197	-0,129203284	0,232118187	-0,159204067	0,016127413	-0,111656439	0,140697944	0,131715134	0,207511624	0,020982083
13283630	0,407651848	0,311319223	0,33315284	0,33075058	0,479525792	0,266617332	0,044925529	0,307683662	-0,215933356	-0,135166748	0,377043056	-0,096250929	0,07030798	-0,01231842	0,209888226	0,117513312	0,109493056	-0,122863179	-0,254033155
12964078	0,429086977	-0,019997421	-0,191601701	-0,114703071	0,038155647	0,208130638	-0,044616038	0,080469506	-0,004292579	-0,138304432	-0,006125399	0,124588369	0,02413404	-0,30145282	0,16070689	-0,079612904	0,138839589	-0,071257706	0,219754364
13081404	0,168343788	0,306183332	0,049819735	-0,167045622	-0,31580185	-0,056325369	-0,264233147	0,058805928	-0,098819506	0,052269182	-0,031699334	0,037922119	0,040327541	0,054742113	-0,163031361	-0,096882919	0,06258302	-0,008548284	0,269882005
13094209	-0,035751769	0,026440913	0,22235434	0,172269171	0,334812057	-0,019548459	0,281492855	0,128941099	0,114306604	-0,094934777	-0,059416867	0,023961165	0,016083874	-0,196252386	-0,266725722	-0,250764066	0,027628026	-0,16410067	-0,000634955
13054773	0,006974129	0,005554638	0,042656876	0,050818214	-0,025982668	0,042645128	-0,061330057	-0,012977652	0,013884526	0,00677338	0,006161768	-0,006105412	-0,02071426	0,00302414	0,007954276	-0,038975363	-0,051361038	-0,000299309	-0,021320968
13065823	0,02068783	-0,136939626	0,092705592	0,116122889	0,13347806	-0,34774562	0,193796274	-0,347340234	0,282059233	-0,080314455	0,141294212	-0,275992301	-0,067046691	-0,14083432	0,316834778	0,014892083	0,358151586	-0,129370713	-0,056692238
13234461	0,036286478	-0,033087419	0,410379013	0,075873265	0,121641215	-0,373507567	0,045142871	-0,230372969	0,095105367	0,221821632	-0,040505624	-0,227878102	-0,048543275	0,120546602	0,155811992	-0,14202392	0,211541025	-0,072262205	-0,109665237
12956364	0,145953588	-0,114851768	-0,123942338	0,046112465	0,050698908	-0,212324977	-0,08808741	0,165832643	-0,104894181	-0,092450201	0,126394313	0,047749303	0,023200767	0,058469066	0,132737914	0,098951563	-0,157892139	-0,049565894	0,029493864
13034897	-0,075025826	-0,033747792	-0,126948721	0,058584279	-0,099741985	-0,141041123	0,002162557	-0,051435486	0,04019181	0,109016162	-0,048411583	-0,033978534	-0,066817858	-0,037301577	0,067692654	0,103543648	0,013219591	-0,068261954	-0,00093799
13278988	-0,208446538	-0,650832615	0,175277998	0,194972277	0,162187768	0,02134612	0,307888121	0,037843188	0,193240349	0,161768072	0,065661252	-0,117906636	-0,302763039	-0,28033847	0,013901734	0,068995397	-0,955898237	-0,089874837	0,086100927
13200912	-0,026143469	0,034238816	0,141909835	0,131248939	0,03163983	-0,067160295	-0,012729693	-0,007690818	-0,058242668	0,124298088	-0,045640767	0,073283155	-0,093697809	0,148239215	0,069931172	-0,000967437	0,093032956	0,061759404	0,177064838
13036819	0,121593197	0,524798672	-0,3428237	0,038518086	-0,148783111	-0,058259204	-0,057520507	0,136080165	-0,073674998	-0,017920884	-0,013773932	0,281213104	-0,175843289	0,021662228	0,129200515	0,321695337	-0,027533776	-0,018880563	-0,027722196
13166102	-0,220899698	0,045147719	-0,05889427	-0,268949776	0,016680365	-0,374360839	-0,208603577	0,284812763	0,135825225	-0,06699446	-0,054835983	0,018837913	-0,032832694	-0,06664196	-0,202985203	0,210920937	-0,101645535	-0,26104947	0,056371934
13153157	0,240081483	-0,039358954	-0,136811042	0,09660335	0,20267645	0,287961464	0,762750957	-0,135564601	0,134845747	-0,055335799	0,125177904	-0,102725343	-0,10196251	-0,214907819	0,070580695	0,038796524	0,135288824	-0,178081316	0,109203403
12992494	0,454286049	-0,675978528	0,407842054	0,600943371	0,717864707	1,449031587	-0,360305328	1,072049761	-0,026072344	-0,386367935	1,106666492	0,395772242	-1,089998457	-1,311654643	-1,277239403	-1,234695909	-0,896499712	-1,486169245	-0,268310889
13176029	-0,161956576	0,310877532	-0,097864751	-0,165780573	-0,074203301	-0,063095929	-0,101093545	-0,31526795	-0,091247033	-0,2387263	-0,02690479	0,025890917	0,330987209	0,010846297	0,025259468	-0,111952298	-0,055072259	-0,075452125	-0,170141219
13223058	0,291014625	0,14021144	-0,145315389	-0,190171282	0,222667734	-0,001738821	0,208826792	0,016304533	-0,0727851	0,17189015	-0,041059467	-0,047866302	-0,010179281	0,174271305	0,296292851	-0,055720111	-0,211681461	0,053791928	-0,067439188
13048660	0,050869618	0,062289569	0,276819434	0,032100086	-0,02538487	-0,014041338	0,13401505	0,601136133	0,104050343	-0,154365943	0,170595473	-0,230438095	0,110158219	-0,054944777	0,273180713	-0,074480229	-0,049191951	0,089825271	0,01355031
13109885	0,048884234	-0,030552448	-0,014003841	0,149125164	-0,092380332	-0,050721609	-0,27827237	-0,072148909	-0,083924439	0,031504296	0,315749102	-0,038028987	-0,225299973	-0,083638266	-0,034237568	-0,248959002	-0,146173622	-0,106369462	-0,11080573
13109885	0,048884234	-0,030552448	-0,014003841	0,149125164	-0,092380332	-0,050721609	-0,27827237	-0,072148909	-0,083924439	0,031504296	0,315749102	-0,038028987	-0,225299973	-0,083638266	-0,034237568	-0,248959002	-0,146173622	-0,106369462	-0,11080573
13109885	0,048884234	-0,030552448	-0,014003841	0,149125164	-0,092380332	-0,050721609	-0,27827237	-0,072148909	-0,083924439	0,031504296	0,315749102	-0,038028987	-0,225299973	-0,083638266	-0,034237568	-0,248959002	-0,146173622	-0,106369462	-0,11080573
13109885	0,048884234	-0,030552448	-0,014003841	0,149125164	-0,092380332	-0,050721609	-0,27827237	-0,072148909	-0,083924439	0,031504296	0,315749102	-0,038028987	-0,225299973	-0,083638266	-0,034237568	-0,248959002	-0,146173622	-0,106369462	-0,11080573
13109885	0,048884234	-0,030552448	-0,014003841	0,149125164	-0,092380332	-0,050721609	-0,27827237	-0,072148909	-0,083924439	0,031504296	0,315749102	-0,038028987	-0,225299973	-0,083638266	-0,034237568	-0,248959002	-0,146173622	-0,106369462	-0,11080573
13176029	-0,119855864	0,064750946	0,013388939	-0,116002538	0,04615139	0,196365524	-0,239541303	-0,131214216	0,057822174	0,127783019	-0,191634342	0,039720812	-0,033691664	0,055200248	0,082602226	0,048651376	-0,081502004	0,205835139	0,320187516
13071605	0,051736133	0,126139831	0,01681698	-0,020334419	0,148465697	-0,222378895	0,315102244	-0,005973953	-0,007569677	0,151708126	-0,063507457	0,170532428	-0,251163419	-0,029807134	0,34944994	0,155251701	-0,164423009	-0,028362755	-0,21966638
13223058	0,129577911	-0,54094595	-0,190476754	-0,019637508	-0,00642818	-0,050210444	-0,380545958	-0,116131438	-0,054051771	-0,091036204	0,041852742	0,105293489	-0,002058257	-0,198089908	-0,096995472	0,11570156	-0,477475896	0,024452403	-0,057049455
13071605	0,63885925	0,336120314	-0,187470993	0,013133139	0,050511004	-0,154202246	-0,055685824	-0,112650331	-0,135387239	0,166315181	0,271259863	-0,315556743	0,013368941	-0,071027585	0,318307283	0,573909994	0,31006873	0,246719551	0,175692972
13176029	0,016492653	-0,18400238	-0,180665354	-0,011149736	0,050486602	-0,147856858	0,023163545	-0,028750406	0,041788056	0,045073697	-0,179190559	0,015155237	0,077173569	0,146550673	-0,144541837	0,010036013	0,079350596	-0,150349219	-0,281217412
13280104	-0,183930012	0,405906223	0,070182708	-0,021585152	0,069606034	0,31420219	-0,273822991	0,384568079	-0,103272891	-0,20811643	0,04106473	0,081533711	0,188790883	0,267082679	0,019332399	0,072716481	0,134743218	0,004585991	-0,074977659
13048660	-0,299293111	-0,215555953	0,089230925	-0,246236939	-0,166819643	0,052435601	-0,321136215	-0,085697659	0,275085108	-0,15771552	0,089326568	-0,258777766	0,052081611	0,146219644	0,087593814	-0,047391309	-0,144525088	0,022238456	0,021606599
13176029	0,41478713	0,169185615	0,232128671	0,277092308	0,269339624	0,292432118	0,33318025	0,123229867	0,324490943	0,061825611	-0,143119119	-0,159256663	-0,083940771	-0,048400219	-0,088616151	0,305096607	0,266963592	-0,161685605	-0,110858223
13223058	0,061919259	-0,152848544	0,375947581	0,432672107	-0,636639821	0,179551676	-0,845744684	0,532065097	0,101632112	-0,019177223	0,593500204	-0,041045418	-0,634909678	-0,424308114	-0,277383502	-0,921736123	-0,619325775	-0,812264838	-0,790328065
13071605																			
13103533																			
13149335																			
13108001																			
13168252																			
13300520																			
13024318																			
13106669																			
12988489																			
13287022																			
13271005																			
13115203																			
13031162																			
13282574																			
13284122																			
13218627																			
12976741																			
13043707																			
13008652																			
13049400																			
13092976																			
13181059																			
13261534																			
13078348																			
12971056																			
13008742																			
12947809																			
13305278																			
13222673																			

Supplementary Table 6 Continued

TranscriptID	CsA_32_M_4	CsA_33_M_4	CsA_34_M_4	CsA_36_H_4	CsA_37_H_4	CsA_38_H_4	CsA_39_H_4	CsA_40_H_4	CsA_41_C_11	CsA_42_C_11	CsA_43_C_11	CsA_44_C_11	CsA_45_C_11	CsA_46_L_11	CsA_47_L_11	CsA_48_L_11	CsA_49_L_11	CsA_50_L_11	CsA_51_M_11
13003871	-0,026404528	0,116486894	-0,118826566	-0,001817666	0,180969526	0,127307407	0,091080787	-0,024541714	-0,196238095	-0,171916787	0,006013587	0,135959703	0,226181589	0,08429258	-0,204727095	-0,056781053	0,115706078	-0,180750054	-0,013833163
13110453	-0,158792049	0,102198553	0,033156648	0,052468476	0,031065043	0,078629246	-0,014965477	-0,118667174	0,133704529	-0,176918126	0,015977597	-0,135727553	0,162963557	0,025699732	0,165081842	-0,081362443	0,145147551	-0,180158302	0,184148828
13305252	0,102596874	0,127608083	0,131429146	-0,003845694	-0,068366447	-0,170688416	-0,068529347	0,054154649	-0,027599294	0,121831635	-0,106603407	-0,028245373	0,040616437	-0,090939399	-0,083511744	0,007250303	0,098672061	-0,057286232	0,107278544
13283206	0,046002552	0,032630419	-0,002835226	0,058991038	0,014118017	-0,095327476	0,032087208	0,015223503	-0,087667142	0,17941064	0,115419465	-0,095895372	-0,111267592	0,004331041	-0,095823163	-0,164665556	-0,22533882	-0,1901241	-0,173986755
13284362	0,046002552	0,032630419	-0,002835226	0,058991038	0,014118017	-0,095327476	0,032087208	0,015223503	-0,087667142	0,17941064	0,115419465	-0,095895372	-0,111267592	0,004331041	-0,095823163	-0,164665556	-0,22533882	-0,1901241	-0,173986755
13131516	0,057349901	0,026055727	0,340337162	-0,233344593	0,072448756	-0,24934645	0,072686592	-0,007774229	0,073734252	-0,046029285	-0,238425458	0,038818046	0,171902445	-0,036262325	0,456979387	-0,039180689	-0,029810058	0,134865024	-0,12976281
13113617	-0,168180075	-0,276453765	0,164705073	0,065703454	0,126373029	-0,064800145	0,096283202	-0,137162764	-0,045557412	0,319382006	0,155958118	-0,243826093	-0,185956622	-0,38931658	-0,0241136	-0,399883809	-0,374382137	-0,276499216	-0,189249234
13079367	-0,17825775	0,018317116	-0,035196349	-0,066948271	0,026610449	-0,356114061	-0,104588617	-0,122495101	-0,116553604	-0,030905621	0,230720364	-0,121604256	0,038343119	-0,202298025	-0,141341591	-0,024922404	0,126769896	0,089510226	-0,134559745
13152298	0,015899022	-0,067055744	-0,16998336	-0,042581182	0,116613965	0,014599778	-0,226966365	-0,110652778	-0,055751855	0,067833329	0,063755705	-0,085188017	0,009350837	-0,023605216	-0,106536675	-0,06766927	-0,054784939	0,152951842	-0,081961977
13283630	0,222801752	-0,006851268	-0,16190839	-0,035302797	0,179071733	0,078443568	0,119857974	0,081688315	-0,216327948	0,041614413	0,42331032	-0,024576498	-0,224020287	-0,040547492	-0,386511113	-0,210604476	-0,128887778	0,095347265	0,036630106
12964078	0,067719157	0,29390908	0,055951843	0,037297698	0,096992981	0,03607856	-0,026305243	0,017664285	-0,118672427	-0,013400975	0,140021515	-0,117858014	0,1099099	-0,125571935	-0,045266219	0,367947355	0,095196703	0,120557586	0,053527565
13081404	0,033278857	0,265669415	0,093836769	0,276993897	0,070096547	0,71408859	0,069291741	0,082367145	-0,228353248	-0,295488411	-0,222389699	0,594545708	0,151685648	0,28056961	-0,072295261	-0,128909926	0,197145525	-0,386320194	-0,469015286
13094209	-0,052678673	0,154582687	-0,226691044	0,140313617	0,086033869	-0,473019571	0,166604576	-0,232174064	0,077257814	-0,024562234	-0,274531576	-0,096707424	0,318543422	0,113716054	0,080155991	-0,131722784	0,190967213	0,243131008	-0,114425264
13054773	-0,042365526	-0,098938296	0,056797073	-0,012349542	-0,001040796	0,062958969	0,074589681	0,001134165	0,036500241	-0,102058854	0,061006489	0,063613912	-0,059061791	0,037627052	0,051360577	0,032708501	-0,045640366	0,082029101	0,029037885
13065823	0,380121374	-0,240710774	-0,079992675	-0,233442799	0,169155018	-0,359441697	-0,032329972	0,089134647	0,146451921	0,072738654	0,005572366	-0,162345665	-0,062417276	0,102124374	0,432352214	0,01322797	-0,076666947	0,287771865	-0,270739553
13234461	-0,050373515	-0,108434089	0,126213298	0,065789274	0,019496116	-0,024568421	-0,265770992	0,385872857	0,040690864	0,026348713	0,190068317	-0,103406066	-0,15370183	-0,175335234	0,403593886	0,05160287	-0,143603925	0,03405471	-0,206072921
12956364	-0,127438644	-0,185913971	-0,047655597	-0,113523439	-0,11626672	0,128755375	0,071209924	-0,160531922	0,118047877	-0,026834418	-0,0004115	-0,089421802	-0,001380159	0,144780342	0,025088812	-0,007205222	0,176361108	0,203747247	0,226203143
13034897	0,17812029	-0,030197347	-0,285798292	0,06079939	0,060550991	-0,100557464	-0,176296536	0,11061974	-0,130213104	-0,058357962	-0,214157052	0,096689074	0,306039048	-0,071347372	-0,138610029	0,015309216	-0,030827512	-0,004355496	-0,200573941
13278988	-0,182145737	-0,423339731	-0,388565546	-0,236565021	0,233682486	-0,240546615	0,344246799	-0,10377802	-0,119707472	0,254248418	-0,034229218	0,002692499	-0,103004228	-0,073178158	-0,121586727	-0,591392089	-0,360406341	-0,286327981	-0,226860662
13200912	-0,080121432	0,023571883	0,083699973	0,0801958	0,037209985	0,222832379	0,178232894	0,216670816	0,190888802	-0,147763116	-0,128415288	0,008082966	0,077206637	0,082841891	0,118573332	0,087438082	0,127518743	0,063590907	0,049764916
13036819	0,141678184	0,01189394	-0,171878428	0,382253753	0,160406078	0,359263918	-0,005596089	-0,139306858	-0,006023788	-0,037625129	-0,083878655	-0,086925826	0,214453395	0,055478376	-0,005050577	0,13205955	-0,048850546	-0,221662738	0,204846353
13166102	-0,005309819	0,075089073	-0,251299689	-0,103302602	-0,02687861	-0,126876852	-0,199583515	0,163530108	-0,285345317	0,13702432	-0,09853988	0,021888047	0,224972827	0,059707308	0,048357106	0,192648917	0,251501672	-0,173042112	-0,083109388
13153157	-0,09657014	-0,240070077	-0,034179142	-0,328594934	-0,011808156	0,295677906	-0,157507801	-0,033908699	0,259179873	-0,050908664	0,09859807	-0,357649742	0,050780463	0,377285395	0,343280236	-0,11378546	-0,086557405	0,294657045	0,269191531
12992494	-0,701528682	-0,973120976	-1,056641629	0,104612696	0,198206544	-1,021897956	0,438887316	-1,49650315	-0,247060428	-0,287171971	-0,792120117	1,019036287	0,307316227	0,534845058	-0,073952422	-0,227532766	0,6313639	-0,003848634	-0,166352639
13176029	-0,062211548	0,10857295	-0,143221203	-0,081072946	-0,078384174	-0,012407539	-0,048466233	0,017308543	-0,082177119	0,044634017	-0,225513209	0,162868524	0,100187788	-0,090846302	0,004326008	-0,028129443	0,007412006	-0,016473933	-0,071538946
13223058	-0,045831203	0,111216606	-0,031006067	0,084207399	-0,300600142	-0,191634319	-0,051105344	-0,032769466	-0,06629649	0,100023853	-0,051497197	-0,03915911	0,056928943	0,053684041	0,031253665	0,041295424	0,210233288	-0,025566863	-0,028017468
13048660	-0,072244061	0,289157895	0,017005662	0,045794088	0,027919601	0,069742114	0,349849434	-0,056272547	0,16475214	0,129212597	-0,10501229	-0,015134155	-0,173818291	0,088718168	0,030767308	-0,293116238	0,18010504	-0,04498848	0,051869959
13109885	-0,26441684	-0,045747756	-0,173364339	0,089626117	-0,059087659	0,118109591	-0,128643989	0,001534397	-0,136604689	0,145275777	-0,005037963	0,135073296	-0,138706423	0,160450212	-0,116109431	-0,080713174	-0,181347445	-0,058176102	-0,190187844
13109885	-0,26441684	-0,045747756	-0,173364339	0,089626117	-0,059087659	0,118109591	-0,128643989	0,001534397	-0,136604689	0,145275777	-0,005037963	0,135073296	-0,138706423	0,160450212	-0,116109431	-0,080713174	-0,181347445	-0,058176102	-0,190187844
13109885	-0,26441684	-0,045747756	-0,173364339	0,089626117	-0,059087659	0,118109591	-0,128643989	0,001534397	-0,136604689	0,145275777	-0,005037963	0,135073296	-0,138706423	0,160450212	-0,116109431	-0,080713174	-0,181347445	-0,058176102	-0,190187844
13109885	-0,26441684	-0,045747756	-0,173364339	0,089626117	-0,059087659	0,118109591	-0,128643989	0,001534397	-0,136604689	0,145275777	-0,005037963	0,135073296	-0,138706423	0,160450212	-0,116109431	-0,080713174	-0,181347445	-0,058176102	-0,190187844
13109885	-0,26441684	-0,045747756	-0,173364339	0,089626117	-0,059087659	0,118109591	-0,128643989	0,001534397	-0,136604689	0,145275777	-0,005037963	0,135073296	-0,138706423	0,160450212	-0,116109431	-0,080713174	-0,181347445	-0,058176102	-0,190187844
13176029	-0,053102614	-0,023200165	0,252376439	0,157029168	0,02510542	-0,00219677	-0,201792048	0,070791642	-0,11253845	0,016130622	0,124133341	-0,042934232	0,015208717	0,214713321	0,069796429	0,082588315	0,097732735	-0,226706221	-0,097910115
13071605	-0,032187002	-0,285674821	0,150666988	0,076049975	0,029502825	0,421834368	0,118678449	0,263662987	0,043768172	0,087921656	-0,004538336	-0,026036819	-0,101114671	0,020784773	0,351555342	0,037682186	0,020484792	0,206717191	0,052578794
13223058	-0,111333812	-0,15565984	-0,265939107	-0,093772099	0,013306646	-0,201069448	-0,441488835	-0,200180521	-0,0144764	0,140537696	-0,022187638	0,053335401	-0,157209058	0,016569905	0,106329876	-0,079524605	-0,225135393	0,194598348	0,349271576
13071605	0,232187252	0,046126596	-0,091625229	0,185710116	-0,141644598	0,053398538	0,010724349	-0,004886819	-0,020295091	-0,009215232	0,218608642	-0,000813263	-0,188285055	-0,231719299	-0,024241068	0,021638254	-0,072674179	0,153887463	0,020212192
13176029	-0,144611075	0,21945563	-0,035535793	-0,00997022	-0,043705011	-0,14830564	-0,017782068	-0,053550881	-0,069777921	-0,021926985	0,003988711	0,136184257	-0,048468064	-0,090414499	0,064232792	-0,009304366	-0,117139544	0,052094167	-0,144174329
13280104	0,056601308	0,010908943	0,244868856	-0,129161323	0,104386381	0,187068801	0,209601741	-0,186247286	-0,060566446	0,136376795	0,054288382	-0,047709178	-0,082389552	-0,055283736	0,044688565	0,0867571	0,26187294	-0,147575212	0,007157721
13048660	-0,295086857	0,242406623	0,082928131	-0,057781992	0,298981521	0,197597295	0,072770675	-0,028565751	-0,039537805	0,07797692	0,10126477	-0,292568444	0,152864556	-0,140982556	0,103792304	0,085327663	0,286874419	0,184029719	-0,108906688
13176029	-0,205805611	-0,113429181	0,160042928	-0,369977305	-0,276967523	-0,104003454	-0,191417033	0,002296908	-0,1194282	-0,216222148	-0,047030359	0,233968156	0,148712549	0,314553532	0,197868991	0,035075015	-0,010523755	0,071332112	0,141293374
13223058	-0,264425678	-0,249836962	-0,256168506	0,038382147	-0,513676636	-1,118684276	0,48791043	-0,497819303	-0,271630686	-0,499556439	0,406401372	0,112069448	0,252716307	-0,378427091	-0,015753757	-0,350931014	0,121683336	-0,735293273	0,073845067
13071605																			
13103533																			
13149335																			
13108001																			
13168252																			
13300520																			
13024318																			
13106669																			
12988489																			
13287022																			
13271005																			
13115203																			
13031162																			
13282574																			
13284122																			
13218627																			
12976741																			
13043707																			
13008652																			
13049400																			
13092976																			
13181059																			
13261534																			
13078348																			
12971056																			
13008742																			
12947809																			
13305278																			
13222673																			

Supplementary Table 6 Continued

TranscriptID	CsA_52_M_11	CsA_53_M_11	CsA_54_M_11	CsA_55_M_11	CsA_56_H_11	CsA_57_H_11	CsA_58_H_11	CsA_59_H_11	CsA_60_H_11
13003871	-0,074707624	0,298938244	0,068123096	-0,046002185	0,069862869	-0,010529149	0,123975456	0,136567407	-0,023114481
13110453	-0,080257004	0,184769125	-0,017222083	0,284906472	-0,008431517	-0,076597459	0,309155868	-0,109646657	-0,082853614
13305252	0,074680898	-0,107339958	0,094745868	-0,013215905	0,050554041	0,093522847	-0,032053433	0,16788184	0,068100019
13283206	-0,202288127	-0,243269595	-0,114528757	-0,121083899	-0,193866062	0,008017726	-0,134171402	0,206817835	-0,227469808
13284362	-0,202288127	-0,243269595	-0,114528757	-0,121083899	-0,193866062	0,008017726	-0,134171402	0,206817835	-0,227469808
13131516	0,215276952	-0,03687153	0,254691477	0,223654823	0,047693624	0,438114144	-0,275506838	0,001396447	-0,120781575
13113617	-0,338881101	-0,151932784	-0,435170683	-0,207309508	-0,148588376	-0,137640482	-0,133365413	-0,427227602	-0,179107727
13079367	-0,148178338	-0,269688355	-0,054663504	-0,148600164	0,092843622	0,053651132	-0,098077772	0,066382433	-0,11400303
13152298	0,12121716	0,108838424	-0,072369059	0,056521208	0,000795583	0,034488417	0,006161628	0,059583445	0,123581914
13283630	-0,281646334	0,016510395	0,029197417	-0,425022886	-0,25134127	-0,083268536	-0,050393395	0,162785883	-0,071458284
12964078	-0,24865474	0,068993628	-0,063322042	0,139345025	-0,001717273	0,347869483	-0,114006487	-0,045147455	0,086725277
13081404	-0,427021251	-0,059661478	-0,016171919	-0,100243111	-0,074417811	-0,055280476	-0,027157123	-0,172157953	-0,458727495
13094209	0,183735132	0,670057597	0,278912685	0,172488548	0,364708035	0,27556414	0,103737776	0,41488399	0,601262778
13054773	-0,00218492	0,010912402	0,008633772	0,003273997	0,049554259	0,018300656	0,002136663	-0,024986346	0,078792221
13065823	-0,208072956	0,057474133	-0,201745277	-0,047152471	-0,030157169	0,112025644	-0,137058608	0,268465739	0,097912517
13234461	-0,013732711	-0,246133975	-0,284368845	0,389883207	-0,126197973	0,152923939	-0,142361295	-0,097877889	0,204764668
12956364	0,132137869	0,411682304	0,045418705	0,243196521	0,103332992	0,262572837	-0,044302921	-0,139618838	0,135905732
13034897	0,060292482	-0,194851145	-0,028568071	-0,201363142	-0,129867951	-0,250297752	-0,183258635	-0,018331685	-0,067463014
13278988	0,109536999	-0,071992818	-0,595612299	-0,07323793	0,291349876	-0,018384468	0,280391815	-0,385036273	0,222896101
13200912	0,106111263	0,082057115	0,03276839	0,069323444	0,251688921	-0,016154977	-0,003403895	-0,01171703	0,247952629
13036819	-0,017264215	-0,105105372	0,224466239	0,023407991	0,126246882	0,229712037	-0,297223529	0,117176524	-0,077574509
13166102	0,096298223	0,201015565	0,076611096	0,046581551	-0,050077553	-0,009743276	0,010025897	0,160434342	-0,093118782
13153157	0,226431509	0,105148347	0,032864867	0,208784622	0,030455452	0,441041787	0,165805346	-0,036160615	0,111955439
12992494	-0,042156187	1,278868491	0,352167591	-0,106255293	-0,69226633	-0,569258119	0,513600642	0,788561608	-0,039918754
13176029	0,061763761	-0,12194529	0,114912514	0,194334802	-0,150180135	-0,045575681	0,134089103	0,040477256	0,02937827
13223058	0,082521301	0,027299388	-0,038779836	0,21157349	0,103366927	0,000151444	0,062293265	-0,106164404	-0,102347451
13048660	-0,284946136	0,150347976	0,136863129	0,04025026	-0,138082512	-0,225004278	0,129014975	0,206323606	0,026148458
13109885	0,240639074	-0,015470393	-0,228389667	-0,281850041	-0,005920744	-0,255644023	-0,06831785	-0,031977846	0,056001112
13109885	0,240639074	-0,015470393	-0,228389667	-0,281850041	-0,005920744	-0,255644023	-0,06831785	-0,031977846	0,056001112
13109885	0,240639074	-0,015470393	-0,228389667	-0,281850041	-0,005920744	-0,255644023	-0,06831785	-0,031977846	0,056001112
13109885	0,240639074	-0,015470393	-0,228389667	-0,281850041	-0,005920744	-0,255644023	-0,06831785	-0,031977846	0,056001112
13109885	0,240639074	-0,015470393	-0,228389667	-0,281850041	-0,005920744	-0,255644023	-0,06831785	-0,031977846	0,056001112
13176029	-0,009208352	-0,183597674	-0,036766057	-0,07439171	0,203738932	-0,048741313	-0,089928478	0,060415297	0,098578603
13071605	0,109732242	-0,161357794	-0,018647982	-0,227635571	0,159195741	0,008441771	-0,040478457	-0,202456247	-0,157701933
13223058	-0,105066533	0,189462493	0,07178124	-0,005042542	0,3150719	-0,425352099	-0,032571559	0,094558127	-0,06594176
13071605	0,27990231	0,122985782	-0,002341485	-0,108415633	0,154424966	-0,012676048	0,200988397	0,23415637	0,137306971
13176029	-0,275362615	-0,161023776	-0,172563607	-0,01021497	0,152550382	0,016223889	0,037388863	-0,156103507	-0,190861665
13280104	-0,135573018	-0,119081927	0,021548562	0,016620672	0,014762821	-0,339988153	0,111570214	0,021924792	0,187301387
13048660	-0,186903014	0,307530638	0,082113791	-0,086269068	0,096567963	0,265786011	0,251635217	-0,253508341	0,340138797
13176029	0,144724478	0,0272187	-0,121182032	0,077273182	-0,064557663	0,062209319	-0,019752371	-0,082798844	0,002013832
13223058	0,185876124	0,434534104	-0,068838729	-0,1075865	0,07447799	0,253124512	0,515822959	0,549902918	0,472936714
13071605									
13103533									
13149335									
13108001									
13168252									
13300520									
13024318									
13106669									
12988489									
13287022									
13271005									
13115203									
13031162									
13282574									
13284122									
13218627									
12976741									
13043707									
13008652									
13049400									
13092976									
13181059									
13261534									
13078348									
12971056									
13008742									
12947809									
13305278									
13222673									

Supplementary Table 1

AffyIDs	AM	APAP	CPZ	CsA	EE2	PQ	TAA	TET	VPA
100000036	-0,171753271	0,994558693	0,883286757	0,259600864	-0,072346688	0,806281679	0,947009202	-0,116059093	0,095273707
100000132	0,184733656	0,317114223	0,190603118	0,152732361	0,348934648	-0,442267112	-0,300548748	0,427757272	0,129784798
100000156	4,532301731	0,593075193	-0,358253637	0,291698087	1,061930484	-0,887705789	-0,417221615	0,017588077	1,8556851
100000294	0,564475715	0,105887726	-0,327645615	0,553166229	0,12158635	0,328479482	-0,249702664	-0,012704742	-0,609689536
100000322	-0,158337727	0,145903297	0,037139887	1,212722572	-0,106745298	0,832034163	0,067772715	0,289605877	0,116872442
100000332	-0,298907456	-0,279785272	-0,676019138	0,08728971	-0,214177921	0,785726322	0,059754505	-0,381773537	-0,039284651
100000389	0,074270741	-0,008390961	-0,309773116	0,302620517	0,104812013	0,653842302	-0,00038274	0,110646924	-0,037542332
100000517	-0,489511754	-0,141176248	-0,12351997	0,163729342	-0,286847216	0,147770979	0,063200048	-0,27291443	-0,635071196
100000574	-0,284519426	0,031185743	0,056693863	-0,465582811	0,234757314	-0,30269841	-0,361064108	0,033582981	0,073421319
100000832	0,21687603	0,151449355	-0,052117962	0,000120982	-0,049846854	1,408380668	0,147561904	-0,230057448	0,142941983
100000842	0,280729766	0,209986805	0,277464121	0,189468199	0,379182628	0,236133806	0,023109064	0,184687759	0,511944366
100001552	-0,136250393	0,007879202	-0,270816327	0,042663457	-0,044174289	-0,497086002	-0,166429943	-0,031367011	0,280827941
100001584	0,172954034	0,165996803	-0,091762431	-0,074606085	-0,097697376	-0,117649381	0,117416943	0,189954117	0,520280747
100001617	-0,124805766	-0,001280333	-0,169622409	0,004637371	-0,186836714	0,475370372	0,088041664	-0,142936788	-0,263419907
100001628	0,695949532	0,061606813	0,174558124	0,205590351	0,158866578	-0,080997066	0,104364453	0,050426507	0,5534511
100001845	-0,169372145	-0,27020336	-0,129931819	-0,272262102	-0,111407938	-0,171861868	0,110731488	-0,221757434	0,389411949
100002108	0,056304025	0,163172918	0,072727528	0,217647579	-0,178228375	-0,305819283	0,628905431	0,219630948	0,030794883
100002272	0,262104718	0,036945915	-0,011480321	0,108027693	-0,177310896	0,115926074	-0,045806079	-0,074836197	0,724775583
100002292	-0,135604022	-0,469446057	-0,554579256	-0,150979309	-0,366009734	0,610343266	0,023250918	-0,383811605	-0,586324293
100002785	-0,09962916	-0,226129604	-0,182118386	0,047200795	-0,117656427	0,416885052	0,335872052	-0,149941252	-0,341899871
100003115	-0,649776691	-0,51841365	-0,531576249	-0,701500548	-0,469963178	0,546645029	-0,023014319	-0,715876425	-0,846877855
100003524	-0,039831879	-0,242083874	-0,512913073	0,043096234	-0,163761006	0,631705951	0,329030574	-0,381262027	-0,624279772
100003553	0,150830828	-0,021767584	0,129623553	0,115755203	0,177595236	-0,063788304	-0,094682506	0,04854699	0,46202776
100003570	0,448493672	-0,042582722	0,037914549	0,04350256	0,021634714	-0,027852722	0,193453925	-0,008791462	0,376136986
100003669	0,414268416	0,057765482	-0,014686631	0,344224722	0,334018646	1,817978914	0,137471706	0,190072057	-0,307761811
100003679	0,124493655	-0,286957552	-0,025774466	-0,067068007	-0,064430698	1,047243436	0,297181968	-0,062429865	-0,13021951
100003849	-0,081822397	-0,255208547	-0,112217879	-0,247419151	-0,076915792	-0,165853679	0,128753449	-0,164799973	0,440362281
100004607	-0,533619504	-0,092639523	-0,425865698	0,375514354	-0,671069656	0,884908234	0,093725319	0,048654202	-0,686952
100004700	0,38289664	-0,482620257	-1,00392061	1,718373932	0,62194222	1,304603866	0,099723912	-1,279130027	-1,061747089
100004810	-0,270460596	-0,231512453	-0,232015978	-0,51503176	-0,117660069	-0,399210637	-0,316164817	-0,472390444	-0,480123009
100004946	0,585945159	0,090283828	0,142931901	0,15796247	0,296550173	0,486067129	-0,105372885	0,373379565	0,52051873
100004951	0,185457774	0,016250183	0,681912156	0,063545683	-0,053678069	-0,262192707	0,331818871	0,036594401	0,292461879
100005008	0,387709766	-0,139378894	-0,264707098	-0,060493462	-0,195703654	0,5719491	-0,005868451	-0,043626314	-0,113420329
100005016	0,225726209	0,219683942	0,046095067	-0,092101753	0,06779974	5,040336803	0,537176296	1,015217331	0,026247346
100005587	-0,258486418	-0,17172291	-0,091068889	-0,046496165	0,056926923	-0,140775862	0,172712397	-0,106053395	-0,471253738
100005588	-0,591351482	-0,548983552	-0,499132369	-0,485095818	0,943005663	-0,263585414	-0,079396152	-0,511110927	-0,407482767
100005729	0,579014679	0,145194036	0,11756052	0,501522252	-0,29123529	-0,109648774	-0,362112714	0,10139387	0,000978077
100006246	-0,088901348	0,0000823	0,02720519	-0,119947849	-0,025209217	-0,203901764	0,02571511	0,003780327	0,481426191
100006303	0,340496015	-0,177423536	-0,396553014	-0,12762375	-1,048955525	0,161492801	-0,168895504	-0,155005438	-0,192905237
100007591	-0,076736485	0,284265301	0,062499247	0,051510926	0,042960202	0,04491751	-0,053345944	0,187631418	0,749354604
100007793	-0,625279959	0,170631632	-0,419765162	0,292003719	-0,122032184	0,469523301	-0,027616464	0,040258566	-0,746476216
100008021	-0,055919025	0,146809301	0,145636172	-0,202043795	-0,034912718	0,030860155	0,323996633	0,019284919	0,857067448
100009638	1,551912393	0,351399658	0,503471583	1,011043856	0,089489495	0,637342541	-0,947383061	0,183733963	-0,16984059
100009650	-0,009750141	-0,024609984	0,085306876	-0,101125155	-0,255846883	-0,310984345	-0,013744125	-0,105343466	-0,619046773
100009654	0,385871868	-0,029117227	-0,361176603	0,32771638	0,011946666	-0,189793819	-0,279140335	0,066643051	-0,726514172
100034383	0,015908898	0,02249868	-0,052088825	-0,074187099	0,098972393	-0,00020436	-0,165067171	-0,064328738	0,518205682
100034480	0,178001223	0,526483163	0,069475804	0,281954598	0,194366572	-0,038998928	0,242235865	0,933906095	0,185320561
100034647	-0,275616383	-0,466580958	-0,278896189	0,041657176	0,079953065	-0,91588565	0,028103848	-0,62862766	-0,975853508
100037315	-0,365545699	-0,014828186	-0,050820837	-0,215912573	-0,474340203	0,207910188	-0,030266658	0,055871264	-0,064409688
100037363	0,199107673	-0,211052223	0,128865621	0,152287185	0,002687391	-0,365173169	-0,411185063	-0,034220449	0,054534262
100038777	0,865100123	0,817568918	0,352716271	0,371165677	0,462632281	2,979678142	0,477908059	1,073200061	0,551453169
100073336	0,068994674	0,060012832	-0,285836947	0,24481592	0,010354165	-0,079825707	-0,301697703	0,115407024	-0,687742055
100124622	0,271605636	0,035645032	0,124289592	0,056044109	0,069223053	3,743294796	0,177634366	0,525944552	0,068467988
100126128	-0,046563043	0,080781813	-0,151826947	0,049099164	-0,110454731	2,108786623	0,420361388	0,705343991	-0,102686341
100134974	-0,198172685	0,201616066	-0,146404196	0,104551854	-0,34598481	0,133310997	-0,080231527	0,180163001	-0,814387904
100136852	-0,071823228	0,034250195	-0,175069942	-0,597837903	-0,034008708	0,234703281	0,432469375	-0,210843145	-0,375682981
100137108	-0,237951975	-0,663432645	-0,785125259	1,138778955	-0,899104685	0,55464888	-0,188652926	-0,582939167	-0,276796925
100137120	0,032362639	0,103307245	-0,179445239	-0,230358288	-0,584900195	-0,114938526	-0,032920533	-0,073372963	-0,551550892
100141332	0,097486834	0,274324286	-0,056929719	0,188189719	0,05060852	-0,564891957	-0,17585439	0,138210554	-0,392969904
100144772	-0,101850386	-0,174218392	-0,249808877	-0,148102294	-0,176772137	-0,800581524	-0,314334637	-0,116514431	-0,842976352
100147863	-0,15324099	-0,184611226	-0,322877953	-0,368182905	-0,301880033	0,55386977	0,175193541	-0,023398149	-0,425341465
100147904	-0,335119278	0,030683551	-0,442741175	0,408037937	-0,494271764	-0,024728518	-0,435889665	0,072686828	-1,109171646
100148962	-0,182266606	-0,154680624	-0,316929787	0,011454125	-0,213193228	0,071772954	0,026936492	-0,203237597	-0,705916209
100149028	-0,185236467	-0,214196454	-0,105341653	-0,018737575	0,080837382	-0,541691457	-0,432916624	-0,148620866	-0,524115609
100149104	0,251105292	0,187514553	0,19133458	0,298827208	0,121947321	-0,222770205	-0,375882518	0,277530592	0,412584288
100149254	-0,051883384	-0,064157706	0,001777005	0,046939447	0,102412249	-0,050183838	0,021444171	-0,061654792	-0,565083311
100149353	0,249148441	-0,024648259	0,041970407	0,018058673	0,257302698	-0,680700442	0,064621058	0,129706775	0,014694674
100149745	0,15630288	-0,019866527	0,159429407	0,120752597	0,167493388	0,896584415	0,260878614	0,312035292	0,220789293
100150054	0,344066466	0,241774753	0,311153458	0,197817425	0,082167981	-0,194923594	-0,187176044	-0,045771413	0,720321037
100150068	-0,247781303	-0,084228296	-0,274051559	-0,063220197	-0,248362903	0,002447801	0,268933892	0,071506754	-0,488565638
100150223	-0,07031979	0,15431961	-0,097263093	-0,094107364	0,084748703	-0,148590601	0,009945963	0,111248974	0,575922514
100150269	-0,401753508	-0,166942304	0,001499435	-0,043581553	-0,24992408	-0,07024829	0,148962757	-0,205809294	-0,978427857
100150939	0,749607043	0,538698147	0,433847031	0,567955392	0,429069031	-0,032495901	0,089746032	0,458417928	0,889387929
100151009	1,900677331	0,48870256	-0,005823798	1,091595913	0,662891848	-0,748688624	-0,527075098	0,700676253	0,645047506

Supplementary Table 1 Continued

AffyIDs	AM	APAP	CPZ	CsA	EE2	PQ	TAA	TET	VPA
100151171	0,106367717	0,654800002	-0,150898818	-0,178133091	-0,035130731	0,212719069	0,432289262	-0,032891352	-0,070329541
100151256	0,534508098	0,312008999	-0,092138961	-0,118902787	0,561583114	2,097329666	0,721397766	0,279632229	0,593421942
100151368	-0,902500564	0,135904748	-0,197332763	0,194087947	-0,578146401	0,050558308	0,26845441	-0,44277976	-0,083752932
100151549	0,014302964	0,033265291	-0,163800999	-0,127424221	-0,117598388	0,089886483	0,556396902	-0,010131895	0,03957044
100170786	-0,34903726	-0,326413899	-0,728060311	-0,244521847	-0,993138679	-0,000314832	-0,006438159	-0,339208467	-0,644714894
100170833	0,218600217	0,060059956	0,206835664	1,139227834	0,146563513	2,913636046	0,315040153	0,638244552	-0,009863891
100174951	-0,290384871	-0,211950348	-0,46126594	-0,185499648	-0,236284792	0,250978912	0,518787832	-0,314765711	-0,299684428
100318173	-0,062370012	0,139802384	-0,161701862	-0,049262721	-0,12225827	-0,319945699	-0,18308546	0,158889627	-0,541433392
100329344	-0,148928839	-0,300771203	0,05589495	0,156895653	-0,057821307	-0,223640506	-0,532779457	-0,10983594	0,016227266
100329429	0,695388715	0,174027182	-0,474602566	0,478246126	-0,507571242	-0,470984199	-0,536840781	0,191747309	-0,575596413
100329446	0,220352158	0,211844289	0,413830837	-0,092962414	0,118882512	-0,280540465	-0,013806069	0,380561108	0,225732137
100329514	1,167582575	0,45455526	0,50055342	0,749503529	0,236830465	0,169118434	0,279601759	0,404561031	0,51109955
100329543	-0,396429889	0,255355606	0,014564524	-0,277659445	0,441932656	-0,737997536	-0,212379394	0,418731801	-0,43324934
100329560	-0,036541927	-0,594613206	0,014450684	-0,201179686	-0,016807832	0,018539312	-0,566349291	-0,362303154	-0,098453698
100329625	-0,22149574	-0,361438929	-0,309602037	-0,243836688	-0,204483098	-1,314704707	-0,370706643	-0,346868113	-1,541437562
100329702	-0,002696219	-0,061582829	-0,22084709	-0,017132172	-0,569627633	-0,103340988	-0,309025476	-0,107127229	-0,43107408
100329888	0,079452473	0,323523836	-0,044850899	0,370830801	-0,074840213	0,039336419	-0,190424794	0,100331213	-0,387205458
100330160	-0,123360106	-0,20563742	-0,213403092	-0,326075704	-0,219229128	0,681919565	0,191892033	-0,283005713	-0,054532386
100330229	-0,972399257	-0,661636281	-0,611246595	-0,686373357	-0,664501547	0,907428676	0,208950101	-1,082910722	-0,413948338
100330479	0,419440731	0,371727659	0,399908831	0,417338326	0,626782654	-0,157824368	0,217932887	0,455780876	0,920782338
100330576	-0,073620496	0,280721123	0,183933231	0,128950595	0,233674865	-0,417994759	-0,060994221	0,086057557	-0,514916142
100330672	0,614373197	-0,190572484	-0,021510089	0,83247212	-0,176283282	0,175363233	-0,555627404	0,273704078	-0,60739527
100330864	-0,329203694	0,019938301	-0,26137412	-0,641969414	-0,083007645	0,107757743	0,061156006	0,250357397	-0,3390433
100330886	-0,298492701	-0,173785198	-0,125651716	-0,262882067	-0,326882534	-0,424830566	-0,616739482	-0,184371676	-0,162907168
100331027	0,011448622	0,303614992	0,065994672	0,223097168	-0,084384008	-0,172097854	0,029781112	0,365792769	-0,391707775
100331065	0,32886393	0,206220589	-0,181897918	-0,185443308	0,242601638	-0,795112313	-0,367352022	0,125647201	0,010888768
100331081	0,231609613	0,075161932	0,191368107	0,109135173	0,008630318	-0,094877714	0,02979315	0,530040451	0,05810396
100331113	0,757543385	0,204277032	-0,049674295	0,252104269	-0,225837007	0,605117252	-0,266522372	0,017812411	-0,013833183
100331214	0,19640331	0,234333131	-0,039817643	0,168743546	0,050782939	-0,001193272	-0,250430395	0,244635443	-0,425908721
100331959	0,116487726	-0,340786949	-0,387928807	0,177309242	-0,447194838	-0,329588526	-0,564799495	-0,584470008	-0,452519003
100332207	-0,128788708	-0,231630602	-0,370530476	-0,342327672	-0,481918112	0,017251386	0,198555881	-0,35074678	-0,46125682
100332237	-0,245903738	-0,432384778	-0,649647823	-0,320126394	-0,302990109	0,549853031	-0,215447762	-0,560936637	-0,566154551
100332378	0,618109931	0,189165067	-0,124834251	0,131191425	-0,110906917	-0,240006849	-0,183327884	0,142310765	0,450548568
100332563	-0,118495696	-0,168415166	-0,158156866	-0,125961213	-0,139242473	0,068158989	0,470145095	-0,098040592	0,104106429
100332613	-0,197820551	0,302146899	-0,387905835	-0,071825232	-1,35101207	-0,187087408	-0,417372412	0,154061554	-0,463449017
100332843	-0,355522755	-0,208743238	-0,492659009	-0,180673894	-0,264388867	-0,24543233	0,190178702	-0,363995231	-0,168819592
100332846	0,19181766	-0,08037726	0,124988851	0,028177449	0,153339932	0,049542215	-0,253597291	0,001172757	0,51532418
100333031	0,372049752	0,5343192	0,37874426	0,569450094	0,674932721	-0,382661216	-0,631162821	0,091407199	0,16354601
100333658	0,004780704	-0,524900337	-0,382964574	0,033416429	-0,326877253	-0,302595583	-0,465257908	-0,466478345	-0,407697259
100333680	-0,083483435	-0,254776203	-0,191377513	-0,425648549	-0,524045014	0,263193933	0,324433906	-0,152162372	-0,008910274
100333855	0,590199496	0,262316587	0,127588569	0,260441171	0,039315215	0,518014592	-0,020986676	-0,011701937	0,090516724
100333888	0,926999256	0,134803409	0,449381854	0,887826786	0,483701335	0,115146225	0,107671867	0,417609575	0,773612944
100333889	0,325368619	0,281063431	0,178522309	0,054680924	0,000509444	-0,094262878	0,0365853	0,224333295	0,613272467
100334018	0,118069262	0,286039586	-0,228213777	-0,023515116	0,063939867	0,413350464	-0,119507834	-0,220088276	0,473550136
100334345	-0,171900581	-0,030574082	-0,077374799	-0,15577402	-0,036078906	0,124306216	0,092300927	-0,125544052	-0,949030006
100334383	0,737108835	0,17291526	-0,113590106	-0,043525334	-0,106543353	0,81391525	-0,236242375	0,320089743	0,183503464
100334568	-0,957120365	-0,335816765	-0,495275551	-0,213358284	-0,700004671	-0,10956755	-0,654048694	-0,375924093	-0,783256454
100334600	-0,051526148	0,109330172	0,06289682	-0,186461797	-0,154090612	0,048881701	0,423012772	-0,006940754	0,524957309
100334649	-0,164925631	0,06548314	-0,037108828	-0,079580775	-0,144134964	-0,074095563	0,38867787	-0,112049113	-0,106001022
100334868	-0,185246189	-0,083151313	-0,206332266	-0,251613789	0,330750373	-0,169771763	-0,84237831	-0,283858985	0,255882947
100335000	-0,141306046	-0,184256097	0,096194294	-0,238943247	0,17647389	-0,183105661	-0,455605207	-0,059934232	0,090312041
100384895	0,818491875	0,450829973	0,352429386	0,473071572	0,801862242	0,174755045	0,310679782	0,246688809	0,504846079
100415798	0,749366148	-0,006628617	0,007938482	0,04274899	-0,059891043	0,148105398	0,083436611	0,281423946	0,002805518
100463516	-0,260415394	-0,460260503	-0,195093237	-0,423117891	-0,36088731	-0,167159717	-0,213804932	-0,662579651	-0,38777762
100534893	0,186249207	0,199444944	0,121152746	0,709853226	0,228040162	-0,14840376	-0,165088086	0,214831623	0,230369763
100534947	0,257253616	-0,183259621	-0,26105716	0,167800697	-0,165098265	0,223418674	-0,01648663	-0,08403818	-0,679095817
100535111	0,078995725	0,051214816	-0,267457565	-0,192741678	-0,416728604	0,265169818	0,251358308	-0,396976167	0,034405599
100535154	0,260165863	-0,082801553	-0,032240583	0,719736969	-1,34495764	0,19753875	-0,039294422	-0,189516393	-0,38557948
100535166	-0,429254532	-0,414811164	-0,544351817	-0,451744223	-0,552955365	0,274073962	-0,000254146	-0,535902759	-0,643544147
100535194	0,796357015	-0,011262288	-0,356795858	-0,002315099	-0,407710104	0,64537823	-0,680692311	-0,091850459	-0,644268733
100535203	0,12980339	0,286638857	0,240753513	0,205511314	0,162772036	0,966597754	-0,028180092	0,249566691	0,047885906
100535309	-0,292128576	-0,189605915	-0,249085488	0,180602868	-0,107533636	-0,453978656	-0,79911984	-0,090878989	-0,654682216
100535470	-0,118779308	-0,599948895	-0,203681686	-0,340430052	-0,170362341	0,059358834	0,25688894	-0,447790179	-0,133945164
100535513	-0,33069154	0,801814731	0,50780567	-0,437886779	-0,152265421	0,573305504	1,251282134	0,05559148	0,041271526
100535729	0,04684546	0,570075459	1,273219552	0,792137068	0,525406287	-0,783210961	-0,702511588	0,414457362	0,621518976
100536248	-0,085389354	0,175520857	0,371287386	-0,230439061	-0,148850116	0,471024444	1,173046109	-0,43731369	-0,201672475
100536600	-0,594532132	-0,234706884	-0,394210842	-0,611027914	-0,253211252	0,58407683	0,175584796	-0,421021956	-0,404473318
100536675	-0,127376959	-0,458305774	-0,291141192	-0,321894008	-0,11164672	-0,146161578	-0,074356541	-0,087092459	0,387397074
100536788	0,978352676	0,043974146	0,004386981	-0,023810233	0,131477482	-0,11419397	0,220862348	0,237364189	0,404566082
100536902	0,426994693	0,52579344	0,26912005	0,590609665	0,531504152	-0,09825588	-0,290841632	0,463207296	0,632507004
100537314	0,214309955	0,065332014	0,753442072	-0,013843812	0,429326838	-0,314443696	-0,307082517	0,441387546	0,530539591
100537419	0,055992863	-0,075999391	0,190197346	0,151974822	0,295065277	-0,18367741	-0,163904449	0,220075781	0,661912656
100537442	0,073495507	0,19250291	0,363288189	0,119844962	0,489399185	0,056998433	0,150986477	0,11163835	1,043069749
100537446	-0,038692159	-0,110631483	0,029067303	-0,066724342	0,090139201	0,235350368	0,514631867	0,054962015	0,190879708

Supplementary Table 1 Continued

AffyIDs	AM	APAP	CPZ	CsA	EE2	PQ	TAA	TET	VPA
100537540	0,032080102	0,019188718	-0,067362311	0,029042973	-0,023024287	0,233075253	0,229199158	0,024246087	0,547341539
100537689	0,075054204	0,27715898	0,197770607	0,152611281	0,033972845	-0,112522427	-0,178243751	0,268143174	0,552500516
100537894	0,139526985	0,176243635	0,270368246	-0,345348038	0,107918232	-0,640562214	-0,515878741	0,39094572	0,069956986
100537990	-0,161751133	0,214261935	0,077384327	0,217983354	-0,064899189	-0,649314856	-0,672587299	0,163215326	0,12667035
100538016	0,109236185	-0,078924435	-0,506766637	-0,242709709	0,005924669	1,194630922	0,100168636	-0,209478658	-0,114270644
100538043	-0,875779408	0,001833752	-0,649342497	-0,509547028	-0,564143056	-0,15330632	0,037082468	-0,431715201	-0,516602091
100538068	0,330761312	-0,24958458	0,347289939	-0,22397333	0,162651124	-0,251153263	0,048149253	0,243072607	0,802978875
100538165	0,555524991	0,151131649	0,088247659	0,810305372	0,048898559	0,153603367	0,103055676	-0,036635942	-0,4131546
114417	-0,829668097	0,282259895	-0,151621075	0,006606543	0,319509247	0,015439921	-0,423048711	0,135801627	-0,632313598
114426	-0,804474709	-0,379760871	-0,490820441	-0,521128963	-0,259974523	0,471812795	-0,243538888	-0,518093017	-0,219711745
114551	-1,114296675	-0,36378373	-0,660637741	-0,855229073	-0,572338757	-0,462802137	-0,519617523	-0,147916972	-0,49062445
140428	-0,607171975	-0,009991584	0,139084058	0,006018427	-0,308245127	-0,214245708	-0,599248221	0,152227399	-0,39085239
140817	-0,181251706	-0,337606996	-0,754891599	-0,166575384	-1,144050877	0,314589025	-0,227052705	-0,438325168	-0,627026119
266992	-0,057355588	-0,107258711	-0,017989728	-0,004787528	-0,106497386	0,043691723	-0,139558009	-0,193176863	-0,459972242
286746	0,063561992	0,052225312	-0,215107467	0,133081226	0,019999248	0,41747166	0,000130053	-0,07650219	-0,255823527
286834	0,220346786	0,104239405	0,138535349	0,124038187	-0,164150244	-0,312625284	0,058096596	-0,107824914	-0,500172612
30086	-0,014470083	-0,027644472	-0,19417272	-0,053460251	-0,062479493	-0,041562994	-0,233976586	0,074570192	0,440749385
30104	-0,073032879	0,017108497	-0,159022564	-0,39766273	-0,300465044	0,482059968	0,181992645	-0,018778779	-0,093866758
30295	-0,738767634	-0,039758529	-0,040997825	-0,127248129	-0,214533935	-0,24672687	-0,281473189	-0,088369709	-0,155857975
30452	0,025087411	0,014793907	-0,056990759	-0,072617107	-0,109608218	-0,018760696	-0,216012391	0,036645215	-0,619759445
30466	0,138575589	0,090904252	0,083407239	0,135930728	0,375786105	-0,299744676	-0,090689499	0,107481429	0,573803943
30480	0,117610147	0,175067935	0,093117405	0,119461934	0,07322665	-0,032991584	-0,420858077	0,315253707	0,132140481
30629	-0,046759478	0,021682009	0,286919855	-0,020962274	-0,027281687	0,102102668	0,414910132	0,242444645	-0,243010485
30719	0,216838595	0,134197896	-0,295464939	0,369064151	-0,406205832	-0,039946257	-0,361565845	0,093087923	-0,228112811
30735	0,126954683	0,009496784	0,146304491	0,276170751	0,114300072	-0,234723989	0,122999547	-0,011980144	-0,826535192
317638	-0,061942212	-0,277161748	-0,891841228	0,180168597	0,393354756	1,470029155	-0,011478034	-0,268037063	-0,39624624
317743	-0,066740182	-0,144855986	-0,017024801	-0,002209039	-0,016082954	-0,157725436	0,002846678	-0,056924944	-0,407369291
321129	0,041384016	0,057754253	0,167113214	-0,0717624	0,230920796	0,169937421	0,056375964	0,073843062	0,593579633
321505	0,195259945	0,027531398	0,333394074	0,270075954	0,280167764	0,032104848	0,15849645	-0,006564412	0,639130643
321622	-0,214336525	-0,153431376	0,053344446	-0,110605037	0,210701423	-0,017382784	0,262123452	-0,19275815	-0,870803171
321837	0,32942248	-0,058662854	-0,167128663	-0,036880518	-0,066451373	1,181644931	0,237526182	0,035488939	-0,102098145
322226	-0,07281608	-0,187858769	-0,06062425	0,03259414	0,030116573	-0,035121981	-0,049042079	-0,106146706	0,416342019
322468	0,153934244	-0,030259379	-0,257898552	0,251327549	-0,065519463	0,224069263	-0,09446873	0,108643797	-1,068383805
322508	-0,415186681	-0,424084155	-0,452399589	-0,214171426	-0,339023084	0,28377805	-0,003310885	-0,327189323	0,218151093
322527	0,039123723	-0,060910686	0,087549213	-0,087031098	0,073524647	-0,043820415	-0,082241107	0,034674395	0,423051017
322846	-0,003746594	-0,108414621	-0,274585122	-0,139962236	-0,42214816	0,495043879	0,013374438	-0,075155552	-0,031171688
323099	-0,055716321	-0,106653809	-0,190353974	0,024011296	-0,717308474	-0,051304781	-0,118827488	-0,015022049	-0,183909569
323500	-0,081131318	-0,205045544	-0,176127798	-0,119244945	-0,119714706	0,060162102	0,068601536	-0,051966829	0,431870786
323630	0,405802777	-0,020444162	0,256739827	0,287107201	0,265176	-0,210989938	-0,430836443	-0,019629613	0,200723683
323754	-0,076454657	-0,466954849	-0,346768982	-0,025723827	0,127578691	-0,386969966	-0,221325325	-0,362154747	-0,998420553
324487	-0,340722358	-0,20718248	-0,09528501	-0,097791434	-0,132552454	0,316827978	0,523779424	-0,24928233	-0,202950515
324490	-0,064531104	-0,103819013	-0,499293959	0,045142708	-0,743156046	0,243874403	-0,122667698	-0,182323152	-0,309974526
326281	-0,106729333	0,160705075	-0,126280056	0,080002685	-0,023317772	-0,164527029	-0,022819883	0,028488588	-0,428825311
326672	-0,473662213	-0,454598548	-0,574064663	-0,410957695	-0,599799329	0,195065118	-0,256967867	-0,707155174	-0,570402763
326857	0,132428388	0,02694755	0,161879684	0,068647522	0,004319688	1,396224817	0,200636087	0,051305189	-0,09368274
327060	0,278154422	-0,150552045	0,260083671	-0,461590315	0,369090075	0,631288496	0,385994583	-0,039658447	0,060950831
327226	-0,471143647	0,007929183	0,091013254	-0,411414493	0,015921376	0,176280848	0,253800566	-0,008439797	-0,05915265
327322	-0,003614095	-0,435522825	0,070979245	-0,056827903	-0,004971905	0,377419674	0,158951944	0,180868199	0,41203126
327556	0,630516096	0,061467151	-0,579247738	0,093271884	-0,474945643	0,572019374	-0,213058419	-0,267180093	-0,374962667
327572	-0,06733764	-0,247487695	-0,214634427	-0,234845783	-0,297509961	-0,01636767	0,051811982	-0,138434706	-0,49230272
327586	-0,209419448	-0,017232089	-0,689884677	0,308693881	-1,046276833	-0,022267786	-0,841251731	-0,308506777	-1,373834151
327588	1,97174875	0,013483844	-0,273182862	-0,010831849	-0,356878798	0,35347623	-0,119076536	-0,203651481	-0,092585891
333974	0,103242717	-0,09965203	-0,16650687	-0,170167051	-0,109515151	1,269957311	0,314183227	0,205948877	-0,144366955
334054	0,124425286	0,041735907	-0,075777131	-0,029943213	0,022293024	-0,182008588	-0,109132829	-0,005605785	0,413767885
334271	0,034249428	-0,222213088	-0,149334809	0,124222473	-0,075592569	0,208377659	-0,001572543	-0,517322569	-0,327043296
334351	-0,251362068	0,08378895	-0,082538065	0,160999651	-0,100779214	-0,359772824	-0,406150346	-0,007058294	0,440228554
334402	-0,120335178	-0,075664276	-0,086696877	-0,049852391	-0,035871057	0,440033938	0,153284902	-0,058144864	-0,124449739
335134	0,437049911	0,333986326	0,550258945	0,222657053	0,14271089	-0,011038236	0,141034693	0,581018763	0,388988901
335152	0,612182388	-0,202314648	0,207524534	0,545547749	-0,222854125	0,916706771	-0,193600373	0,26705807	-0,025395312
335386	0,052616482	0,16022175	-0,028849387	0,06814039	-0,038932365	-0,457202317	-0,327017164	0,117468432	0,356955643
335654	-0,260783368	-0,043842967	-0,122782911	-0,250572107	-0,817566738	-0,154088948	-0,193133986	-0,022152179	-0,819458415
335709	0,509383463	-0,21847259	0,040848543	0,25001569	-0,080827975	-0,056639402	-0,136697386	-0,323524818	-0,1884919
335722	0,177843009	0,118837082	-0,15552817	-0,022141396	0,053091576	-0,257030275	0,133468857	0,192857985	0,610196849
335732	-0,368120965	0,131618812	0,341580132	-0,220769294	-0,0552383	-0,117914102	-0,417320948	0,1959891	0,046674349
336057	0,754871955	0,68898351	0,529281449	0,491796701	0,431887272	-0,030426956	0,116908785	0,649570443	0,637991998
336798	-0,284722479	-0,286912225	-0,350429923	-0,302628503	-0,33214571	0,028124511	0,117072088	-0,414294268	-0,779602038
337153	0,331296258	0,042052928	0,093965216	0,008918522	0,094739213	0,046031949	0,106410382	0,209918559	0,609258051
337556	-0,028919122	-0,126205872	-0,023435841	-0,058714886	0,04427985	-0,095132376	0,253083744	-0,167412894	-0,608605601
337583	0,477873732	0,048170092	0,376396769	0,071793929	0,032077062	-0,028283972	-0,128816231	0,092781763	0,429114371
337597	1,222801611	0,083747414	0,420537461	-0,100865576	0,159951027	-0,220230415	-0,293894151	-0,056189795	0,145049089
338306	-0,025674784	0,216389225	0,37996087	-0,042732976	0,393921156	-0,067835675	0,107603416	0,192940476	0,53991606
352913	-0,297251965	-0,05495135	-0,159574466	-0,190477742	-0,228062002	0,007429112	0,057333748	-0,12774422	0,537003131
352924	0,324048885	0,028193968	-0,180249464	0,15672711	-0,05877417	1,015209699	0,194456458	0,151527457	0,100419589
352926	0,15084056	0,134611725	-0,026433044	0,209486251	0,02635727	0,928649516	-0,024831997	-0,109063014	-0,215185818

Supplementary Table 1 Continued

AffyIDs	AM	APAP	CPZ	CsA	EE2	PQ	TAA	TET	VPA
100537540	0,032080102	0,019188718	-0,067362311	0,029042973	-0,023024287	0,233075253	0,229199158	0,024246087	0,547341539
100537689	0,075054204	0,27715898	0,197770607	0,152611281	0,033972845	-0,112522427	-0,178243751	0,268143174	0,552500516
100537894	0,139526985	0,176243635	0,270368246	-0,345348038	0,107918232	-0,640562214	-0,515878741	0,39094572	0,069956986
100537990	-0,161751133	0,214261935	0,077384327	0,217983354	-0,064899189	-0,649314856	-0,672587299	0,163215326	0,12667035
100538016	0,109236185	-0,078924435	-0,506766637	-0,242709709	0,005924669	1,194630922	0,100168636	-0,209478658	-0,114270644
100538043	-0,875779408	0,001833752	-0,649342497	-0,509547028	-0,564143056	-0,15330632	0,037082468	-0,431715201	-0,516602091
100538068	0,330761312	-0,24958458	0,347289939	-0,22397333	0,162651124	-0,251153263	0,048149253	0,243072607	0,802978875
100538165	0,555524991	0,151131649	0,088247659	0,810305372	0,048898559	0,153603367	0,103055676	-0,036635942	-0,4131546
114417	-0,829668097	0,282259895	-0,151621075	0,006606543	0,319509247	0,015439921	-0,423048711	0,135801627	-0,632313598
114426	-0,804474709	-0,379760871	-0,490820441	-0,521128963	-0,259974523	0,471812795	-0,243538888	-0,518093017	-0,219711745
114551	-1,114296675	-0,36378373	-0,660637741	-0,855229073	-0,572338757	-0,462802137	-0,519617523	-0,147916972	-0,49062445
140428	-0,607171975	-0,009991584	0,139084058	0,006018427	-0,308245127	-0,214245708	-0,599248221	0,152227399	-0,39085239
140817	-0,181251706	-0,337606996	-0,754891599	-0,166575384	-1,144050877	0,314589025	-0,227052705	-0,438325168	-0,627026119
266992	-0,057355588	-0,107258711	-0,017989728	-0,004787528	-0,106497386	0,043691723	-0,139558009	-0,193176863	-0,459972242
286746	0,063561992	0,052225312	-0,215107467	0,133081226	0,019999248	0,41747166	0,000130053	-0,07650219	-0,255823527
286834	0,220346786	0,104239405	0,138535349	0,124038187	-0,164150244	-0,312625284	0,058096596	-0,107824914	-0,500172612
30086	-0,014470083	-0,027644472	-0,19417272	-0,053460251	-0,062479493	-0,041562994	-0,233976586	0,074570192	0,440749385
30104	-0,073032879	0,017108497	-0,159022564	-0,39766273	-0,300465044	0,482059968	0,181992645	-0,018778779	-0,093866758
30295	-0,738767634	-0,039758529	-0,040997825	-0,127248129	-0,214533935	-0,24672687	-0,281473189	-0,088369709	-0,155857975
30452	0,025087411	0,014793907	-0,056990759	-0,072617107	-0,109608218	-0,018760696	-0,216012391	0,036645215	-0,619759445
30466	0,138575589	0,090904252	0,083407239	0,135930728	0,375786105	-0,299744676	-0,090689499	0,107481429	0,573803943
30480	0,117610147	0,175067935	0,093117405	0,119461934	0,07322665	-0,032991584	-0,420858077	0,315253707	0,132140481
30629	-0,046759478	0,021682009	0,286919855	-0,020962274	-0,027281687	0,102102668	0,414910132	0,242444645	-0,243010485
30719	0,216838595	0,134197896	-0,295464939	0,369064151	-0,406205832	-0,039946257	-0,361565845	0,093087923	-0,228112811
30735	0,126954683	0,009496784	0,146304491	0,276170751	0,114300072	-0,234723989	0,122999547	-0,011980144	-0,826535192
317638	-0,061942212	-0,277161748	-0,891841228	0,180168597	0,393354756	1,470029155	-0,011478034	-0,268037063	-0,39624624
317743	-0,066740182	-0,144855986	-0,017024801	-0,002209039	-0,016082954	-0,157725436	0,002846678	-0,056924944	-0,407369291
321129	0,041384016	0,057754253	0,167113214	-0,0717624	0,230920796	0,169937421	0,056375964	0,073843062	0,593579633
321505	0,195259945	0,027531398	0,333394074	0,270075954	0,280167764	0,032104848	0,15849645	-0,006564412	0,639130643
321622	-0,214336525	-0,153431376	0,053344446	-0,110605037	0,210701423	-0,017382784	0,262123452	-0,19275815	-0,870803171
321837	0,32942248	-0,058662854	-0,167128663	-0,036880518	-0,066451373	1,181644931	0,237526182	0,035488939	-0,102098145
322226	-0,07281608	-0,187858769	-0,06062425	0,03259414	0,030116573	-0,035121981	-0,049042079	-0,106146706	0,416342019
322468	0,153934244	-0,030259379	-0,257898552	0,251327549	-0,065519463	0,224069263	-0,09446873	0,108643797	-1,068383805
322508	-0,415186681	-0,424084155	-0,452399589	-0,214171426	-0,339023084	0,28377805	-0,003310885	-0,327189323	0,218151093
322527	0,039123723	-0,060910686	0,087549213	-0,087031098	0,073524647	-0,043820415	-0,082241107	0,034674395	0,423051017
322846	-0,003746594	-0,108414621	-0,274585122	-0,139962236	-0,42214816	0,495043879	0,013374438	-0,075155552	-0,031171688
323099	-0,055716321	-0,106653809	-0,190353974	0,024011296	-0,717308474	-0,051304781	-0,118827488	-0,015022049	-0,183909569
323500	-0,081131318	-0,205045544	-0,176127798	-0,119244945	-0,119714706	0,060162102	0,068601536	-0,051966829	0,431870786
323630	0,405802777	-0,020444162	0,256739827	0,287107201	0,265176	-0,210989938	-0,430836443	-0,019629613	0,200723683
323754	-0,076454657	-0,466954849	-0,346768982	-0,025723827	0,127578691	-0,386969966	-0,221325325	-0,362154747	-0,998420553
324487	-0,340722358	-0,20718248	-0,09528501	-0,097791434	-0,132552454	0,316827978	0,523779424	-0,24928233	-0,202950515
324490	-0,064531104	-0,103819013	-0,499293959	0,045142708	-0,743156046	0,243874403	-0,122667698	-0,182323152	-0,309974526
326281	-0,106729333	0,160705075	-0,126280056	0,080002685	-0,023317772	-0,164527029	-0,022819883	0,028488588	-0,428825311
326672	-0,473662213	-0,454598548	-0,574064663	-0,410957695	-0,599799329	0,195065118	-0,256967867	-0,707155174	-0,570402763
326857	0,132428388	0,02694755	0,161879684	0,068647522	0,004319688	1,396224817	0,200636087	0,051305189	-0,09368274
327060	0,278154422	-0,150552045	0,260083671	-0,461590315	0,369090075	0,631288496	0,385994583	-0,039658447	0,060950831
327226	-0,471143647	0,007929183	0,091013254	-0,411414493	0,015921376	0,176280848	0,253800566	-0,008439797	-0,05915265
327322	-0,003614095	-0,435522825	0,070979245	-0,056827903	-0,004971905	0,377419674	0,158951944	0,180868199	0,41203126
327556	0,630516096	0,061467151	-0,579247738	0,093271884	-0,474945643	0,572019374	-0,213058419	-0,267180093	-0,374962667
327572	-0,06733764	-0,247487695	-0,214634427	-0,234845783	-0,297509961	-0,01636767	0,051811982	-0,138434706	-0,49230272
327586	-0,209419448	-0,017232089	-0,689884677	0,308693881	-1,046276833	-0,022267786	-0,841251731	-0,308506777	-1,373834151
327588	1,97174875	0,013483844	-0,273182862	-0,010831849	-0,356878798	0,35347623	-0,119076536	-0,203651481	-0,092585891
333974	0,103242717	-0,09965203	-0,16650687	-0,170167051	-0,109515151	1,269957311	0,314183227	0,205948877	-0,144366955
334054	0,124425286	0,041735907	-0,075777131	-0,029943213	0,022293024	-0,182008588	-0,109132829	-0,005605785	0,413767885
334271	0,034249428	-0,222213088	-0,149334809	0,124222473	-0,075592569	0,208377659	-0,001572543	-0,517322569	-0,327043296
334351	-0,251362068	0,08378895	-0,082538065	0,160999651	-0,100779214	-0,359772824	-0,406150346	-0,007058294	0,440228554
334402	-0,120335178	-0,075664276	-0,086696877	-0,049852391	-0,035871057	0,440033938	0,153284902	-0,058144864	-0,124449739
335134	0,437049911	0,333986326	0,550258945	0,222657053	0,14271089	-0,011038236	0,141034693	0,581018763	0,388988901
335152	0,612182388	-0,202314648	0,207524534	0,545547749	-0,222854125	0,916706771	-0,193600373	0,26705807	-0,025395312
335386	0,052616482	0,16022175	-0,028849387	0,06814039	-0,038932365	-0,457202317	-0,327017164	0,117468432	0,356955643
335654	-0,260783368	-0,043842967	-0,122782911	-0,250572107	-0,817566738	-0,154088948	-0,193133986	-0,022152179	-0,819458415
335709	0,509383463	-0,21847259	0,040848543	0,25001569	-0,080827975	-0,056639402	-0,136697386	-0,323524818	-0,1884919
335722	0,177843009	0,118837082	-0,15552817	-0,022141396	0,053091576	-0,257030275	0,133468857	0,192857985	0,610196849
335732	-0,368120965	0,131618812	0,341580132	-0,220769294	-0,0552383	-0,117914102	-0,417320948	0,1959891	0,046674349
336057	0,754871955	0,68898351	0,529281449	0,491796701	0,431887272	-0,030426956	0,116908785	0,649570443	0,637991998
336798	-0,284722479	-0,286912225	-0,350429923	-0,302628503	-0,33214571	0,028124511	0,117072088	-0,414294268	-0,779602038
337153	0,331296258	0,042052928	0,093965216	0,008918522	0,094739213	0,046031949	0,106410382	0,209918559	0,609258051
337556	-0,028919122	-0,126205872	-0,023435841	-0,058714886	0,04427985	-0,095132376	0,253083744	-0,167412894	-0,608605601
337583	0,477873732	0,048170092	0,376396769	0,071793929	0,032077062	-0,028283972	-0,128816231	0,092781763	0,429114371
337597	1,222801611	0,083747414	0,420537461	-0,100865576	0,159951027	-0,220230415	-0,293894151	-0,056189795	0,145049089
338306	-0,025674784	0,216389225	0,37996087	-0,042732976	0,393921156	-0,067835675	0,107603416	0,192940476	0,53991606
352913	-0,297251965	-0,05495135	-0,159574466	-0,190477742	-0,228062002	0,007429112	0,057333748	-0,12774422	0,537003131
352924	0,324048885	0,028193968	-0,180249464	0,15672711	-0,05877417	1,015209699	0,194456458	0,151527457	0,100419589
352926	0,15084056	0,134611725	-0,026433044	0,209486251	0,02635727	0,928649516	-0,024831997	-0,109063014	-0,215185818

Supplementary Table 1 Continued

AffyIDs	AM	APAP	CPZ	CsA	EE2	PQ	TAA	TET	VPA
359839	0,479687327	0,109981014	0,30926214	0,162151669	0,093266595	0,0113315	-0,025023544	0,132775056	0,169536433
360208	0,459206006	-0,149742358	-0,290689873	0,297535571	-0,100303616	-1,740937902	-0,410042471	-0,346398683	-0,380541284
368234	-0,921592701	0,154292205	-0,276882408	-0,168083465	0,107833036	-0,034663386	-0,194832748	-0,073825985	-0,543916532
368278	0,282829636	0,174953409	0,198744307	0,066170989	0,392525244	0,076903004	0,065584825	-0,004090836	0,886144023
368323	-0,077963329	-0,167186126	-0,132929648	-0,095527171	-0,435635453	0,34431153	-0,038128519	-0,008992468	-0,16002908
368410	-0,603875338	0,114410518	0,072999116	-0,10852379	0,062499376	-0,243617873	-0,10235456	0,322540516	-0,443289483
368620	-0,005451226	-0,037655535	-0,194356452	-0,084813868	-0,212467248	0,983532236	-0,035392498	-0,03829026	-0,044107728
368924	-0,585808425	-0,59918175	-0,828545118	-0,685756297	-4,157908747	-0,086400219	-0,434469585	-0,501681499	-0,435406943
373084	-0,276493882	-0,153125048	-0,395185391	-0,385696614	-0,285893647	1,091642557	-0,272995838	-0,242800126	-0,21843825
373102	-0,000500607	-0,252644329	-0,681951694	-0,041223235	-0,789393842	0,513213896	0,075580766	-0,336475222	-0,27047218
378720	0,28234515	-0,089112553	-0,093863504	-0,033899656	0,052691823	0,19058295	0,272378513	0,105697299	0,436285005
378721	0,078716802	-0,080464315	-0,014823277	-0,067595093	-0,007473072	1,025444209	0,153468801	-0,024365191	0,044191726
378727	-0,582030485	-0,288850776	-0,794884703	-0,087708203	-1,840422004	0,457097112	-0,29104465	-0,127073922	-1,150999772
378855	-0,045057265	-0,050396399	-0,130179368	-0,370473299	-0,507166576	0,137394341	-0,268989711	-0,215792062	-0,366382841
378963	-0,036365645	-0,226588197	-0,111409429	0,119962801	-0,029189251	-0,27136137	-0,09314123	-0,150608706	-0,575941301
378998	0,046093058	-0,281845323	-0,426262009	-0,074956481	-0,241536703	0,145288924	0,36688363	-0,123364332	0,068092506
386638	-0,064575856	0,486949756	0,439258279	0,233457463	0,81416921	0,228314436	0,292764444	-0,028649705	0,702876212
386663	-0,398012476	-0,105493613	-0,192763377	0,001339172	-1,299189566	-0,172685574	-0,452080822	0,040861364	-0,012448659
386920	-0,215585807	-0,342935205	-0,240719243	-0,098575358	-0,233346576	-0,001470128	-0,093563009	-0,344587516	-0,639854524
393129	0,6806382	0,36183664	0,186791252	0,223710988	0,283639699	-0,008836717	-0,129360837	0,231655951	-0,060757341
393148	0,127654994	0,16756214	0,245315457	0,037604479	0,237936371	-0,188080078	0,035001677	0,082579109	0,515144242
393155	0,321692355	0,050437981	0,042030735	-0,224620365	-0,0190612	1,115012921	0,122057451	-0,076167136	-0,162018192
393167	0,320817204	0,322042963	-0,236637393	0,018556757	-0,048635077	1,725752562	-0,436324702	0,114294343	0,093168268
393174	0,055743498	0,157037691	0,061679897	0,151911923	0,161664057	-0,213998995	-0,24059598	0,26331524	0,475251383
393180	-0,38567209	-0,340270944	-0,213452615	-0,115504544	-0,379070042	-0,259577411	-0,231330032	-0,485446003	-0,20957612
393187	-0,069201846	0,032967144	-0,107335179	0,051593854	-0,076658348	-0,140239108	-0,151138124	-0,094228765	-0,482415721
393195	-0,021979669	-0,008303654	0,402252195	0,136456397	0,117204214	-0,267830114	-0,284339223	-0,028604514	0,256506421
393247	0,541418561	0,225374405	0,03431093	0,215660909	0,011704921	-0,239119699	-0,292013841	0,239295375	0,259779644
393307	0,099675597	-0,026612783	-0,243557617	0,024063286	-0,018155981	0,681048784	0,046796173	-0,022871277	-0,47203523
393358	-0,09746647	0,070456761	0,080284541	-0,131348324	0,059433522	-0,013511526	-0,111497829	0,231407057	0,581467624
393412	0,430385063	0,301327621	-0,045540897	0,536058045	-0,116761584	-0,03506636	-0,14328556	0,208897371	-0,114561171
393461	0,153376059	0,341119886	0,25779791	0,329906228	0,316989501	0,682162712	-0,205455277	0,406840076	0,747801875
393464	0,078719981	-0,01959624	0,026238509	-0,147620139	-0,174825481	0,080096686	-0,141880221	0,043770786	0,440682966
393484	2,874037128	0,336366008	0,049139838	0,066624806	-0,024066496	0,198602279	0,016432913	0,205066943	1,374450382
393486	-0,333127514	-0,052086721	-0,390855711	0,137715071	-0,000627169	0,072932136	0,061497019	0,088242739	-0,651115996
393489	0,052681319	-0,083724903	-0,156829923	-0,082538616	0,007345232	0,592483736	0,013809016	0,055148152	0,019069285
393500	-0,282592442	-0,225259295	-0,058324671	-0,220358508	-0,518526653	0,030452897	-0,015549802	-0,071438188	-0,202994103
393511	0,176904014	-0,074734531	-0,206254236	-2,152264826	-0,25349777	-0,370291972	0,264273699	-0,252598459	-0,669340652
393530	0,211052206	0,317883683	0,058971437	0,638420695	-0,073317002	-0,211282831	-0,326368857	-0,056403009	0,039818252
393541	-0,069364152	0,063004358	-0,12025215	-0,058697707	-0,753769145	0,082468115	0,004775871	-0,02252417	-0,144755874
393548	0,54572582	0,068603444	0,140376979	0,363267782	0,14466193	0,779054092	-0,010284944	0,394456357	-0,063493332
393556	2,037621597	0,129070088	0,097600501	0,07910088	0,287308104	0,447060649	0,261230704	0,294361627	0,686881345
393561	1,446555276	0,046592034	-0,156609752	0,33198864	0,164590445	1,037914845	0,212710971	0,031634944	-0,006134476
393608	0,286889425	0,029908819	-0,04168862	0,175475634	-0,105631773	-0,067424119	-0,416995136	-0,077495234	0,146661526
393612	0,524338562	0,238555478	0,248461934	0,07080861	0,385216983	-0,092531913	-0,091518393	0,349206983	0,422787919
393661	-0,080646094	0,102169055	-0,294179298	0,195000131	-0,732269521	-0,196557444	-0,116003515	-0,217970967	-0,068810719
393673	0,091218984	0,089954989	0,043448632	0,103970832	-0,557536884	0,235737522	0,136102612	-0,012020483	0,220364345
393699	-0,531884857	-0,638772647	-0,741942331	-0,716632646	-0,767288922	0,064534036	0,29494605	-0,489534569	-0,455697591
393813	-0,036675856	-0,294016388	-0,254161645	-0,118519465	-0,098450608	0,061570566	-0,125587154	-0,55362855	-0,205041011
393856	-0,071607431	-0,051482055	-0,004092601	-0,006209617	-0,072439586	-0,134848776	0,181416983	-0,164538241	0,526018823
393910	0,003203895	0,119649448	0,190118766	-0,061743718	0,018460736	-0,077594315	0,052426659	0,11258411	0,502424575
393923	0,03940439	-0,129959864	-0,352001294	-0,010774026	-0,350844589	0,206632377	0,015048906	-0,58398356	-0,499095474
393939	0,236553395	-0,402061048	-0,444344827	-0,37772028	-0,068515321	1,397726762	0,129311869	0,013038227	-0,26488883
393940	0,5190899	-0,046551632	-0,261776152	0,266193731	-0,250690792	0,307783979	-0,090928476	-0,150944312	-0,192464769
393984	-0,266652216	-0,119867427	0,025454453	-0,434836793	-0,185065041	-0,035115945	0,046126031	-0,031759976	-0,02847595
393989	-0,568519401	-0,316880102	-0,022224972	-0,031176563	-0,354718931	-0,088652429	-0,256404199	-0,050855925	-0,578122556
393993	0,104614932	0,105172673	0,199349363	-0,174507528	-0,282123035	0,111523101	0,503176304	0,171231377	0,540948191
394028	0,445826761	0,3239982	0,11101987	0,105058495	0,174256152	0,054959352	0,028845512	0,33981957	0,433043373
394050	-0,084527392	-0,03653309	0,00785986	-0,074583353	-0,033458912	-0,071045975	-0,011679024	0,025207567	-0,60175834
399483	0,052105216	0,136590999	0,004492458	0,03451445	0,19866668	-0,315645849	-0,09916448	0,157390622	0,407457554
399650	-0,473194326	-0,384570164	-0,70652566	-0,307693771	-1,294317309	0,466983224	0,157854179	-0,792418496	-0,065831063
402815	-0,235151692	-0,182479727	-0,115526876	-0,044247577	-1,214842009	-0,152368793	-0,065583773	-0,152465407	-0,335779162
402940	0,247226887	0,138155016	-0,490396825	0,256329147	-1,230497249	-0,127064672	-0,759476404	0,199915213	-0,496687984
402981	1,067303294	0,03154631	0,060629647	0,453187023	0,097366006	0,361541066	-0,190781743	0,070542352	0,155901315
403002	0,221352367	0,468323118	-0,008987873	0,234164068	-0,127157284	-0,287405084	-0,361077682	0,255048277	-0,068549254
403031	-0,046598346	0,217779273	0,317393919	0,035393131	0,256107766	-0,065983044	-0,013415112	0,451354123	0,145410518
403075	0,064507455	0,213921597	0,274771834	0,075129186	0,100145446	-0,076296903	0,302558444	0,083425824	1,008609157
403307	-0,361867348	0,045854675	-0,343575837	-0,533785	0,226221977	-0,426274904	-0,403112397	0,349979429	-0,226451923
403309	-0,182687565	-0,161011093	-0,4626039	-1,250403535	-0,251336523	0,280906553	-0,521304967	0,132206238	-0,234179716
404625	0,08110349	-0,393224226	-0,303638037	-0,23824307	-0,342602852	0,370333864	0,207009907	-0,04108762	-0,093063729
404730	0,450084155	0,087517907	-0,373322377	0,160666943	-0,063011599	0,517928187	-0,155499515	-0,073398784	-0,59126289
405758	0,0357032	-0,194925686	-0,033297264	-0,034623597	-0,00649407	0,122642366	0,793305913	0,085330011	0,13967882
405769	-0,321554571	-0,29731936	-0,114827069	-0,398089789	-0,234361117	-0,022600625	-0,020161203	-0,094123575	-0,595706952
405781	0,1077811	-0,073051388	-0,506489356	-0,103670795	-0,178314049	0,953398805	0,246890801	-0,369465358	-0,27303013

Supplementary Table 1 Continued

AffyIDs	AM	APAP	CPZ	CsA	EE2	PQ	TAA	TET	VPA
405805	-0,07069949	0,008145049	-0,367890618	-0,06730752	-0,191990448	1,135812295	-0,054018161	-0,183544236	-0,140406465
405817	-0,620178509	-0,08053643	-0,254933453	-0,173634574	-0,611386018	-0,243315272	-0,515131927	-0,230967725	-0,675633267
405865	-0,049343012	0,052701952	-0,411526538	0,133580957	0,108350056	1,408675367	0,073587461	0,346039855	-0,111240307
406247	0,175946517	0,085685198	0,219653303	-0,049137497	0,279089912	0,002401509	0,052482973	0,279806668	0,818910183
406265	0,180992127	0,144089542	0,253250161	0,058910636	0,261893821	-0,007049197	0,073875795	0,170360073	0,463789378
406270	0,235955395	0,228016692	0,329872846	0,225641531	0,340930064	-0,236031394	-0,019391822	0,174899595	0,445009895
406278	0,205861517	-0,408517859	-0,407881754	0,35018501	-0,389204295	0,12949153	-0,00639888	-0,224145012	-0,247773436
406290	-0,144031056	-0,045096179	-0,38846352	0,069825462	-0,200384757	0,18081698	0,056313991	0,029541446	-0,459492723
406304	0,01839155	-0,273273474	-0,721477485	-0,10679396	-1,07997758	-0,10245331	0,077130089	-0,107706219	-0,49321596
406311	-0,333997276	-0,283081456	-0,257774183	-0,318208188	-1,078446025	0,127952753	0,0563582	-0,173728402	-0,32181412
406312	-0,155532348	-0,098743038	-0,462005417	-0,003117318	-0,500849949	-0,045317325	-0,083510931	-0,454667092	-0,346327828
406376	-0,044741107	-0,208783497	-0,195750063	-0,148903073	0,114351093	0,594414516	-0,057967747	-0,037513898	0,031544233
406424	0,231365322	0,020902598	-0,205666065	0,436590077	-0,763333297	0,107810913	-0,485136126	-0,038635096	-0,513424145
406433	0,358520512	0,101688246	-0,385242228	0,120935628	0,203595931	1,692636001	0,303753168	0,045604259	-0,143731832
406452	0,577280663	0,040766955	-0,014190855	0,352926791	0,282385129	1,844254603	0,083267949	-0,043137342	-0,011168681
406484	-0,895566754	-0,55674095	-0,844593058	-0,938151687	-0,312491319	-0,428211918	-0,438878531	-0,649488343	-0,730645338
406537	-0,807156214	-0,079325554	-0,533593746	0,235809168	-0,733658664	-0,183253037	-0,567108547	-0,188068658	-1,185169412
406590	-0,315322519	-0,047290431	-0,194532864	-0,046910843	0,054034466	-0,440660757	-0,236712099	-0,084369014	-0,420483682
406762	0,42286332	0,157601164	0,107569873	0,187835436	0,256772292	1,554485793	0,301352942	0,156437203	0,273288144
406782	-0,116038449	-0,306029132	-0,109351984	-0,396685704	-0,307930072	0,239086546	0,226030898	-0,303390041	0,191719903
406812	-0,317260198	-0,304638512	-0,572522442	-0,294928906	-0,791233779	0,662385234	0,191623705	-0,3633874	-0,520522116
407629	-0,051744669	0,103538334	0,050191088	0,294235521	0,261193007	-0,398648898	-0,31875499	0,030832812	0,233655322
407661	-0,236223831	-0,087907302	0,0057648	-0,198679627	-0,073852228	-0,05803256	0,230851705	0,040652775	0,43154581
407667	-0,424434282	-0,566805922	-0,527967344	-0,064655535	-0,409740378	-0,075895218	-0,055728042	-0,166472537	-0,498608797
407732	-0,188394232	-0,136140393	-0,104577688	-0,201952174	-0,033791171	-0,010873287	0,049984103	-0,172648409	-0,453038985
415096	0,338904407	0,214333471	0,050761083	0,07955962	0,01409585	-0,073814423	-0,319514873	0,345756137	0,542166735
415164	0,637475212	0,150628822	-0,158393222	0,357757224	-0,014404177	0,117743018	-0,29633887	-0,075434122	-0,486449634
431765	-1,548002322	-0,308684643	-0,280906912	-0,677551021	-0,628396957	-0,129376783	-1,778524163	-0,329294425	-0,558441002
432384	0,877971264	-0,079815641	-0,29771337	-0,016312837	0,024808414	-0,070915923	-0,078134657	-0,290788515	-0,507533305
436612	0,12783633	0,069415864	0,122435802	0,182296887	0,091322997	0,112849803	0,180639216	0,103559201	0,539192532
436636	-0,148780145	0,003602372	-0,568765371	0,241642201	-0,419917404	-0,02880496	-0,24183478	-0,192658922	-1,043798641
436641	-0,000176919	-0,158078717	-0,515613317	-0,016535074	-0,345051769	-0,661784366	-0,611494546	-0,160767151	-1,623436962
436648	-0,034189297	-0,103522631	0,201106787	-0,271844713	0,164458638	-0,41149715	-0,064265598	0,146037145	-0,208916613
436651	0,402835766	-0,115027578	0,044689663	0,01831942	0,027146712	1,241924738	0,398746105	0,105288956	0,060811983
436726	-0,081758674	-0,21553419	-0,281262351	-0,138904728	-0,750954252	0,194093189	0,072312307	-0,191730764	-0,444752771
436734	0,351331695	0,227991381	-0,106634996	0,192046696	0,119484841	2,283202129	0,905187938	0,141426901	0,226466277
436762	0,344337757	0,459655617	0,25092441	0,106120828	0,30008401	0,189256803	0,54713925	0,16979714	0,981028825
436804	-0,080870938	-0,018494536	-0,022369067	0,032757332	-0,185870888	-0,11213335	0,041698342	-0,089758156	-0,786531329
436812	0,585339244	0,193702401	0,234418899	0,150608171	0,357498672	-0,128936346	-0,034195321	0,359851762	0,47265317
436823	0,347271025	0,143134542	0,160502164	0,258257998	0,221049173	2,190027565	0,611422825	0,511700252	0,288605519
436837	-0,503102191	-0,300619103	-0,313019758	0,120526679	0,056056413	0,339780418	0,867999086	0,240272953	0,638706346
436894	0,088824379	-0,042671085	-0,450225284	-0,10258565	-0,109975485	1,122692609	0,359735884	0,136835131	-0,182958605
436896	0,437499866	0,079740981	-0,137334935	0,100438613	-0,145683587	0,182002929	0,221068899	-0,042426549	-0,162112485
436914	-0,036697452	-0,067880143	0,084141896	-0,029065353	0,135932342	-0,157907771	-0,10029042	0,075646616	0,406822293
436917	0,404002512	-0,012668756	-0,322501248	-0,34174287	-0,184305258	0,269124343	0,046647662	-0,094897477	-0,040995107
436934	-0,043928744	-0,024418542	-0,014748983	0,00950792	0,170374629	-0,105950719	-0,139060184	0,168668894	0,585737441
436958	0,309836021	-0,097629301	0,047128543	0,23213349	-0,420907232	0,058633043	-0,206028261	-0,028900138	0,205824079
436969	1,410036396	0,067551571	-0,121793276	0,044534006	-0,004448061	1,131181732	0,369152918	0,186557036	0,536009018
437023	-0,191817582	0,01015733	0,152444818	-0,049976255	0,021633238	-0,016361728	0,074462048	0,068404615	0,429477506
445032	0,010016361	0,249493105	-0,053373563	-0,063260433	-0,060323074	-0,388326015	-0,711453706	-0,277964656	-0,452147664
445042	0,422974448	0,178231316	0,10212843	0,428111663	0,149724071	-0,229109595	-0,350435078	0,057351111	-0,077015141
445044	0,114015274	0,002273058	0,196285722	0,034006607	-0,049985816	-0,086201599	0,06321973	0,004560087	0,563232923
445072	-0,04719872	-0,471176942	-0,033096704	-0,187976702	-0,017846074	-0,097289164	0,032394857	0,056693084	0,021143381
445073	-0,215988862	0,370619723	-0,541439964	-0,132169857	-0,662756411	-0,46402632	-0,68897645	0,332873607	-0,220597739
445111	-0,014123703	-0,393790656	-0,277864901	0,356923402	-0,018158004	-0,194601585	-0,429471451	-0,699395447	-0,412747929
445155	0,405058333	0,188824663	-0,141706618	0,195606533	0,083565672	0,146942079	-0,205027277	0,036478348	0,40342752
445166	-0,220671394	-0,358696671	-0,313025111	-0,17376453	-0,008223394	0,500481767	-0,022982166	-0,098174224	-0,214341452
445175	1,072065553	0,120791731	0,173332214	0,460143232	0,155946788	-0,206673228	-0,306261451	0,196981838	0,061360607
445214	-0,244236363	-0,028214116	-0,155922272	-0,449106596	0,101466435	-0,218790013	-0,062586185	-0,062063138	0,434857068
445220	0,054608134	0,00479216	-0,055496587	-0,106622549	0,039964929	0,696390642	0,079343983	-0,047596376	0,227664698
445222	0,057903714	0,034251721	-0,000763035	-0,538162551	0,104616759	0,238245973	0,315820002	0,136192065	0,068591784
445315	0,478230817	0,003407486	0,028871467	0,339803454	-0,076107801	0,026029095	-0,163233565	-0,049835806	0,197528223
447825	-0,300146526	-0,148111532	-0,495474707	-0,160711633	-0,36951088	0,354173317	0,102232249	-0,083719131	-0,205899326
447836	0,065670482	-0,220445465	-0,112023448	0,226737345	-0,915118206	-0,100117781	-0,484078349	-0,425551186	-0,335448446
447840	0,199348321	0,025957991	-0,10503191	0,180045103	-0,317917461	-0,210456702	-0,349991956	0,026572453	-0,501335155
447859	0,038423628	-0,459888817	-0,317774007	-0,031247213	0,133670936	0,331395595	-0,20697872	-0,238489506	-0,165659556
447898	0,286617145	0,317159156	0,123743974	0,348019946	0,105702671	-0,459960727	-0,280523304	0,051332647	0,403451444
447911	0,08727481	0,164913188	0,231107257	0,018126694	0,056236303	-0,03037688	-0,071849934	0,136118916	0,822369523
447932	0,228024074	0,096111092	0,21699391	0,147681809	0,202317383	-0,222100587	0,115053516	0,176353137	0,651804789
447944	0,683356492	0,036968076	-0,096980392	0,100784743	0,260631659	0,121267252	-0,024556888	0,079708181	0,452104375
448857	-0,046598972	0,006213458	-0,024337715	0,050501938	0,004919488	0,394435016	0,099009095	0,022739424	-0,158257566
448859	0,139530516	0,011125854	0,042021935	-0,071455264	-0,01732576	0,512467388	0,365168621	-0,201390593	0,206151568
449537	0,071664157	0,061245628	0,071572514	0,2868765	-0,050815607	-0,106427996	0,768267375	0,296332114	0,134527657
449552	-0,05024328	0,029128784	-0,141879896	-0,022832664	-0,01508144	0,209478548	0,018373538	-0,038811771	0,907399915

Supplementary Table 1 Continued

AffyIDs	AM	APAP	CPZ	CsA	EE2	PQ	TAA	TET	VPA
449555	0,326583304	0,201346699	0,422037158	0,367804783	0,413538615	-0,039505862	-0,431995804	0,404977822	0,47328512
449656	-0,194165228	-0,090598288	-0,174371012	-0,061209988	-0,271779793	0,093055586	-0,071778364	-0,111150657	-0,512084178
449773	1,018979309	0,153384081	0,033222664	0,429634698	0,157865327	0,186737315	0,606511915	0,506429669	-0,289556919
449796	0,185782375	-0,000656304	-0,14537475	0,146749191	0,048870422	-0,332340562	-0,474802616	-0,218795739	-0,067882966
449797	0,074186995	-0,125196038	-0,054536087	0,135312055	0,099414849	0,243685745	0,425268564	0,135435729	0,324328444
449866	0,718329113	-0,044035983	-0,137516386	0,243622818	0,231548929	1,300241618	-0,030685331	0,299611059	0,130890941
450038	-0,228866994	-0,009257965	-0,507060742	-0,283020466	-0,206243817	0,241582339	0,130811954	-0,241067275	-0,038786291
450061	0,255680681	0,365443811	0,197560299	0,042592846	0,43449831	-0,044119415	-0,440519216	0,068221163	0,01234495
450066	0,125932245	0,332665524	0,390719068	0,227427492	0,178341426	0,006333391	0,05099075	0,231110177	0,390216799
450084	-0,155900376	0,021849218	-0,20074352	-0,099345386	0,054651151	1,260270859	-0,062704583	-0,159361236	0,088525706
474346	-0,386046328	-0,024055131	-0,058623622	-0,086714906	-0,033848051	0,02563634	0,24221495	-0,080850695	-0,250969901
492339	-0,122310423	-0,180771639	-0,122282437	-0,030981236	0,084544729	0,453801135	0,369859637	-0,103630252	-0,062892342
492409	0,117998182	-0,018121139	-0,09238308	0,054564393	-0,456259883	0,048500439	-0,004047936	-0,21481757	0,107755561
492647	-0,492010941	0,009473052	-0,232029037	-0,145761929	-0,318202466	0,285979746	-0,188728923	-0,012451342	0,020829851
492792	0,237616519	-0,068704204	-0,115476644	-0,034303988	-0,162372372	-0,035142587	0,199942513	-0,034969641	0,386885248
493608	0,136988258	-0,056798261	-0,106712865	-0,050392277	0,017276077	0,281001593	-0,234713371	0,051974848	0,452375196
494035	-0,055026903	-0,283498151	-0,558085988	-0,271358489	-0,086218725	0,375087036	0,147156708	-0,099226519	-0,161018985
494036	0,070949152	-0,193389401	-0,175852936	0,397556556	0,029867023	-0,499912411	-0,691461986	-0,451797449	-0,159687779
494176	-0,035883735	-0,125488688	-0,02082541	-0,191536474	-0,175004269	0,887360751	0,329674493	0,305194765	0,163010511
494476	0,066036062	-0,213843251	-0,419901753	0,116867745	-0,093946498	0,442957283	0,427336921	-0,187632689	-0,601924434
494487	-0,172397033	-0,039595908	-0,338793751	0,032054847	-0,589396657	-0,16476942	-0,34025898	-0,137662447	-0,739857952
494573	-0,682332502	0,07734739	-0,06701214	0,246397266	-0,230821882	-0,403711072	-1,672347785	-0,026239341	-0,547471214
497122	0,08735711	-0,137447673	0,096747206	0,027062141	-0,170606546	0,032876038	0,048879265	-0,094669015	-0,475960189
503516	0,084106811	0,031264651	0,096067131	-0,020284698	0,064978798	0,093961038	0,12802279	0,16467242	0,425049916
503751	-0,03780442	0,011807252	0,086221619	0,148860742	0,217684204	0,069054587	0,733223667	0,111569288	0,173183313
503752	-0,007117697	0,221518722	0,20421752	-0,064851275	0,297953127	1,006114191	0,081299099	0,300706248	0,491545381
503792	-0,152603337	-0,022144409	0,10197531	-0,224844696	0,144413958	-0,303414175	0,039170256	0,082855686	0,562131542
541319	-0,236799994	-0,078136501	-0,227302032	0,256227085	-0,504476351	0,215187676	-0,189105188	-0,047131133	-0,391411413
541344	0,218497801	0,099879849	-0,074442189	-0,180896606	0,234660272	2,756072692	1,67083357	0,219156644	0,056164071
541347	0,136165461	0,072110525	0,206624413	0,19497105	0,270818218	0,081650966	-0,072140437	0,142835241	0,467613485
541382	-0,305010553	-0,12921295	0,02532021	-0,247581649	-0,23691707	-0,092933932	0,25499419	-0,146415312	-0,481095003
541423	0,138868312	-0,191259876	-0,203801593	0,079057571	0,018514805	-0,314220765	-0,239673823	-0,070243395	0,400901734
541442	0,147680364	0,224996029	0,168588674	0,310944007	0,262192659	0,117535795	0,183191034	0,185194109	0,623949611
541449	0,265203584	-0,199006388	0,078476832	0,081074663	0,056452405	0,324590879	0,380367502	0,276809796	0,493937812
541523	-0,312005741	0,103792429	-0,052904388	-0,192235528	0,290229287	-0,356417813	-0,065652012	-0,02183802	-0,567810505
541544	0,329811805	0,207446946	0,181665443	0,218389328	0,135989274	-0,401627503	0,03108131	0,23032343	0,38942052
541548	0,025538059	-0,112252736	-0,175817046	-0,069998367	-0,064051569	0,439358921	0,027802733	-0,290310869	-0,070293843
544655	0,032393787	-0,140018485	0,031216156	-0,055707943	-0,02471436	-0,203926715	-0,196789423	0,004255314	0,419244939
550132	-0,003917016	-0,023558684	-0,09506466	-0,065121329	-0,030582767	0,06991645	-0,227493711	-0,022262418	0,41210176
550134	0,360102044	0,122555145	0,035839089	0,254328077	0,035633757	0,73437961	0,124509666	-0,044126105	0,064593605
550264	-0,190838111	-0,336278368	-0,336154764	-0,040486507	-0,142792155	0,43402901	-0,192471658	-0,1333544	-0,025462806
550276	0,391802713	0,301393053	0,021180115	0,070244413	0,136113825	1,331329423	0,140005646	0,082666724	-0,054009028
550345	-0,307521198	-0,044977841	0,009965386	-0,268165921	-0,221564629	-0,197172234	-0,028638326	0,056024168	-0,570580856
550360	0,099864567	0,140673973	0,105539918	-0,062965526	0,217727654	0,612705384	0,431374967	0,262096464	0,760844361
550385	0,059516459	-0,003752435	0,19149972	-0,033480131	0,099034526	-0,213697891	-0,371242708	0,062224231	0,449108881
550436	-0,012475283	0,053622408	-0,080770718	0,217185905	0,041193555	-0,299627003	-0,120364953	-0,064516725	-0,593705644
550446	0,358448903	0,21082742	0,206813866	0,309355362	0,20400292	-0,083678352	0,243036047	0,277593519	0,663818647
550460	0,466309679	-0,018999246	0,089294336	-0,022454652	0,050783208	-0,20125312	0,078228389	-0,295390769	0,336246831
550489	0,125698085	0,040784456	-0,196119579	-0,178682456	0,078097643	0,025366765	0,266400835	0,213926302	0,663276392
550515	0,310980397	0,159779636	0,066850658	0,021812567	0,301326836	-0,042989639	-0,111829737	0,164027868	0,53248237
550569	0,215050669	-0,199555464	-0,232477727	0,481411892	0,03684662	-0,145381291	-0,337080662	-0,408232795	-0,185853614
550580	0,536930417	-0,124719753	-0,175455528	0,21413403	0,184652346	2,128515444	0,307136054	0,18240314	0,384413185
550603	0,229715231	0,277084589	0,305667265	-0,01988602	-0,081536856	-0,042169082	0,003541231	0,142724081	0,76026528
552924	0,558208972	0,212070381	0,444708612	0,158100409	0,31831046	-0,085846655	0,192199494	0,284702668	0,46981057
552944	-0,233383386	-0,120045227	-0,228538683	-0,525872617	0,107538145	0,218343801	0,200199237	-0,17145513	-0,323556427
553062	-0,344415559	-0,141652604	-0,203063727	-0,26924431	-0,323289384	0,473617133	0,122032466	-0,077820749	-0,563024243
553066	-0,299319798	0,119229502	0,145034292	-0,463708745	-0,044711748	-0,045206144	0,152706739	0,15584053	-0,334363683
553256	-0,551027109	0,073251945	-0,487437072	-0,17715029	-1,373500045	-0,103169252	-0,205558489	-0,136477385	-0,993366656
553411	0,155515825	0,05904747	0,194460065	0,093511747	0,1064215	-0,071066377	0,211722277	0,236055349	0,645158757
553423	0,63221577	-0,137330675	-0,179659597	0,137832722	0,066935323	0,168853153	0,304300455	-0,07248171	0,273802357
553474	0,098383991	0,295444044	0,262356071	0,013109128	0,293449669	0,0250099	0,010658124	0,264751894	0,60937751
553495	0,130044962	0,096284674	0,367088174	0,171297644	0,409056519	-0,403565601	-0,419081248	0,160054055	0,367078732
553530	-0,069910037	0,430916731	-0,203096007	0,986612301	-0,139019768	-0,240482038	-0,803200573	0,272148205	-0,996542884
553537	0,613232948	-0,184137992	-0,047584052	-0,038124438	-0,224754682	1,839070554	0,244576807	0,234917789	0,106800449
553552	0,274772625	0,001834862	-0,073239517	-0,057734555	-0,022840441	2,684857148	0,705534178	0,459158976	-0,084161209
553575	0,391935938	0,077990378	-0,038909808	-0,018178744	0,141683178	1,824312139	0,673422676	0,206112966	0,041437752
553622	-0,041734896	-0,005096252	-0,051801489	-0,064176783	0,227365704	1,443460107	0,169490405	-0,038803138	-0,095166647
553688	0,334190206	0,055400491	-0,032057	0,104578538	-0,110882625	1,230508019	0,383444095	-0,108796406	-0,237303263
553694	0,290843316	0,020925958	0,076518105	0,52387814	-0,62901897	0,197722418	-0,385372493	0,013095126	0,199627139
553716	0,138419785	-0,093877015	-0,070019892	-0,223685916	-0,171596399	0,026496476	-0,001312815	0,068932302	0,492772335
553729	0,147122876	0,116942456	0,099689469	0,033023702	0,109997695	-0,128444105	-0,039994541	0,103453931	0,534169096
553770	0,342748279	0,188609899	0,280239717	0,499892788	0,571654808	-0,029719851	0,062735534	0,283200999	0,632018584
554036	0,178861216	0,282556484	0,16704213	-0,049628959	0,334346933	0,080121584	-0,167082148	0,325849951	0,417144706
554046	0,270052002	-0,204660191	-0,076899504	0,319136327	-0,528112706	0,022574332	-0,025127469	0,041311956	-0,114442838

Supplementary Table 1 Continued

AffyIDs	AM	APAP	CPZ	CsA	EE2	PQ	TAA	TET	VPA
554095	0,428577125	-0,022501303	-0,389207073	0,031464024	-0,31425628	-0,097605031	0,172005845	0,042436745	-0,041613194
554103	0,297787204	0,032983786	-0,027419333	0,519440865	0,031011651	0,083947337	-0,278601049	-0,251193343	-0,164081442
554150	0,005420948	0,049644683	-0,055266345	0,050317649	0,073802294	0,058924225	-0,068978056	0,078406976	0,616317282
554200	0,40407098	0,258023049	0,224566114	0,186327024	0,351474476	0,123929211	-0,214714088	0,423890412	0,513233387
554477	0,140580053	-0,288042865	-0,584898246	-0,031536113	-0,517412843	1,056977108	-0,005036342	-0,550816592	-0,446714513
555134	-0,023002678	0,008297096	0,11065884	-0,249270144	0,047811429	-0,201786507	-0,084536813	0,103182302	0,491452289
555196	0,061848131	0,129487204	0,149088955	0,154273403	0,150137699	0,152058096	0,102419171	0,197100759	0,547842127
555251	-0,135160853	-0,192185039	-0,051075115	0,008622973	-0,323794876	-0,329882938	-0,352683508	-0,190752733	-0,900026991
555297	0,11805001	0,10900451	-0,397995774	0,440456684	0,227608662	0,494947679	0,279999934	0,40464793	-0,343417998
555305	-0,57633899	-0,165497708	-0,261160353	0,044600117	-0,212944905	-0,496499332	-0,990369803	-0,20577095	-0,334522503
555334	-0,389935517	0,277401085	-0,042545719	-0,825721823	-0,649090204	0,101043448	0,093067366	0,187931747	-0,588064649
555344	0,032639875	-0,027406953	-0,116630595	-0,157716469	-0,337989251	0,255107558	0,738228067	-0,189890185	0,093428171
555467	-0,520830353	-0,347865574	-0,136388818	-0,210955609	-0,245467854	-0,125168338	-0,22790788	-0,279523264	0,32563182
555481	-0,680168497	-0,071460527	-0,700351107	0,406354276	-0,89166443	-0,707926071	-0,962753645	-0,036940436	-1,039583123
555510	0,787998127	0,123448759	-0,246742122	0,370920591	0,197479709	-0,063606715	-0,355062827	0,244004204	-0,427997703
555595	-0,04021652	-0,151388458	-0,15610002	0,025247719	-0,417247786	-0,055950985	-0,116501757	-0,108844727	-0,194547293
555795	0,285381567	-0,130450813	-0,42081701	-0,097829633	-0,782091959	0,256398899	-0,031093255	-0,289194784	-0,278959432
555812	-0,082615675	-0,095609778	-0,255426572	-0,080392024	-0,981508925	0,612650735	-0,113676701	-0,170150766	-0,115758798
555939	0,050672335	0,184753487	-0,038516594	0,069095003	0,032317729	-0,413258402	-0,594602524	-0,073154987	-0,528199961
555983	0,500866634	0,180113418	0,222479994	0,143816185	0,326098486	0,003275951	-0,070028647	0,298219164	0,358129046
556024	0,342950051	0,203602042	0,274293673	0,435830132	0,132399285	0,920133461	0,469691028	0,438449678	0,252217617
556199	0,152873064	-0,184491829	0,005435968	0,063915025	-0,438461476	0,119775067	-0,119892244	-0,211444506	0,139550524
556236	0,177777341	0,011385084	-0,1931642	-0,06406924	-0,479835818	0,022723029	-0,295375116	-0,085958272	-0,318005532
556258	-0,612174143	-0,649712285	-0,741749555	0,679851933	-0,953443404	0,240613824	0,101407155	-0,700667583	-0,623011746
556307	0,799591268	-0,016583578	0,056990356	0,037224166	0,168267608	0,044275378	0,037866507	-0,024627559	0,273261823
556765	-0,0772392	-0,005699905	0,081921403	-0,130676305	0,07775953	-0,015419209	0,07219171	-0,058341878	0,409907583
556898	-0,009478861	0,038199458	-0,031075565	0,406086397	0,051345738	-0,632725073	-0,409319253	0,2615822	0,229189459
556973	-0,147280494	-0,170704124	-0,153144454	-0,242467951	-0,247574649	-0,026835002	0,111195703	-0,147715065	0,556462592
557232	0,455963528	0,029321943	0,056666371	0,362908546	0,155982674	-0,084350477	-0,000642322	0,177028379	-0,055803951
557269	0,110443051	0,025141917	-0,308237642	0,413621133	-0,20243417	0,088485879	0,0810231	0,051995385	-0,456698482
557383	-0,471269472	-0,276868472	-0,30654746	-0,35885985	-0,517948748	-0,161555507	0,193674899	-0,253796942	-0,280247374
557565	-0,277025785	0,131808609	0,067883481	-0,051725682	0,006969904	-0,285044901	0,006737612	-0,137061914	0,537705103
557652	-0,002600933	0,008076957	0,131358869	-0,102296903	-0,07720355	1,171570017	0,08634497	-0,15201239	0,28284409
557660	-0,055116353	-0,204017879	-0,373503284	-0,054212789	-0,085726929	0,236768336	0,097406992	-0,181533605	-0,303051821
557898	0,556748403	0,110420652	0,262172439	0,168008488	0,130440712	0,400146864	0,16635844	0,067577906	0,502254011
557919	0,112519948	0,12508754	0,125773542	0,046317402	0,266116164	-0,312667592	-0,081505684	0,164458433	0,650424083
558146	-0,316286874	-0,091860275	-0,079838076	-0,034973097	-0,183526	-0,459192821	0,367568905	-0,343409416	-0,626621388
558154	0,533591167	0,019546723	-0,076556842	-0,064914309	0,258770879	0,00794058	0,03634981	-0,126510444	-0,009230706
558156	-0,174041593	-0,041414018	0,02441182	-0,015714194	-0,206569986	-0,141384924	-0,142560628	-0,094481927	0,483882818
558461	0,378549927	-0,175899977	-0,053152872	0,428265058	0,035478048	-0,069224155	0,013593495	0,15608499	-0,352659248
558552	0,366397561	-0,180618578	-0,023427922	-0,103855413	-0,079102361	0,704310572	0,166184408	0,251798676	-0,174577911
558687	0,493404157	0,100305757	-0,074880796	0,017241247	-0,179097211	-0,060009829	0,242975653	-0,037117449	0,323949667
558758	0,253998737	0,225624183	0,148232087	0,069180094	-0,078513908	0,531062111	0,139864022	-0,034341054	0,983312589
558800	-0,118039629	-0,049956099	-0,238179524	0,426105314	0,148559868	-0,116213998	-0,388651399	-0,266969589	-0,327809524
558816	0,201514831	-0,331858858	0,009022329	0,32241968	0,107992165	3,752250311	0,617670684	1,514705196	-0,346865786
558921	-0,505946946	-0,369754881	-0,546368052	-0,488279252	-0,34439486	0,295075161	-0,296736145	-0,410886006	-0,450505823
558924	-0,064697707	-0,426039056	-0,366319184	-0,02951143	-0,386035035	0,261620135	-0,008712996	-0,49946614	-0,353248615
558938	0,953788166	0,295787128	-0,048915433	0,425147174	-0,438396705	1,587541199	0,044568633	0,065063126	-0,274017225
559018	-0,325493298	-0,018517891	-0,051307906	0,362056916	0,253910634	-0,10815118	-0,536036333	-0,043307035	-1,211177917
559054	0,07054028	0,001580301	0,024611459	-0,585834635	-0,770280178	-0,175469251	-0,495638685	0,059874862	-0,17514655
559160	0,627233033	0,189536134	-0,330759217	0,186188336	-0,113824062	0,28584619	-0,030923252	-0,135492327	-0,036082591
559358	0,067171889	0,138142245	0,250370912	-0,122446869	0,231954617	0,005458174	0,370328241	0,275940544	0,660369869
559575	0,276716836	0,345607503	0,288835991	0,296748517	0,074314222	-0,105242251	0,17435317	0,284390352	0,582001626
559664	0,460113552	-0,05223341	-0,337631712	0,068999923	-0,819927992	0,061401025	-0,03329165	-0,376838123	-0,366952381
559721	0,252917972	0,44312579	0,084109484	-0,049254071	0,043957071	-0,195161767	-0,066800886	0,295352986	0,326919466
559746	0,038164062	-0,437581297	-0,505555601	0,466322596	-0,396897728	-0,368387618	-0,278803291	-0,613255354	-0,619656383
559754	0,921093115	0,315290582	0,014419227	0,360905	0,139367878	1,620194292	0,37323201	0,480747384	0,366310952
559790	0,335041212	0,242191563	-0,02322568	0,530628873	-0,033461173	-0,167492282	-0,086835969	0,117640379	0,03991245
559868	-0,091938456	-0,056958673	0,076907285	-0,215631948	-0,307220384	-0,065558132	0,18493011	-0,148478995	-0,527314897
560060	0,178405873	-0,033202707	0,104580304	0,07790719	0,043265992	-0,368690001	-0,173568976	0,132182096	0,20839889
560115	0,360476984	-0,00176506	-0,225951478	0,520789545	0,126845785	0,025978276	-0,089995392	-0,01887613	0,019433723
560140	0,178369473	-0,026771254	-0,164388148	-0,049043183	-0,579059053	-0,05262818	-0,349287769	-0,149964126	-0,467619213
560234	-0,170985527	-0,054035762	0,079396412	-0,100835381	-0,110312042	-0,253727465	-0,121613954	0,174413047	0,481393654
560548	0,540930502	-0,005019282	-0,250231279	0,369117252	-0,202918531	0,604665529	0,103568287	-0,127804573	-0,119088064
560591	0,17099449	0,476329215	0,146180081	0,165804466	0,285085249	-0,765962855	-0,003977932	0,147914888	0,307217122
560620	0,533680088	0,209241787	-0,070522317	0,508338849	0,340582412	0,391150661	0,445406734	-0,043023571	-0,298448436
560647	-0,080039658	0,202842361	0,097567748	-0,028217751	-0,110848889	-0,433494229	-0,397794893	0,127901587	0,319588514
560745	0,022164827	-0,447661087	-0,257225465	-0,092113921	-0,136119745	-0,018800007	-0,098579846	-0,313850562	0,110084439
560765	-0,078698143	-0,004683206	0,04033683	-0,019268395	0,001382883	-0,496672427	-0,159788209	0,080240645	0,406569189
560787	0,186741979	-0,018714889	-0,193415186	0,226414683	0,145617801	0,164904303	-0,062480804	0,010181251	-0,510574868
560827	-0,092292447	-0,276719468	-0,065337486	-0,358379492	0,101964019	0,093423329	0,253176906	-0,042719384	0,471145687
560910	-0,156238476	-0,166551803	0,125865837	-0,201529887	0,339566123	-0,307339893	-0,820608275	0,027400878	-0,132887149
560955	0,037975347	0,337795802	0,225966555	-0,123510389	0,122007839	-0,421510867	-0,152427759	0,089208857	-0,497567431
561007	-0,088272701	-0,166141505	-0,281734938	-0,068590194	-0,844252402	0,251668895	-0,26102017	-0,360049508	-0,308957472

Supplementary Table 1 Continued

AffyIDs	AM	APAP	CPZ	CsA	EE2	PQ	TAA	TET	VPA
561018	0,216081604	0,261948819	0,490739676	0,095764116	0,299318556	-0,223307552	-0,046527731	0,328285501	0,489259654
561287	-0,01538897	-0,158638367	-0,067894882	-0,50409361	-0,199938213	0,380025571	0,087617184	0,057794272	-0,393879229
561339	0,398856229	0,075710113	0,141611923	0,216811218	0,034185622	-0,441444916	-0,30136354	0,05007021	0,006310747
561360	0,477190263	0,250511182	-0,087290766	0,046335702	0,066739533	0,256653052	-0,193101922	0,267692379	0,064289011
561542	-0,863872019	-0,020192474	-0,228146714	-0,278030904	-0,298750047	0,073095319	0,294149488	-0,50356257	-0,695884123
561563	-0,240185993	-0,1821304	-0,184255653	-0,123524546	-0,749532336	0,176812908	0,157162867	-0,073928951	-0,178234848
561694	-0,26558914	0,023648112	0,149156154	-0,440493097	0,080514659	1,274440098	0,435963711	-0,159285874	-0,208949221
561766	-0,447214677	-0,208584229	-0,044898206	0,084276681	-0,361832868	0,980937503	0,540865756	-0,230888107	0,11433658
561964	0,462015764	-0,095366633	-0,027222009	0,097367138	-0,152891961	0,412997561	0,120604754	-0,090196801	0,017257824
561995	0,212345807	0,219214312	0,116978796	0,200226079	0,199070055	0,110245443	0,215749842	0,168620206	0,688681206
562008	0,577806498	0,41190999	0,274779476	0,616382049	0,679520432	-0,017859824	0,199347247	0,103552613	0,124182383
562062	-0,358647621	0,047928456	-0,238021041	-0,381299355	-0,173895216	-0,152363113	-1,121138557	-0,069522506	-0,408142759
562292	0,120607437	0,306839807	0,22078955	0,225162498	0,355140357	-0,508273102	-0,110680438	0,301331817	0,194678476
562304	2,073014463	1,505876246	1,104887741	1,145220976	1,187254421	-0,742812124	-0,392260934	1,284707633	0,792902944
562327	0,126426417	0,073520133	-0,177576631	-0,118163211	0,022035613	0,264624733	-0,222420039	-0,244464954	-0,537316169
562371	1,028849428	0,095473234	0,274964356	0,314338272	0,151721782	-0,056163636	0,352555578	0,207757776	0,382962615
562402	0,366295935	-0,203935864	-0,254462176	0,347931131	-1,041092361	-0,159371924	-0,316046854	-0,295586542	-0,041642599
562406	-0,185577945	0,000947889	0,048933765	-1,680385851	-0,084978985	-0,208243438	-0,140993755	-0,031749784	-0,38878492
562414	-0,33754876	-0,145048087	-0,087830103	0,258375439	0,2132474	-0,399378965	-0,745170908	-0,143042806	-0,339503072
562466	-0,521556752	-0,189120019	0,014104571	-0,026536401	0,204662379	-0,330405752	-0,444436673	-0,116122432	-0,45640333
562524	0,247637754	-0,387819076	0,520821234	-0,003317701	0,29194036	-0,241555765	0,317119046	0,36698374	0,20754844
562639	0,06661577	-0,06311411	-0,358608105	0,102358261	-0,010402174	0,030606821	-0,444121045	-0,024066162	-0,307279665
562682	0,554417997	0,386889957	0,12654943	-0,058569497	0,033271153	0,427663847	1,121497367	0,0684817	0,376009371
562734	-0,124286088	-0,065011201	-0,180713288	0,016602582	-0,182355092	0,459184895	-0,055524887	-0,459236292	-0,133081978
562845	-0,589656599	0,252817003	0,1916427	-0,021159707	0,129024882	-0,471944737	-0,444081263	0,025510567	-0,449846888
563067	0,342947564	0,174506162	0,230311759	0,161602438	0,203754453	-0,026144833	0,279923881	0,076024837	0,482670187
563089	0,173918726	0,197185661	0,181225735	-0,098198903	-0,224929905	-0,453187556	-0,311239879	0,335353023	0,288419836
563192	0,040041918	-0,110403065	-0,141952931	-0,023373204	0,039761391	0,605272616	0,044260665	0,008224677	0,049920795
563215	0,47861498	-0,081838959	0,034691866	0,224117104	0,033365095	-0,087402577	-0,037701028	-0,022973862	-0,057764445
563265	0,570181401	0,285142403	-0,042351576	0,094937403	-0,054692072	1,904750335	0,525052851	0,331660056	0,198430577
563325	-0,003176777	-0,029021894	0,105416747	-0,008300291	-0,175477178	0,419991266	0,748390483	0,007604404	0,574051942
563332	0,018559781	-0,171775823	-0,026727168	-0,300828633	-0,011805381	-0,024332822	0,25021016	0,338554028	0,503688808
563341	-0,543717717	-0,57130288	-1,490935536	-1,332134593	-1,442744699	0,633477161	-0,708836352	-1,173675095	-1,587565112
563489	0,127598467	0,158501822	0,133505553	0,138568164	0,345209387	0,105841324	0,230044104	0,400609055	0,791394845
563551	0,325099481	0,045274728	0,218809665	0,46995393	-0,061573595	-0,122770808	-0,028995489	0,296621131	0,381988453
563649	-0,044366753	-0,070013613	-0,251036385	0,10255392	0,003155624	0,635363768	0,262229643	0,02307101	-0,016174378
563826	0,772084594	0,088562198	-0,044184611	0,645319945	-1,004118053	0,037224805	-1,150800418	-0,491087338	-0,485287783
563834	-0,212598972	0,054254131	-0,119250968	0,07604587	-0,149943281	-0,106587343	0,183273298	-0,396354034	0,182131734
563887	0,237667884	0,209945452	0,484487405	0,352371944	0,261468238	-0,103226415	0,008447592	0,311632566	0,699900629
563896	0,183116848	0,423216854	0,06886198	0,550485932	0,547049705	1,02555084	0,312977261	0,529322581	-0,617534333
563923	-0,21486281	-0,148035575	-0,01587981	-0,040438696	-0,1523357	0,197738228	0,441065384	-0,086031799	-0,265325242
563926	-0,170194769	-0,361803456	-0,457252646	0,06576831	-1,069907158	-0,079479107	-0,255182287	-0,272913189	-0,672514521
564048	0,118835679	-0,213254501	-0,192484705	0,130401666	-0,587651297	-0,166066156	-0,223794223	-0,061458233	-0,152590462
564067	0,084695603	0,024464654	0,306678555	-0,170502572	0,088686952	1,145293799	0,169490122	-0,031204145	-0,026587442
564077	0,518693731	0,149232563	0,268895723	0,118647847	0,156692878	-0,010586311	0,095379804	0,096591482	0,565783087
564159	0,479446203	-0,186351033	-0,205358552	0,520106219	-0,980353804	-0,13845805	-0,68870892	-0,003735463	0,284374695
564166	0,144304626	-0,12466094	-0,329842735	0,069025052	0,18685247	0,160138787	-0,351223175	-0,262455295	-0,481923094
564413	-0,233220936	-0,195107471	-0,342171659	-0,119548246	-0,165013578	-0,005996789	-0,033341784	-0,374589431	-0,492598184
564474	-0,287730401	-0,141272321	-0,366406578	-0,575476226	-0,364613018	-0,372293029	-0,470819978	-0,204907324	-1,019174696
564731	-0,00544274	0,123407323	0,074681718	-0,068750045	-0,01726532	-0,18485252	0,100561169	0,093731739	0,812883339
564750	0,161157397	-0,071909214	-0,151542601	-0,087349471	-0,19675617	0,181195352	-0,109106586	-0,080551208	0,449609915
564849	-0,100408429	-0,207712747	-0,417507578	0,042294174	-0,398134782	0,759611249	0,227755626	0,093528444	-0,114857936
564862	0,061385336	0,12014094	0,022047969	0,071719226	-0,04727811	0,024073079	0,024114492	0,058037822	0,631476566
564916	-0,400331853	-0,303277575	-0,358618115	-0,409451298	-0,281484736	-0,093881623	0,069832657	-0,258212205	-0,856038152
564970	0,5088723	0,423761339	0,22220038	0,177047322	-0,050489498	0,15156922	0,743587672	0,298782682	0,625514595
564989	-0,035375589	0,017045985	0,018087938	0,023348497	0,078259136	-0,519527148	-0,270217361	0,082232984	-0,02716194
565154	-0,285710589	-0,236614125	-0,167784684	-0,45105412	-0,287183321	-0,038882136	-0,152057878	-0,213354622	-0,045069408
565335	0,00125434	0,131618643	0,011483854	0,085310978	-0,203239705	0,342731906	0,05953873	0,099101473	0,66871388
565379	0,018644191	-0,119581246	0,086734896	0,071404558	-1,087648476	-0,082565493	-0,226242875	0,004446687	-0,538163135
565439	0,519027948	-0,026174998	-0,091326507	0,52934062	-0,07551925	0,261580556	0,185836261	0,210903229	-0,143505498
565535	-0,155778277	-0,000706808	-0,474621213	0,606943434	-0,622696917	-0,423235326	-0,942978905	-0,017761465	-1,060634866
565591	0,501226893	0,30988539	0,354401187	0,348557323	0,364789336	-0,407826669	-0,093737133	0,385900394	0,306127608
565844	-0,228946598	-0,157367238	-0,055152218	-0,209089276	-0,319011881	0,02542592	-0,019522452	-0,072169095	-0,580429832
565869	-0,211310844	-0,065178917	-0,570931264	-0,299572329	-1,469363067	-0,273011436	-0,602482699	-0,062926839	-0,601183834
565911	0,254659809	-0,115306699	-0,218835675	-0,114146826	-0,962177166	0,507770407	-0,121864336	-0,09403144	-0,264415332
565952	-0,219647462	-0,070551893	0,030093706	-0,406941857	-0,202960927	-0,205118889	0,009805654	-0,066961149	-0,166990624
565970	-0,095352236	-0,049836042	-0,067188646	-0,085023216	-0,080519313	-0,178788471	0,016583769	-0,093400308	-0,541414557
566074	-0,343749531	-0,124541825	-0,242653229	-0,273940842	-0,179640757	-0,168776464	0,349008012	-0,212325297	0,52146582
566203	-0,107973531	-0,371508363	-0,074118384	-0,185949827	-0,294082101	0,131711706	0,51761528	-0,270381443	0,449813123
566313	0,360975398	0,498735138	0,086263343	0,156946821	0,381335311	-0,0018545	-0,301830408	0,294402515	0,330311614
566336	0,400123652	0,382546915	0,312445416	0,067360847	0,08003204	0,572046094	0,251078439	0,289811677	0,323272005
566492	-0,314129768	-0,138422183	-0,109035231	-0,235802407	-0,155323658	-0,092079041	0,136580588	-0,348355939	-0,485666912
566845	-0,495332399	-0,654011979	-0,717352511	-0,597684116	-1,007586631	-0,118996634	-0,823493281	-0,726605696	-0,686122286
566921	-0,235422995	0,577961161	0,435052045	0,410706181	0,480041855	-1,520292125	-0,598067798	-0,205545643	0,28137594

Supplementary Table 1 Continued

AffyIDs	AM	APAP	CPZ	CsA	EE2	PQ	TAA	TET	VPA
566996	1,227106044	0,143269411	0,038093042	0,134104342	0,171336972	3,835799254	0,116969598	0,566220176	0,225708697
567225	0,019399928	0,124719138	0,260734027	0,039120176	0,105968538	-0,117358495	0,020165171	0,062111445	0,573600857
567241	0,340641339	0,185564683	-0,065253018	0,17761832	-0,077750489	0,645731547	0,011474898	-0,155880391	0,16811698
567253	0,17950561	0,085963264	-0,106237939	0,253148137	0,135523834	0,555318393	-0,025644953	-0,107608355	0,081434117
567263	-0,15317959	0,060719828	-0,078269813	-0,140830012	-0,051632127	-0,061250339	0,139169573	-0,051051496	-0,718530129
567306	0,074816366	0,036168047	0,21437101	-0,034256851	0,09742442	0,024428353	-0,231970673	0,246232326	0,530411597
567375	0,325549129	0,251608788	0,066225494	0,194818497	0,042638712	-0,077242131	0,062551756	0,109376192	0,485149446
567528	-0,092079647	-0,109045921	-0,396340424	-0,047060195	-0,119202524	0,317384931	0,363996043	-0,221156439	-0,375937348
567611	0,066789289	0,105194954	0,1728277	0,291386758	0,230037676	-0,158045606	0,035113678	0,273125714	0,784581038
567822	1,206099261	0,263576899	0,058767699	0,140416701	0,06003084	0,864906963	-0,031414159	0,321571488	0,212013924
567944	0,257283491	0,198964998	-0,030875985	0,272243361	0,36534679	-0,315297695	-0,023686724	0,232475713	0,520381259
567956	0,485743599	0,294435635	0,402209926	0,461853632	0,377993807	0,268053765	-0,051149207	0,271613927	0,169200878
568001	0,459779989	0,055660855	-0,074441365	0,451630143	-0,14535673	-0,012306974	-0,461812377	0,273897506	0,130373713
568021	-0,141138982	-0,29036889	-0,237151746	-0,057215568	-0,744525723	0,298923966	-0,013377987	-0,32560504	-0,328005525
568180	0,290229205	0,361233971	0,035863171	-0,213277729	-0,274748161	-0,41194076	-0,185336181	0,148813613	0,076044486
568219	0,262453695	0,070733507	-0,183615553	-0,010300177	0,039246558	-0,245638191	-0,097250245	0,183764385	0,437734121
568265	0,366488248	-0,149125021	0,075344701	-0,027264111	0,000455781	0,683412047	0,222920416	0,049526413	0,09304216
568360	0,098275561	0,022315811	0,055578247	-0,527873484	0,299786873	0,38833323	0,259273899	0,166324302	0,09474233
568367	-0,068291678	-0,183930805	-0,153592159	0,030112398	0,036904469	0,493992897	0,067110987	-0,22208411	-0,261505346
568457	-0,020564934	0,155377564	0,2591648	0,222659558	0,16039454	0,120134024	0,272081019	0,191695122	0,728125495
568482	1,802846867	0,129478552	-0,056525446	-0,04429706	0,3526441	1,528759286	0,0344843	0,094684007	0,402077505
568707	-0,81107454	-0,384437727	-0,788718396	0,470281598	-1,062410086	0,449090932	-0,484160018	-0,0542935	-0,653831138
568754	-0,047491199	0,124421078	-0,038180057	0,062748397	-0,122515636	-0,278845142	-0,269753306	-0,087524668	-0,735685083
568768	-0,19948519	-0,175953196	0,041456027	-0,285735432	-0,078107466	-0,243741315	0,092751832	-0,20332157	-0,454695863
568800	-0,104725049	-0,253259662	-0,034567077	-0,199790262	-0,195080014	0,117173499	0,250992748	0,14027699	0,583612777
568883	0,061015487	-0,030283748	-0,037210991	0,021575913	0,04443524	0,126039835	-0,188140857	0,02318652	0,609378737
568958	0,308879478	0,018326527	0,055247891	-0,23696147	-0,187064039	-0,053560108	0,194314972	-0,072001967	0,707494823
569294	-0,016234579	0,103733772	0,139187677	0,037991228	0,300464437	0,21037568	-0,010025385	0,193351669	0,790163019
569298	0,880168671	0,192219537	-0,018817964	0,008327774	0,208582206	-0,471350334	-0,40104456	-0,150608747	-1,087855912
569320	-0,208372009	-0,230956179	-0,046867206	-0,265302694	-0,254964082	0,312081614	0,265334902	-0,263814768	-0,431997996
569329	0,382142792	0,26118571	0,174561918	0,101256154	0,116702988	-0,08994798	-0,093193041	0,27736111	0,539050173
569340	-0,025733595	-0,19357128	-0,008736687	-0,137918832	-0,189537423	-0,511854944	-0,238148128	-0,150539908	-0,825129533
569344	-0,013881317	-0,066764931	0,05640374	-0,239988576	-0,067854622	0,06223687	0,212043601	-0,021703139	-0,691441222
569543	0,005325906	-0,290824498	-0,028612064	-0,066687544	-0,334373648	0,487947676	0,030366236	-0,250388353	-0,307392541
569620	-0,103384246	-0,085953755	-0,017630064	-0,009866407	-0,005304354	-0,031900855	0,484897664	-0,115462238	-0,103370523
569727	-0,28717701	-0,097198496	-0,1066877	-0,220880912	-0,05541426	-0,208526912	-0,057068963	-0,086617271	-0,519291854
569940	0,16645605	0,311037326	0,183207761	0,202084112	0,285148075	-0,177818449	-0,18643437	0,116708169	0,621211639
570077	-0,051926964	0,017862256	0,092184669	-0,018959892	0,112665403	0,194262202	-0,166002351	-0,087207904	0,52578943
570148	-0,15952173	0,015834631	0,024025541	-0,050995482	-0,114332038	0,802502916	0,43091964	-0,05220261	0,144907708
570409	0,21887346	0,059134639	0,207958987	0,059616557	0,068674585	0,131014121	0,318413558	0,285217112	-0,658860815
570567	-0,176958803	-0,160273559	-0,353394372	0,056255708	-0,447363	-0,35034633	-0,710521313	0,077285675	-1,248783002
570579	0,421475981	0,022304956	-0,03341654	0,01716627	0,052552217	0,998357899	0,122766978	0,127039269	0,341582417
570589	0,023543586	-0,060479453	0,017532722	-0,068305606	0,068060554	0,470609272	0,270447475	-0,037042656	-0,122739806
570782	0,410954961	-0,090154115	0,174736369	0,111788645	-0,01315002	0,200679539	-0,27435873	-0,11643973	-0,019981786
570867	-0,313476222	-0,335566134	-0,25794389	-0,327851464	-0,198899761	0,656693835	0,220497098	-0,226197368	-0,44984497
571219	0,191650587	-0,16567527	-0,020236715	0,768519229	-0,119753353	0,101325657	0,089218799	-0,087518046	-0,007417031
571470	0,018174291	-0,103289227	-0,055754339	0,224629175	-0,031342601	0,992659779	-0,133035496	-0,1186355	0,310317527
571743	0,300426765	-0,068145157	0,181273317	-0,078300796	0,078458812	-0,013320892	0,213308848	0,359627842	0,689839718
571770	-0,316224932	-0,589572725	-0,221434228	0,026188612	-0,554060287	0,358709867	0,046905051	-0,476693536	-0,101329122
572002	-0,319049161	-1,021400377	-0,558918605	-0,388509297	-0,496322127	-0,03317126	0,282261996	-0,653412369	-0,36509429
572087	-0,2085431	-0,20845709	-0,287993438	-0,406371161	-0,145714269	-0,005738602	0,379771998	-0,29756503	-0,035142387
572114	0,192149497	0,563339834	0,434659532	0,224112206	0,247441415	-0,448717609	-0,151756614	0,20045137	0,383507879
572492	-0,010117971	0,107652519	-0,043929003	0,102016313	-0,187834546	0,062039908	-0,340120568	0,064035748	-0,579189699
572518	-0,106650804	-0,33062465	-0,391406932	-0,241369001	-0,724418496	0,284813384	-0,138192318	-0,429027766	-0,420291441
572649	1,14720348	0,171426922	-0,395826697	0,375567895	-0,357011903	0,8073316	0,053508451	0,277919679	-0,195020913
573111	0,822582164	0,425561669	0,240279555	0,515566311	0,50279237	2,003493444	0,572968075	0,363530167	0,138092707
58027	-0,165299485	-0,387226119	0,058328116	-0,309875346	-0,285700588	-0,017204879	0,281386101	-0,25082458	-0,619562477
58108	0,289475006	0,026796105	-0,233645044	0,021075868	0,001810632	0,437012708	0,015687384	-0,073138494	-0,005719844
58122	0,296682549	-0,086163479	-0,34075581	0,176922745	-0,102170789	0,538304543	-0,231022444	-0,291942938	-0,225249633
60640	1,077819781	0,565155946	0,773665033	-0,061105757	2,024945484	0,213988057	0,437604214	0,06000886	0,277509972
619256	-0,053138016	-0,145587683	-0,032712384	0,050545537	-0,07294891	0,013711972	0,242643991	0,088845338	0,592392824
619266	-0,152378799	0,160465494	0,219625862	0,074279699	-0,023773217	-0,011375586	-0,118452136	0,233592243	0,682082305
619268	-1,169071726	-0,117216524	-0,234248839	-0,451723909	-0,325473376	-0,120476097	0,082594412	-0,274372734	-0,446386265
641422	-0,136452245	-0,097802068	-0,204585077	-0,140996272	0,003017624	4,060414267	0,232214568	0,183731955	-0,228941376
641427	0,215527012	0,162372218	0,230499705	0,122640881	-0,01185272	-0,331539298	-0,262580485	0,281911243	0,486703425
641479	1,293167316	-0,105521154	-0,088106063	0,134222177	-0,425952121	1,563382734	0,162713069	0,177158779	0,266477845
641576	-0,684369268	-0,319459482	-0,542628846	-0,3034418	-0,956948773	-0,333972483	-0,353624227	-0,410115045	-0,649765427
64265	0,440173331	0,094749686	0,243285681	-0,100460606	0,039593099	0,094566341	0,527254814	0,109108322	0,282546944
64605	0,137530576	0,004632563	-0,266980125	0,130151649	-0,150598338	1,049589768	0,722602906	0,220100806	0,325851891
64608	1,794804191	0,137434176	-0,011033607	-0,034323509	0,337996471	1,240705069	-0,319620348	0,245863313	0,143129655
64611	-0,025209239	-0,173494161	-0,102278241	-0,056248163	-0,562580966	-0,190860988	-0,270108039	-0,213513743	-0,689391493
64812	0,034949982	0,209986681	0,229037915	0,07165671	0,101564175	0,340497192	0,43438243	0,329600681	0,606142777
65233	0,281394011	0,344742478	0,128443846	0,269748999	0,160507373	-0,466550067	-0,14394914	0,259987325	0,261374206
664754	0,05165192	-0,121849796	-0,075936751	0,007731961	0,296039859	-0,371285573	-0,159710496	-0,132775741	-0,726829526

Supplementary Table 1 Continued

AffyIDs	AM	APAP	CPZ	CsA	EE2	PQ	TAA	TET	VPA
677747	-0,536888575	0,403487689	0,014973865	-0,04928194	0,480227708	0,041797178	-0,130321665	0,441753438	-0,549510639
678514	0,219297313	0,533408046	0,142739578	0,604306634	0,553419165	-0,276429221	0,054646335	0,702229968	0,191976572
678555	0,519431375	-0,06504481	0,003719108	0,148897485	-0,089556184	0,133253975	0,056927099	-0,144631079	0,324656156
678628	0,523404632	-0,065699988	0,085049876	0,141062576	-0,064129544	-0,04533527	-0,076806116	0,03014328	0,036505829
724004	0,04237559	-0,214687863	-0,315908888	0,4543777	-0,115239224	-0,03973586	0,062871492	-0,387372168	-0,354593504
751093	0,170052547	0,224619653	0,093547952	-0,045951401	0,268745136	-0,182481206	-0,235040292	0,090334515	0,821904883
751627	0,345545268	0,199943646	-0,120054413	0,096154953	0,109279431	0,881779554	-0,278457673	0,015037307	0,14655131
751668	-0,614102075	-0,381824912	0,673956853	-0,240834971	-0,729435167	-0,010088072	-0,496148009	0,195240134	0,87023948
751731	0,475880887	0,151000438	-0,431184204	-0,090275094	-0,02147264	0,566443221	-0,246669197	0,118370848	-0,815129328
751751	-0,516420242	-0,183775922	0,232104686	-0,449774635	-0,123122488	0,106770461	-0,018098649	-0,061944995	0,304407976
751793	0,301002934	-0,013494871	0,01992594	0,717920997	0,137314258	-0,056999703	-0,110263051	0,117808991	-0,174127722
767640	0,010733708	0,051736564	0,196293257	-0,042760468	-0,041943111	-0,508977774	-0,049249237	0,007626138	0,356004201
767649	0,016234673	-0,044923758	-0,284462248	-0,035056141	-0,127373869	0,686371683	0,113678852	-0,140898741	-0,126645514
767662	-0,029417113	0,023701599	0,172755637	-0,092127969	-0,223939324	0,874431999	0,316545964	0,055336159	-0,202636641
767687	-0,005193025	0,213637563	0,085294556	-0,090167204	0,153152124	-0,16993805	-0,124698463	0,210307335	0,579248286
767730	-0,097564866	0,050250943	-0,052071033	0,07143884	-0,024680746	0,646402841	0,102198896	-0,122302649	-0,020325105
767756	0,578803169	-0,014203287	0,031041891	0,015199254	-0,096469042	0,222092596	-0,208032253	0,052182509	0,082816209
767778	0,11881481	0,02694642	0,368151432	0,163308412	0,281583103	0,224285894	-0,229387224	0,14670833	0,663557026
768152	0,138567789	0,165823843	0,23719107	-0,154174404	0,30976662	-0,321317755	0,208302896	0,387649107	0,298277525
768172	-0,164765018	0,041368877	-0,198203825	-0,0920927	0,066024086	1,504238493	0,293564663	0,252393535	-0,086087797
768292	-0,078126721	-0,228013425	-0,830345315	0,466446333	-1,469189391	0,342778186	-0,313298326	-0,086088543	-1,682372148
777641	-0,169370522	-0,110547789	-0,125752948	0,067135997	-0,128438539	-0,082877569	-0,058955533	0,009334406	-0,453745308
790919	0,170958555	0,238648364	0,19753809	-0,19872763	0,163614149	0,283961997	0,135629431	0,121695946	0,871046693
790941	0,528856539	-0,118088966	-0,038890965	0,203693209	0,082202855	0,351000545	-0,028969933	-0,132702944	-0,196632061
790945	0,013758597	-0,108163148	0,01542399	0,251635234	-0,9757986	0,444216242	-0,25301857	-0,101034142	0,182821442
791159	0,508629242	0,055771092	0,027297733	0,224429861	-0,032013486	0,536083304	0,110434552	0,20953614	0,37012665
791197	-0,235138468	-0,152316721	-0,259025688	0,026109109	-0,289590793	0,48019183	-0,162533137	-0,004798396	-0,230797316
791215	0,902465834	-0,001792642	-0,054536678	0,435976344	0,08683308	0,219060255	-0,23800526	-0,189589897	0,29902674
791218	0,361655831	0,175865638	0,277579009	0,162470885	0,397050772	1,920366768	0,475587258	0,584316143	0,540849259
791453	1,180408242	-0,107451148	-0,455731981	1,03761924	0,307338875	0,216396785	0,5287588	0,244037198	0,284316811
791613	3,09882815	-0,134772118	-0,822761673	-0,395157155	0,093578606	1,310401827	0,511594845	-0,609649592	0,734207943
791773	0,218627018	-0,174015941	-0,242381535	0,091153928	-0,13788315	0,053239902	0,201340959	0,153277501	-0,541875488
792211	-0,202011856	-0,412274967	-0,052654884	-0,195900028	-0,234297156	-0,1727877	-0,002882047	-0,144771481	-0,347198775
792319	-0,834291509	-0,369318949	-0,063339133	-0,015353977	-0,165293475	-0,089069111	-0,170856992	-0,175913199	-0,383782252
792566	0,45866571	0,292238991	0,351082153	0,589437119	0,178424977	-0,40344108	0,325813214	0,418607801	-0,337330904
792610	0,396016479	-0,286314703	-0,351889208	0,488667226	-1,43458763	0,246162013	-0,476882745	-0,518067997	0,187327925
792692	-0,078693872	-0,008589003	0,034016505	0,014388155	0,027702147	-0,31981646	-0,198885024	0,31341832	-0,635376553
792697	-0,204403229	-0,06682429	-0,26278957	-0,008272743	-0,026857405	-0,394074774	-0,125083511	-0,143608823	0,360797287
792944	0,063655495	0,343686807	0,354078687	-0,032047403	0,35811305	-0,174366026	-0,444594082	0,376308654	0,048408882
793278	0,375774507	0,194403904	0,07267287	0,484775399	0,389551736	0,193080013	-0,142326602	0,070964061	0,648762675
793796	-0,127184499	-0,139011086	-0,181232321	-0,29355075	-0,235848126	-0,202930429	-0,305614877	0,03750735	-0,792066883
79381	0,264638857	-0,075506148	-0,107834111	-0,158145101	0,251215823	1,62445544	0,56971429	0,140696971	0,111779877
793907	0,451176285	-0,405519309	-0,568264978	1,047768359	0,009988545	1,403429535	0,209140518	-0,280745005	-0,919134201
793937	0,764562664	0,431938281	0,525617458	0,046934478	0,300804894	-0,225830153	-0,292289725	0,296822121	0,420628722
794083	-0,164309316	-0,124646602	-0,373587643	-0,246650144	-0,558634703	0,352874556	-0,178401762	-0,336667631	-0,460070301
794117	-0,085629251	0,36989533	-0,175970775	-0,092438937	0,024507192	0,083562079	0,093689535	0,35511259	-0,638065585
794145	-0,198971985	0,026274355	-0,0359061	-0,230247563	0,083639238	0,219076205	0,307855715	-0,434613838	-0,236420162
794188	0,258544633	0,17631824	0,433611578	-0,038454364	0,097484606	-0,029568679	0,413502483	0,189640065	0,335406112
794234	-0,131412241	-0,127870371	0,04544464	-0,162155912	-0,479517596	-0,030405731	0,078751863	-0,112230678	-0,044491088
794406	-0,060189088	0,024779518	-0,000981943	-0,152070092	0,146848321	-0,165601432	-0,376768616	-0,022530802	0,039816222
795520	0,090222345	-0,096935607	-0,242816723	-0,460998654	0,063073744	-0,293990392	-0,028191686	0,290603304	0,531550549
795664	-0,16267212	-0,20287389	-0,633853794	0,121016301	-0,557259027	-0,664028797	-0,554558391	-0,171474748	-0,86126872
796215	-0,328264553	-0,161993036	-0,019978119	-0,490558587	-0,112805697	0,098324074	0,290824181	-0,428717299	0,364501639
796392	-0,418026801	-0,479950886	-0,256492077	-0,180920573	-0,379421812	-0,381081825	-0,099006906	-0,306501362	-0,741620359
796618	0,61118348	0,063559279	0,051231248	0,146533384	0,207691929	-0,268631138	0,145825292	0,028817822	0,063632319
797243	0,16839611	0,548975411	0,173898123	0,174803314	0,359577103	-0,094313632	-0,039867024	0,248564875	0,274890589
797371	0,248711496	-0,13377757	-0,494840086	0,413488606	-0,164018229	1,075525246	-0,284750043	0,240461586	-0,582757194
797969	-0,038898411	-0,282616085	-0,534295818	-0,263623302	-0,356918321	0,042777264	0,147504697	-0,612643536	-0,514427612
798023	-0,472640466	0,008599799	-0,703217034	-0,444036015	-0,862870397	-0,306167207	-0,892498642	-0,477617237	-1,079429438
798527	0,73710933	-0,223033106	-0,250187097	0,462372188	-0,164830905	0,280950845	-0,340454469	-0,221975817	-0,029807727
799290	-0,47171135	0,10862064	-0,036616003	-0,070631531	-0,018157942	-0,053173692	0,03687248	0,068847304	-0,667869793
799373	0,239030578	-0,039631934	-0,183611649	0,064133024	-0,389166106	0,741547415	-0,114876636	-0,118648844	0,160778786
799473	0,008032341	-0,230820692	0,009698374	-0,009085233	-0,181043995	-0,194620372	-0,157964447	-0,174952763	-0,414543374
799492	0,200752775	-0,188835897	-0,358755165	0,414057884	-0,283178384	-0,320290726	-0,562184991	-0,470026918	-0,734007065
799656	0,045935792	-0,144515819	-0,475007089	0,212412016	-0,286775281	0,986326096	-0,196556556	-0,217274489	-0,373836192
83908	-0,71683263	-0,222928442	-0,865677489	0,178155397	-0,962276157	0,193569653	-0,602459411	-0,320497437	-1,402201459

Supplementary Table 1 Dosing and time points in the models included in the comparison

	Model	**Zebrafish embryo (ZFE)**	**mouse *in vivo* (MIV)**	**Mouse primary hepatocytes (MPH)**	**Rat *in vivo* single dose (RIVS)**	**Rat *in vivo* repeated dose (RIVR)**	**Rat primary hepatocytes (RPH)**	**Human primary hepatocytes (HPH)**
	Time	48 hours	1, 2, 4, 11 days	24, 48 hours	3, 6, 9, 24 hours	4, 8, 15, 29 days	2, 8, 24 hours	2, 8, 24 hours
	Dose unit	µM	mg/kg	µM	mg/kg	mg/kg	µM	µM
Compound								
Amiodarone (AMD)	doses	1.1 - 3.3 - 10	6.7 - 20 - 60	1 - 25	200 - 600 - 2000	20 - 60 - 200	0.28 – 1.4 - 7	0.28 – 1.4 - 7
	Accession #	GSE55618	GSE48126		E-MTAB-799	E-MTAB-800	E-MTAB-797	E-MTAB-798
Acetaminophen (APAP)	dose L-M-H	73.3 - 220 - 660	168.8 - 225 - 300	1000 - 10000	300 - 600 - 1000	300 - 600 - 1000	1000 - 3000 - 10000	200 - 1000 - 5000
	Accession #	GSE55618	GSE51969		E-MTAB-799	E-MTAB-800	E-MTAB-797	E-MTAB-798
Cyclosporine A (CsA)	dose L-M-H	1 - 3 - 6	3 - 8.9 - 26.7	10 - 50	30 - 100 - 300	10 - 30 - 100	0.24 - 1.2 - 6	0.24 - 1.2 - 6
	Accession #	GSE55618	GSE31540		E-MTAB-799	E-MTAB-800	E-MTAB-797	E-MTAB-798
Original publication		Driessen et al., 2013; Driessen et al., 2014	Kienhuis et al., 2013; Vitins et al., 2014	Van Summeren et al., 2013	Noriyuki et al., 2012; Uehara et al., 2010	Noriyuki et al., 2012; Uehara et al., 2010	Noriyuki et al., 2012; Uehara et al., 2010	Noriyuki et al., 2012; Uehara et al., 2010

L-M-H, Low – Mid – High dose, respectively.
There is no accession number for MPH while it is a in-house dataset

Supplementary Table 2

Entrez_ID	Gene_symbol	Compound	Condition
2	A2M	AMD	in_vivo
968	CD68	AMD	in_vivo
1581	CYP7A1	AMD	in_vivo
1582	CYP8B1	AMD	in_vivo
1717	DHCR7	AMD	in_vivo
1728	NQO1	AMD	in_vivo
1891	ECH1	AMD	in_vivo
1990	CELA1	AMD	in_vivo
3171	FOXA3	AMD	in_vivo
3484	IGFBP1	AMD	in_vivo
4199	ME1	AMD	in_vivo
6307	MSMO1	AMD	in_vivo
9415	FADS2	AMD	in_vivo
25987	TSKU	AMD	in_vivo
51316	PLAC8	AMD	in_vivo
51703	ACSL5	AMD	in_vivo
54677	CROT	AMD	in_vivo
54884	RETSAT	AMD	in_vivo
56898	BDH2	AMD	in_vivo
57035	C1orf63	AMD	in_vivo
84263	HSDL2	AMD	in_vivo
220441	RNF152	AMD	in_vivo
1962	EHHADH/ECHD	AMD	In_vitro
4239	MFAP4	AMD	In_vitro
5649	RELN	AMD	In_vitro
9963	SLC23A1	AMD	In_vitro
57715	SEMA4G	AMD	In_vitro
1581	CYP7A1	APAP	in_vivo
1582	CYP8B1	APAP	in_vivo
1647	GADD45A	APAP	in_vivo
1675	CFD	APAP	in_vivo
2643	GCH1	APAP	in_vivo
2645	GCK	APAP	in_vivo
3303	HSPA1A	APAP	in_vivo
4323	MMP14	APAP	in_vivo
4958	OMD	APAP	in_vivo
9099	USP2	APAP	in_vivo
10110	SGK2	APAP	in_vivo
51084	CRYL1	APAP	in_vivo

Supplementary Table 2 Continued

Entrez_ID	Gene_symbol	Compound	Condition
54884	RETSAT	APAP	in_vivo
55269	PSPC1	APAP	in_vivo
2152	F3	APAP	In_vitro
2289	FKBP5	APAP	In_vitro
3303	HSPA1A	APAP	In_vitro
4320	MMP11	APAP	In_vitro
4547	MTTP	APAP	In_vitro
5009	OTC	APAP	In_vitro
11069	RAPGEF4	APAP	In_vitro
54463	FAM134B	APAP	In_vitro
55055	ZWILCH	APAP	In_vitro
64240	ABCG5	APAP	In_vitro
123920	CMTM3	APAP	In_vitro
1582	CYP8B1	CsA	in_vivo
1595	CYP51A1	CsA	in_vivo
1728	NQO1	CsA	in_vivo
3484	IGFBP1	CsA	in_vivo
4597	MVD	CsA	in_vivo
4837	NNMT	CsA	in_vivo
5313	PKLR	CsA	in_vivo
8835	SOCS2	CsA	in_vivo
9601	PDIA4	CsA	in_vivo
10110	SGK2	CsA	in_vivo
10912	GADD45G	CsA	in_vivo
23423	TMED3	CsA	in_vivo
25819	CCRN4L	CsA	in_vivo
26118	WSB1	CsA	in_vivo
57546	PDP2	CsA	in_vivo
57761	TRIB3	CsA	in_vivo
64240	ABCG5	CsA	in_vivo
83595	SOX7	CsA	in_vivo
219972	MPEG1	CsA	in_vivo
1039	CDR2	CsA	In_vitro
1543	CYP1A1	CsA	In_vitro
11069	RAPGEF4	CsA	In_vitro
57761	TRIB3	CsA	In_vitro
64240	ABCG5	CsA	In_vitro

Supplementary Table 3

RIVS AMD Pathways p<0.05

#	Maps	pValue
1	Regulation of metabolism_Bile acids regulation of glucose and lipid metabolism via FXR	8,189E-10
2	Cell cycle_Role of SCF complex in cell cycle regulation	1,182E-06
3	Development_Thromboxane A2 pathway signaling	2,707E-06
4	Development_Endothelin-1/EDNRA signaling	6,131E-06
5	Development_WNT signaling pathway. Part 2	6,131E-06
6	Cytoskeleton remodeling_TGF, WNT and cytoskeletal remodeling	7,920E-06
7	Development_Role of IL-8 in angiogenesis	8,390E-06
8	Cell adhesion_Chemokines and adhesion	9,286E-06
9	Immune response_MIF-induced cell adhesion, migration and angiogenesis	1,053E-05
10	Immune response_MIF - the neuroendocrine-macrophage connector	1,053E-05
11	Transcription_ChREBP regulation pathway	1,117E-05
12	Development_Leptin signaling via PI3K-dependent pathway	1,291E-05
13	Regulation of lipid metabolism_Regulation of lipid metabolism via LXR, NF-Y and SREBP	1,397E-05
14	Reproduction_Progesterone-mediated oocyte maturation	2,183E-05
15	Development_Gastrin in cell growth and proliferation	2,959E-05
16	Immune response_IL-12-induced IFN-gamma production	6,935E-05
17	Immune response_IL-18 signaling	1,182E-04
18	Development_A3 receptor signaling	1,193E-04
19	Immune response_IL-6 signaling pathway	1,787E-04
20	G-protein signaling_Proinsulin C-peptide signaling	1,921E-04
21	Cytoskeleton remodeling_Cytoskeleton remodeling	2,034E-04
22	Regulation of lipid metabolism_Insulin regulation of fatty acid methabolism	2,082E-04
23	Putative pathways for stimulation of fat cell differentiation by Bisphenol A	2,209E-04
24	Cell cycle_Role of APC in cell cycle regulation	2,209E-04
25	Development_BMP signaling	2,709E-04
26	Cell cycle_ESR1 regulation of G1/S transition	2,709E-04
27	PGE2 pathways in cancer	2,987E-04
28	Immune response_IL-1 signaling pathway	3,070E-04
29	Development_Thrombopoietin-regulated cell processes	3,605E-04
30	G-protein signaling_Rap2A regulation pathway	4,172E-04
31	Development_Prolactin receptor signaling	4,500E-04
32	Regulation of CFTR activity (normal and CF)	4,500E-04
33	Cytoskeleton remodeling_Keratin filaments	4,773E-04
34	Development_EGFR signaling pathway	4,898E-04
35	Transport_Alpha-2 adrenergic receptor regulation of ion channels	4,905E-04
36	Development_WNT5A signaling	4,905E-04
37	wtCFTR and deltaF508 traffic / Membrane expression (normal and CF)	6,735E-04
38	Development_GM-CSF signaling	7,543E-04
39	Translation_Non-genomic (rapid) action of Androgen Receptor	9,288E-04
40	Development_G-CSF-induced myeloid differentiation	1,041E-03
41	Immune response_HMGB1 release from the cell	1,082E-03
42	Immune response_HMGB1/RAGE signaling pathway	1,122E-03
43	ENaC regulation in normal and CF airways	1,122E-03
44	Cytoskeleton remodeling_Reverse signaling by ephrin B	1,248E-03

Supplementary Table 3 Continued

RIVS AMD Pathways p<0.05

#	Maps	pValue
45	Transport_ACM3 in salivary glands	1,255E-03
46	Immune response_CCL2 signaling	1,272E-03
47	Development_VEGF signaling and activation	1,448E-03
48	Development_Transcription regulation of granulocyte development	1,485E-03
49	DNA damage_ATM/ATR regulation of G1/S checkpoint	1,485E-03
50	Immune response_MIF-mediated glucocorticoid regulation	1,505E-03
51	Development_S1P1 signaling pathway	1,664E-03
52	G-protein signaling_Regulation of CDC42 activity	1,755E-03
53	Normal and pathological TGF-beta-mediated regulation of cell proliferation	1,755E-03
54	Ca(2+)-dependent NF-AT signaling in cardiac hypertrophy	1,820E-03
55	Immune response_IL-33 signaling pathway	1,820E-03
56	Cell cycle_Nucleocytoplasmic transport of CDK/Cyclins	1,844E-03
57	Immune response_IL-12 signaling pathway	1,861E-03
58	Apoptosis and survival_Beta-2 adrenergic receptor anti-apoptotic action	1,861E-03
59	Transcription_Androgen Receptor nuclear signaling	1,904E-03
60	Immune response_PGE2 signaling in immune response	1,904E-03
61	Signal transduction_Erk Interactions: Inhibition of Erk	2,060E-03
62	Neurophysiological process_ACM regulation of nerve impulse	2,170E-03
63	Reproduction_GnRH signaling	2,200E-03
64	Development_Growth hormone signaling via STATs and PLC/IP3	2,404E-03
65	Development_Beta-adrenergic receptors regulation of ERK	2,464E-03
66	Development_HGF signaling pathway	2,464E-03
67	Cytoskeleton remodeling_Neurofilaments	2,751E-03
68	Transcription_Transcription regulation of aminoacid metabolism	2,751E-03
69	Immune response_Histamine H1 receptor signaling in immune response	2,788E-03
70	Immune response_TLR5, TLR7, TLR8 and TLR9 signaling pathways	2,788E-03
71	G-protein signaling_G-Protein alpha-s signaling cascades	2,789E-03
72	Development_Lipoxin inhibitory action on PDGF, EGF and LTD4 signaling	2,789E-03
73	Development_Alpha-2 adrenergic receptor activation of ERK	3,131E-03
74	Immune response_IL-2 activation and signaling pathway	3,143E-03
75	G-protein signaling_RhoB regulation pathway	3,146E-03
76	Development_Cross-talk between VEGF and Angiopoietin 1 signaling pathways	3,296E-03
77	DNA damage_ATM / ATR regulation of G2 / M checkpoint	3,296E-03
78	Cell cycle_Regulation of G1/S transition (part 2)	3,296E-03
79	Transcription_PPAR Pathway	3,465E-03
80	Apoptosis and survival_HTR1A signaling	3,532E-03
81	Immune response_Histamine signaling in dendritic cells	3,532E-03
82	Immune response_C5a signaling	3,532E-03
83	Signal transduction_cAMP signaling	3,697E-03
84	Transcription_Role of AP-1 in regulation of cellular metabolism	3,697E-03
85	Signal transduction_PKA signaling	3,957E-03
86	Some pathways of EMT in cancer cells	3,957E-03
87	Regulation of lipid metabolism_Regulation of acetyl-CoA carboxylase 1 activity in lipogenic tissue	3,986E-03
88	Immune response_CD40 signaling	4,214E-03

Supplementary Table 3 Continued

RIVS AMD Pathways p<0.05

#	Maps	pValue
89	Muscle contraction_Regulation of eNOS activity in endothelial cells	4,214E-03
90	Development_PACAP signaling in neural cells	4,224E-03
91	Development_FGF-family signaling	4,419E-03
92	Cytoskeleton remodeling_Role of PKA in cytoskeleton reorganisation	4,806E-03
93	Apoptosis and survival_Role of PKR in stress-induced apoptosis	4,921E-03
94	Development_A1 receptor signaling	4,921E-03
95	Immune response_Oncostatin M signaling via JAK-Stat in mouse cells	4,965E-03
96	CFTR-dependent regulation of ion channels in CF	5,444E-03
97	Immune response_HSP60 and HSP70/ TLR signaling pathway	5,464E-03
98	Immune response_Fc epsilon RI pathway	6,051E-03
99	Regulation of lipid metabolism_PPAR regulation of lipid metabolism	6,143E-03
100	Apoptosis and survival_Lymphotoxin-beta receptor signaling	6,143E-03
101	Development_VEGF signaling via VEGFR2 - generic cascades	6,257E-03
102	Cell adhesion_Gap junctions	6,263E-03
103	Regulation of lipid metabolism_Insulin regulation of glycogen metabolism	6,685E-03
104	Chemotaxis_CCL2-induced chemotaxis	6,685E-03
105	Immune response_CD28 signaling	6,685E-03
106	Muscle contraction_Regulation of eNOS activity in cardiomyocytes	6,685E-03
107	Nicotine signaling in dopaminergic neurons, Pt. 2 - axon terminal	6,904E-03
108	Signal transduction_AKT signaling	6,904E-03
109	Apoptosis and survival_TNFR1 signaling pathway	6,904E-03
110	Development_A2A receptor signaling	6,904E-03
111	cAMP/ Ca(2+)-dependent Insulin secretion	6,904E-03
112	Apoptosis and survival_Role of IAP-proteins in apoptosis	7,227E-03
113	Immune response_ETV3 affect on CSF1-promoted macrophage differentiation	7,227E-03
114	Immune response_Role of PKR in stress-induced antiviral cell response	7,366E-03
115	Immune response_Oncostatin M signaling via JAK-Stat in human cells	7,380E-03
116	Impaired Lipoxin A4 signaling in CF	7,731E-03
117	Immune response_IL-5 signalling	7,731E-03
118	Cell cycle_Role of Nek in cell cycle regulation	8,291E-03
119	Neurophysiological process_Glutamate regulation of Dopamine D1A receptor signaling	8,628E-03
120	Development_Ligand-independent activation of ESR1 and ESR2	8,628E-03
121	Role of alpha-6/beta-4 integrins in carcinoma progression	8,628E-03
122	Signal transduction_Calcium signaling	8,628E-03
123	Cell cycle_Cell cycle (generic schema)	8,833E-03
124	Cell cycle_Chromosome condensation in prometaphase	8,833E-03
125	Cytoskeleton remodeling_Thyroliberin in cytoskeleton remodeling	9,458E-03
126	LRRK2 in neurons in Parkinson's disease	9,458E-03
127	Cell cycle_Spindle assembly and chromosome separation	9,458E-03
128	Development_G-Proteins mediated regulation MAPK-ERK signaling	9,596E-03
129	Immune response_NF-AT signaling and leukocyte interactions	9,596E-03
130	Immune response_IL-17 signaling pathways	9,717E-03
131	Glycine, serine, cysteine and threonine metabolism	1,023E-02
132	Transcription_CREM signaling in testis	1,046E-02
133	Development_Thrombopoetin signaling via JAK-STAT pathway	1,046E-02

Supplementary Table 3 Continued

RIVS AMD Pathways p<0.05

#	Maps	pValue
134	Cell cycle_Role of 14-3-3 proteins in cell cycle regulation	1,046E-02
135	Regulation of lipid metabolism_Insulin signaling:generic cascades	1,064E-02
136	Development_TGF-beta-dependent induction of EMT via MAPK	1,064E-02
137	Development_PDGF signaling via MAPK cascades	1,064E-02
138	Chemotaxis_CCR4-induced chemotaxis of immune cells	1,073E-02
139	Mechanism of action of CCR4 antagonists in asthma and atopic dermatitis (Variant 1)	1,073E-02
140	CCR4-dependent immune cell chemotaxis in asthma and atopic dermatitis	1,073E-02
141	Oxidative stress_Role of ASK1 under oxidative stress	1,073E-02
142	Immune response_IL-22 signaling pathway	1,073E-02
143	Development_Role of CDK5 in neuronal development	1,073E-02
144	Glycine, serine, cysteine and threonine metabolism/ Rodent version	1,147E-02
145	Development_EPO-induced Jak-STAT pathway	1,212E-02
146	Cell adhesion_Plasmin signaling	1,212E-02
147	Transport_Macropinocytosis regulation by growth factors	1,258E-02
148	Development_Melanocyte development and pigmentation	1,296E-02
149	Transcription_CREB pathway	1,296E-02
150	Immune response_IL-9 signaling pathway	1,363E-02
151	Development_Regulation of epithelial-to-mesenchymal transition (EMT)	1,365E-02
152	Development_A2B receptor: action via G-protein alpha s	1,425E-02
153	Proteolysis_Role of Parkin in the Ubiquitin-Proteasomal Pathway	1,427E-02
154	Development_Glucocorticoid receptor signaling	1,427E-02
155	Immune response_MIF-JAB1 signaling	1,427E-02
156	Immune response_IL-27 signaling pathway	1,427E-02
157	Mechanism of action of DGAT1 inhibitors in obesity and diabetes mellitus, type II (Variant 1)	1,427E-02
158	Triacylglycerol biosynthesis in obesity and diabetes mellitus, type II	1,427E-02
159	G-protein signaling_G-Protein alpha-12 signaling pathway	1,525E-02
160	Development_Delta-type opioid receptor mediated cardioprotection	1,525E-02
161	Development_Leptin signaling via JAK/STAT and MAPK cascades	1,647E-02
162	Cell cycle_Initiation of mitosis	1,647E-02
163	Cytoskeleton remodeling_ACM3 and ACM4 in keratinocyte migration	1,700E-02
164	Immune response_Human NKG2D signaling	1,700E-02
165	Development_Gastrin in differentiation of the gastric mucosa	1,700E-02
166	Development_IGF-1 receptor signaling	1,708E-02
167	Immune response_PGE2 common pathways	1,708E-02
168	Cell adhesion_ECM remodeling	1,708E-02
169	Muscle contraction_GPCRs in the regulation of smooth muscle tone	1,773E-02
170	Neurophysiological process_Dopamine D2 receptor transactivation of PDGFR in CNS	1,886E-02
171	Transcription_Receptor-mediated HIF regulation	1,888E-02
172	Cell adhesion_PLAU signaling	1,888E-02
173	Transcription_P53 signaling pathway	1,888E-02
174	G-protein signaling_Regulation of p38 and JNK signaling mediated by G-proteins	1,888E-02
175	Mucin expression in CF airways	2,002E-02
176	Membrane-bound ESR1: interaction with G-proteins signaling	2,028E-02
177	Immune response _IFN gamma signaling pathway	2,028E-02

Supplementary Table 3 Continued

RIVS AMD Pathways p<0.05

#	Maps	pValue
178	Immune response_BCR pathway	2,028E-02
179	Development_Neurotrophin family signaling	2,089E-02
180	G-protein signaling_G-Protein alpha-i signaling cascades	2,146E-02
181	Development_GH-RH signaling	2,304E-02
182	Development_VEGF-family signaling	2,304E-02
183	Airway smooth muscle contraction in asthma	2,387E-02
184	Immune response_Murine NKG2D signaling	2,532E-02
185	Development_Growth hormone signaling via PI3K/AKT and MAPK cascades	2,532E-02
186	Immune response_TLR2 and TLR4 signaling pathways	2,581E-02
187	Cytoskeleton remodeling_FAK signaling	2,581E-02
188	Apoptosis and survival_p53-dependent apoptosis	2,729E-02
189	Development_Angiotensin signaling via PYK2	2,775E-02
190	Regulation of metabolism_Role of Adiponectin in regulation of metabolism	2,775E-02
191	Immune response_HTR2A-induced activation of cPLA2	2,775E-02
192	Regulation of lipid metabolism_Regulation of acetyl-CoA carboxylase 1 activity in keratinocytes	2,858E-02
193	Transcription_Transcription factor Tubby signaling pathways	2,858E-02
194	G-protein signaling_Rap2B regulation pathway	2,943E-02
195	Immune response_PGE2 in immune and neuroendocrine system interactions	3,031E-02
196	Neurophysiological process_Kappa-type opioid receptor in transmission of nerve impulses	3,052E-02
197	DNA damage_Brca1 as a transcription regulator	3,052E-02
198	Regulation of lipid metabolism_RXR-dependent regulation of lipid metabolism via PPAR, RAR and VDR	3,052E-02
199	Development_Osteopontin signaling in osteoclasts	3,052E-02
200	Development_Adiponectin signaling	3,302E-02
201	Cytoskeleton remodeling_Fibronectin-binding integrins in cell motility	3,398E-02
202	Development_Inhibition of angiogenesis by PEDF	3,398E-02
203	Immune response_IL-3 activation and signaling pathway	3,398E-02
204	Regulation of lipid metabolism_FXR-dependent negative-feedback regulation of bile acids concentration	3,398E-02
205	Regulation of lipid metabolism_G-alpha(q) regulation of lipid metabolism	3,461E-02
206	Transcription_Role of VDR in regulation of genes involved in osteoporosis	3,461E-02
207	Development_GDNF family signaling	3,588E-02
208	Development_Angiotensin activation of Akt	3,588E-02
209	Muscle contraction_Oxytocin signaling in uterus and mammary gland	3,708E-02
210	Development_PDGF signaling via STATs and NF-kB	3,764E-02
211	Development_Angiotensin signaling via STATs	3,764E-02
212	Cell cycle_Start of DNA replication in early S phase	3,764E-02
213	Development_Alpha-1 adrenergic receptors signaling via cAMP	3,841E-02
214	Development_WNT signaling pathway. Part 1. Degradation of beta-catenin in the absence WNT signaling	3,841E-02
215	Regulation of lipid metabolism_Regulation of acetyl-CoA carboxylase 2 activity in muscle	3,841E-02
216	Regulation of lipid metabolism_Regulation of fatty acid synthase activity in hepatocytes	3,841E-02
217	Development_PIP3 signaling in cardiac myocytes	3,888E-02
218	Development_EGFR signaling via small GTPases	4,153E-02
219	Muscle contraction_Role of kappa-type opioid receptor in heart	4,153E-02
220	Muscle contraction_Relaxin signaling pathway	4,204E-02
221	Immune response_IL-15 signaling	4,236E-02
222	Immune response_Bacterial infections in normal airways	4,534E-02
223	Cell adhesion_Alpha-4 integrins in cell migration and adhesion	4,564E-02
224	Development_S1P1 receptor signaling via beta-arrestin	4,564E-02
225	Apoptosis and survival_Role of CDK5 in neuronal death and survival	4,564E-02
226	Immune response_CXCR4 signaling via second messenger	4,564E-02
227	Hypoxia-induced EMT in cancer and fibrosis	4,785E-02
228	Neurophysiological process_Corticoliberin signaling via CRHR1	4,880E-02
229	Development_TGF-beta receptor signaling	4,880E-02
230	Development_Angiopoietin - Tie2 signaling	4,996E-02

The full supplementary table can be requested by sending an email to marja.driessen@embl.de

Supplementary Table 4

Overlapping pathways between MPH and ZFE AMD
Blood coagulation_Blood coagulation
Protein folding and maturation_Angiotensin system maturation \ Human version
Cell adhesion_ECM remodeling
Regulation of metabolism_Bile acids regulation of glucose and lipid metabolism via FXR
Protein folding and maturation_Angiotensin system maturation \ Rodent version
Fructose metabolism
Phenylalanine metabolism/ Rodent version
Glycolysis and gluconeogenesis p. 1
Phenylalanine metabolism
Role of ZNF202 in regulation of expression of genes involved in atherosclerosis
Immune response_Alternative complement pathway
Fructose metabolism/ Rodent version
Tyrosine metabolism p.2 (melanin)
Regulation of lipid metabolism_FXR-dependent negative-feedback regulation of bile acids concentration
Regulation of lipid metabolism_PPAR regulation of lipid metabolism
Glycolysis and gluconeogenesis (short map)
Propionate metabolism p.2
Histamine metabolism

Overlapping pathways between MPH and ZFE CsA
Blood coagulation_Blood coagulation
Cytoskeleton remodeling_TGF, WNT and cytoskeletal remodeling
Development_TGF-beta-dependent induction of EMT via SMADs
Immune response_Alternative complement pathway
Cell adhesion_ECM remodeling
Cell adhesion_Plasmin signaling
Regulation of metabolism_Bile acids regulation of glucose and lipid metabolism via FXR
Cytoskeleton remodeling_Cytoskeleton remodeling
Fructose metabolism
Cell adhesion_PLAU signaling
Regulation of lipid metabolism_PPAR regulation of lipid metabolism
Fructose metabolism/ Rodent version
Glycolysis and gluconeogenesis p. 1
Development_Growth hormone signaling via STATs and PLC/IP3
Glycolysis and gluconeogenesis (short map)
Regulation of lipid metabolism_Regulation of fatty acid synthesis: NLTP and EHHADH
Regulation of lipid metabolism_FXR-dependent negative-feedback regulation of bile acids concentration
Regulation of lipid metabolism_Insulin regulation of glycogen metabolism
(L)-Alanine, (L)-cysteine, and (L)-methionine metabolism
(L)-Alanine, (L)-cysteine, and (L)-methionine metabolism / Human version